



Universiteit  
Leiden  
The Netherlands

## Next generation lipopeptide antibiotics

Al Ayed, U.K.

### Citation

Al Ayed, U. K. (2024, January 23). *Next generation lipopeptide antibiotics*. Retrieved from <https://hdl.handle.net/1887/3714346>

Version: Publisher's Version

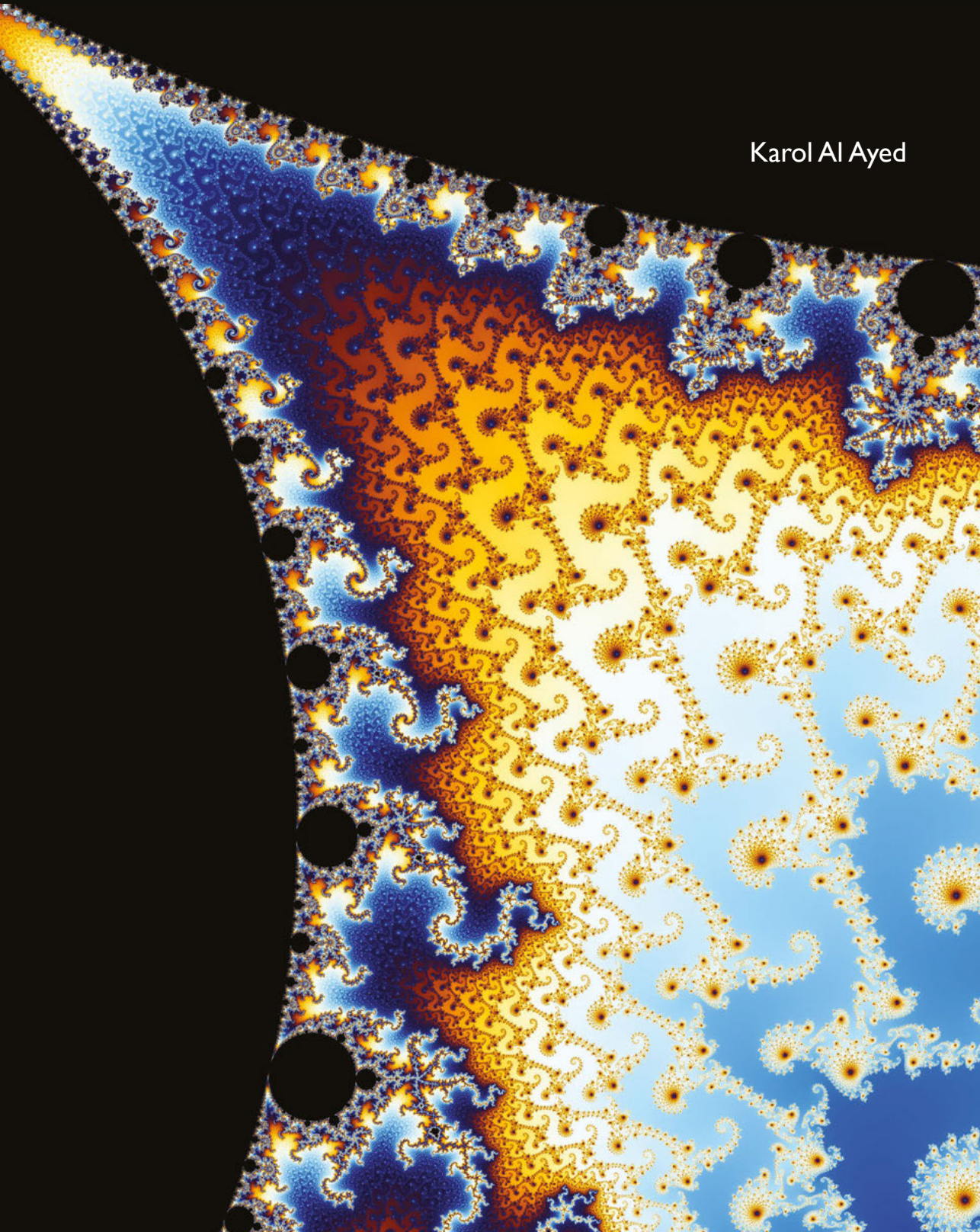
License: [Licence agreement concerning inclusion of doctoral thesis in the Institutional Repository of the University of Leiden](#)

Downloaded from: <https://hdl.handle.net/1887/3714346>

**Note:** To cite this publication please use the final published version (if applicable).

# Next Generation Lipopeptide Antibiotics

Karol Al Ayed





# Next Generation Lipopeptide Antibiotics

Proefschrift

ter verkrijging van

de graad van doctor aan de Universiteit Leiden,

op gezag van rector magnificus prof.dr.ir. H. Bijl,

volgens besluit van het college voor promoties

te verdedigen op dinsdag 23 januari 2024

klokke 13:45 uur

door

Usama Karol Al Ayed

geboren te Gdynia

in 1990

***Promotor:***

Prof.dr. N.I. Martin

***Co-promotor:***

Dr. P. Innocenti

***Promotiecommissie:***

Prof.dr. A.H. Meijer

Prof.dr. D. Claessen

Prof. dr. J. van Maarseveen

Dr. S. Cochrane

Dr. S.J. Pomplun

Printed by Gildeprint

Cover art created by Wolfgang Beyer with the program Ultra Fractal 3

Financial support for printing the thesis: Leiden University

Copyright © 2024 by Karol Al Ayed. All rights reserved. No part of this publication may be reproduced or transmitted in any form or by any means without prior written permission of the author, or where appropriate, of the publisher of the article.

*Aut inveniam viam aut faciam*

Hannibal Barca

# Table of Contents

<b>List of Abbreviations</b>	<b>5</b>
<b>Chapter 1</b>	<b>9</b>
General Introduction	
<b>Chapter 2</b>	<b>19</b>
Synthetic Studies with the Brevicidine and Laterocidine Lipopeptide Antibiotics Including Analogues with Enhanced Properties and <i>In Vivo</i> Efficacy	
<b>Chapter 3</b>	<b>67</b>
Synthesis and Structure–Activity Relationship Studies of N-terminal Analogues of the Lipopeptide Antibiotics Brevicidine and Laterocidine	
<b>Chapter 4</b>	<b>83</b>
Linearization of the Brevicidine and Laterocidine Lipopeptides Yields Analogues that Retain Full Antibacterial Activity 81	
<b>Chapter 5</b>	<b>101</b>
Total Synthesis and Structure Assignment of the Relacidine Lipopeptide Antibiotics and Preparation of Analogues with Enhanced Stability	
<b>Chapter 6</b>	<b>129</b>
Summary and Outlook	
<b>Appendices</b>	<b>137</b>
<b>Samenvatting</b>	<b>138</b>
<b>List of publications</b>	<b>145</b>
<b>Curriculum Vitae</b>	<b>146</b>

## List of Abbreviations

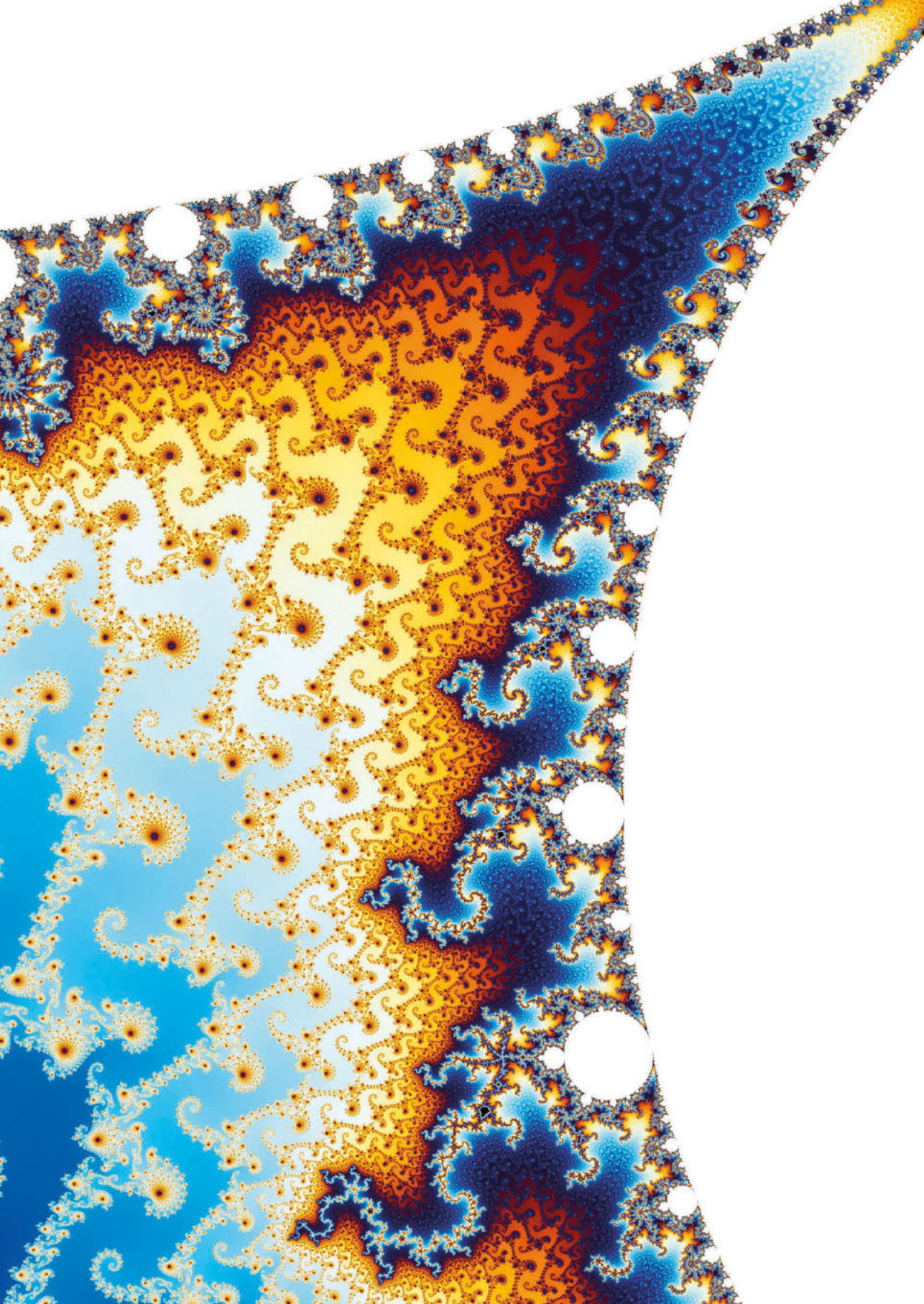
2-CT	2-Chlorotrityl
AA	Amino acid
ACS	American Chemical Society
All	Allyl
Alloc	Allyloxycarbonyl
AMR	Antimicrobial resistance
BGC	Biosynthetic gene cluster
Boc	tert-Butyloxycarbonyl
BOP	Benzotriazol-1-yloxytris(dimethylamino)phosphonium hexafluorophosphate
Brev	Brevicidine
C55-PP	Undecaprenyl pyrophosphate
CFU	Colony forming unit
CLED	Cystine-lactose-electrolyte-deficient
CLSI	Clinical and Standards Laboratory Institute
COVID	Coronavirus disease
DCM	Dichloromethane
DIC	N,N-Diisopropylcarbodiimide
DIPEA	N,N-Diisopropylethylamine
DMAP	4-Dimethylaminopyridine
DMEM	Dulbecco's Modified Eagle Medium
DMF	N,N-Dimethylformamide
DMSO	Dimethylsulfoxide
EDC	1-Ethyl-3-(3-dimethylaminopropyl)carbodiimide
ESKAPE	<i>E. faecium</i> , <i>S. aureus</i> , <i>K. pneumoniae</i> , <i>A. baumannii</i> , <i>P.aeruginosa</i> , and <i>Enterobacter</i> spp.
Fmoc	Fluorenylmethoxycarbonyl
HATU	Hexafluorophosphate azabenzotriazole tetramethyl uronium
HEPA	High-efficiency particulate air
HFIP	Hexafluoro-2-propanol
HMM	Hidden Markov model
HPLC	High-performance liquid chromatography
ICR	Institute of Cancer Research
IM	Intramuscular



Lat	Laterocidine
LB	Luria-Bertani
LC-MS	Liquid chromatography–mass spectrometry
LPS	Lipopolysaccharide
MCR	Mobilized colistin resistance
MHB	Mueller–Hinton broth
MIC	Minimum inhibitory concentration
MOA	Mechanism of action
MTBE	Methyl-tert-butylether
MTT	3-(4,5-dimethylthiazol-2-yl)-2,5-diphenyltetrazolium bromide
NMR	Nuclear magnetic resonance
NRP	Non-ribosomal peptide
NRPS	Non-ribosomal peptide synthase
OD <sub>600</sub>	Optical density at 600 nm
PARAS	Predictive algorithm for resolving A-domain specificity
PBS	Phosphate-buffered saline
PDB	Protein data bank
PK	Pharmacokinetics
PMF	Proton-motive force
RA	Rink amide
RP	Reverse-phase
RT	Room temperature
SAR	Structure-activity relationship
SPPS	Solid-phase peptide chemistry
tBu	tert-Butyl
tBuOH	tert-Butanol
TCA	Trichloroacetic acid
TFA	Trifluoroacetic acid
TIPS	Triisopropyl silane
TOF	Time of flight
TriA <sub>1</sub>	Tridecaptin A <sub>1</sub>
TSB	Tryptic soy broth
UPLC	Ultra-high performance liquid chromatography
UV	Ultraviolet
WHO	World Health Organization

## **Amino Acids**

Ala	Alanine
Asn	Asparagine
Asp	Aspartic acid
Cys	Cysteine
Dab	Diaminobutyric acid
Dap	Diaminopropionic acid
Glu	Glutamic acid
Gly	Glycine
His	Histidine
Ile	Isoleucine
Leu	Leucine
Lys	Lysine
Orn	Ornithine
Phe	Phenylalanine
Ser	Serine
Val	Valine



# **Chapter 1**

## **General Introduction**

## ***History of infectious disease***

At the end of the 19<sup>th</sup> century, Robert Koch definitively established the causative relationship between infectious disease and microbes, or what we now call the germ theory of disease.<sup>1</sup> Prior to Koch's work, the miasma theory was broadly used to explain disease. The word "miasma" comes from ancient Greek "μίασμα" meaning "to soil/to corrupt" and was used to describe a mist of bad air filled with particles from decomposed matter that was believed to cause various illnesses.<sup>2</sup> These particles were thought to spontaneously appear and could not be transmitted from one person to another. Interestingly, the beginnings of germ theory, can be traced back to a much earlier period than that of Koch. In ancient India the physician Sushruta theorized in the *Sushruta Samhita* (Sashruta's Compendium), which some scholars date to around 600 BC, that various infectious diseases were spread through contact.<sup>3</sup> Subsequently, many generations of scholars studied this now widely understood natural phenomenon. For example, the idea that disease could be spread by microbes was first described in ca. 37 BC by the statesman and scholar Marcus Terentius Varro in his book *Rerum Rusticarum Libri III* (Agricultural Topics in Three Books).<sup>4</sup> In this work he warned the reader to avoid swamps as "...there are bred certain minute creatures which cannot be seen by the eyes, but which float in the air and enter the body through the mouth and nose and cause serious diseases."

Many centuries later in 1546 the Italian physician, poet, and scholar Girolamo Fracastoro published *De Contagione et Contagiosis Morbis* (On Contagion and Contagious Diseases) in which he used the term "*seminaria morbi*" or "seeds of disease" to represent unseen particles as causative agents of disease.<sup>5</sup> His work outlined the concept that each disease is caused by different multiplying particles that could be spread from one person to another either by direct contact, soiled linen or air. Another notable mention is the work of Italian physician, naturalist, biologist, and poet Francesco Redi, who famously wrote "*omne vivum ex vivo*" (all life comes from life) and is referred to as the founder of experimental biology. His experiments published in 1668 as *Esperienze intorno alla generazione degl'insetti* (Experiments on the Generation of Insects) disapproved the theory of spontaneous generation of life.<sup>6</sup> At the time it was thought that maggots spontaneously appeared from rotting meat. Redi however showed that maggots would not grow in jars filled with rotting meat that were covered with gauze, while they readily grew in open jars. Later, Louis Pasteur would perform similar experiments, proving that microbes likewise do not generate spontaneously.<sup>7</sup>

It was not until the Dutch microbiologist and microscopist Antonie van Leeuwenhoek developed a method for creating powerful magnifying lenses that it became possible to see and experiment with microbes. He initially called these creatures "*kleine dierkens*" later translated to latin to "*animalculum*" as van Leeuwenhoek only wrote in his native Dutch. He was not particularly enthusiastic to publish his findings as he saw himself more as a businessman than a scientist but was pushed by his friend and famous Dutch physician Reinier de Graaf to publish his findings at the Royal Society in London. While his findings were initially questioned, they were ultimately officially fully acknowledged in 1677 by the Royal Society.<sup>8</sup>

Sometime later in 1861, the Hungarian physician and scientist Ignaz Semmelweis, also called the "savior of mothers" published his book *Die Ätiologie, der Begriff und die Prophylaxe des Kindbettfiebers* (Etiology, Concept and Prophylaxis of Childbed Fever) which drew attention to the importance of sterility in reducing infection in clinical practice.<sup>9</sup> Semmelweis observed

that the doctors ward at the Vienna General Hospital's First Obstetrical Clinic had three times the mortality rate of the midwives' ward due to new mothers acquiring "childbed fever". Based on the observation that doctors were less likely than midwives to wash their hands between visiting patients, in 1847 he proposed the practice of hand washing with chlorinated lime solutions (calcium hypochlorite) which reduced the mortality rate to below 1%. Notably, this advice was not well received by Semmelweis' peers and it took the work of the Scottish surgeon Joseph Lister, inspired by the findings of French chemist and microbiologist Louis Pasteur, to popularize the practice.<sup>10</sup>

While Louis Pasteur is regarded as one of the founders of modern microbiology, he was in fact a true multidisciplinary scientist. Although less popularly known than his microbiological work, Pasteur's investigations with tartaric acid crystallization led to the discovery of optical isomerism and can be considered among his greatest achievements.<sup>11</sup> Pasteur noticed that solutions of tartaric acid from natural sources rotated the plane of polarization of light passing through the solution while tartaric acid made through chemical synthesis did not possess this quality. After crystalizing the substances in the solutions he noticed that in racemic mixtures of tartrates two types of crystals could form that were non-superimposable mirror images of each other. Pasteur linked the optical activity and shape of the crystals to the asymmetric arrangement of the molecules, thus discovering molecular chirality and isomerism. The chemical separation method in which chiral salts can be separated is called Pasteur crystallization to this day. While chemists owe a debt to Pasteur for his foundational contributions to stereochemistry, he is more widely known for his work on microbial fermentation. He was the first to determine that yeast produces alcohol from sugar and that less sugar was fermented under aerobic condition. An effect that is nowadays called the Pasteur effect. He also discovered that micro-organisms were responsible for spoiling beverages and that heating the beverages killed most bacteria and increased their shelf life, a process called pasteurization. His work on the spoiling of beverages led Pasteur to the idea that micro-organism could also infect animals and humans and cause disease.

The many ideas and experiments of scholars throughout the ages contributed to the germ theory of disease. However, it was the experimental methods devised by German physician and microbiologist Robert Koch at the end of the 19th century that made it possible to prove the theory. What made Koch so effective was the combination of his individual discoveries which allowed for a leap in understanding of the natural world. Koch was not only a pioneer in bacterial staining and was the first to use an oil immersion lens and a condenser in microscopy but also pioneered the use solid growth media that made it possible to grow pure bacterial cultures on agar.<sup>12</sup> In 1876 he published "*Die Ätiologie der Milzbrand-Krankheit, Begründet auf die Entwicklungsgeschichte des Bacillus Anthracis*" (The Etiology of Anthrax Disease, Based on the Developmental History of Bacillus Anthracis) in which he described the discovery of *Bacillus anthracis* being the causative agent of anthrax.<sup>13</sup> This work formed the basis for the four Koch postulates that were later formulated by Koch's assistant Friedrich Loeffler. These postulates enabled the determination of the cause of many infectious diseases and state that the same organism must be present in every case of the disease. The organism must be isolated from the patient and grown in a pure culture. When a healthy subject is inoculated by the pure culture it must cause the same disease and finally the same organism must then be isolated from the inoculated subject. Although this might seem simple or obvious to a reader

today it was a huge leap in human understanding at the time and created an opportunity for Koch to discover the causative agent of tuberculosis, *Mycobacterium tuberculosis* which paved the way for the discovery of many more pathogenic bacteria by his students and peers. In 1905 he was awarded the Nobel prize in physiology/medicine for his work on tuberculosis.

## History of antibiotics

Following the discovery that microbes are the causative agents of many infectious diseases, it still took several decades before safe and effective antibiotic treatments were developed and even to this day there exists some ambiguity in what is considered an antibiotic. The origin of the term antibiotic can be traced back to an article of Paul Vuillemin, in which he used the word “*antibiose*” as an antonym to symbiosis to describe the antagonistic effect microbes can have on each other in culture.<sup>14</sup> In this sense, the term antibiotic was originally used specifically for natural products produced by bacteria and fungi with bactericidal or bacteriostatic properties against other bacteria or fungi. Today, however, the term antibiotic is used to describe both naturally occurring and synthetically produced compounds, that exhibit antibacterial activity and are suitable to treat infections *in vivo*.

With the present-day definition in mind, the first antibiotic to be discovered was arsphenamine (Salvarsan, Figure 1). Salvarsan is an organoarsenic compound that was first synthesized by Alfred Bertheim in the laboratory of Paul Ehrlich.<sup>15</sup> It was approved in 1910 as the first effective treatment for syphilis, a sexually transmitted disease caused by the bacterium *Treponema pallidum*. The discovery of Salvarsan was a major milestone in the history of medicine and it paved the way for the development of many other important drugs. The discovery of Salvarsan had a major impact on public health, and it was widely used to treat syphilis in the years following its discovery. However, the drug was not without its problems. Salvarsan had many side effects including rash and liver damage and did not always cure syphilis completely.<sup>16</sup> If discovered today, it would most certainly not be approved for clinical use. It is for this reason that the natural product penicillin is often mentioned as the first antibiotic (Figure 1.).

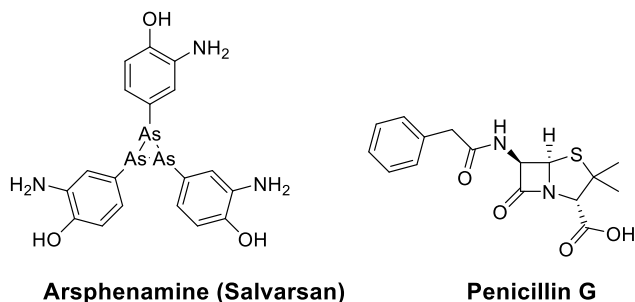


**Figure 1.** Structures of Salvarsan and penicillin G

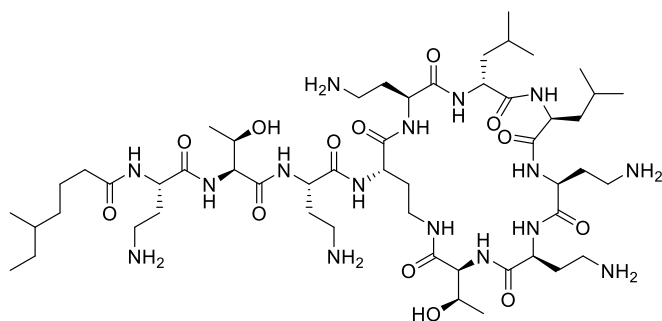
The discovery of penicillin is probably the most well-known drug discovery story of all time. On the third of September 1928 Alexander Fleming came back to his laboratory after a vacation and found a fungal contamination in one of his plates of *Staphylococcus aureus*. He found a

ring around the fungal contamination where the growth of the bacterium was inhibited and now famously remarked “That’s funny”.<sup>17</sup> After growing a pure culture of the fungus he was able to show that it was producing a substance that caused this inhibition, that he later named penicillin. He was not, however, able to purify penicillin nor test its effect against bacterial infections in animals and humans. Fleming’s findings would flounder in relative obscurity until 1939 when Howard Florey and Ernst Chain at Oxford University resumed research on the topic. They were quick to confirm Fleming’s findings and with the help of Norman Heatley they were able to purify enough penicillin to perform the first animal experiments in the early 1940s.<sup>18</sup> It wasn’t until February 1941 when they were able to produce enough penicillin to begin human trials. Charles Fletcher, a young doctor from Radcliffe Infirmary in Oxford was recruited to perform the clinical trial and the first patient Albert Alexander, a 43-year-old policeman suffering from sepsis, was treated on 12 February 1941.<sup>19</sup> Alexander was injected with penicillin and within a day his health greatly improved. He was injected regularly with penicillin over the next four days at which point the supply of the drug was exhausted. In desperation, Florey’s team tried to extract penicillin from Alexander’s urine and reinject it, however this was not sufficient and due to a lack of material Alexander ultimately succumbed to the infection.<sup>20</sup> In the months that followed, a great effort was made to increase penicillin production, which led to the first fully successful treatment of several other patients and penicillin’s reputation as a new miracle drug. A massive collaborative effort was subsequently undertaken to mass produce the drug by the British and Americans that finally led to the allies landing in Normandy on D-day in 1944 with a million doses of penicillin.

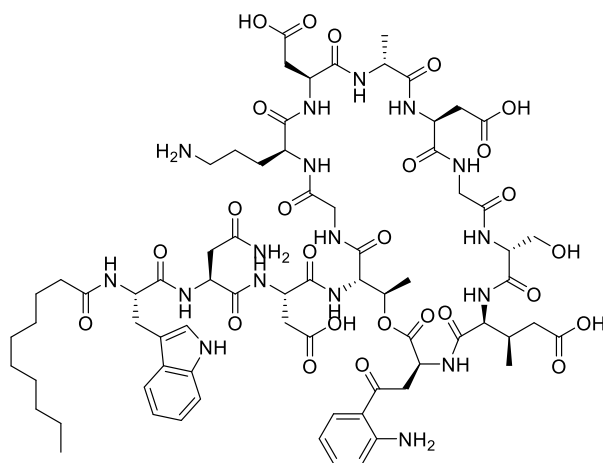
The significance of natural products and their derivatives in medicine has been extensively proven not only through their direct application in clinical settings, but also as tools to uncover biological pathways and targets for pharmacological intervention. After the successful development of penicillin, there was a heightened interest in discovering new antibiotics and other bioactive compounds from nature, as demonstrated by the surge in their discovery following World War II. Many of these agents were subsequently developed into drugs to treat a range of diseases, including bacterial infections and cancer. The work in this thesis describes the modern continuation of such efforts and is concerned with synthetic studies on a specific class of natural products, lipopeptide antibiotics.

At present there are two clinically relevant classes of lipopeptide antibiotics: the polymyxins and daptomycin (Figure 2). In literature one often finds that the polymyxins are considered as a separate antibiotic class and that daptomycin falls within the lipopeptide class, causing confusion. From a structural viewpoint however both should be viewed as lipopeptides. While daptomycin is used to treat Gram-positive infections and the polymyxins are used to treat Gram-negative infections, both classes of lipopeptides exert their activity through interaction with the bacterial cell wall. This has proven an effective strategy in the chemical warfare between the bacteria that produce these antibiotics and their surrounding environment. Lipopeptides often do not target a protein target and as such, resistance development through point mutation is less likely. Furthermore, not having to cross the outer membrane makes one of the common resistance strategies used by microorganisms, namely efflux pumps, irrelevant. On the other hand, the membrane-disrupting properties that often underline the mechanism of action of lipopeptides can sometimes cause off target toxicity by damaging mammalian cell membranes as well. Moreover the large size and physicochemical properties of





**Polymyxin E (Colistin)**



**Daptomycin (Cubicin)**

**Figure 2.** Structures of polymyxin E and daptomycin

lipopeptides, as well as their potential for inactivation by proteases, forms a challenge in their development as new pharmaceuticals.

In part it is also the success of other antibiotics such as penicillin that slowed down the development of new anti-infective drugs. The need for superiority trials in order to get a new drug approved and the general low cost of treatment with currently marketed alternatives, makes antibiotics development a financially dangerous endeavor. Nevertheless, it is still important to study new classes of antibiotics as our society is currently losing the arms race against pathogenic bacteria, which could lead to a post-antibiotic era and future deaths of millions of people if nothing is done to tip the scales in our favor.

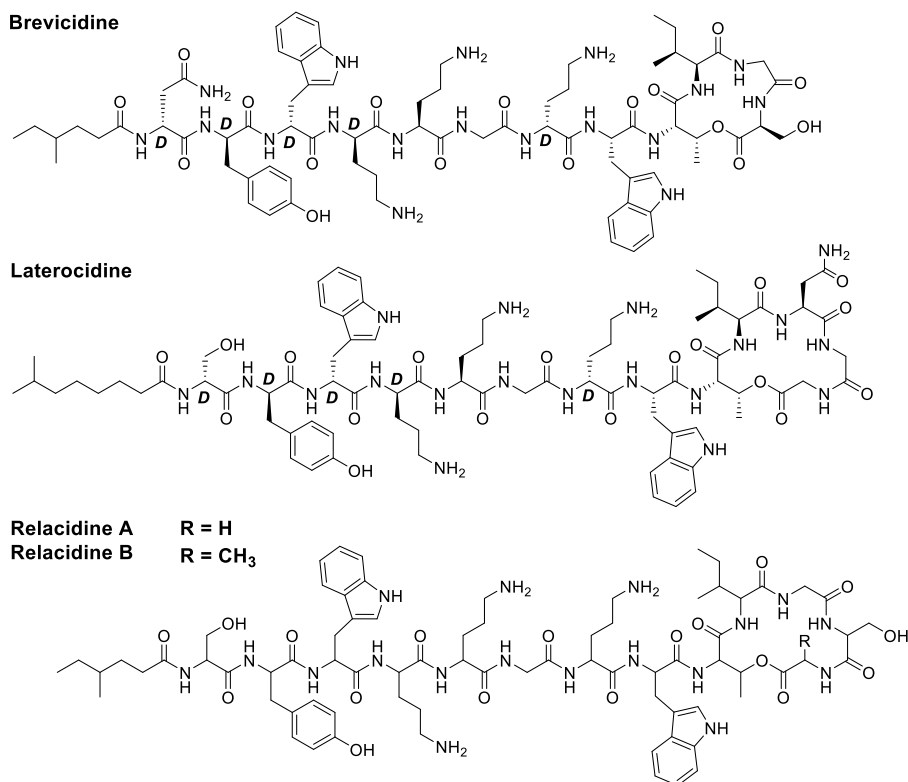


**Figure 3.** Structures of brevicidine, laterocidine and relacidine A and B

### *Within this thesis*

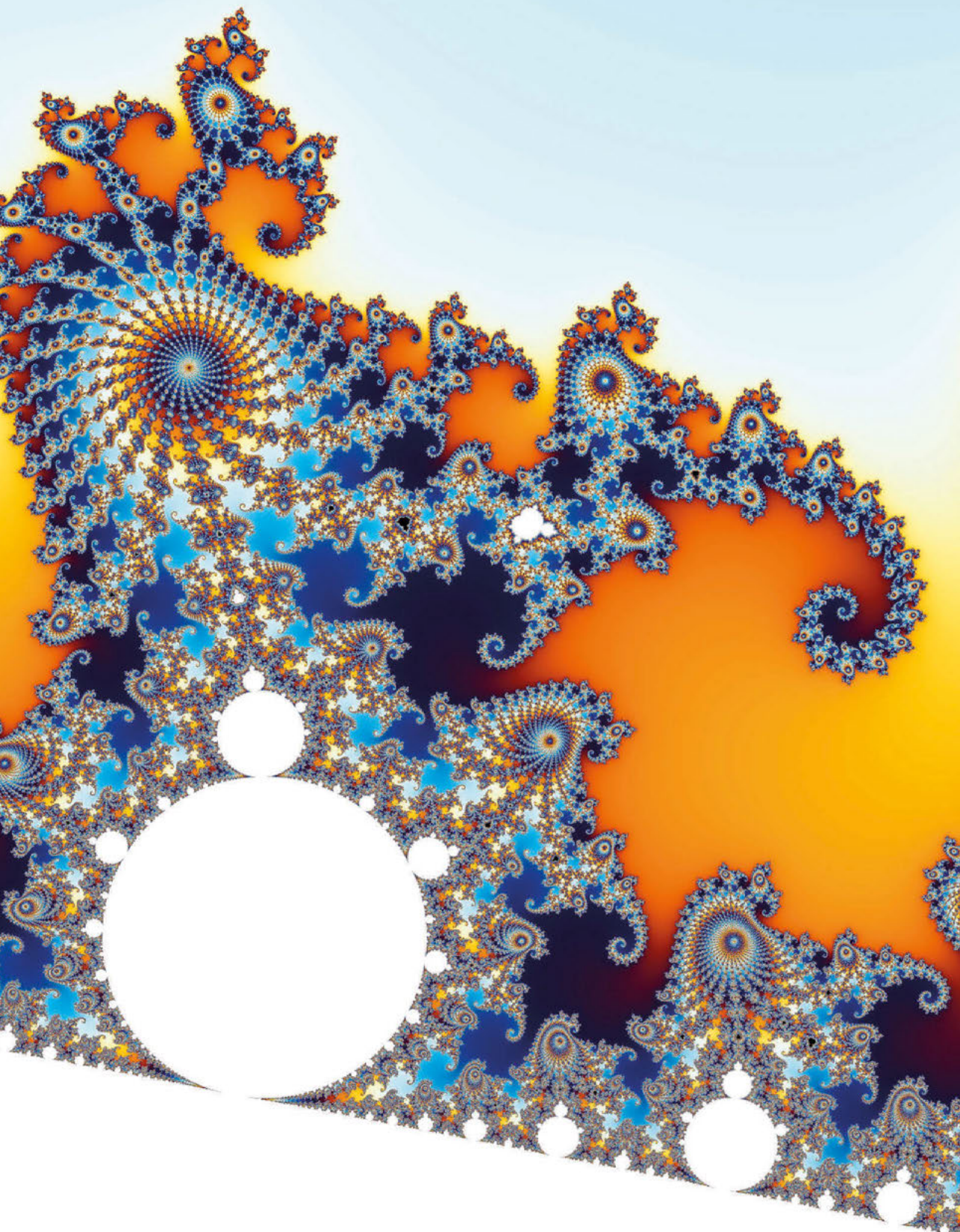
This thesis describes the evaluation of novel natural products with antibacterial activity enabled by total chemical synthesis. In **Chapter 2** the first total synthesis of the two recently discovered lipopeptide antibiotics, brevicidine and laterocidine (Figure 3), is described. These natural products structurally resemble the polymyxins but unlike the polymyxins are active against Gram-negative bacterial strains carrying the *mcr-1* resistance gene, responsible for polymyxin resistance. The methodology described in this chapter made it possible to produce enough material to gain more insight into the activity and toxicity profile of this class of antibiotics. The modular approach of the solid-phase synthesis also allowed for convenient access to structural analogues of brevicidine and laterocidine that showed increased stability in human serum. Finally one of the laterocidine analogues was also shown to be active *in vivo* in a mouse thigh infection model. **Chapter 3** describes structure-activity relationship studies of N-terminal analogues of brevicidine and laterocidine that were made possible by the synthetic methodology described in the previous chapter. Substitution of the branched lipids found in the natural products with a saturated decanoyl tail did not negatively impact antibacterial activity. However, substitution by either shorter or longer lipids compared to the lipids found in the natural products was found to have a negative effect on *in vitro* activity. In addition, a longer lipid chain was found to correlate with increased hemolytic activity. **Chapter**

4 describes the discovery of linear laterocidine and brevicidine analogues that retain activity against Gram-negative bacteria. Previously it was thought that the peptide macrocycles found in laterocidine and brevicidine were essential for their activity. However, amidation of the C-terminus and substitution of the threonine on position 9 led to active compounds that are synthesized more readily without a visible increase in hemolytic activity. The results in this chapter raise the question if such a linearization and amidation strategy could be employed more generally for other cyclic non-ribosomal peptides. **Chapter 5** describes the bioinformatics guided total synthesis of the naturally occurring lipopeptides relacidine A and B (Figure 3). The relacidines are non-ribosomal peptide antibiotics that structurally resemble brevicidine and laterocidine, described in chapters 2-4. In contrast to brevicidine and laterocidine the stereochemistry of the relacidines was not fully assigned in the original publication that reported their discovery. With the use of genome mining, fermentation, and total synthesis we were able to achieve the full stereochemical characterization of these compounds as well as to study their activity and toxicity profile. An amide analogue of relacidine A was also shown to be active *in vivo* in a *Galleria mellonella* larvae infection model. Finally, **Chapter 6** summarizes the findings in this thesis and reflects on the potential applications and future prospects for the lipopeptides here studied.

## References

- (1) Münch, R. Robert Koch. *Microbes Infect* **2003**, 5 (1), 69–74. [https://doi.org/10.1016/S1286-4579\(02\)00053-9](https://doi.org/10.1016/S1286-4579(02)00053-9).
- (2) Malouin, P.-J. Miasma. *Encyclopedia of Diderot & d'Alembert - Collaborative Translation Project* **2004**.
- (3) Tipton, C. M. Susruta of India, an Unrecognized Contributor to the History of Exercise Physiology. *J Appl Physiol* **2008**, 104 (6), 1553–1556.
- (4) Varro, M. T. Rerum Rusticarum de Agri Cultura. *Documento digital disponible en: <http://www.readme.it/libri/2/2048022.shtml> (Fecha de acceso: octubre de 2020)* **1971**.
- (5) Leake, C. D. Hieronymi Fracastorii De Contagione et Contagiosis Morbis et Eorum Curatione, Libri III. JSTOR 1931.
- (6) Roncalli Amici, R. The History of Italian Parasitology. *Vet Parasitol* **2001**, 98 (1), 3–30. [https://doi.org/https://doi.org/10.1016/S0304-4017\(01\)00420-4](https://doi.org/https://doi.org/10.1016/S0304-4017(01)00420-4).
- (7) Roll-Hansen, N. Experimental Method and Spontaneous Generation: The Controversy between Pasteur and Pouchet, 1859–64. *J Hist Med Allied Sci* **1979**, 34 (3), 273–292.
- (8) Porter, J. R. Antony van Leeuwenhoek: Tercentenary of His Discovery of Bacteria. *Bacteriol Rev* **1976**, 40 (2), 260–269.
- (9) Semmelweis, I. F. *The Etiology, Concept, and Prophylaxis of Childbed Fever*; Univ of Wisconsin Press, **1983**.
- (10) Pitt, D.; Aubin, J.-M. Joseph Lister: Father of Modern Surgery. *Canadian Journal of Surgery* **2012**, 55 (5), E8.
- (11) Bordenave, G. Louis Pasteur (1822–1895). *Microbes Infect* **2003**, 5 (6), 553–560. [https://doi.org/10.1016/S1286-4579\(03\)00075-3](https://doi.org/10.1016/S1286-4579(03)00075-3).
- (12) Blevins, S. M.; Bronze, M. S. Robert Koch and the 'Golden Age' of Bacteriology. *International Journal of Infectious Diseases* **2010**, 14 (9), e744–e751. <https://doi.org/10.1016/j.ijid.2009.12.003>.
- (13) Koch, R. Die Ätiologie Der Milzbrand-Krankheit, Begründet Auf Die Entwicklungsgeschichte Des Bacillus Anthracis. **2010**.
- (14) Vuillemin, P. J. Antibiose et Symbiose. *Assoc. Franc. pour l'Avanc. Sci.* **1890**, 2, 525–543.
- (15) Schwartz, R. S. Paul Ehrlich's Magic Bullets. *N Engl J Med* **2004**, 350 (11), 1079–1080. <https://doi.org/10.1056/NEJMP048021>.
- (16) Kaufmann, S. H. E. Paul Ehrlich: Founder of Chemotherapy. *Nature Reviews Drug Discovery* **2008** 7:5 2008, 7 (5), 373–373. <https://doi.org/10.1038/nrd2582>.

- (17) Ligon, B. L. Penicillin: Its Discovery and Early Development. *Semin Pediatr Infect Dis* **2004**, *15* (1), 52–57. <https://doi.org/10.1053/J.SPID.2004.02.001>.
- (18) Bennett, J. W.; Chung, K. T. Alexander Fleming and the Discovery of Penicillin. *Adv Appl Microbiol* **2001**, *49*, 163–184. [https://doi.org/10.1016/S0065-2164\(01\)49013-7](https://doi.org/10.1016/S0065-2164(01)49013-7).
- (19) Aldridge, S.; Parascandola, J.; Sturchio, J. L. *The Discovery and Development of Penicillin 1928-1945: The Alexander Fleming Laboratory Museum, London, UK, November 19, 1999 : An International Historic Chemical Landmark*; American Chemical Society, **1999**.
- (20) Abraham, E. P.; Chain, E.; Fletcher, C. M.; Gardner, A. D.; Heatley, N. G.; Jennings, M. A.; Florey, H. W. Further Observations on Penicillin. *The Lancet* **1941**, *238* (6155), 177–189.



## Chapter 2

# Synthetic Studies with the Brevicidine and Laterocidine Lipopeptide Antibiotics Including Analogues with Enhanced Properties and *In Vivo* Efficacy

### **Abstract**

Brevicidine and laterocidine are two recently discovered lipopeptide antibiotics with promising antibacterial activity. Possessing a macrocyclic core, multiple positive charges, and a lipidated N-terminus, these lipopeptides exhibit potent and selective activity against Gram-negative pathogens, including polymyxin-resistant isolates. Given the low amounts of brevicidine and laterocidine accessible by fermentation of the producing microorganisms, synthetic routes to these lipopeptides present an attractive alternative. We here report the convenient solid-phase syntheses of both brevicidine and laterocidine and confirm their potent anti-Gram-negative activities. The synthetic routes developed also provide convenient access to novel structural analogues of both brevicidine and laterocidine that display improved hydrolytic stability while maintaining potent antibacterial activity in both *in vitro* assays and *in vivo* infection models.

### **Parts of this chapter have been published in Chemical Science:**

Al Ayed, K.\*; Ballantine, R. D.\*; Hoekstra, M.; Bann, S. J.; Wesseling, C. M. J.; Bakker, A. T.; Zhong, Z.; Li, Y.-X.; Bröchle, N. C.; Van Der Stelt, M.; Cochrane, S. A.; Martin, N. I. Synthetic Studies with the Brevicidine and Laterocidine Lipopeptide Antibiotics Including Analogues with Enhanced Properties and *in Vivo* Efficacy. *Chem. Sci.* **2022**, 13 (12), 3563–3570. <https://doi.org/10.1039/D2SC00143H>

### **Parts of the data in this chapter are part of a patent:**

"Antibiotic natural product analogues"; Cochrane, S.A.; Ballantine, R. D.; Martin, N. I.; Al Ayed, K.; Hoekstra, M.; Zamarride Losada, S.D.; Priority Date: 28 January 2021; Published: 4 August 2022; WO2022162332A1

\*Authors contributed equally

## Introduction

The accelerated appearance of multi-drug resistant bacterial pathogens has led to the worrying speculation that society may soon face a “post-antibiotic” era.<sup>1-3</sup> The gravity of the antimicrobial resistance (AMR) crisis is most clearly reflected by the spread of the “ESKAPE” pathogens (*E. faecium*, *S. aureus*, *K. pneumoniae*, *A. baumannii*, *P. aeruginosa*, and *Enterobacter* species), a group of organisms that are increasingly difficult or impossible to treat with conventional antibiotics. Globally, deaths due to infections with drug-resistant bacteria are nearing one million per year.<sup>4</sup> Even more worrying are recent projections suggesting that by the year 2050 the number of AMR associated deaths will grow to a staggering ten million per year.<sup>4</sup>

To prioritize the greatest threats currently associated with AMR, the World Health Organization (WHO) recently published its list of priority pathogens.<sup>5</sup> Among these pathogens, it is exclusively the Gram-negative members of the ESKAPE family that are labeled as “critical”, the highest threat level on the WHO list. This is due to the rapidly accelerating rise in antibiotic resistance among *Acinetobacter*, *Pseudomonas*, and various *Enterobacteriaceae* (including *Klebsiella* and *Escherichia coli*) causing severe and often deadly bloodstream and pulmonary infections. The AMR threat underscores the importance of pursuing new strategies in discovering and developing the antibiotics of the future.

Using a biosynthetic gene cluster mining strategy, Li and co-workers recently reported the discovery of a promising new class of macrocyclic lipopeptides termed the brevicidines and laterocidines (Figure 1).<sup>6</sup> Produced by strains of *Brevibacillus laterosporus*, brevicidine and laterocidine specifically kill all Gram-negative members of the ESKAPE family, including drug-resistant strains. The antibacterial activity of these lipopeptides is promising, with MIC values comparable to the polymyxins, the only class of lipopeptides presently used in the clinical treatment of serious Gram-negative infections. Of particular note is the finding that brevicidine and laterocidine effectively kill pathogenic strains featuring the recently reported MCR-type polymyxin resistance mechanism.<sup>6</sup> Furthermore, the initial report describing the discovery of brevicidine and laterocidine also indicates that these lipopeptide antibiotics show little propensity to induce resistance and have low toxicity towards mammalian cells.<sup>6</sup>

While brevicidine and laterocidine are promising new anti-Gram-negative antibiotics, both compounds are difficult to isolate in significant quantities from natural sources, presenting a major obstacle to investigate their full potential. Brevicidine and laterocidine can be obtained by fermentation of the producing microorganisms, however this labour-intensive process provides limited amounts of material (sub-milligram-per-litre yields in the case of laterocidine).<sup>6</sup> For this reason, reliable synthetic routes to these lipopeptides present an attractive alternative as a means of providing larger amounts of material for both clinical evaluation and mechanistic studies.<sup>7,8</sup> Herein we report the total syntheses of brevicidine and laterocidine by solid-phase peptide synthesis (SPPS).<sup>9</sup> The synthetic compounds and natural products have identical <sup>1</sup>H-NMR spectra, RP-HPLC retention times, and antibacterial activities. Using the same synthetic approach, the enantiomers of brevicidine and laterocidine were also prepared to probe the role of stereochemistry in the antibacterial mechanism of these unique lipopeptides. Furthermore, novel analogues wherein the ester moiety of the peptide macrocycle was replaced by an amide linkage, were prepared and their stability and antibacterial activities assessed both *in vitro* and *in vivo*.

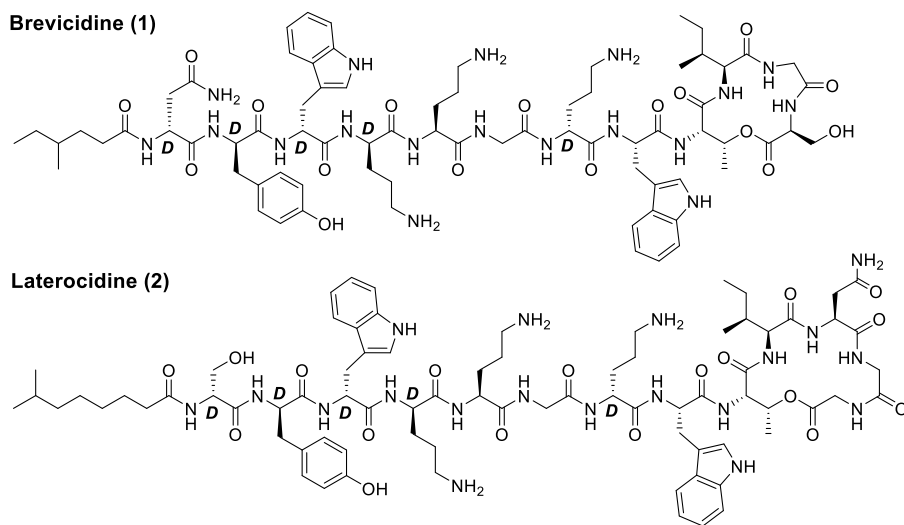


**Figure 1.** Structures of brevicidine (1) and laterocidine (2)

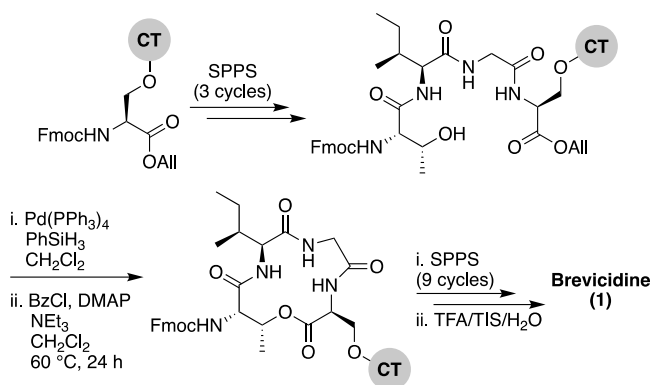
## Results and discussion

Brevicidine and laterocidine share several structural features, including a C-terminal ester-linked macrocycle of 4- or 5- amino acids, a number of conserved residues including three positively charged ornithines, and a lipidated N-terminus. It was previously demonstrated that the macrocycle is necessary for antibacterial activity of these peptides.<sup>6</sup> Key to the syntheses of both brevicidine and laterocidine was therefore development of a reliable approach for the introduction of the macrocycle formed via an ester linkage between the C-terminal carboxylate and the corresponding threonine side chain hydroxyl group. For both brevicidine and laterocidine, convenient solid phase approaches were developed that allowed on-resin formation of the key macrocycle and installation of all other amino acids.

In approaching the synthesis of brevicidine, we initially investigated a strategy starting from Gly11 loaded on 2-chlorotrityl resin (CT) to generate a linear peptide that would subsequently be cyclized in solution. We envisaged installation of the required Thr9-Ser12 linkage as a preformed, ester-linked dipeptide. However, while incorporation of the Thr9-Ser12 unit was achieved, further elongation of the peptide failed due to an O→N acyl shift that occurred upon removal of the Thr9 Fmoc group (see supporting Scheme S1). As an alternative, we next examined formation of the macrocycle at an earlier stage to assess whether the ester linkage might be more stable when contained in the more conformationally restricted ring system. To implement this approach, Fmoc-Ser-OAll was loaded on to CT resin via its free side-chain hydroxyl group. Notably, the initial conditions used (1 h, RT) resulted in a lower loading than required (0.07 mmol/g), so the reaction time was extended to 24 h along with heating at 45 °C, resulting in an improved loading of 0.13 mmol/g. Resin-bound Fmoc-Ser-OAll was then extended to the tetrapeptide using standard Fmoc-SPPS (Scheme 1). At this stage, the C-terminal allyl ester was cleanly removed on resin using Pd(PPh<sub>3</sub>)<sub>4</sub>/PhSiH<sub>3</sub> in CH<sub>2</sub>Cl<sub>2</sub>. Subsequent closure of the macrolactone was then investigated using different coupling



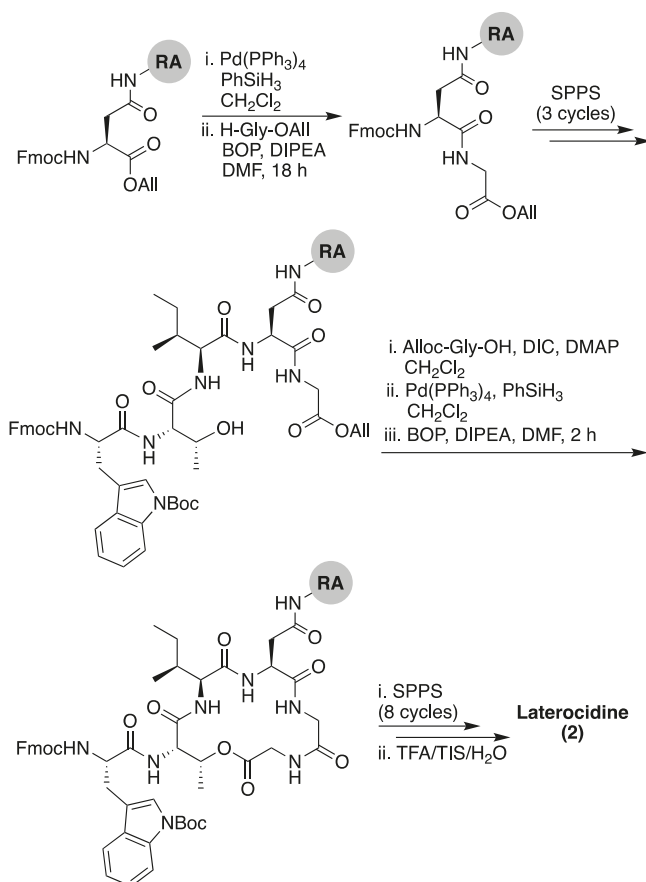
conditions. Cyclization of the on-resin tetrapeptide proved to be refractory to both the use of 1-ethyl-3-(3-dimethylaminopropyl) carbodiimide (EDC) and diisopropylcarbodiimide (DIC), with only starting material being obtained after 48 h. To circumvent this lack of reactivity, we next attempted a modified Yamaguchi esterification, utilizing benzoyl chloride as the coupling reagent, along with a 24 h reaction time run at RT. Although only a small amount of the desired cyclic product was obtained using these conditions, increasing the reaction temperature to 60 °C resulted in near complete conversion. Building from the successful formation of the resin-bound tetrapeptide macrolactone, all that remained was to extend the peptide from the N-terminal threonine residue with SPPS. It was thought best to proceed with caution at the initial Fmoc deprotection to avoid unwanted *O*→*N* acyl migration. Therefore, less aggressive Fmoc deprotection conditions (10% piperidine in DMF) were used in the first deprotection. Gratifyingly, we did not detect any *O*→*N* acyl migration, even using standard Fmoc deprotection conditions, validating our hypothesis that preforming the C-terminal macrocycle would overcome this issue. The remainder of the peptide was constructed without incident along with coupling of the N-terminal 4-methylhexanoic acid. Following global deprotection and resin cleavage and purification by RP-HPLC, synthetic brevicidine was obtained in an overall yield of 9% over 28 steps.



**Scheme 1.** Total SPPS of brevicidine (1). CT = 2-chlorotrityl resin.

The synthetic strategy initially pursued for the preparation of laterocidine was inspired by the successful route developed for brevicidine (see supporting Scheme S2). Unfortunately, formation of the macrolactone proved refractory towards a variety of conditions, including the modified Yamaguchi esterification, with all failing to provide the desired product in appreciable yield. We ascribe this difficulty in ester formation to the larger five-amino-acid macrocycle found in laterocidine versus the four-amino-acid ring found in brevicidine. As an alternative, we next investigated the possibility of closing the macrocycle via amide bond formation between Gly12 and Gly13 (Scheme 2). Following allyl ester cleavage of Fmoc-Asp-OAll loaded Rink amide (RA) resin, an allyl ester protected Gly was coupled after which the peptide was built out to Trp8. The ester linkage between the free Thr9 side chain hydroxyl and the Gly13 C-terminal carboxylate was successfully introduced by coupling Alloc-Gly-OH using an on-resin Steglich esterification approach inspired by the Albericio group's synthesis

of pipecolidepsin A.<sup>10</sup> Following removal of the allyl and Alloc protecting groups, a BOP/DIPEA mediated macrolactamization resulted in the clean formation of the macrocyclic product. From there the peptide was completed using standard Fmoc-SPPS conditions, including N-terminal lipidation with isopelargonic acid. Following cleavage from resin and global deprotection, the crude lipopeptide was subsequently purified using RP-HPLC, yielding laterocidine in 2% purified yield over 29 steps.



**Scheme 2.** Total SPPS of laterocidine (2). RA = Rink amide resin.

Our route to brevicidine and laterocidine was originally disclosed in preprint form (uploaded to ChemRxiv on 10 Jan 2021).<sup>9</sup> Subsequently, Hermant and co-workers reported a different synthetic strategy also providing access brevicidine and laterocidine.<sup>11</sup> As described above, our syntheses are performed entirely on solid support, wherein a side-chain residue is immobilized (Ser 12 for brevicidine and Asn11 for laterocidine) allowing for on resin formation of the peptide macrocycle. Hermant and co-workers opted for an alternate approach combining solid-phase and solution phase synthesis, wherein linear peptide precursors were assembled on resin followed by macrolactamization in solution.

To confirm the equivalency of the synthetic and natural lipopeptides, their  $^1\text{H-NMR}$  spectra were compared with published data for the natural products, revealing them to be indistinguishable (Figure 2, also see supporting Figures S1-2). In addition, LC-MS/MS analysis of the synthetic lipopeptides and comparison to the natural products further verified their identity (see experimental methods Figure 5). Antibacterial assays were also performed against a range of Gram-negative bacteria, which confirmed that synthetic brevicidine and laterocidine possess the same activity profile as the natural products (Table 1). To confirm that the antibacterial activity of brevicidine and laterocidine is intrinsically dependent on the chirality of the molecules, we synthesized the enantiomeric forms of both lipopeptides. The syntheses of *ent*-brevicidine (**ent-1**) and *ent*-laterocidine (**ent-2**) were achieved by following the same routes developed for the natural lipopeptides, but employing the corresponding mirror image amino acid building blocks (see supporting Schemes S3 and S4). Of note, similar mirror-image strategies have been used to characterize the stereochemical aspects in the antibacterial mechanisms of other peptide antibiotics.<sup>12-16</sup> In cases where an achiral target is implicated, the enantiomeric peptide antibiotic typically shows activity on par with the natural product, as in the case of bacitracin, which targets undecaprenyl pyrophosphate (C55-PP),<sup>12</sup> and laspartomycin, which targets undecaprenyl phosphate (C55-P).<sup>13</sup> Conversely, in the case of tridecaptin A1, which targets the chiral cell wall precursor lipid II,<sup>14</sup> thanatin, which targets the LptA and LptD proteins involved in LPS biosynthesis,<sup>15</sup> and daptomycin, which targets phosphatidylglycerol,<sup>16</sup> the activities of the corresponding enantiomers is significantly reduced. In their initial investigations with brevicidine and laterocidine, Li and co-workers found that addition of exogenous lipopolysaccharides (LPS) strongly antagonized the activity of both peptides, suggesting an interaction with LPS as part of the mechanism of action.<sup>6</sup> Given the inherent chirality of LPS, we hypothesized that *ent*-brevicidine and *ent*-laterocidine might exhibit decreased antibacterial activities relative to the natural products in the event that stereochemically defined binding interactions with LPS, rather than nonspecific electrostatic interactions, are central to the working mechanism of the lipopeptides. As confirmation of this hypothesis, the antibacterial activities of *ent*-brevicidine and *ent*-laterocidine were found

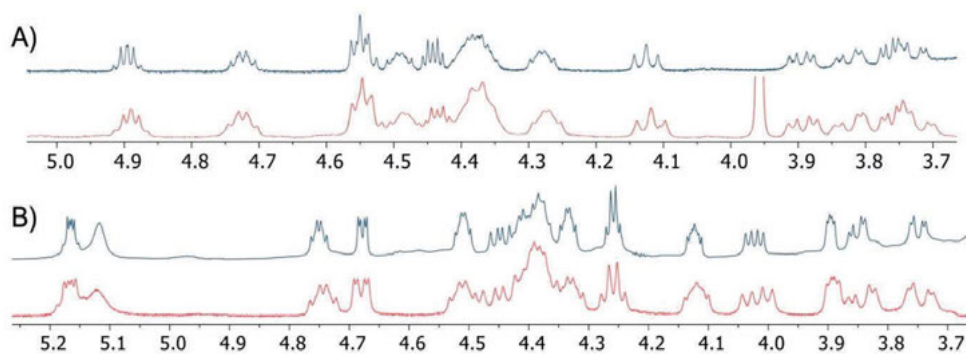


**Figure 2.** Overlaid portions of  $^1\text{H-NMR}$  spectra obtained for synthetic lipopeptides (blue traces) and previously published spectra (red traces) corresponding to: A) brevicidine (**1**) and B) laterocidine (**2**). The peak at ca. 3.96 ppm in the published spectrum of brevicidine is attributed to an impurity not present in the synthetic material. Spectra recorded in  $\text{DMSO-d}_6$  at RT.

to be consistently lower than the natural products, with the MIC values ranging from 8- to 32-fold higher (Table 1). Interestingly, the antibacterial activities of both laterocidine and *ent*-laterocidine were found to be antagonized upon addition of LPS (see experimental methods Figure 6). In the presence of LPS, the activities of laterocidine and *ent*-laterocidine decrease by 8-fold or more, indicating that the interaction with LPS may be driven by nonspecific electrostatic interactions. This finding suggest another chiral biomolecular target might be involved in the mechanism of action associated with these lipopeptides. Studies are underway to identify this target.

To probe the role of the Thr9 side chain methyl group on the conformational requirements of the brevicidine and laterocidine macrocycles, analogues were synthesized in which the Thr9 residue was substituted for Ser (Figure 3). The synthetic route used in preparing Ser9 analogues 3 and 4 was essentially the same as for the natural products (see supporting Schemes S5 and S6), although it was found that more strictly anhydrous conditions were necessary to prevent product degradation during the cyclization step. The antibacterial activities of the Ser9 analogues were similar to the natural products, suggesting the  $\beta$ -methyl group in Thr9 does not play a crucial role in dictating the biologically active conformation of either peptide.

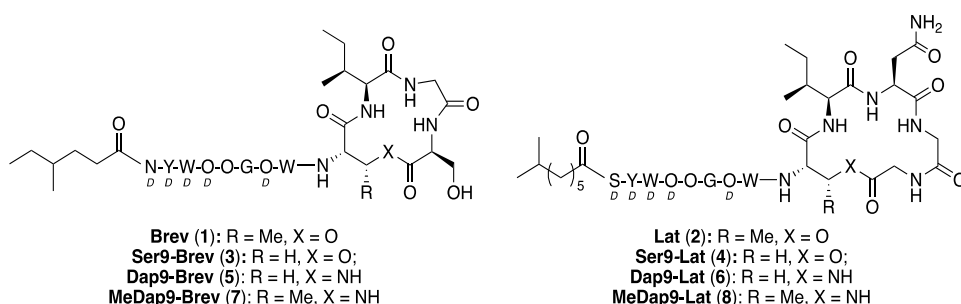


**Figure 3.** Brevicidine and laterocidine analogues containing modified macrocycles. Non-ring amino acids shown as one-letter codes. D-amino acids labelled D.

We next explored the effect of replacing the ester linkage between the Thr9 side chain and the C-terminus with the corresponding amide. For several macrocyclic depsipeptide antibiotics, it has been shown that such amide for ester substitutions can have a positive effect on hydrolytic stability, as in the case of analogues of ramoplanin,<sup>17</sup> fusaricidin,<sup>18</sup> daptomycin,<sup>19</sup> and fengycin.<sup>20</sup> Additionally, from a synthetic perspective, macrocyclic ring closure via formation of an amide linkage can be more facile than formation of the corresponding macrolactone due to the enhanced reactivity of amines over alcohols. To this end, amide analogues of brevicidine and laterocidine were prepared, and their hydrolytic stability and antibacterial activities assessed. For both lipopeptides, we examined the effect of replacing Thr9 with either (*S*)-2,3-diaminopropanoic acid (Dap) or (2*S*, 3*R*)-2,3-diaminobutanoic acid (MeDap) to yield analogues 5-8 (Figure 3). The synthesis of Dap9-Brev (5) started from CT resin loaded with Fmoc-Ser-OAll via its side-chain hydroxyl group (Scheme 3). Iterative Fmoc-SPPS was then used to construct the linear protected on-resin tetrapeptide incorporating Fmoc-

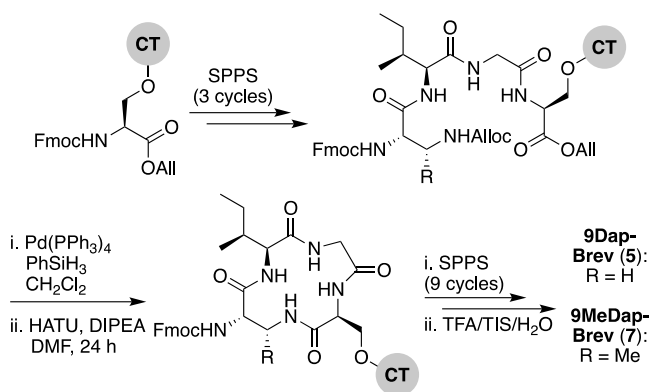
**Table 1.** *In vitro* minimum inhibitory concentrations (MICs) of peptide analogues determined using microbroth-dilution assays

	Brev (1)	ent-Brev (ent-1)	Ser9-Brev (3)	Dap9-Brev (5)	MeDap9-Brev (7)	Lat (2)	ent-Lat (ent-2)	Ser9-Lat (4)	Dap9-Lat (6)	MeDap9-Lat (8)	Col	PolyB
<i>Ec</i> ATCC 25922	1-2	16	4	8-16	16	1	8	0.5	1	1	0.25-0.5	0.5
<i>Ec</i> ATCC 25922 MCR-1	2	16	4	16	8	2	8-16	0.5	1-2	1	2-4	2-4
<i>Ec</i> MCR-1	1-2	16	2	8-16	8	0.5	8-16	0.5	1	0.5	2-4	2-4
<i>Ec</i> EQAS MCR-2	2	16-32	4-8	8-16	8-16	1	8-16	0.5-1	1	0.5	4	4
<i>Kp</i> ATCC 11228	1-2	32	2	16-32	8	2	16	1-2	2	1-2	<0.25	<0.25
<i>Kp</i> ATCC 13883	1	32	2	32	8	1	16	1-2	2	1-2	0.25	0.25
<i>Kp</i> 2048	1-2	32	4	16-32	8-16	2	16	2	2	2	0.5-1	0.5-1
<i>Kp</i> JS-123	1	8	2	8	4-8	0.5	4	0.5	0.5	0.5	<0.25	<0.25
<i>Ab</i> ATCC 17961	2-4	32	0.5-1	4	8-16	0.5	4	4	4	2	<0.25	<0.25
<i>Ab</i> ATCC 17978	4	16-32	2	16	16	0.5	4	2	4	2	<0.25	<0.25
<i>Ab</i> 2018-006	4	8-16	2	8	16	2	4	4	4	4	<0.25	<0.25
<i>Ab</i> MDR	4	16	1-2	8	16	1	4-8	2	4	4	<0.25	<0.25
<i>Pa</i> ATCC 27853	≤0.5	16	1	8	2-4	≤0.5	8	0.5-1	0.5-1	0.5	<0.25	<0.25
<i>Pa</i> PAO1	2	32	2-4	16-32	4	1	16	2	1-2	2	0.25-0.5	0.25-0.5
<i>Pa</i> NRZ-03961	2	32	4	16-32	8	1-2	16	1-2	2	2	0.25-0.5	0.25-0.5
<i>Pa</i> M-120	2-4	16	2	16	4	1	16	1	1-2	1	<0.25	<0.25
<i>Sa</i> USA300	64	>64	>64	>64	>64	64	64	>64	>64	32	>64	64

*Ec* = *E. coli*, *Kp* = *K. pneumoniae*, *Ab* = *A. baumannii*, *Sa* = *S. aureus*, Col = colistin, PolyB = polymyxin B. MICs reported in µg/mL.

Dap(Alloc)-OH. Both the allyl and Alloc groups were removed in a single deprotection with Pd(PPh<sub>3</sub>)<sub>4</sub>/PhSiH<sub>3</sub> in CH<sub>2</sub>Cl<sub>2</sub>. With the amine of Dap9 and the C-terminal carboxylic acid of the peptide liberated, an overnight macrolactamization was effected using HATU/DIPEA. Fmoc-SPPS was continued to complete the linear peptide backbone, followed by capping with 4-methylhexanoic acid. Finally, a global cleavage of the peptide from resin and subsequent purification by RP-HPLC yielded Dap9-Brev (5) in a 13% yield over 28 steps. The synthesis of the MeDap9-Brev (7) followed a similar strategy, with the exception that the corresponding Fmoc-MeDap(Alloc)-OH building block was incorporated at position 9. The antibacterial activities of brevicidine amide analogues 5 and 7 were evaluated, which in both cases revealed a significant loss of activity relative to brevicidine itself (Table 1). This reduced activity may be due to a loss of flexibility in the brevicidine macrocycle, caused by the ester to amide substitution preventing it from accessing its fully active conformation. In addition, the serum stability of Dap9-Brev (5) was assessed, revealing it to be much more stable than brevicidine

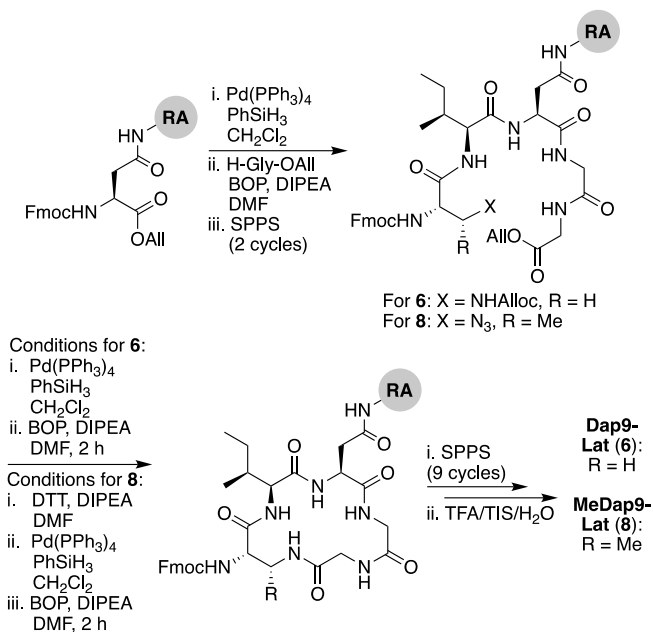
(see experimental methods Figure 7). Dap9-Lat (**6**) was prepared from Fmoc-Asp-OAll loaded Rink amide resin (Scheme 4). Treatment with  $\text{Pd}(\text{PPh}_3)_4/\text{PhSiH}_3$  in  $\text{CH}_2\text{Cl}_2$ , followed by activation and coupling to  $\text{H}_2\text{N-Gly-Gly-OAll}$ , yielded an on-resin tripeptide, which was then elongated to the macrocycle precursor. After removal of the Alloc and allyl groups, on-resin macrocyclization was effected using BOP/DIPEA. The peptide was then completed using standard Fmoc-SPPS conditions, including N-terminal lipidation with isopelargonic acid. After cleavage from the resin, and global deprotection, the crude lipopeptide was purified using RP-HPLC, yielding Dap9-Lat (**6**) in 3% overall yield over 27 steps. MeDap9-Lat (**8**) was synthesized following essentially the same on-resin protocol used for **6**, with the exception that the MeDap residue was installed as the corresponding azido species and reduced on-resin before the macrolactamization step (this strategy was also attempted for MeDap9-Brev (**7**) but the on-resin azide reduction step caused peptide decomposition).



**Scheme 3.** Total SPPS of Dap9-Brev (**5**) and MeDap9-Brev (**7**).

In addition to the total SPPS of Dap9-Lat (**6**), we also investigated an operationally more straightforward approach, wherein the amide linked macrocycle was formed in solution at the end of the synthesis (see supporting Scheme S7). This approach yielded Dap9-Lat (**6**) in an excellent overall yield of 29% (over 30 steps). Notably, this solution phase cyclization strategy was found to scale well, providing convenient access to **6** in multi-gram quantities. Assessment of the antibacterial activities of laterocidine amide analogues **6** and **8** revealed them to largely mirror the activity of laterocidine itself, with the exception of the *A. baumannii* strains tested (Table 1). This is in marked contrast to the significant loss of activity observed for the corresponding brevicidine amide analogues **5** and **7**, suggesting that the larger macrocycle present in laterocidine is more amenable to the ester-to-amide substitution. The serum stability of Dap9-Lat (**6**) was also found to be enhanced relative to laterocidine, with nearly 60% of the amide analogue still intact after 24 h incubation with serum, versus 45% for laterocidine itself (see experimental methods Figure 7).

Building on these findings, brevicidine (**1**), laterocidine (**2**), and the synthetically more tractable amide analogues **5** and **6** were taken forward for further characterisation in cell toxicity assays. All compounds were found to be non-hemolytic up to the highest concentration tested (128  $\mu\text{g}/\text{mL}$ ) (see experimental methods Figure 8). Brevicidine, laterocidine, and Dap9-Lat (**6**) were also found to be non-toxic to HepG2 cells at 128  $\mu\text{g}/\text{mL}$ , while Dap9-Brev (**5**) showed



**Scheme 4.** Total SPPS of Dap9-Lat (**6**) and MeDap9-Lat (**8**).

a slight indication of toxicity at the same concentration (see experimental methods Figure 9). Based on the favourable balance of antibacterial activity, stability, low cell toxicity, and synthetic accessibility, Dap9-Lat (**6**) was selected for further *in vivo* evaluation. To begin, the tolerability of the compound was assessed in naïve ICR mice, showing it to be well tolerated when dosed subcutaneously at 40 mg/kg every q8h over a 24 h period (total daily dose 120 mg/kg). Building from this, an efficacy study was performed wherein Dap9-Lat (**6**) was further assessed for its capacity to reduce thigh infection in neutropenic mice infected with *E. coli* ATCC 25922. To gain an indication of dose-response, Dap9-Lat (**6**) was administered subcutaneously q8h at 10, 20, and 40 mg/kg and compared with groups treated with vehicle or polymyxin B as a clinical reference antibiotic administered subcutaneously q8h at 20 mg/kg (Figure 4). A clear dose response was observed in the mice treated with Dap9-Lat (**6**), with the highest 40 mg/kg dose tested resulting in an approximate 5-log reduction in bacterial load relative to the untreated group, an antibacterial effect comparable to that observed for polymyxin B administered at 20 mg/kg. Notably, these *in vivo* activities reflect the results of the *in vitro* activity assays, wherein Dap9-Lat (**6**) and polymyxin B were found to have MIC values against *E. coli* ATCC 25922 of 1.0 and 0.5 µg/mL respectively (Table 1). It is worthy of mention that in the original report describing the discovery and characterization of brevicidine and laterocidine the quantities of material obtained from fermentation were not sufficient for comprehensive *in vivo* efficacy studies. In contrast, the convenient and scalable synthesis of laterocidine amide analogue **6** provides the opportunity for further optimization and evaluation of these promising lipopeptide antibiotics.

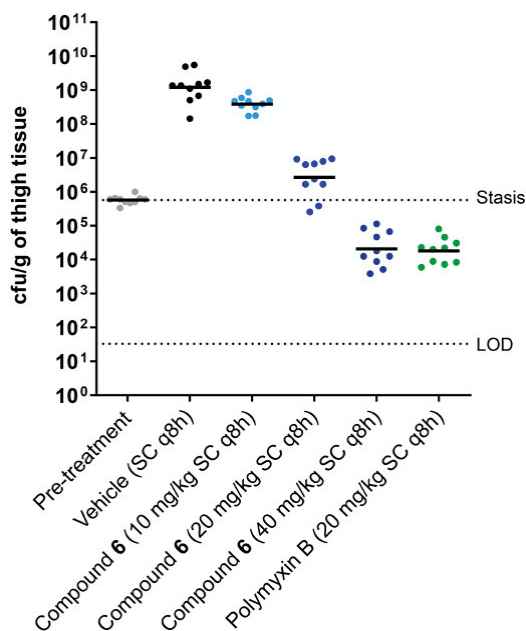


**Figure 4.** *In vivo* efficacy study. Scattergram of mouse thigh burdens (cfu/g) following infection with *E. coli* ATCC 25922 and treatment with test articles, as indicated on the x-axis. The geometric mean burden of each treatment is indicated by the horizontal bar. LOD = Limit of detection

## Conclusions

In conclusion, we here report the total syntheses of the recently discovered lipodepsipeptide antibiotics brevicidine and laterocidine. In addition, a number of analogues of each were prepared including a particularly interesting variant of laterocidine wherein the ester linkage in the peptide macrocycle was substituted as an amide. This laterocidine analogue (**6**) maintains the potent anti-Gram-negative activity of the natural product *in vitro* and was also found to be efficacious *in vivo*. The *in vivo* efficacy of **6** is noteworthy given that in the original report describing the discovery of laterocidine, only modest *in vivo* activity was observed for the natural product,<sup>6</sup> likely attributable to the low quantities of material available for dosing, coupled with its hydrolytic instability. In contrast, laterocidine amide analogue **6** exhibits enhanced stability, is readily synthesized on gram-scale, and exhibits a clear dose-dependent effect *in vivo*.

The routes here reported also provide reliable access to the natural products themselves. Brevicidine was obtained in 28 steps from 2-chlorotrityl resin in an overall yield of 9%, and laterocidine was obtained in 29 steps from Rink-amide resin in an overall yield of 2%. In both syntheses, formation of the macrocycle on-resin at an early stage was found to be most effective, serving to limit deleterious O→N acyl shifts at the ester linkage on Thr9, and provided the desired peptides as the major products after cleavage from resin, allowing



for facile HPLC purification. Overall, both synthetic strategies are highly robust, yielding brevicidine and laterocidine in quantities that compare well with those obtained by isolation of the natural products from fermentation of the producing organisms. Synthetic brevicidine and laterocidine were shown to have identical <sup>1</sup>H-NMR spectra and RP-HPLC elution profiles compared to their natural counterparts, confirming the previously reported structures. The antibacterial activities of synthetic brevicidine and laterocidine were also assessed against a panel of Gram-negative pathogens, demonstrating their potent antibacterial effect.

The methodology reported offers an efficient alternative to isolating these promising natural products from bacterial fermentation, and in doing so provides access to quantities of material suitable for further evaluation and mechanistic studies. Furthermore, the synthetic approaches we describe also provide access to novel analogues of both brevicidine and laterocidine. Of particular note is the finding that the enantiomeric forms of both brevicidine and laterocidine exhibit severely reduced antibacterial activities, a finding that supports a mechanism of action involving a stereospecific interaction with the bacterial target. Also of note is the finding that the macrocycles in brevicidine and laterocidine have varying tolerances for modification. Specifically, the ester-to-amide substitution, investigated as a means of both enhancing hydrolytic stability and increasing synthetic accessibility, was found to be detrimental to the activity of the brevicidines, while the laterocidine amide analogues largely maintain the activity of the natural product. Evaluation of the serum stability, haemolytic activity, and eukaryotic cell toxicity of the brevicidines and laterocidines here investigated in turn led the selection of laterocidine amide analogue **6** for further *in vivo* assessment. As noted above, these studies showed compound **6** to be well tolerated and capable of effectively reducing bacterial infection in a murine thigh-infection model. Also, while the clinically used polymyxins were found to be consistently more active (generally 2-to-4-fold lower MICs) than the brevicidines and laterocidines here studied, it is notable that in the case of *mcr*-positive polymyxin resistant strains, the brevicidines and laterocidines maintained their antibacterial activity. Given the “last-resort” status of the polymyxins, it is imperative that new antibacterial agents capable of overcoming polymyxin resistance be pursued.

In light of the increasing occurrence of Gram-negative pathogens with resistance to conventional antibacterial therapies, the brevicidine and laterocidine family of lipopeptide antibiotics represent promising leads for further development. In this regard, the recent discovery of the relacidines,<sup>21</sup> which show high structural similarity to laterocidine, indicates that these lipopeptide antibiotics may be widespread in nature. The encouraging results we here report pave the way for future investigations aimed at further developing these promising lipopeptides with an eye to more fully characterizing their therapeutic potential. To this end, the synthetic approaches here described provide a convenient means to access structurally diverse analogues. In addition, mechanistic studies into how the brevicidines and laterocidines prevent the growth of polymyxin resistant strains are ongoing and will be reported in due course.

## Experimental methods

### Reagents and general methods

All reagents employed were of American Chemical Society (ACS) grade or higher and were used without further purification unless otherwise stated. Fmoc-Ser-OAll,<sup>22</sup> Fmoc-Asp-OAll,<sup>23</sup> TFA·NH<sub>2</sub>-Gly-OAll,<sup>24</sup> TFA·NH<sub>2</sub>-Gly-Gly-OAll<sup>25</sup> and (2S,3R)-2-(((9H-fluoren-9-yl)methoxy)carbonyl)amino)-3-azidobutanoic acid<sup>26</sup> were synthesized according to referenced literature procedures. The NMR characterization of brevicidine in DMSO-d<sub>6</sub> was obtained using a Bruker Ascend 600 (600 MHz). The NMR characterization of laterocidine in DMSO-d<sub>6</sub> was obtained on a Bruker AV850 spectrometer (850 MHz). LC-MS analyses were performed on a Shimadzu LC-20AD system with a Shimadzu Shim-Pack GISS-HP C18 column (3.0 x 150 mm, 3 μm) at 30°C and equipped with a UV detector. The following solvent system, at a flow rate of 0.5 mL/min, was used: solvent A, 0.1 % formic acid in water; solvent B, acetonitrile. Gradient elution was as follows: 95:5 (A/B) for 2 min, 95:5 to 0:100 (A/B) over 13 min, 0:100 (A/B) for 2 min, then reversion back to 95:5 (A/B) over 1 min, 95:5 (A/B) for 2 min. This system was connected to a Shimadzu 8040 triple quadrupole mass spectrometer (ESI ionisation). The NMR characterisation of brevicidine and derivatives in DMSO-d<sub>6</sub> was obtained using a Bruker Ascend 600 (600 MHz). LC-MS analyses were conducted on an Agilent 1260 HPLC (equipped with an Infinity II quaternary pump, vial sampler, integrated column compartment and a variable wavelength detector) and MSD single quadrupole mass spectrometer. Samples were analysed using an Agilent Infinitylab poroshell 120 column (2.1 x 150 mm, 2.7 μm) under acetonitrile/water gradient with 0.1% formic acid as an additive. The following solvent system, at a flow rate of 0.3 mL/min, was used: solvent a, 0.1 % formic acid in water, solvent B, 0.1 % formic acid in acetonitrile. Gradient elution was as follows: 95:5 to 0:100 (A/B) over 5 min, 0:100 (A/B) for 1 min, then reversion back to 95:5 (A/B) over 0.1 min.

### Synthesis of brevicidine (1)

To a flame dried 25 mL round bottom flask was added Fmoc-Ser-OAll (110 mg, 0.300 mmol) and dry dichloromethane (DCM) (10.0 mL). 2-Chlorotrityl chloride resin (CT) (1.00 g, 0.81 mmol g<sup>-1</sup>) and DIPEA (210 μL, 1.20 mmol) were added. The suspension was stirred under argon for 48 h, after which the resin was filtered through a manual SPPS vessel and washed with DCM (4 x 5 mL). The resin was then capped by adding a solution of methanol, DIPEA and DCM (3 mL, 10 : 5 : 85) and bubbled with argon for 1 h. The solution was discharged and the resin was washed with DCM (3 x 5 mL) before being dried under a stream of argon. A small portion of resin was then used to ascertain the loading. Estimation of loading level of first residue onto resin (0.15 mmol g<sup>-1</sup>) was calculated via an Fmoc loading test, as described by Gude *et al.*<sup>27</sup>

Standard Fmoc SPPS protocol was used to extend the peptide to the linear Fmoc-Thr-Ile-Gly-Ser stage. Specifically, resin (670 mg, 0.1 mmol) was added to a manual SPPS vessel and bubbled in DMF (3 mL) to swell. The solvent was discharged and the resin was bubbled in an Fmoc deprotection solution of 20% piperidine in DMF (3 x 3 mL, 2 x 1 min then 1 x 5 min) with argon. The resin was washed with DMF (3 x 3 mL) and a coupling solution of amino acid (6 equiv), HATU (6 equiv) and DIPEA (12 equiv) in DMF (3 mL) was added. The solution was then bubbled with argon for 1 h, before the solution was discharged and the resin washed with DMF (3 x 3 mL). This process was repeated to obtain on-resin linear Fmoc-

tetrapeptide. At this stage the resin was split and a portion of this on-resin allyl-protected tetrapeptide (78.0 mg, 0.01 mmol) was added to a manual SPPS vessel and bubbled in DCM (3 mL) with argon for 15 min. The solvent was discharged and an allyl deprotection solution of tetrakis(triphenylphosphine) palladium (231 mg, 0.200 mmol) and phenylsilane (123  $\mu$ L, 0.998 mmol) in DCM and DMF (1:1, 2 mL) was added. The solution was bubbled with argon for 2 h in darkness, after which the deprotection solution was discharged and the resin was washed with DMF (3 x 3 mL), 0.5 % sodium diethyldithiocarbamate solution in DMF (4 x 5 mL), DMF (4 x 5 mL) and DCM (4 x 5 mL). The resin was dried under argon, then added to a 5 mL flame dried round bottom flask under argon. Dry dichloromethane (3 mL) was added and the suspension stirred for 15 min. Benzoyl chloride (13.0  $\mu$ L, 0.112 mmol), triethylamine (3.00  $\mu$ L, 22.0  $\mu$ mol) and catalytic DMAP (1 crystal) were added and the reaction mixture was stirred overnight at 60 °C. The resin was then filtered through a manual SPPS vessel and washed with DMF (3 x 5 mL) and DCM (3 x 5 mL) before being dried under argon. To ascertain reaction progress, a small sample was cleaved using a 2 % TFA solution in DCM (1 mL). The cleavage cocktail was gently agitated for 1 h and filtered through a glass wool plug. The filtrate was concentrated with a gentle stream of argon before being analysed by LC-MS. Desired cyclic product was identified ( $[M+H]^+$  calculated for  $C_{30}H_{36}N_4O_8$  581.2, found (LC-MS) 581.5) Following this modified Yamaguchi esterification, the synthesis of brevicidine was completed using standard Fmoc SPPS protocols as described above, after which 4-methylhexanoic acid was coupled to the N-terminus. The dried resin was then added to a cleavage cocktail of TFA, TIPS and distilled water (10 mL, 95 : 2.5 : 2.5) and heated to 37°C for 1 h. The suspension was filtered through a glass wool plug and the filtrate concentrated under vacuum. Diethyl ether was used to precipitate the crude peptide, which was then centrifuged and washed with additional diethyl ether. The suspension was centrifuged and the pellet dissolved in a minimal amount of 1:1 acetonitrile and water solution with 0.1% TFA. The crude mixture was subsequently purified by RP-HPLC (See [HPLC purification of synthetic peptides](#)). Fractions were assessed by LC-MS and product-containing fractions were pooled, frozen and lyophilized to yield brevicidine as a white powder. Yield: 13 mg, 9% over 28 steps. HPLC retention time 23.3 min (Method A);  $[M+3H]^{3+}$  calculated for  $C_{74}H_{106}N_{18}O_{17}$  507.2734, found (HR-MS) 507.2688.

### Synthesis of *ent*-brevicidine (*ent*-1)

To a flame dried 25 mL round bottom flask was added Fmoc-D-Ser-OAll (112 mg, 0.305 mmol) and dry dichloromethane (10.0 mL). 2-Chlorotrityl chloride resin (CT) (1.00 g, 0.81 mmol  $g^{-1}$ ) and DIPEA (210  $\mu$ L, 1.20 mmol) were added. The suspension was stirred under argon for 48 h at 45 °C, after which the resin was filtered through a manual SPPS vessel and washed with DCM (4 x 5 mL). The resin was then capped and loading level of the first residue onto resin (0.25 mmol  $g^{-1}$ ) was calculated as per the synthesis of brevicidine.

Standard Fmoc SPPS protocol was used to extend the peptide to the linear Fmoc-D-Thr-D-Ile-Gly-D-Ser peptide on a 0.1 mmol scale (400 mg) similar to the synthesis of brevicidine. Following SPPS of the tetrapeptide, an allyl deprotection solution of tetrakis (triphenylphosphine) palladium (231 mg, 0.200 mmol) and phenylsilane (123  $\mu$ L, 0.998 mmol) in DCM and DMF (1:1, 2 mL) was added. The solution was bubbled with argon for 2 h in darkness, after which the deprotection solution was discharged and the resin was washed with DMF (3 x 3 mL), 0.5 % sodium diethyldithiocarbamate solution in DMF (4 x 5 mL),

DMF (4 x 5 mL) and DCM (4 x 5 mL). The resin was dried under argon, then added to a 5 mL flame dried round bottom flask under argon. Dry dichloromethane (3 mL) was added and the suspension stirred for 15 min. Benzoyl chloride (13.0  $\mu$ L, 0.112 mmol), triethylamine (3.00  $\mu$ L, 22.0  $\mu$ mol) and catalytic DMAP (1 crystal) were added and the reaction mixture was stirred overnight at 60°C. The resin was then filtered through a manual SPPS vessel and washed with DMF (3 x 5 mL) and DCM (3 x 5 mL) before being dried under argon. A small sample was cleaved using a 2 % TFA solution in DCM (1 mL). The cleavage cocktail was gently agitated for 1 h and filtered through a glass wool plug. The filtrate was concentrated with a gentle stream of argon before being analysed by LC-MS ( $[M+Na]^+$  calculated for  $C_{30}H_{36}N_4O_8$  603.2, found (LC-MS) 603.5). Following this modified Yamaguchi esterification, the synthesis of *ent*-brevicidine was completed using standard Fmoc SPPS protocols as described above after which 4-methylhexanoic acid was coupled to the N-terminus. The peptide was cleaved from resin, precipitated and purified by RP-HPLC (See [HPLC purification of synthetic peptides](#)) following the procedure for synthesising brevicidine. Yield: 3 mg, 2% over 28 steps. HPLC retention time 22.9 min;  $[M-H]^-$  calculated for  $C_{74}H_{106}N_{18}O_{17}$  1517.7910, found (HR-MS) 1517.7943.

### Synthesis of Ser9-brevicidine (3)

The desired Fmoc-tetrapeptide was synthesized from Fmoc-Ser-OAll as described above, with Fmoc-Ser used in place of Fmoc-Thr. This resin-bound tetrapeptide (0.065 mmol, 0.14 mmol/g) was added to a manual SPPS vessel and bubbled with DMF (5 mL) for 15 min then the solvent was discharged. An allyl deprotection solution of tetrakis (triphenylphosphine) palladium (150 mg, 0.130 mmol) and phenylsilane (80.0  $\mu$ L, 0.649 mmol) in DCM and DMF (1:1, 2 mL) was added. The solution was bubbled with argon for 2 h in darkness, after which the deprotection solution was discharged and the resin was washed with DMF (3 x 3 mL), 0.5 % sodium diethyldithiocarbamate solution in DMF (4 x 5 mL), DMF (4 x 5 mL) and DCM (4 x 5 mL). The resin was dried under argon, then added to a 5 mL flame dried round bottom flask under argon. Dry dichloromethane (3 mL) was added and the suspension stirred for 15 min. Benzoyl chloride (8.00  $\mu$ L, 68.9  $\mu$ mol), triethylamine (20.0  $\mu$ L, 0.143 mmol) and catalytic DMAP (1 crystal) were added and the reaction mixture was stirred overnight at 60°C. The resin was then filtered through a manual SPPS vessel and washed with DMF (3 x 5 mL) and DCM (3 x 5 mL) before being dried under argon. A small sample was cleaved using a 2 % TFA solution in DCM (1 mL). The cleavage cocktail was gently agitated for 1 h and filtered through a glass wool plug. The filtrate was concentrated with a gentle stream of argon before being analysed by LC-MS ( $[M+H]^+$  calculated for  $C_{30}H_{36}N_4O_8$  567.2, found (LC-MS) 567.5). Following this modified Yamaguchi esterification, the synthesis of Ser9-brevicidine was completed using standard Fmoc SPPS protocols as described above. The peptide was cleaved from resin, precipitated and purified by RP-HPLC (See [HPLC purification of synthetic peptides](#)) following the procedure for synthesising brevicidine. Yield: 13 mg, 13% over 28 steps. HPLC retention time 22.1 min;  $[M+2H]^{2+}$  calculated for  $C_{73}H_{104}N_{18}O_{17}$  753.3986, found (HR-MS) 753.3980

### Synthesis of Dap9-brevicidine (5)

The desired Fmoc-tetrapeptide was synthesized from Fmoc-Ser-OAll as described above, with Fmoc-Dap(Alloc) used in place of Fmoc-Thr. This resin-bound tetrapeptide (0.1 mmol, 0.13 mmol/g) was added to a manual SPPS vessel and bubbled with DMF (5 mL) for 15 min then

the solvent was discharged. An allyl deprotection solution of tetrakis (triphenylphosphine) palladium (462 mg, 0.400 mmol) and phenylsilane (246  $\mu\text{L}$ , 2.00 mmol) in DCM and DMF (1:1, 8 mL) was added. The solution was bubbled with argon for 2 h in darkness, after which the deprotection solution was discharged and the resin was washed with DMF (3 x 3 mL), 0.5 % sodium diethyldithiocarbamate solution in DMF (6 x 10 mL), DMF (4 x 5 mL) and DCM (4 x 5 mL). A solution of HATU (76.0 mg, 0.200 mmol) and DIPEA (70.0  $\mu\text{L}$ , 0.402 mmol) in DMF (3 mL) and bubbled with argon overnight. The coupling solution was discharged, and the resin was washed with DMF (3 x 5 mL) then DCM (3 x 5 mL) and dried under a stream of argon. The synthesis of Dap9-brevicidine was completed using standard Fmoc SPPS protocols as described above. The peptide was cleaved from resin, precipitated and purified by RP-HPLC (See [HPLC purification of synthetic peptides](#)) following the procedure for synthesising brevicidine. Yield: 20 mg, 13% over 28 steps. HPLC retention time 21.6 min;  $[M+2H]^{2+}$  calculated for  $C_{73}H_{105}N_{19}O_{16}$  752.9066, found (HR-MS) 752.9368.

### Synthesis of MeDap9-brevicidine (7)

The desired Fmoc-tetrapeptide was synthesized from Fmoc-Ser-OAll as described above, with Fmoc-MeDap(Alloc)-OH (IUPAC name: (2S,3R)-2-[[[(9H-fluoren-9-ylmethoxy)carbonyl]amino]-3-[[[(2-propen-1-yloxy)carbonyl]amino]-butanoic acid) used in place of Fmoc-Thr. The synthesis of Fmoc-MeDap(Alloc)-OH was adapted from a previously reported literature precedent (R. Moran Ramallal, R. Liz & V. Gotor, *J. Org. Chem.*, 2010, 75, 19, 6614-6624) - To a flame dried 25 mL round bottom flask was added Fmoc-L-Abu(3R-N<sub>3</sub>)-OH (146 mg, 0.398 mmol) and 10% Pd/C (63 mg, 59.2  $\mu\text{mol}$ ). The flask was evacuated and a balloon of hydrogen was attached. Methanol (10 mL) was added and the suspension was stirred for 30 min before being filtered through a celite plug. The filtrate was concentrated under vacuum and re-dissolved in dichloromethane (10 mL). The solution was stirred at 0 °C then allyl chloroformate (51  $\mu\text{L}$ , 0.478 mmol) and DIPEA (83  $\mu\text{L}$ , 0.478 mmol) were added. The reaction was stirred at 0 °C for 3 h and concentrated under vacuum. The crude solid was subsequently purified by flash chromatography (1 % MeOH in DCM with 1% acetic acid). The fractions containing product were pooled, concentrated and co-evaporated with toluene (3 x 10 mL) then chloroform (3 x 10 mL) to yield a white solid (70 mg, 41%); TLC:  $R_f$  0.44 (10 % MeOH in DCM);  $\alpha_D^{20}$ : +31.9 (0.6,  $\text{CHCl}_3$ );  $^1\text{H}$  NMR (400 MHz,  $\text{CDCl}_3$ ):  $\delta$  7.74 (2H, d,  $J = 7.5$  Hz, Fmoc), 7.58 (2H, t,  $J = 6.7$  Hz, Fmoc), 7.38 (2H, t,  $J = 7.3$  Hz, Fmoc), 7.28 (2H, t,  $J = 7.3$  Hz, Fmoc), 6.09 (1H, d,  $J = 7.7$  Hz, -NH), 5.84 (1H, br,  $-\text{OCH}_2\text{CH}=\text{CH}_2$ ), 5.32 (1H, d,  $J = 6.7$  Hz,  $-\text{CHCH}(\text{CH}_3)\text{NH}-$ ), 5.23 (1H, d,  $J = 17.1$  Hz,  $-\text{OCH}_2\text{CH}=\text{CH}_2$ ), 5.15 (1H, d,  $J = 9.9$  Hz,  $-\text{OCH}_2\text{CH}=\text{CH}_2$ ), 4.52 - 4.35 (6H, m,  $-\text{CHCH}(\text{CH}_3)\text{NH}-$ ,  $-\text{CHCH}(\text{CH}_3)\text{NH}-$ , Fmoc- $\text{CHCH}_2$ ), 4.19 (1H, t,  $J = 6.9$  Hz, Fmoc- $\text{CHCH}_2$ ), 1.23 (3H, br,  $-\text{CHCH}(\text{CH}_3)\text{NH}-$ );  $[M+H]^+$  calculated for,  $C_{23}H_{24}N_2O_6$  425.1707, found (LC-MS) 425.4.

This resin-bound tetrapeptide (0.05 mmol, 0.14 mmol/g) was added to a manual SPPS vessel and bubbled with DMF (5 mL) for 15 min then the solvent was discharged. An allyl deprotection solution of tetrakis (triphenylphosphine) palladium (231 mg, 0.200 mmol) and phenylsilane (123  $\mu\text{L}$ , 0.998 mmol) in DCM and DMF (1:1, 6 mL) was added. The solution was bubbled with argon for 2 h in darkness, after which the deprotection solution was discharged and the resin was washed with DMF (3 x 3 mL), 0.5 % sodium diethyldithiocarbamate solution in DMF (6 x 10 mL), DMF (4 x 5 mL) and DCM (4 x 5 mL). A solution of HATU (95.0 mg, 0.250 mmol) and DIPEA (87.0  $\mu\text{L}$ , 0.499 mmol) in DMF (3 mL) and bubbled with argon overnight

at 50 °C. The coupling solution was discharged, and the resin was washed with DMF (3 x 5 mL) then DCM (3 x 5 mL) and dried under a stream of argon. A small sample was cleaved using a 2 % TFA solution in DCM (1 mL). The cleavage cocktail was gently agitated for 1 h and filtered through a glass wool plug. The filtrate was concentrated with a gentle stream of argon before being analysed by LC-MS ( $[M+H]^+$  calculated for  $C_{30}H_{36}N_4O_8$  580.3, found (LC-MS) 580.6). The synthesis of MeDap9-brevicidine was completed using standard Fmoc SPPS protocols as described above. The peptide was cleaved from resin, precipitated and purified by RP-HPLC (See [HPLC purification of synthetic peptides](#)) following the procedure for synthesising brevicidine. Yield: 3 mg, 2% over 28 steps. HPLC retention time 21.2 min;  $[M+H]^+$  calculated for  $C_{74}H_{107}N_{19}O_{16}$  1518.8216, found (HR-MS) 1518.4032.

### Synthesis of laterocidine (2)

Rink Amide MBHA resin (5.0 g, 0.67 mmol g<sup>-1</sup>) was loaded by overnight coupling via the free sidechain carboxylate of Fmoc-Asp-OAll (2.65 g, 6.70 mmol, 2 eq.) with BOP (2.96 g, 6.70 mmol, 2 eq.) and DiPEA (2.33 mL, 13.4 mmol, 4 eq.) in 150 mL of DMF. After capping with AcO<sub>2</sub> : pyridine (3 : 2, v/v) for 30 min the resin loading was determined to be 0.37 mmol g<sup>-1</sup>. The loaded resin (680 mg, 0.25 mmol) was treated with Pd(PPh<sub>3</sub>)<sub>4</sub> (75 mg, 0.075 mmol, 0.3 eq.) and PhSiH<sub>3</sub> (0.75 mL, 7.5 mmol, 30 eq.) in DCM (ca. 15 mL) under nitrogen for 1 h. The resin was subsequently washed with DCM (5 x 10 mL), followed by a solution of diethyldithiocarbamic acid trihydrate sodium salt (5 mg mL<sup>-1</sup> in DMF, 5 x 10 mL), and DMF (5 x 10 mL). TFA·H<sub>2</sub>N-Gly-OAll (115 mg, 0.5 mmol, 2 eq.) was then coupled using BOP (221 mg, 0.5 mmol, 2 eq.) and DiPEA (174 μL, 1.0 mmol, 4 eq.) under nitrogen flow for 1 h. The next 3 amino acids (Ile10, Thr9, Trp8) were coupled manually (1 h) under nitrogen flow via standard Fmoc solid-phase peptide synthesis (SPPS) (resin : Fmoc-AA : BOP : DiPEA, 1 : 4 : 4 : 8 molar eq.). DMF (5 mL) was used as solvent and Fmoc deprotections (2 min then 10 min) were carried out with 5 mL piperidine : DMF (1 : 4, v/v). The following Fmoc amino acids were used: Fmoc-Ile-OH, Fmoc-Thr-OH (used without side chain protection), and Fmoc-Trp(Boc)-OH. After coupling of Fmoc-Trp(Boc)-OH esterification of the Thr side chain was achieved by treating the resin-bound peptide with Alloc-Gly-OH (596 mg, 3.75 mmol, 15 eq.), DIC (0.59 mL, 3.75 mmol, 15 eq.) and DMAP (15 mg, 0.13 mmol, 0.5 eq.) in 8 mL DCM : DMF (3 : 1, v/v) for 18 h under nitrogen. The resin was treated with Pd(PPh<sub>3</sub>)<sub>4</sub> (75 mg, 0.075 mmol) and PhSiH<sub>3</sub> (0.75 mL, 7.5 mmol) in DCM (ca. 15 mL) under nitrogen for 2 h before being washed with DCM (5 x 10 mL), followed by a solution of diethyldithiocarbamic acid trihydrate sodium salt (5 mg mL<sup>-1</sup> in DMF, 5 x 10 mL), and DMF (5 x 10 mL). The peptide was then cyclized using BOP (442 mg, 1.0 mmol, 4 eq.) and DiPEA (0.35 mL, 2.0 mmol, 8 eq.) for 2 h in 5 mL DMF under nitrogen flow. The remaining linear N-terminal section of the peptide was then synthesized using the standard SPPS protocol mentioned above. The following Fmoc amino acids were used: Fmoc-D-Ser(tBu)-OH, Fmoc-D-Tyr(tBu)-OH, Fmoc-D-Trp(Boc)-OH, Fmoc-D-Orn(Boc)-OH, Fmoc-L-Orn(Boc)-OH, Fmoc-Gly-OH. Following the final Fmoc removal step, isopelargonic acid (79 mg, 0.5 mmol, 2 eq.) was coupled using BOP (221 mg, 0.5 mmol, 2 eq.) and DiPEA (174 μL, 1.0 mmol, 4 eq.) in 5 mL of DMF overnight, under nitrogen flow. Final deprotection was carried out by treating the resin with TFA : TIS : H<sub>2</sub>O (95 : 2.5 : 2.5, 10 mL) for 90 min. The reaction mixture was filtered through cotton, the filtrate precipitated in MTBE : petroleum ether (1 : 1), and the resulting precipitate washed once more with MTBE : petroleum ether (1 : 1). The crude cyclic peptide was lyophilized from tBuOH : H<sub>2</sub>O (1 : 1) and purified with reverse phase HPLC

(See [HPLC purification of synthetic peptides](#)). Pure fractions were pooled and lyophilized to yield laterocidine in >95% purity as a white powder. Yield: 8 mg, 2% over 29 steps.  $[M+2H]^{2+}$  calculated for,  $C_{78}H_{113}N_{19}O_{18}$  802,9329, found (HR-MS) 802,9326.

### Synthesis of *ent*-laterocidine (**ent-2**)

Rink Amide MBHA resin (5.0 g, 0.67 mmol  $g^{-1}$ ) was loaded by overnight coupling via the free sidechain carboxylate of Fmoc-D-Asp-OAll (2.65 g, 6.70 mmol, 2 eq.) with BOP (2.96 g, 6.70 mmol, 2 eq.) and DiPEA (2.33 mL, 13.4 mmol, 4 eq.) in 150 mL of DMF. After capping with  $AcO_2$  : pyridine (3 : 2, v/v) for 30 min the resin loading was determined to be 0.37 mmol  $g^{-1}$ . The loaded resin (675 mg, 0.25 mmol) was treated with  $Pd(PPh_3)_4$  (75 mg, 0.075 mmol, 0.3 eq.) and  $PhSiH_3$  (0.75 mL, 7.5 mmol, 30 eq.) in DCM (ca. 15 mL) under nitrogen for 1 h. The resin was subsequently washed with DCM ( $5 \times 10$  mL), followed by a solution of diethyldithiocarbamic acid trihydrate sodium salt (5 mg  $mL^{-1}$  in DMF,  $5 \times 10$  mL), and DMF ( $5 \times 10$  mL). TFA- $H_2N$ -Gly-OAll (115 mg, 0.5 mmol, 2 eq.) was then coupled using BOP (221 mg, 0.5 mmol, 2 eq.) and DiPEA (174  $\mu$ L, 1.0 mmol, 4 eq.) under nitrogen flow for 1 h. The next 3 amino acids (D-Ile10, D-Thr9, D-Trp8) were coupled manually (1 h) under nitrogen flow via standard Fmoc solid-phase peptide synthesis (SPPS) (resin : Fmoc-AA : BOP : DiPEA, 1 : 4 : 4 : 8 molar eq.). DMF (5 mL) was used as solvent and Fmoc deprotections (2 min then 10 min) were carried out with 5 mL piperidine : DMF (1 : 4, v/v). The following Fmoc amino acids were used: Fmoc-D-Ile-OH, Fmoc-D-Thr-OH (used without side chain protection), and Fmoc-D-Trp(Boc)-OH. After coupling of Fmoc-D-Trp(Boc)-OH esterification of the D-Thr side chain was achieved by treating the resin-bound peptide with Alloc-Gly-OH (596 mg, 3.75 mmol, 15 eq.), DIC (0.59 mL, 3.75 mmol, 15 eq.) and DMAP (15 mg, 0.13 mmol, 0.5 eq.) in 8 mL DCM : DMF (3 : 1, v/v) for 18 h under nitrogen. The resin was treated with  $Pd(PPh_3)_4$  (75 mg, 0.075 mmol) and  $PhSiH_3$  (0.75 mL, 7.5 mmol) in DCM (ca. 15 mL) under nitrogen for 2 h before being washed with DCM ( $5 \times 10$  mL), followed by a solution of diethyldithiocarbamic acid trihydrate sodium salt (5 mg  $mL^{-1}$  in DMF,  $5 \times 10$  mL), and DMF ( $5 \times 10$  mL). The peptide was then cyclized using BOP (442 mg, 1.0 mmol, 4 eq.) and DiPEA (0.35 mL, 2.0 mmol, 8 eq.) for 2 h in 5 mL DMF under nitrogen flow. The remaining linear N-terminal section of the peptide was then synthesized using the standard SPPS protocol mentioned above. The following Fmoc amino acids were used: Fmoc-L-Ser(tBu)-OH, Fmoc-L-Tyr(tBu)-OH, Fmoc-L-Trp(Boc)-OH, Fmoc-L-Orn(Boc)-OH, Fmoc-D-Orn(Boc)-OH, Fmoc-Gly-OH. Following the final Fmoc removal step, isopelargonic acid (79 mg, 0.5 mmol, 2 eq.) was coupled using BOP (221 mg, 0.5 mmol, 2 eq.) and DiPEA (174  $\mu$ L, 1.0 mmol, 4 eq.) in 5 mL of DMF overnight, under nitrogen flow. Final deprotection was carried out by treating the resin with TFA : TIS :  $H_2O$  (95 : 2.5 : 2.5, 10 mL) for 90 min. The reaction mixture was filtered through cotton, the filtrate precipitated in MTBE : petroleum ether (1 : 1), and the resulting precipitate washed once more with MTBE : petroleum ether (1 : 1). The crude cyclic peptide was lyophilized from tBuOH :  $H_2O$  (1 : 1) and purified with reverse phase HPLC (See [HPLC purification of synthetic peptides](#)). Pure fractions were pooled and lyophilized to yield *ent*-laterocidine in >95% purity as a white powder. Yield: 30 mg, 7.4% over 29 steps.  $[M+2H]^{2+}$  calculated for,  $C_{78}H_{113}N_{19}O_{18}$  802,9329, found (HR-MS) 802,9327.

### Synthesis of Ser9-laterocidine (**4**)

The loaded resin (274 mg, 0.1 mmol) was treated with  $Pd(PPh_3)_4$  (30 mg, 0.03 mmol, 0.3 eq.) and  $PhSiH_3$  (0.30 mL, 3.0 mmol, 30 eq.) in DCM (ca. 7 mL) under nitrogen for 1 h. The resin was

subsequently washed with DCM ( $5 \times 10$  mL), followed by a solution of diethyldithiocarbamic acid trihydrate sodium salt ( $5 \text{ mg mL}^{-1}$  in DMF,  $5 \times 10$  mL), and DMF ( $5 \times 10$  mL). TFA- $\text{H}_2\text{N}$ -Gly-OAll (115 mg, 0.5 mmol, 2 eq.) was then coupled using BOP (88 mg, 0.2 mmol, 2 eq.) and DiPEA ( $87 \mu\text{L}$ , 0.4 mmol, 4 eq.) under nitrogen flow for 2 h. The next 3 amino acids (Ile10, Ser9, Trp8) were coupled manually (1 h) under nitrogen flow via standard Fmoc solid-phase peptide synthesis (SPPS) (resin : Fmoc-AA : BOP : DiPEA, 1 : 4 : 4 : 8 molar eq.). Dry DMF (3 mL) was used as solvent and Fmoc deprotections (2 min then 10 min) were carried out with 3 mL piperidine : DMF (1 : 4, v/v). The following Fmoc amino acids were used: Fmoc-Ile-OH, Fmoc-Ser-OH (used without side chain protection), and Fmoc-Trp(Boc)-OH. After coupling of Fmoc-Trp(Boc)-OH esterification of the Ser side chain was achieved by treating the resin-bound peptide with Alloc-Gly-OH (238 mg, 1.5 mmol, 15 eq.), DIC (0.24 mL, 1.5 mmol, 15 eq.) and DMAP (6 mg, 0.05 mmol, 0.5 eq.) in 3 mL DCM : DMF (3 : 1, v/v) for 18 h under nitrogen. The resin was treated with  $\text{PhSiH}_3$  (0.30 mL, 3.0 mmol, 30 eq.) in DCM (ca. 7 mL) under nitrogen for 2 h before being washed with DCM ( $5 \times 10$  mL), followed by a solution of diethyldithiocarbamic acid trihydrate sodium salt ( $5 \text{ mg mL}^{-1}$  in DMF,  $5 \times 10$  mL), and DMF ( $5 \times 10$  mL). The peptide was then cyclized using BOP (177 mg, 0.4 mmol, 4 eq.) and DiPEA (0.14 mL, 0.8 mmol, 8 eq.) for 2 h in 3 mL DMF under nitrogen flow. The remaining linear N-terminal section of the peptide was then synthesized using the standard SPPS protocol mentioned above. The following Fmoc amino acids were used: Fmoc-D-Ser(tBu)-OH, Fmoc-D-Tyr(tBu)-OH, Fmoc-D-Trp(Boc)-OH, Fmoc-D-Orn(Boc)-OH, Fmoc-L-Orn(Boc)-OH, Fmoc-Gly-OH. Following the final Fmoc removal step, isopelargonic acid (79 mg, 0.5 mmol, 2 eq.) was coupled using BOP (88 mg, 0.2 mmol, 2 eq.) and DiPEA ( $87 \mu\text{L}$ , 0.4 mmol, 4 eq.) in 3 mL of DMF overnight, under nitrogen flow. Final deprotection was carried out by treating the resin with TFA : TIS :  $\text{H}_2\text{O}$  (95 : 2.5 : 2.5, 5 mL) for 90 min. The reaction mixture was filtered through cotton, the filtrate precipitated in MTBE : petroleum ether (1 : 1), and the resulting precipitate washed once more with MTBE : petroleum ether (1 : 1). The crude cyclic peptide was lyophilized from tBuOH :  $\text{H}_2\text{O}$  (1 : 1) and purified with reverse phase HPLC (See [HPLC purification of synthetic peptides](#)). Pure fractions were pooled and lyophilized to yield laterocidine in >95% purity as a white powder. Yield: 4 mg, 2% over 29 steps  $[\text{M}+2\text{H}]^{2+}$  calculated for,  $\text{C}_{78}\text{H}_{113}\text{N}_{19}\text{O}_{18}$  795.9250, found (HR-MS) 795,9249.

### Synthesis of Dap9-laterocidine (6)

The loaded resin (680 mg, 0.25 mmol) was treated with  $\text{Pd}(\text{PPh}_3)_4$  (75 mg, 0.075 mmol, 0.3 eq.) and  $\text{PhSiH}_3$  (0.75 mL, 7.5 mmol, 30 eq.) in DCM (ca. 15 mL) under nitrogen for 1 h. The resin was subsequently washed with  $\text{CH}_2\text{Cl}_2$  ( $5 \times 10$  mL), followed by a solution of diethyldithiocarbamic acid trihydrate sodium salt ( $5 \text{ mg mL}^{-1}$  in DMF,  $5 \times 10$  mL), and DMF ( $5 \times 10$  mL). TFA- $\text{H}_2\text{N}$ -Gly-Gly-OAll (143 mg, 0.5 mmol, 2 eq.) was then coupled using BOP (221 mg, 0.5 mmol, 2 eq.) and DiPEA ( $174 \mu\text{L}$ , 1.0 mmol, 4 eq.) under nitrogen flow for 1 h. The next two amino acids (Ile and Dap) were coupled manually (1 h) under nitrogen flow via standard Fmoc solid-phase peptide synthesis (SPPS) (resin : Fmoc-AA : BOP : DiPEA, 1 : 4 : 4 : 8 molar eq.). DMF (5 mL) was used as solvent and Fmoc deprotections (2 min then 10 min) were carried out with 5 mL piperidine : DMF (1 : 4, v/v). The following Fmoc amino acids were used: Fmoc-Ile-OH and Fmoc-Dap(Alloc)-OH. The resin was then treated two times with  $\text{Pd}(\text{PPh}_3)_4$  (75 mg, 0.075 mmol) and  $\text{PhSiH}_3$  (0.75 mL, 7.5 mmol) in DCM (ca. 15 mL) under nitrogen for 3 h with washing in between with DCM ( $5 \times 10$  mL), followed by a solution of diethyldithiocarbamic acid trihydrate sodium salt ( $5 \text{ mg mL}^{-1}$  in DMF,  $5 \times 10$  mL),



and DMF (5 × 10 mL). The macrocycle was then closed by treatment with BOP (442 mg, 1.0 mmol, 4 eq.) and DiPEA (0.35 mL, 2.0 mmol, 8 eq.) for 2 h in 5 mL DMF under nitrogen flow. Following cyclization the remaining linear N-terminal section of the peptide was added using a CEM Liberty Blue automated peptide synthesizer with microwave irradiation, on standard settings (resin : Fmoc-AA : DIC : Oxyma, 1 : 5 : 5 : 5 molar eq.). DMF was used as solvent and Fmoc deprotections were carried out with piperidine : DMF (1 : 4, v/v). The following Fmoc amino acids were used: Fmoc-D-Ser(tBu)-OH, Fmoc-D-Tyr(tBu)-OH, Fmoc-D-Trp(Boc)-OH, Fmoc-L-Orn(Boc)-OH, Fmoc-L-Orn(Boc)-OH, Fmoc-Gly-OH and Fmoc-Trp(Boc)-OH. Following the final Fmoc removal step, the resin was removed from the CEM Liberty Blue and washed with DCM and DMF before isopelargonic acid (79 mg, 0.5 mmol, 2 eq.) was coupled manually using BOP (221 mg, 0.5 mmol, 2 eq.) and DiPEA (174 μL, 1.0 mmol, 4 eq.) in 5 mL of DMF overnight, under nitrogen flow. Final deprotection was carried out by treating the resin with TFA : TIS : H<sub>2</sub>O (95 : 2.5 : 2.5, 10 mL) for 90 min. The reaction mixture was filtered through cotton, the filtrate was precipitated in MTBE : petroleum ether (1 : 1) and the resulting precipitate washed once more with MTBE : petroleum ether (1 : 1). The crude cyclic peptide was lyophilized from tBuOH : H<sub>2</sub>O (1 : 1) and purified with reverse phase HPLC (See [HPLC purification of synthetic peptides](#)). Pure fractions were pooled and lyophilized to yield Dap9-laterocidamide in >95% purity as a white powder. Yield 10 mg, 3 % yield over 27 steps. [M+2H]<sup>2+</sup> calculated for, C<sub>77</sub>H<sub>112</sub>N<sub>20</sub>O<sub>17</sub> 795,4330 found (HR-MS) 795,43

### Synthesis of Dap9-laterocidine (6) via Solution-Phase Cyclization.

2-Chlorotrityl resin (5.0 g, 1.60 mmol g<sup>-1</sup>) was loaded with Fmoc-Gly-OH. Resin loading was determined to be 0.67 mmol g<sup>-1</sup>. The linear peptide was assembled manually on a 3 mmol scale under nitrogen flow via standard Fmoc solid-phase peptide synthesis (SPPS) (1 h couplings, resin : Fmoc-AA : BOP : DiPEA, 1 : 4 : 4 : 8 molar eq.). DMF (60 mL) was used as solvent and Fmoc deprotections (2 min then 10 min) were carried out with 60 mL piperidine : DMF (1 : 4, v/v). The following Fmoc amino acids were used: Fmoc-D-Ser(tBu)-OH, Fmoc-D-Tyr(tBu)-OH, Fmoc-D-Trp(Boc)-OH, Fmoc-L-Orn(Boc)-OH, Fmoc-L-Orn(Boc)-OH, Fmoc-Gly-OH and Fmoc-Trp(Boc)-OH, Fmoc-Dap(Alloc)-OH and Fmoc-Ile-OH. Following the final Fmoc removal step, isopelargonic acid (0.95 g, 6 mmol, 2 eq.) was coupled using BOP (2.65 g, 6 mmol, 2 eq.) and DiPEA (2.1 mL, 12 mmol, 4 eq.) in 60 mL of DMF overnight, under nitrogen flow. The resin was then treated three times with Pd(PPh<sub>3</sub>)<sub>4</sub> (0.9 g, 0.075 mmol) and PhSiH<sub>3</sub> (9.0 mL, 7.5 mmol) in CH<sub>2</sub>Cl<sub>2</sub> (ca. 180 mL) under nitrogen for 2 h with washing in between with CH<sub>2</sub>Cl<sub>2</sub> (5 × 120 mL), followed by a solution of diethyldithiocarbamic acid trihydrate sodium salt (5 mg mL<sup>-1</sup> in DMF, 5 × 120 mL), and DMF (5 × 120 mL). The peptide was cleaved off the resin by treating it with HFIP : DCM (1 : 4, v/v, 240 mL) for 1 h and rinsed with additional HFIP : DCM and DCM. The combined washings were then evaporated to yield the linear protected peptide with a free C-terminus and Dap amino sidechain. The partially protected peptide was dissolved in DCM (1.8 L), treated with BOP (2.65 g, 6 mmol, 2 eq.) and DiPEA (2.1 mL, 12 mmol, 4 eq.) and the solution was stirred overnight under nitrogen atmosphere. The reaction mixture was concentrated and directly treated with TFA : TIS : H<sub>2</sub>O (95 : 2.5 : 2.5, 120 mL) for 90 min. The reaction mixture was subsequently filtered through cotton, the filtrate was precipitated in MTBE : petroleum ether (1 : 1) and the resulting precipitate washed once more with MTBE : petroleum ether (1 : 1). The crude cyclic peptide was lyophilized from tBuOH : H<sub>2</sub>O (1 : 1) and purified using a Buchi Pure C-815 Flash system with a Buchi FlashPure ID C18-WP

20  $\mu\text{m}$  irregular 80 g reverse-phase column. The purification was performed while doing 1 g injections of crude peptide. The following solvent system, at a flow rate of 40 mL/min, was used: solvent A, 0.1 % TFA in water; solvent B, 0.1 % TFA in acetonitrile. Gradient elution was as follows: 100:0 to 50:50 (A/B) over 60 min. Pure fractions were pooled and lyophilized to yield Dap9-laterocidamide in >95% purity as a white powder. Yield 1.4 g, 29 % yield over 30 steps.  $[\text{M}+2\text{H}]^{2+}$  calculated for,  $\text{C}_{77}\text{H}_{112}\text{N}_{20}\text{O}_{17}$  795,4330 found (HR-MS) 795,4327.

### Synthesis of MeDap9-laterocidine (8)

Rink amide MBHA resin loaded with Fmoc-Asp-OAll (680 mg, 0.25 mmol) was treated with  $\text{Pd}(\text{PPh}_3)_4$  (75 mg, 0.075 mmol) and  $\text{PhSiH}_3$  (0.75 mL, 7.5 mmol) in DCM (ca. 15 mL) under nitrogen for 2 h before being washed with DCM ( $5 \times 10$  mL), followed by a solution of diethyldithiocarbamic acid trihydrate sodium salt ( $5 \text{ mg mL}^{-1}$  in DMF,  $5 \times 10$  mL), and DMF ( $5 \times 10$  mL). TFA· $\text{H}_2\text{N}$ -Gly-OAll (115 mg, 0.5 mmol, 2 eq.) was then coupled using BOP (221 mg, 0.5 mmol, 2 eq.) and DiPEA (174  $\mu\text{L}$ , 1.0 mmol, 4 eq.) under nitrogen flow for 1 h. The next 2 amino acids Fmoc-Ile-OH and (2S,3R)-Fmoc-azido-aminobutyric acid were coupled manually (1 h) under nitrogen flow via standard Fmoc solid-phase peptide synthesis (SPPS) (resin : Fmoc-AA : BOP : DiPEA, 1 : 4 : 4 : 8 molar eq.). DMF (5 mL) was used as solvent and Fmoc deprotections (2 min then 10 min) were carried out with 5 mL piperidine : DMF (1 : 4, v/v). The azide was then reduced using a DTT (2M) and DiPEA (1M) in DMF (ca. 15 mL) for 2H under  $\text{N}_2$  followed by washings with DMF ( $5 \times 10$  mL). The Allyl protecting group on the C-terminus was then removed using  $\text{Pd}(\text{PPh}_3)_4$  (75 mg, 0.075 mmol) and  $\text{PhSiH}_3$  (0.75 mL, 7.5 mmol) in DCM (ca. 15 mL) under nitrogen for 2 h before being washed with DCM ( $5 \times 10$  mL), followed by a solution of diethyldithiocarbamic acid trihydrate sodium salt ( $5 \text{ mg mL}^{-1}$  in DMF,  $5 \times 10$  mL), and DMF ( $5 \times 10$  mL). The peptide was then cyclized using BOP (442 mg, 1.0 mmol, 4 eq.) and DiPEA (0.35 mL, 2.0 mmol, 8 eq.) for 2 h in 5 mL DMF under nitrogen flow. The remaining linear N-terminal section of the peptide was then synthesized using the standard SPPS protocol mentioned above. The following Fmoc amino acids were used: Fmoc-D-Ser(tBu)-OH, Fmoc-D-Tyr(tBu)-OH, Fmoc-D-Trp(Boc)-OH, Fmoc-D-Orn(Boc)-OH, Fmoc-L-Orn(Boc)-OH, Fmoc-Gly-OH, Fmoc-L-Trp(Boc)-OH. Following the final Fmoc removal step, isopelargonic acid (79 mg, 0.5 mmol, 2 eq.) was coupled using BOP (221 mg, 0.5 mmol, 2 eq.) and DiPEA (174  $\mu\text{L}$ , 1.0 mmol, 4 eq.) in 5 mL of DMF overnight, under nitrogen flow. Final deprotection was carried out by treating the resin with TFA : TIS :  $\text{H}_2\text{O}$  (95 : 2.5 : 2.5, 10 mL) for 90 min. The reaction mixture was filtered through cotton, the filtrate precipitated in MTBE : petroleum ether (1 : 1), and the resulting precipitate washed once more with MTBE : petroleum ether (1 : 1). The crude cyclic peptide was lyophilized from tBuOH :  $\text{H}_2\text{O}$  (1 : 1) and purified with reverse phase HPLC (See [HPLC purification of synthetic peptides](#)). Pure fractions were pooled and lyophilized to yield MeDap9-laterocidine in (9.7 mg, 2.4% over 29 steps, purity >95%)  $[\text{M}+2\text{H}]^{2+}$  calculated for,  $\text{C}_{78}\text{H}_{114}\text{N}_{20}\text{O}_{17}$  802.4408, found (HRMS) 802.4412.

### HPLC purification of synthetic peptides

Brevicidine and analogues were purified using a Perkin Elmer HPLC system composed of a 200 series binary pump, UV/Vis detector monitoring at 220 nm, vacuum degasser and Rheodyne 7725i injector. **Method A (Preparative):** Phenomenex Luna C18 column (21.2 x 250 mm, 5  $\mu\text{m}$ ) with a 2 mL injection loop. The following solvent system, at a flow rate of 10 mL/min, was used: solvent A, 0.1 % TFA in water; solvent B, acetonitrile. Gradient elution

was as follows: 80:20 (A/B) for 5 min, 80:20 to 45:55 (A/B) over 30 min, 45:55 to 0:95 (A/B) over 3 min, 0:95 (A/B) for 3 min then reversion back to 80:20 (A/B) over 2 min, 80:20 (A/B) for 5 min. **Method B (Analytical):** Phenomenex C18 Luna column (4.6 x 150 mm, 5  $\mu$ m) with a 200  $\mu$ L injection loop. The following solvent system, at a flow rate of 2 mL/min, was used: solvent A, 0.1 % TFA in water; solvent B, acetonitrile. Gradient elution was as follows: 95:5 (A/B) for 2 min, 95:5 to 5:95 (A/B) over 18 min then reversion back to 95:5 (A/B) over 0.1 min, 95:5 (A/B) for 3.9 min. Laterocidine and analogues were purified using the following methods. **Method C (Preparative):** BESTA-Technik system equipped with a ECOM Flash UV detector monitoring at 214 nm and 254 nm with a Dr. Maisch Reprosil Gold 120 C18 column (25 x 250 mm, 10  $\mu$ m). The following solvent system, at a flow rate of 12 mL/min, was used: solvent A, 0.1 % TFA in water/acetonitrile 95/5; solvent B, 0.1 % TFA in water/acetonitrile 5/95. Gradient elution was as follows: 100:0 (A/B) for 5 min, 100:0 to 50:50 (A/B) over 50 min, 50:50 to 0:100 (A/B) for 3min, then reversion back to 100:0 (A/B) over 1 min, 100:0 (A/B) for 5 min. **Method D (Analytical):** Shimadzu Prominence-i LC-2030 system with a Dr. Maisch ReproSil Gold 120 C18 column (4.6 x 250 mm, 5  $\mu$ m) at 30 °C and equipped with a UV detector monitoring 214 nm and 254 nm. The following solvent system, at a flow rate of 1 mL/min, was used: solvent A, 0.1 % TFA in water/acetonitrile 95/5; solvent B, 0.1 % TFA in water/acetonitrile 5/95. Gradient elution was as follows: 100:0 (A/B) for 2 min, 100:0 to 50:50 (A/B) over 45 min, 50:50 (A/B) to 0:100 (A/B) over 1 min, 0:100 (A/B) for 6 min then reversion back to 100:0 (A/B) over 1min, 100:0 (A/B) for 5min. HPLC traces of all peptides can be found in the online supplementary material at DOI <https://doi.org/10.1039/D2SC00143H>

### MIC determinations

Minimum inhibitory concentrations (MICs) were determined by broth microdilution according to CLSI guidelines in triplicate. Blood agar plates were inoculated with glycerol stocks of *E. coli* ATCC 25922, *E. coli* MCR-1 (clinical isolate from Utrecht Medical Centre, NL), *E. coli* EQAS MCR-2 (clinical isolate from Wageningen University and Research, NL), *K. pneumoniae* ATCC 11228, *K. pneumoniae* ATCC 13883, *K. pneumoniae* 2048 (clinical isolate from Vrije Universiteit Amsterdam Medical Centre, NL), *K. pneumoniae* JS-123 (clinical isolate from Utrecht Medical Centre, NL), *A. baumannii* ATCC 17961, *A. baumannii* ATCC 17978, *A. baumannii* 2018-006 (clinical isolate from Rijksinstituut voor Volksgezondheid en Milieu, NL), *A. baumannii* MDR (clinical isolate from Vrije Universiteit Amsterdam Medical Centre, NL), *P. aeruginosa* ATCC 27853, *P. aeruginosa* PAO1, *P. aeruginosa* NRZ-03961 (Reference strain from Das Nationale Referenzzentrum für gramnegative Krankenhauserreger, DE), *P. aeruginosa* M-120 (clinical isolate from Leiden University Medical Centre, NL) and *S. aureus* USA300 (clinical isolate from Texas Children's Hospital, USA). *E. coli* 25922 MCR1 was grown on LB agar supplemented with kanamycin. The inoculated agar plates were then incubated for 16 h at 37°C. Individually grown colonies were subsequently used to inoculate 3 mL aliquots of TSB that were then incubated at 37°C with shaking at 220 rpm. In parallel, the lipopeptide antibiotics to be assessed were serially diluted with Mueller-Hinton broth (MHB) in polypropylene 96-well plates (50  $\mu$ L in each well). Once the OD<sub>600</sub> of the bacterial suspensions reached 0.5, the bacteria were diluted with MHB (final concentration  $2 \times 10^5$  CFU mL<sup>-1</sup>) and added to the microplates containing the test compounds (50  $\mu$ L to each well, final volume: 100  $\mu$ L). The well-plates were sealed with an adhesive membrane and after 16 h of incubation at 37°C with shaking at 220 rpm the wells were visually inspected for bacterial

growth. MIC values reported are based on three technical replicates and defined as the lowest concentration of the compound that prevented visible growth of bacteria.

## LC-MS/MS

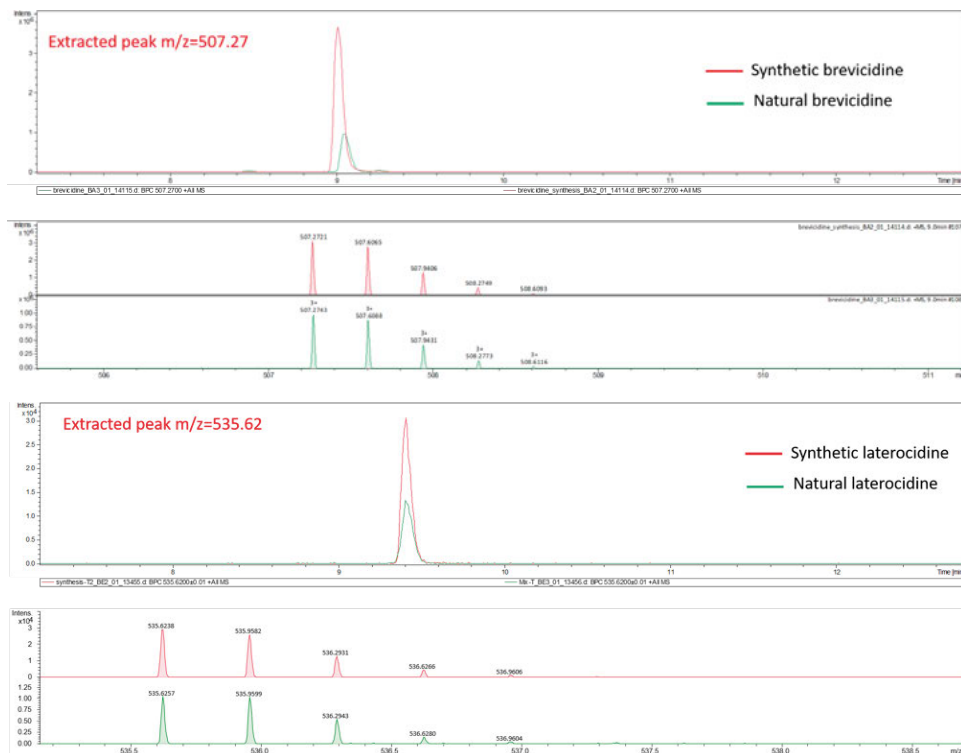


**Figure 5.** Comparison of synthetic lipopeptides with their natural counterparts by LC-MS/MS.

UltiMate 3000 UHPLC Systems coupled to Bruker impact™II Mass Spectrometer (TOF). **Column:** Waters Acquity UPLC BEH C18 column (1.7  $\mu\text{m}$ , 130  $\text{\AA}$ , 2.1  $\times$  150 mm). **LC method:** The column was maintained at 40°C and run at a flow rate of 0.2 mL/min, using 0.1% formic acid in H<sub>2</sub>O as solvent A and 0.1% formic acid in acetonitrile as solvent B. A gradient was employed for chromatographic separation starting at 5% B for 2 min, then 5% to 95% B for 15 min, and finally held at 95% for 4 min, The column was re-equilibrated to 5% B for 1 min before the next run was started. **MS method:** The MS system was tuned using standard sodium formate solution. The same solution was used to calibrate the system before starting. All the samples were analyzed in positive polarity, using data-dependent acquisition mode. Detection range: 100–1500 m/z.

## LPS antagonization assay

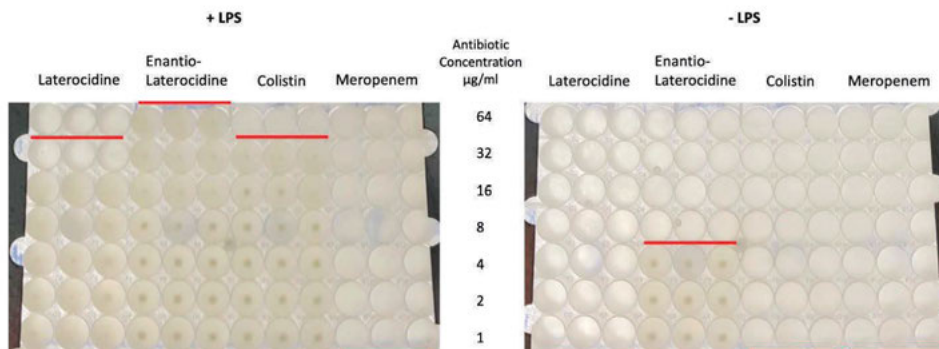


**Figure 6.** LPS antagonization assay.

A blood agar plate was inoculated with a glycerol stock of *E. coli* ATCC 25922. The inoculated agar plate was then incubated for 16 h at 37 °C. An individually grown colony was subsequently used to inoculate 3 mL of TSB that was then incubated at 37 °C with shaking at 220 rpm. In parallel, the compounds to be assessed were serially diluted with Mueller-Hinton broth (MHB) in polypropylene 96-well plates (50 µL in each well). Once the OD600 of the bacterial suspensions reached 0.5, the bacteria were diluted with MHB (final concentration  $2 \times 10^5$  CFU mL<sup>-1</sup>). The media were then either supplemented with 1 mg/mL of LPS (lipopolysaccharides from *E. coli* O55:B5, Sigma-Aldrich) or added directly to the microplates containing the test compounds (50 µL to each well, final volume: 100 µL). The well-plates were sealed with an adhesive membrane and after 16 h of incubation at 37°C with shaking at 220 rpm. The wells were visually inspected for bacterial growth.

## Serum stability assay

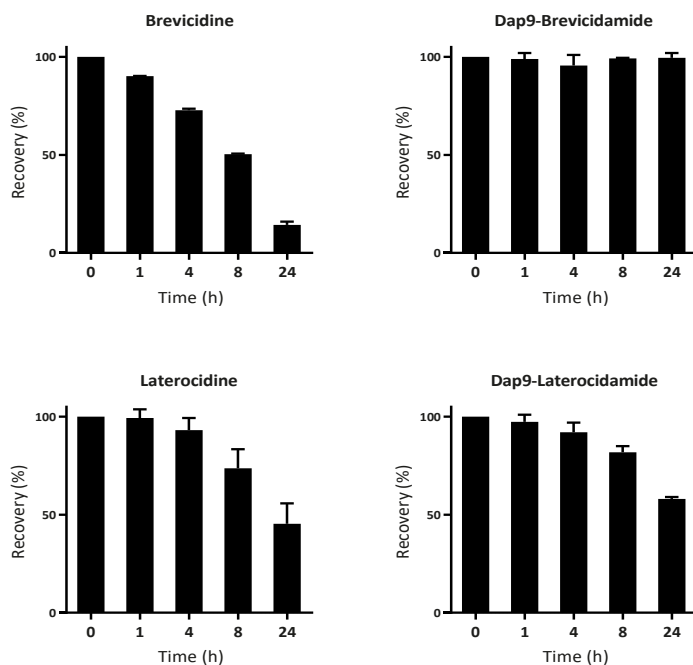


**Figure 7.** Serum stability assays comparing natural lipopeptides to synthetic amide analogues.

10 mg/mL peptide solutions were prepared in Milli-Q water. Samples were prepared with 42  $\mu$ L peptide solution and 518  $\mu$ L human serum (obtained from Sigma Aldrich, product number: H4522) and incubated at 37  $^{\circ}$ C. Samples were taken at  $t = 0, 1, 4, 8$  and 24 h. To 100  $\mu$ L of serum, 100  $\mu$ L of 6% TCA in ACN (containing 0.2  $\mu$ g/mL D-Phenylalanine as internal standard) was added to precipitate the proteins. The samples were vortexed, left for 15 min at room temperature and stored at -20  $^{\circ}$ C. Before analysis the samples were centrifuged for 5 min at 13 000 rpm. The supernatant was analyzed by RP-HPLC using a Shimadzu Prominence-i LC-2030 system with a Dr. Maisch ReproSil Gold 120 C18 column (4.6  $\times$  250 mm, 5  $\mu$ m) at 30  $^{\circ}$ C and equipped with a UV detector monitoring at 220 nm and 254 nm. The following solvent system, at a flow rate of 1 mL/min, was used: solvent A, 0.1 % TFA in water/acetonitrile 95/5; solvent B, 0.1 % TFA in water/acetonitrile 5/95. Gradient elution was as follows: 100:0 (A/B) for 2 min, 100:0 to 50:50 (A/B) over 45 min, 50:50 (A/B) to 0:100 (A/B) over 1 min, 0:100 (A/B) for 6 min then reversion back to 100:0 (A/B) over 1 min, 100:0 (A/B) for 5 min. The peaks were integrated and normalized to the internal standard. Recovery of the peptides at  $t=0$  was compared to control samples without serum and was within the 85%-115% range (data not shown). The  $t=0$  value was then set at 100% for each analogue and all time-points were calculated as a percentage of  $t=0$ . Biological duplicates of the experiment were performed.

## Hemolysis assay

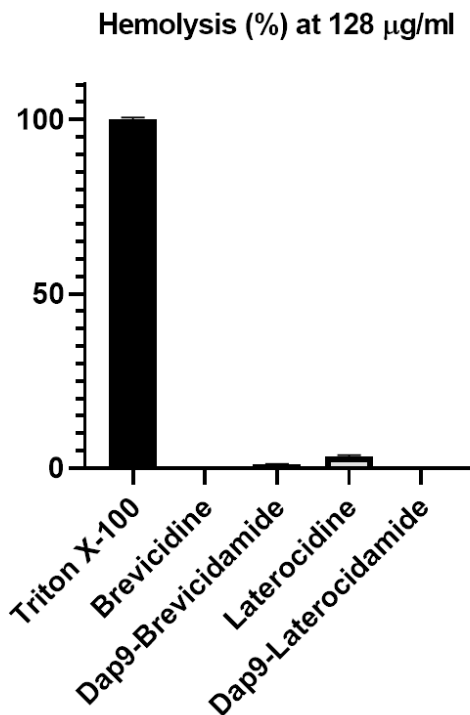


**Figure 8.** Hemolytic activity of selected analogues against sheep red blood cells.

Experiments were performed in triplicate and Triton X-100 used as a positive control. Red blood cells from defibrinated sheep blood obtained from Thermo Fisher were centrifuged (400 g for 15 min at 4°C) and washed with Phosphate-Buffered Saline (PBS) containing 0.002% Tween20 (buffer) for five times. Then, the red blood cells were normalized to obtain a positive control read-out between 2.5 and 3.0 at 415 nm to stay within the linear range with the maximum sensitivity. A serial dilution of the compounds (256 – 8  $\mu\text{g/mL}$ , 75  $\mu\text{L}$ ) was prepared in a 96-well plate. The outer border of the plate was filled with 75  $\mu\text{L}$  buffer. Each plate contained a positive control (0.1% Triton-X final concentration, 75  $\mu\text{L}$ ) and a negative control (buffer, 75  $\mu\text{L}$ ) in triplicate. The normalized blood cells (75  $\mu\text{L}$ ) were added and the plates were incubated at 37 °C for 1 h while shaking at 500 rpm. A flat-bottom plate of polystyrene with 100  $\mu\text{L}$  buffer in each well was prepared. After incubation, the plates were centrifuged (800 g for 5 min at room temperature) and 25  $\mu\text{L}$  of the supernatant was transferred to their respective wells in the flat-bottom plate. The values obtained from a read-out at 415 nm were corrected for background (negative control) and transformed to a percentage relative to the positive control.

## Cytotoxicity assay

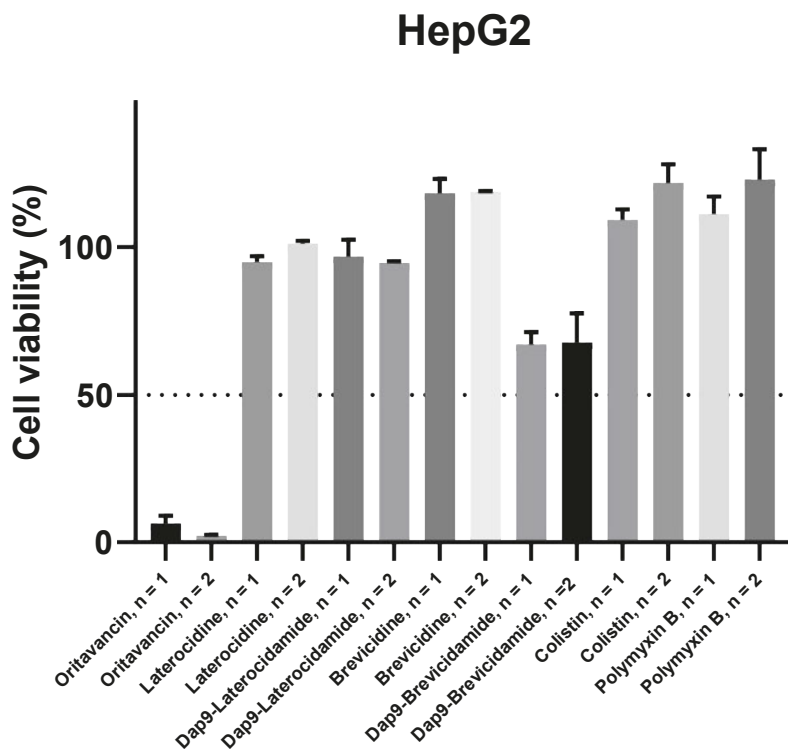


**Figure 9.** Cytotoxicity of selected brevicidine and laterocidine analogues against HepG2 cells compared to oritavancin, colistin and polymyxin B using a (3-(4,5-dimethylthiazol-2-yl)-2,5-diphenyltetrazolium bromide (MTT) assay.

HepG2 cells were seeded at a density of  $1.5 \times 10^4$  cells per well in a clear 96-well tissue culture treated plate in a final volume of 100  $\mu$ L of Dulbecco's Modified Eagle Medium (DMEM), supplemented with Fetal Bovine Serum (1%), Glutamax and Pen/Strep. Cells were incubated for 24 h at 37°C, 7% CO<sub>2</sub> to allow cells to attach to the plates. In addition to a single vehicle control, compounds (diluted from DMSO stock) were added to each well to obtain in a final 128  $\mu$ g/mL concentration (max. final DMSO concentration 0.5%) for all compounds except for oritavancin which was administered at 50  $\mu$ M. Incubation was done for 24 h at 37 °C, 7% CO<sub>2</sub>. After the incubation, MTT was added to each well at a final concentration of 0.40 mg/mL. The plates were then incubated for 2 h at 37 °C, 7% CO<sub>2</sub>. Medium was carefully removed via suction, and purple formazan crystals were resuspended in 100  $\mu$ L DMSO. Absorbance was read at 570 nm using a Clariostar plate reader. The data was then analysed with GraphPad Prism software. Technical triplicates for each condition were used, along with biological duplicates.



### **In vivo tolerability and efficacy studies**

**Ethical Issues.** Animal experiments were performed under UK Home Office Licences P89653310 (tolerability and PK) and PA67E0BAA (high efficacy), with local ethical committee clearance.

**Animal Strain.** Mice used in these studies were supplied by Charles River (Margate UK) and were specific pathogen free. The strain of mice used was ICR (also known as CD1 Mice) which is a well characterized outbred murine strain. Mice (male) were 11-15 g on receipt and were allowed to acclimatise for at least 7 days.

**Animal Housing.** Mice were housed in sterilised individual ventilated cages exposing the mice at all times to HEPA filtered sterile air. Mice had free access to food and water and had aspen chip bedding (changed at least once weekly). The room temperature was 22°C +/- 1°C, with a relative humidity of 60% and maximum background noise of 56 dB. Mice were exposed to 12 h light/dark cycles.

**Test compounds.** Compound **6** was dissolved in water for injection in which it formed a clear colourless solution. Polymyxin B was dissolved in saline for injection to produce a clear colourless solution .

**Tolerability study.** The tolerability of compound **6** was assessed in the same mouse strain used for the efficacy studies. Compound **6** was administered via subcutaneous administration route at 3 8-h intervals indicating good tolerability up to 40 mg/kg. The mice used in the tolerability study were naïve and were not immunosuppressed or infected.

**Efficacy study.** The *in vivo* efficacy of compound **6** was assessed in a mouse thigh abscess model where both thighs of each mouse were infected with *E. coli* ATCC 25922

**Immunosuppression.** Mice were rendered neutropenic with subcutaneous injections of cyclophosphamide at 150 mg/kg 4 days before infection and 100 mg/kg 1 day before infection. The immunosuppression regime leads to neutropenia starting 24 h post administration of the first injection, which continues throughout the study.

**Infection.** The bacterial strain used was *E. coli* ATCC 25922. An aliquot of a previously prepared frozen stock of the strain was thawed and diluted in sterile PBS to the desired inoculum just prior to infection. Mice were infected with 0.05 mL of the bacterial strain suspensions by intramuscular (IM) injection under temporary inhaled anaesthesia (2.5% isoflurane for 3-4 min) into both thighs. The inoculum was 6 x 10<sup>6</sup> cfu/mL, 3 x 10<sup>5</sup> cfu/thigh.

**Analgesia.** At the time of thigh infection, buprenorphine analgesia was administered at 0.03mg/kg subcutaneously using a 0.015mg/mL solution delivered at 2 mL/kg. The same dose was administered again 9 and 17 h post-infection.

**Treatment.** Compound **6** was administered SC every 8 h starting 1 h post-infection at doses of 10, 20, and 40 mg/kg. Additional control groups comprising an infected pre-treatment group, which was euthanised 1 h after infection, a vehicle (WFI) treated group and a group that

received comparator Polymyxin B SC every 8 h dosed at 20 mg/kg were included.

**Endpoints.** One h and 20.5 (planned 25) h post-infection, the clinical condition of all animals was assessed prior to humane euthanasia using pentobarbitone overdose, and the thighs were removed and weighed. Thigh samples were homogenized in 3mL ice cold sterile PBS; the homogenates were quantitatively cultured onto CLED agar and incubated at 37°C for 18 - 24 h before colonies were counted.

**Data analysis.** The data from the culture burdens were analysed using appropriate non-parametric statistical models (Kruskal-Wallis using Conover-Inman to make all pairwise comparisons between groups) with StatsDirect software v. 3.3.5, and compared to vehicle control. For all calculations the thighs from each animal were treated as two separate data points.

## NMR characterization of compounds

## Synthetic brevicidine (1)

Residue	-NH	H $\alpha$	H $\beta$	H $\gamma$	H $\delta$	H $\epsilon$
D-Asn1	8.01 (1H, d, $J$ = 7.8 Hz)	4.54 (1H, m)	2.53 (1H, under DMSO peak) & 2.35 (1H, dd, $J$ = 15.7 & 6.8 Hz)			
D-Tyr2	7.98 (1H, d, $J$ = 7.3 Hz)	4.27 (1H, m)	2.78 (1H, m) & 2.58 (1H, m)	Aromatic: 6.85 (2H, d, $J$ = 8.6 Hz) & 6.55 (2H, d, $J$ = 8.6 Hz)		
D-Trp3	8.11 (1H, m)	4.48 (1H, m)	3.17 (1H, dd, $J$ = 14.6 & 4.3 Hz) & 3.02 (1H, dd, $J$ = 14.8 & 9.9 Hz)	Indole: 10.89 (2H, br d, $J$ = 6.5 Hz), 7.57 (2H, app dd, $J$ = 8.2 & 2.2 Hz), 7.32 (2H, app dd, $J$ = 14.2 & 8.2 Hz), 7.16 (1H, d, $J$ = 2.2 Hz), 7.05 (2H, m) & 6.97 (3H, m)		
D-Orn4	8.07 (1H, d, $J$ = 8.6 Hz)	4.37 (1H, m)	1.73 (1H, m) & 1.53 (1H, m)	1.53 (2H, m)	2.78 (2H, m)	7.76 (2H, br)
Orn5	7.92 (1H, d, $J$ = 8.2 Hz)	4.37 (1H, m)	1.73 (1H, m) & 1.53 (1H, m)	1.53 (2H, m)	2.78 (2H, m)	7.76 (2H, br)
Gly6	8.23 (1H, t, $J$ = 5.4 Hz)	3.82 (1H, dd, $J$ = 16.6 & 6.1 Hz) & 3.73 (1H, dd, $J$ = 18.4 & 7.8 Hz)				
D-Orn7	8.11 (1H, m)	4.37 (1H, m)	1.40 (1H, m) & 1.29 (1H, m)	1.29 (2H, m)	2.58 (2H, m)	7.68 (2H, br)
Trp8	8.19 (1H, m)	4.72 (1H, app q, $J$ = 7.8 Hz)	3.08 (1H, dd, $J$ = 14.6 & 5.6 Hz) & 2.96 (1H, dd, $J$ = 14.4 & 8.6 Hz)	Indole: 10.89 (2H, app d, $J$ = 6.5 Hz), 7.57 (2H, app dd, $J$ = 8.2 & 2.2 Hz), 7.32 (2H, app dd, $J$ = 14.2 & 8.2 Hz), 7.10 (1H, d, $J$ = 2.6 Hz), 7.05 (2H, app q, $J$ = 7.8 Hz) & 6.97 (3H, m)		
Thr9	8.19 (1H, m)	4.54 (1H, m)	4.88 (1H, m)	1.08 (3H, d, $J$ = 6.5 Hz)		
Ile10	8.54 (1H, d, $J$ = 9.6 Hz)	4.12 (1H, t, $J$ = 10.8 Hz)	1.84 (1H, br m)	0.84 (3H, m), 1.51 (1H, m) & 1.06 (1H, m)	0.84 (3H, m)	
Gly11	8.44 (1H, t, $J$ = 6.3 Hz)	3.89 (1H, dd, $J$ = 15.5 & 6.5 Hz) & 3.55 (under H <sub>2</sub> O)				
Ser12	7.62 (1H, d, $J$ = 9.1 Hz)	4.43 (1H, dt, $J$ = 9.0 & 4.7 Hz)	3.76 (1H, dd, $J$ = 11.2 & 4.7 Hz) & 3.60 (1H, dd, $J$ = 10.8 & 4.7 Hz)			
Lipid	2.06 (2H, m, O=CCH <sub>2</sub> -), 1.53 (2H, O=CCH <sub>2</sub> CH <sub>2</sub> -), 1.29 (5H, -CH <sub>2</sub> CH(CH <sub>3</sub> )CH <sub>2</sub> CH <sub>3</sub> ), 1.07 (2H, -CH <sub>2</sub> CH <sub>3</sub> ) & 0.81 (6H, -CH(CH <sub>3</sub> )CH <sub>2</sub> CH <sub>3</sub> )					

**ent-brevicidine (ent-1)**

Residue	-NH	H $\alpha$	H $\beta$	H $\gamma$	H $\delta$	H $\epsilon$
Asn1	8.02 (1H, d, J = 7.9 Hz)	4.54 (1H, m)	2.54 (1H, m) & 2.35 (1H, dd, J = 15.2 & 7.0 Hz)			
Tyr2	7.98 (1H, d, J = 7.5 Hz)	4.49 (1H, m)	2.79 (1H, m) & 2.62 (1H, m)	6.86 (2H, d, J = 8.5 Hz), 6.56 (2H, d, J = 8.5 Hz)		
Trp3	8.13 (1H, d, J = 8.2 Hz)	4.27 (1H, br)	3.17 (1H, dd, J = 14.6 & 3.4 Hz), 3.02 (1H, dd, J = 15.1 & 10.1 Hz)	Indole: 10.80 (2H, app d, J = 12.2 Hz), 7.57 (2H, app dd, J = 7.8 & 2.2 Hz), 7.32 (2H, app dd, J = 12.7 & 8.1 Hz), 7.17 (1H, d, J = 2.1 Hz), 7.05 (2H, m), 6.97 (2H, m)		
Orn4	8.11 (1H, m)	4.39 (1H, m)	1.72 (1H, m) & 1.56 (1H, m)	1.56 (2H, m)	2.78 (2H, m)	7.82 (2H, br m)
D-Orn5	7.92 (1H, d, J = 8.1 Hz)	4.38 (1H, m)	1.76 (1H, m) & 1.56 (1H, m)	1.56 (2H, m)	2.78 (2H, m)	7.82 (2H, br m)
Gly6	8.25 (1H, t, J = 5.4 Hz)	3.81 (1H, dd, J = 17.0 & 6.6 Hz), 3.73 (m)				
Orn7	8.09 (1H, m)	4.36 (1H, m)	1.41 (1H, br m) & 1.32 (1H, m)	1.32 (2H, m)	2.59 (2H, br m)	7.72 (2H, br)
D-Trp8	8.20 (1H, d, J = 8.6 Hz)	4.71 (1H, app q, J = 8.0 Hz)	3.09 (1H, dd, J = 13.8 & 4.9 Hz), 2.96 (1H, dd, J = 15.1 & 8.3 Hz)	Indole: 10.80 (2H, app d, J = 12.2 Hz), 7.57 (2H, app dd, J = 7.8 & 2.2 Hz), 7.32 (2H, app dd, J = 12.7 & 8.1 Hz), 7.11 (1H, d, J = 2.3 Hz), 7.05 (2H, m), 6.97 (2H, m)		
D-Thr9	8.19 (1H, d, J = 9.0 Hz)	4.55 (1H, m)	4.89 (1H, m)	1.09 (3H, d, J = 6.4 Hz)		
D-Ile10	8.58 (1H, d, J = 9.7 Hz)	4.12 (1H, app t, J = 10.5 Hz)	1.86 (1H, br m)	0.84 (3H, m), 1.51 (1H, m), 1.07 (1H, m)	0.84 (3H, m)	
Gly11	8.45 (1H, t, J = 6.3 Hz)	3.87 (1H, dd, J = 14.8 & 5.6 Hz), 3.54 (1H, dd, J = 15.2 & 6.1 Hz)				
D-Ser12	7.68 (1H, d, J = 8.8 Hz)	4.44 (1H, dt, J = 8.9 & 4.4 Hz)	3.78 (1H, m) & 3.62 (1H, br m)			
Lipid	2.06 (2H, m, O=CCH <sub>2</sub> -), 1.50 (2H, O=CCH <sub>2</sub> CH <sub>2</sub> -), 1.27 (5H, -CH <sub>2</sub> CH(CH <sub>3</sub> )CH <sub>2</sub> CH <sub>3</sub> ), 1.09 (2H, -CH <sub>2</sub> CH <sub>3</sub> ), 0.82 (6H, -CH(CH <sub>3</sub> )CH <sub>2</sub> CH <sub>3</sub> )					

## Ser9-brevicidine (3)

Residue	-NH	H $\alpha$	H $\beta$	H $\gamma$	H $\delta$	H $\epsilon$
D-Asn1	8.02 (1H, d, $J$ = 7.6 Hz)	4.54 (1H, app q, $J$ = 7.1 Hz)	2.53 (1H, under DMSO peak) & 2.35 (1H, dd, $J$ = 15.3 & 6.7 Hz)			
D-Tyr2	7.98 (1H, d, $J$ = 7.2 Hz)	4.27 (1H, m)	2.79 (1H, m) & 2.62 (1H, m)	Aromatic: 6.86 (2H, d, $J$ = 8.2 Hz) & 6.55 (2, d, $J$ = 8.2 Hz)		
D-Trp3	8.13 (1H, d, $J$ = 7.2 Hz)	4.49 (1H, br m)	3.17 (1H, br m) & 3.02 (1H, dd, $J$ = 14.4 & 9.8 Hz)	Indole: 10.80 (2H, s), 7.58 (2H, app dd, $J$ = 18.9 & 7.8 Hz), 7.32 (2H, app dd, $J$ = 14.9 & 8.1 Hz), 7.15 (1H, m), 7.05 (2H, m) & 6.97 (3H, m)		
D-Orn4	8.08 (1H, br d, $J$ = 7.8 Hz)	4.38 (1H, m)	1.72 (1H, m) & 1.55 (1H, m)	1.55 (2H, m)	2.78 (6H, m)	7.78 (2H, br)
Orn5	7.93 (1H, d, $J$ = 8.1 Hz)	4.37 (1H, m)	1.72 (1H, m) & 1.55 (1H, m)	1.55 (2H, m)	2.78 (6H, m)	7.78 (2H, br)
Gly6	8.22 (1H, m)	3.81 (1H, m) & 3.73 (1H, m)				
D-Orn7	8.05 (1H, d, $J$ = 8.3 Hz)	4.34 (1H, m)	1.38 (1H, m) & 1.33 (1H, m)	1.33 (2H, m)	2.59 (2H, m)	7.72 (2H, br)
Trp8	8.19 (1H, d, $J$ = 7.9 Hz)	4.64 (1H, m)	3.08 (1H, dd, $J$ = 14.2 & 2.91 (1H, dd, $J$ = 14.2 & 8.8 Hz)	Indole: 10.80 (2H, s), 7.58 (2H, app dd, $J$ = 18.9 & 7.8 Hz), 7.32 (2H, app dd, $J$ = 14.9 & 8.1 Hz), 7.10 (1H, m), 7.05 (2H, m) & 6.97 (3H, m)		
Ser9	8.38 (1H, d, $J$ = 7.2 Hz)	4.69 (1H, m)	4.20 (1H, dd, $J$ = 9.8 & 5.1 Hz) & 3.84 (1H, m)			
Ile10	8.71 (1H, d, $J$ = 9.7 Hz)	4.09 (1H, app t, $J$ = 10.1 Hz)	1.83 (1H, br m)	0.84 (3H, m), 1.54 (1H, m) & 1.11 (1H, m)	0.84 (3H, m)	
Gly11	8.53 (1H, t, $J$ = 6.3 Hz)	3.94 (1H, dd, $J$ = 15.1 & 6.4 Hz) & 3.47 (1H, dd, $J$ = 15.0 & 6.3 Hz)				
Ser12	7.46 (1H, br)	4.43 (1H, m)	3.71 (1H, m) & 3.57 (1H, m)			
Lipid	2.06 (2H, m, O=CCH <sub>2</sub> -), 1.50 (2H, O=CCH <sub>2</sub> CH <sub>2</sub> -), 1.27 (5H, -CH <sub>2</sub> CH(CH <sub>3</sub> )CH <sub>2</sub> CH <sub>3</sub> ), 1.10 (2H, -CH <sub>2</sub> CH <sub>3</sub> ) & 0.81 (6H, -CH(CH <sub>3</sub> )CH <sub>2</sub> CH <sub>3</sub> )					

### Dap9-brevicidine (5)

Residue	-NH	H $\alpha$	H $\beta$	H $\gamma$	H $\delta$	H $\epsilon$
D-Asn1	8.01 (1H, d, $J = 7.8$ Hz)	4.53 (1H, q, $J = 7.2$ Hz)	2.54 (under solvent) & 2.35 (1H, dd, $J = 15.5$ & 7.1 Hz)			
D-Tyr2	7.98 (1H, d, $J = 7.3$ Hz)	4.28 (1H, m)	2.77 (1H, m) & 2.61 (1H, m)	Aromatic: 6.85 (2H, d, $J = 8.5$ Hz), 6.55 (2H, d, $J = 8.4$ Hz)		
D-Trp3	8.11 (1H, d, $J = 7.3$ Hz)	4.46 (1H, m)	3.17 (1H, m) & 3.01 (1H, m)	Indole: 10.78 (2H, br m), 7.32 (2H, dd, $J = 14.9$ & 8.0 Hz), 7.17 (1H, br d, $J = 2.0$ Hz), 7.06 (3H, m) & 6.98 (3H, m)		
D-Orn4	8.05 (1H, d, $J = 8.3$ Hz)	4.35 (1H, m)	1.70 (1H, m) & 1.52 (1H, m)	1.52 (2H, m)	2.77 (2H, m)	7.71 (2H, br)
Orn5	7.92 (1H, d, $J = 7.6$ Hz)	4.35 (1H, m)	1.74 (1H, m) & 1.54 (1H, m)	1.55 (2H, m)	2.77 (2H, m)	7.69 (2H, br)
Gly6	8.22 (1H, t, $J = 5.3$ Hz)	3.82 (1H, dd, $J = 17.1$ & 5.3 Hz) & 3.74 (1H, dd, $J = 16.8$ & 4.8 Hz)				
D-Orn7	8.05 (1H, d, $J = 8.3$ Hz)	4.35 (1H, m)	1.28 (2H, m)	1.28 (2H, m)	2.58 (2H, m)	7.61 (2H, m)
Trp8	8.27 (1H, d, $J = 8.2$ Hz)	4.60 (1H, m)	3.05 (1H, m) & 2.88 (1H, m)	Indole: 10.89 (2H, br m), 7.32 (2H, dd, $J = 14.9$ & 8.0 Hz), 7.06 (3H, m) & 6.98 (3H, m)		
Dap9	8.30 (1H, m)	4.46 (1H, m)	3.44 (1H, dd, $J = 12.7$ & 6.0 Hz) & 3.03 (1H, m)			
Ile10	8.29 (1H, m)	4.05 (1H, app t. $J = 10.0$ Hz)	1.76 (1H, m)	1.48 (1H, m), 1.09 (1H, m) & 0.82 (3H, m)	0.82 (3H, m)	
Gly11	8.29 (1H, m)	3.86 (1H, dd, $J = 14.7$ & 6.1 Hz) & 3.53 (1H, dd, $J = 14.7$ & 6.2 Hz)				
Ser12	7.34 (1H, d, $J = 8.4$ Hz)	4.20 (1H, m)	3.57 (1H, m) & 3.34 (1H, m)			
Lipid	2.06 (2H, m, O=CCH <sub>2</sub> -), 1.49 (2H, O=CCH <sub>2</sub> CH <sub>2</sub> -), 1.25 (5H, -CH <sub>2</sub> CH(CH <sub>3</sub> )CH <sub>2</sub> CH <sub>3</sub> ), 1.08 (2H, m, -CH <sub>2</sub> CH <sub>3</sub> ) 0.80 (6H, -CH(CH <sub>3</sub> )CH <sub>2</sub> CH <sub>3</sub> ).					

## MeDap9-brevicidine (7)

Residue	-NH	H $\alpha$	H $\beta$	H $\gamma$	H $\delta$	H $\epsilon$
D-Asn1	8.03 (1H, d, $J$ = 7.8 Hz)	4.53 (1H, app q, $J$ = 7.2 Hz)	2.52 (Under DMSO peak) & 2.35 (1H, dd, $J$ = 15.2 & 7.0 Hz)			
D-Tyr2	7.98 (1H, d, $J$ = 7.5 Hz)	4.27 (1H, m)	2.79 (1H, m) & 2.62 (1H, m)	Aromatic: 6.86 (2H, d, $J$ = 8.4 Hz), 6.56 (2H, d, $J$ = 8.5 Hz)		
D-Trp3	8.15 (1H, m)	4.42 (1H, m)	3.17 (1H, dd, $J$ = 14.9 & 4.0 Hz) & 3.02 (1H, dd, $J$ = 14.5 & 8.9 Hz)	Indole: 10.81 (2H, d, $J$ = 15.8 Hz), 7.57 (2H, d, $J$ = 7.8 Hz), 7.32 (2H, app dd, $J$ = 11.1 & 8.1 Hz), 7.17 (1H, d, $J$ = 2.1 Hz), 7.05 (2H, m) & 6.97 (2H, m).		
D-Orn4	8.14 (1H, m)	4.37 (1H, m)	1.73 (1H, m) & 1.55 (1H, m)	1.55 (2H, m)	2.78 (2H, m)	7.86 (2H, br m)
Orn5	7.92 (1H, d, $J$ = 8.1 Hz)	4.38 (1H, m)	1.74 (1H, m) & 1.58 (1H, m)	1.58 (2H, m)	2.78 (2H, m)	7.86 (2H, br m)
Gly6	8.27 (1H, t, $J$ = 5.6 Hz)	3.81(1H, dd, $J$ = 16.7 & 5.6 Hz) & 3.73 (1H, dd, $J$ = 17.1 & 5.2 Hz)				
D-Orn7	8.09 (1H, d, $J$ = 8.4 Hz)	4.36 (1H, m)	1.34 (2H, m)	1.34 (2H, m)	2.59 (2H, m)	7.73 (2H, br)
Trp8	8.24 (1H, d, $J$ = 8.2 Hz)	4.68 (1H, m)	3.11 (1H, dd, $J$ = 15.6 & 4.5 Hz) & 2.95 (1H, dd, $J$ = 14.4 & 8.7 Hz)	Indole: 10.81 (2H, d, $J$ = 15.8 Hz), 7.57 (2H, d, $J$ = 7.8 Hz), 7.32 (2H, app dd, $J$ = 11.1 & 8.1 Hz), 7.12 (1H, d, $J$ = 2.1 Hz), 7.05 (2H, m) & 6.97 (2H, m).		
MeDap9	8.14 (1H, m)	4.41 (1H, dd, $J$ = 8.4 & 4.4 Hz)	4.18 (1H, m)	1.01 (3H, d, $J$ = 6.8 Hz), NH: 6.86 (2H, d, $J$ = 8.4 Hz)		
Ile10	8.59 (1H, d, $J$ = 9.5 Hz)	4.07 (1H, app t, $J$ = 10.2 Hz)	1.85 (1H, br)	0.86 (3H, m), 1.54 (1H, m) & 1.07 (1H, m)	0.86 (3H, m)	
Gly11	8.65 (1H, t, $J$ = 5.7 Hz)	3.93 (1H, dd, $J$ = 14.7 & 6.8 Hz) & 3.42 (under H <sub>2</sub> O)				
Ser12	7.54 (1H, d, $J$ = 8.9 Hz)	4.20 (1H, m)	3.66 (1H, m) & 3.52 (1H, m)			
Lipid	2.06 (2H, m, O=CCH <sub>2</sub> -), 1.50 (2H, O=CCH <sub>2</sub> CH <sub>2</sub> -), 1.26 (5H, -CH <sub>2</sub> CH(CH <sub>3</sub> )CH <sub>2</sub> CH <sub>3</sub> ), 1.06 (2H, -CH <sub>2</sub> CH <sub>3</sub> ) & 0.81 (6H, -CH(CH <sub>3</sub> )CH <sub>2</sub> CH <sub>3</sub> ).					

## Synthetic laterocidine (2)

Residue	-NH	H $\alpha$	H $\beta$	H $\gamma$	H $\delta$	H $\epsilon$
D-Ser1	7.85 (1H, d, <i>J</i> = 7.4 Hz)	4.26 (1H, dd, <i>J</i> = 13.5 & 6.4 Hz)	3.50 (2H, m)	5.12 (1H, t, <i>J</i> = 5.4 Hz)		
D-Tyr2	8.00 (1H, m)	4.34 (1H, m)	2.83 (1H, dd, <i>J</i> = 14.3 Hz & 4.4 Hz) & 2.62 (1H, dd, <i>J</i> = 14.1 & 9.5 Hz)	Aromatic: 6.89 (2H, d, <i>J</i> = 8.5 Hz), 6.56 (2H, d, <i>J</i> = 8.5 Hz)		
D-Trp3	8.00 (1H, m)	4.52 (1H, m)	3.15 (1H, m) & 2.93 (1H, m)	Indole: 10.79 (1H, s), 7.57 (1H, d, <i>J</i> = 7.8 Hz), 7.33 (1H, d, <i>J</i> = 8.0 Hz), 7.14 (1H, br s), 7.06 (1H, t, <i>J</i> = 8.0 Hz) & 6.98 (1H, t, <i>J</i> = 7.4 Hz)		
D-Orn4	8.03 (1H, m)	4.39 (1H, m)	1.73 (1H, m) & 1.56 (1H, m)	1.56 (2H, m)	2.82 (2H, m)	7.71 (2H, m)
Orn5	8.09 (1H, d, <i>J</i> = 8.3 Hz)	4.41 (1H, m)	1.70 (1H, m) & 1.52 (1H, m)	1.52 (2H, m)	2.76 (2H, m)	7.71 (2H, m)
Gly6	8.24 (1H, t, <i>J</i> = 5.2 Hz)	3.85 (1H, dd, <i>J</i> = 17.2 & 5.7 Hz) & 3.75 (1H, dd, <i>J</i> = 16.8 & 5.0 Hz)				
D-Orn7	8.07 (1H, d, <i>J</i> = 8.5 Hz)	4.40 (1H, m)	1.43 (1H, m) & 1.29 (1H, m)	1.43 (2H, m)	2.59 (2H, m)	7.63 (2H, m)
Trp8	8.32 (1H, d, <i>J</i> = 8.1 Hz)	4.75 (1H, m)	3.14 (1H, m) & 2.93 (1H, m)	Indole: 10.76 (1H, s), 7.59 (1H, d, <i>J</i> = 8.0 Hz), 7.32 (1H, d, <i>J</i> = 8.1 Hz), 7.12 (1H, br s), 7.04 (1H, t, <i>J</i> = 7.6 Hz) & 6.96 (1H, t, <i>J</i> = 7.6 Hz)		
Thr9	7.92 (1H, d, <i>J</i> = 6.4 Hz)	4.68 (1H, dd, <i>J</i> = 8.8 & 3.1 Hz)	5.17 (1H, m)	1.09 (3H, d, <i>J</i> = 6.4 Hz)		
Ile10	8.30 (1H, d, <i>J</i> = 3.1 Hz)	3.90 (1H, m)	1.57 (1H, m)	1.57 (1H, m), 1.11 (1H, m) & 0.86 (3H, m)	0.86 (3H, m)	
Asn11	9.40 (1H, d, <i>J</i> = 6.7 Hz)	4.12 (1H, m)	2.89 (1H, m) & 2.65 (1H, m)			
Gly12	8.03 (1H, m)	4.02 (1H, dd, <i>J</i> = 16.9 & 8.3 Hz) & 3.58 (1H, dd, <i>J</i> = 17.1 & 4.6 Hz)				
Gly13	7.67 (1H, m)	4.45 (1H, dd, <i>J</i> = 16.6 & 10.0 Hz) & 3.37 (under H <sub>2</sub> O)				
Lipid	2.10 (2H, m, O=CCH <sub>2</sub> -), 1.45 (3H, O=CCH <sub>2</sub> CH <sub>2</sub> - & -CH <sub>2</sub> CH(CH <sub>3</sub> ) <sub>2</sub> ), 1.20 (4H, -CH <sub>2</sub> CH <sub>2</sub> CH(CH <sub>3</sub> ) <sub>2</sub> ), 1.11 (2H, -CH <sub>2</sub> CH(CH <sub>3</sub> ) <sub>2</sub> ) & 0.83 (6H, -CH <sub>3</sub> CH(CH <sub>3</sub> ) <sub>2</sub> )					



**ent-laterocidine (ent-2)**

Residue	-NH	H $\alpha$	H $\beta$	H $\gamma$	H $\delta$	H $\epsilon$
Ser1	7.85 (1H, d, $J$ = 7.4 Hz)	4.27 (1H, q, $J$ = 6.6 Hz)	3.50 (2H, m)	-OH: 5.13 (1H, t, $J$ = 5.3 Hz)		
Tyr2	8.02 (1H, m)	4.34 (1H, td, $J$ = 8.3, 4.7 Hz)	2.82 (1H, dd, $J$ = 14.1, 3.9 Hz) & 2.62 (1H, dd, $J$ = 14.2, 9.8 Hz)	Aromatic: 6.89 (2H, d, $J$ = 8.4 Hz) & 6.56 (2H, d, $J$ = 8.3 Hz) & 9.17 (1H, s, -OH)		
Trp3	8.00 (1H, m)	4.52 (1H, app dd, $J$ = 13.3, 8.0 Hz)	3.15 (1H, dd, $J$ = 15.3, 4.2 Hz) & 2.94 (m)	Indole: 10.79 (1H, s), 7.57 (1H, d, $J$ = 7.9 Hz), 7.33 (1H, d, $J$ = 8.1 Hz), 7.14 (1H, app s), 7.06 (1H, t, $J$ = 7.6 Hz) & 6.98 (1H, t, $J$ = 7.5 Hz)		
Orn4	8.02 (1H, m)	4.38 (1H, m)	1.72 (1H, m) & 1.55 (1H, m)	1.55 (2H, m)	2.78 (2H, m)	7.73 (2H, br)
D-Orn5	8.10 (1H, d, $J$ = 8.1 Hz)	4.41 (1H, m)	1.70 (1H, m) & 1.52 (1H, m)	1.51 (2H, m)	2.76 (2H, m)	7.73 (2H, br)
Gly6	8.24 (1H, app t, $J$ = 5.3 Hz)	3.85 (1H, dd, $J$ = 16.7 & 5.7 Hz) & 3.75 (1H, dd, $J$ = 16.7 & 4.9 Hz)				
Orn7	8.07 (1H, d, $J$ = 8.2 Hz)	4.39 (1H, m)	1.43 (1H, m) & 1.29 (1H, m)	1.29 (1H, m)	2.58 (2H, br s)	7.65 (2H, m)
D-Trp8	8.32 (1H, d, $J$ = 7.7 Hz)	4.75 (1H, app dd, $J$ = 13.9, 8.2 Hz)	3.13 (1H, dd, $J$ = 15.9, 5.5 Hz) & 2.93 (1H, m)	Indole: 10.76 (1H, s), 7.59 (1H, d, $J$ = 7.9 Hz), 7.32 (1H, d, $J$ = 8.0 Hz), 7.13 (1H, app s), 7.04 (1H, t, $J$ = 7.4 Hz) & 6.96 (1H, t, $J$ = 7.4 Hz)		
D-Thr9	7.93 (1H, d, $J$ = 8.6 Hz)	4.69 (1H, dd, $J$ = 8.6, 3.0 Hz)	5.17 (1H, m)	1.09 (2H, d, $J$ = 6.2 Hz)		
D-Ile10	8.30 (1H, d, $J$ = 2.6 Hz)	3.90 (1H, dd, $J$ = 6.6, 3.8 Hz)	1.58 (1H, m)	1.58 (1H, m), 1.10 (1H, m) & 0.87 (2H, m)	0.87 (3H, m)	
D-Asn11	9.41 (1H, d, $J$ = 6.7 Hz)	4.12 (1H, m)	2.89 (1H, dd, $J$ = 16.1, 3.5 Hz) & 2.67 (1H, dd, $J$ = 16.1, 9.5 Hz)	-NH <sub>2</sub> : 7.37 (1H, br s)		
Gly12	8.03 (1H, m)	4.02 (1H, dd, $J$ = 17.0, 8.2 Hz), 3.58 (1H, dd, $J$ = 16.9, 4.3 Hz)				
Gly13	7.67 (1H, m)	4.46 (1H, dd, $J$ = 16.6, 9.9 Hz), 3.38 (under H <sub>2</sub> O) (1H, s)				
Lipid	2.11 (2H, m, O=CCH <sub>2</sub> -), 1.48 (1H, -CH <sub>2</sub> CH(CH <sub>3</sub> ) <sub>2</sub> ), 1.45 (2H, O=CCH <sub>2</sub> CH <sub>2</sub> -), 1.20 (2H, -CH <sub>2</sub> CH <sub>2</sub> CH(CH <sub>3</sub> ) <sub>2</sub> ), 1.19 (2H, br m, O=C(CH <sub>2</sub> ) <sub>2</sub> CH <sub>2</sub> -), 1.10 (2H, -CH <sub>2</sub> CH(CH <sub>3</sub> ) <sub>2</sub> ), 0.83 (6H, -CH <sub>2</sub> CH(CH <sub>3</sub> ) <sub>2</sub> )					

### Ser9-laterocidine (4)

Residue	-NH	H $\alpha$	H $\beta$	H $\gamma$	H $\delta$	H $\epsilon$
D-Ser	7.85 (1H, d, $J = 7.2$ Hz)	4.26 (1H, q, $J = 4.8$ Hz)	3.50 (m)			
D-Tyr2	8.00 (1H, m)	4.34 (1H, m)	2.83 (1H, dd, $J = 14.3$ & 3.8 Hz) & 2.62 (m)	6.89 (2H, d, $J = 8.3$ Hz) & 6.56 (2H, d, $J = 8.3$ Hz)		
D-Trp3	7.99 (1H, m)	4.52 (1H, m)	3.15 (1H, dd, $J = 14.7$ & 4.0 Hz) & 2.94 (m)	10.79 (1H, s), 7.57 (2H, app t, $J = 8.2$ Hz), 7.33 (1H, d, $J = 8.2$ Hz), 7.14 (1H, br s), 7.07 (1H, t, $J = 7.3$ Hz), 6.98 (1H, t, $J = 7.5$ Hz)		
D-Orn4	8.03 (1H, m)	4.38 (1H, m)	1.73 (1H, m), 1.56 (1H, m)	1.56 (2H, m)	2.78 (2H, m)	7.69 (2H, m)
Orn5z	8.08 (1H, d, $J = 8.7$ Hz)	4.41 (1H, m)	1.70 (1H, m), 1.52 (1H, m)	1.52 (2H, m)	2.77 (2H, m)	7.69 (2H, m)
Gly6	8.23 (1H, m)	3.82 (1H, dd, $J = 17.0$ & 5.9 Hz) & 3.76 (1H, dd, $J = 17.4$ & 4.1 Hz)				
D-Orn7	8.08 (1H, m)	4.40 (1H, m)	1.39 (1H, m), 1.29 (1H, m)	1.30 (2H, m)	2.58 (2H, m)	7.61 (2H, m)
Trp8	8.22 (1H, m)	4.69 (1H, m)	3.09 (2H, dd, $J = 14.5$ & 4.6 Hz) & 2.92 (m)	10.76 (1H, s), 7.57 (2H, app t, $J = 8.2$ Hz), 7.31 (1H, d, $J = 8.1$ Hz), 7.10 (1H, br s), 7.04 (1H, t, $J = 7.5$ Hz), 6.95 (1H, t, $J = 7.4$ Hz)		
Ser9	8.23 (1H, m)	4.62 (1H, m)	4.54 (1H, dd, $J = 11.0$ & 3.4 Hz) & 3.87 (1H, dd, $J = 10.4$ & 5.0 Hz)			
Ile10	8.31 (1H, d, $J = 5.0$ Hz)	4.06 (1H, m)	1.65 (1H, m)	1.52 (1H, m), 1.14 (1H, m) & 0.87 (3H, m)	0.86 (3H, m)	
Asn11	9.21 (1H, d, $J = 6.2$ Hz)	4.17 (1H, m)	2.87 (1H, dd, $J = 16.0$ & 3.8 Hz) & 2.62 (m)			
Gly12	7.98 (1H, m)	4.04 (1H, m) & 3.50 (1H, m)				
Gly13	7.60 (1H, m)	4.39 (1H, m) & 3.56 (1H, br m)				
Lipid	2.11 (2H, m, O=CCH <sub>2</sub> ), 1.46 (3H, O=CCH <sub>2</sub> CH <sub>2</sub> & (CH <sub>2</sub> ) <sub>2</sub> CH-), 1.20 (4H, (CH <sub>3</sub> ) <sub>2</sub> CHCH <sub>2</sub> CH <sub>2</sub> CH <sub>2</sub> -), 1.11 (2H, (CH <sub>3</sub> ) <sub>2</sub> CHCH <sub>2</sub> -), 0.83 (6H, (CH <sub>3</sub> ) <sub>2</sub> CHCH <sub>2</sub> -)					

## Dap9-Laterocidine (6)

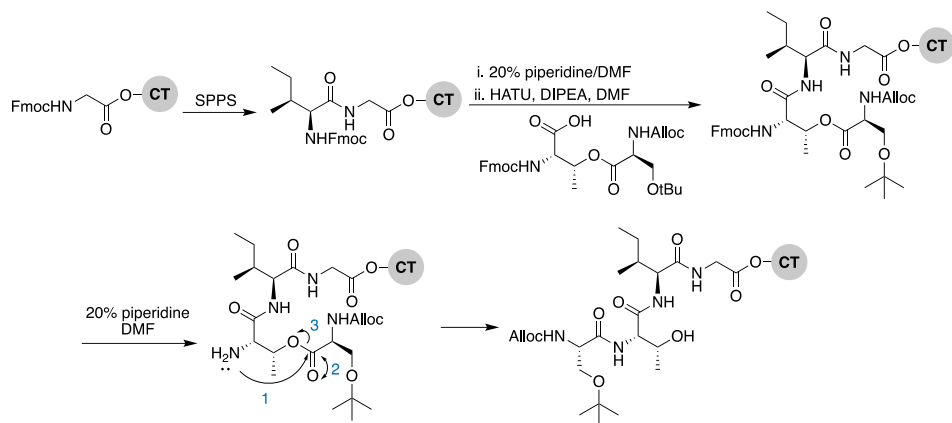
Residue	-NH	H $\alpha$	H $\beta$	H $\gamma$	H $\delta$	H $\epsilon$
D-Ser1	7.86 (1H, d, $J$ = 7.3 Hz)	4.26 (1H, q, $J$ = 6.7 Hz)	3.50 (1H, m) -OH: 5.14 (1H, br s)			
D-Tyr2	8.03 (1H, m)	4.33 (1H, m)	2.83 (1H, dd, $J$ = 14.3, 4.2 Hz) & 2.62 (1H, m)	Aromatic: 6.89 (2H, d, $J$ = 8.4 Hz) & 6.56 (2H, d, $J$ = 8.3 Hz) & 9.18 (1H, s, -OH)		
D-Trp3	8.02 (1H, m)	4.51 (1H, m)	3.15 (1H, dd, $J$ = 14.5, 3.8 Hz) & 2.94 (1H, dd, $J$ = 14.5, 9.3 Hz)	Indole: 10.80 (1H, s), 7.57 (1H, d, $J$ = 7.9 Hz), 7.33 (1H, d, $J$ = 8.1 Hz), 7.14 (1H, d, $J$ = 1.7 Hz), 7.06 (1H, t, $J$ = 7.5 Hz) & 6.98 (1H, t, $J$ = 7.4 Hz)		
D-Orn4	8.03 (1H, m)	4.38 (1H, m)	1.74 (2H, m)	1.56 (2H, m)	2.78 (2H, m)	7.75 (2H, br)
Orn5	8.09 (1H, m)	4.40 (1H, m)	1.70 (2H, m)	1.53 (2H, m)	2.78 (2H, m)	7.76 (2H, br)
Gly6	8.26 (1H, t, $J$ = 5.1 Hz)	3.79 (1H, dd, $J$ = 16.8, 5.7 Hz) & 3.74 (1H, m)				
D-Orn7	8.07 (1H, m)	4.33 (1H, m)	1.36 (1H, m) & 1.29 (1H, m)	1.29 (2H, m)	2.57 (2H, m)	7.67 (2H, m)
Trp8	8.15 (1H, d, $J$ = 8.3 Hz)	4.65 (1H, m)	3.09 (1H, dd, $J$ = 14.1, 3.8 Hz) & 2.88 (1H, br m)	Indole: 10.78 (1H, s), 7.61 (1H, d, $J$ = 7.9 Hz), 7.30 (1H, d, 8.1 Hz), 7.11 (1H, d, $J$ = 1.8 Hz), 7.04 (1H, t, $J$ = 7.4 Hz) & 6.96 (1H, t, $J$ = 7.4 Hz)		
Dap9	8.20 (1H, $J$ = 7.0 Hz)	4.29 (1H, br m)	3.74 (1H, m) & 2.67 (1H, m)	-NH: 7.67 (1H, m)		
Ile10	7.96 (1H, d, $J$ = 9.1 Hz)	4.51 (1H, m)	1.62 (1H, m)	1.05 (1H, br m), 1.40 (1H, m) & 0.85 (3H, m)	0.81 (3H, m)	
Asn11	9.22 (1H, d, $J$ = 6.2 Hz)	4.16 (1H, m)	2.92 (1H, m) & 2.56 (1H, m)	-NH <sub>2</sub> : 7.39 (1H, br s)		
Gly12	8.23 (1H, dd, $J$ = 9.1, 2.5 Hz)	4.23 (1H, dd, $J$ = 17.1, 9.6 Hz) & 3.28 (1H, br m)				
Gly13	7.72 (1H, dd, $J$ = 9.0, 3.5 Hz)	4.15 (1H, m) & 3.39 (under H <sub>2</sub> O)				
Lipid	2.10 (2H, m, O=CCH <sub>2</sub> -), 1.46 (3H, -CH <sub>2</sub> CH(CH <sub>3</sub> ) <sub>2</sub> & O=CCH <sub>2</sub> CH <sub>2</sub> -), 1.20 (4H, m, -CH <sub>2</sub> CH <sub>2</sub> CH(CH <sub>3</sub> ) <sub>2</sub> & O=C(CH <sub>2</sub> ) <sub>2</sub> CH <sub>2</sub> -), 1.11 (2H, -CH <sub>2</sub> CH(CH <sub>3</sub> ) <sub>2</sub> ) & 0.83 (6H, -CH <sub>2</sub> CH(CH <sub>3</sub> ) <sub>2</sub> )					

### MeDap9-laterocidine (8)

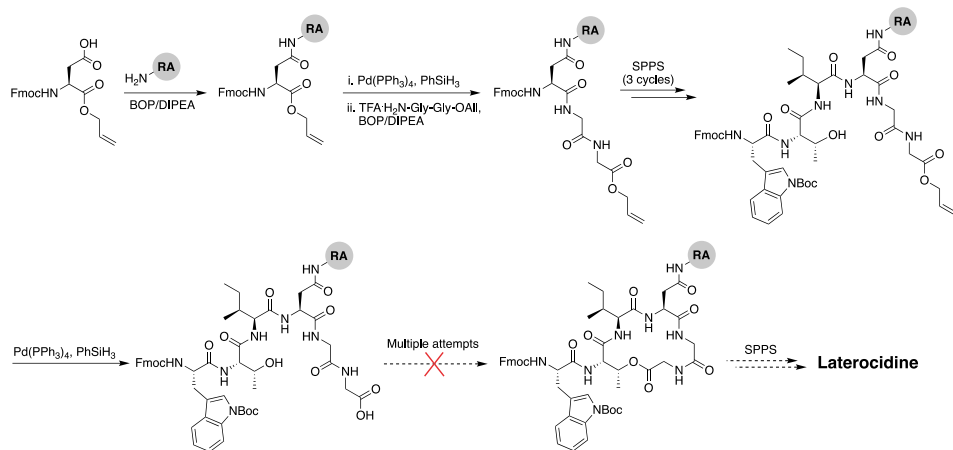
Residue	-NH	H $\alpha$	H $\beta$	H $\gamma$	H $\delta$	H $\epsilon$
D-Ser1	7.85 (1H, d, <i>J</i> = 7.4 Hz)	4.26 (1H, q, <i>J</i> = 6.7 Hz)	3.50 (2H, m) -OH: 5.12 (1H, <i>J</i> = 5.5 Hz)			
D-Tyr2	8.01 (1H, m)	4.33 (1H, m)	2.83 (1H, dd, <i>J</i> = 14.5, 4.2 Hz) & 2.62 (1H, m)	Aromatic: 6.89 (1H, d, <i>J</i> = 8.4 Hz) & 6.56 (1H, d, <i>J</i> = 8.3 Hz), 9.17 (1H, s, -OH)		
D-Trp3	8.00 (1H, m)	4.51 (1H, m)	3.15 (1H, dd, <i>J</i> = 14.3, 3.6 Hz) & 2.93 (1H, br m)	Indole: 10.79 (1H, s), 7.57 (1H, d, <i>J</i> = 7.8 Hz), 7.33 (1H, d, <i>J</i> = 8.1 Hz), 7.14 (1H, br s), 7.06 (1H, t, <i>J</i> = 7.5 Hz) & 6.98 (1H, t, <i>J</i> = 7.4 Hz)		
D-Orn4	8.03 (1H, d, <i>J</i> = 7.8 Hz)	4.38 (1H, m)	1.73 (1H, m) & 1.56 (1H, m)	1.53 (2H, m)	2.78 (2H, m)	7.71 (2H, m)
Orn5	8.08 (1H, m)	4.40 (1H, m)	1.70 (1H, m) & 1.53 (1H, m)	1.53 (2H, m)	2.77 (2H, m)	7.71 (2H, m)
Gly6	8.26 (1H, t, <i>J</i> = 5.0 Hz)	3.82 (1H, dd, <i>J</i> = 17.2, 5.8 Hz) & 3.73 (1H, dd, <i>J</i> = 16.9, 4.8 Hz)				
D-Orn7	8.13 (1H, d, <i>J</i> = 8.4 Hz)	4.38 (1H, m)	1.40 (1H, m) & 1.31 (1H, m)	1.31 (2H, m)	2.58 (2H, m)	7.63 (2H, br m)
Trp8	8.20 (1H, d, <i>J</i> = 7.8 Hz)	4.69 (1H, m)	3.08 (1H, dd, <i>J</i> = 14.6 & 4.1 Hz) & 2.92 (1H, m)	Indole: 10.78 (1H, s), 7.60 (1H, d, <i>J</i> = 7.7 Hz), 7.31 (1H, d, 8.1 Hz), 7.12 (1H, d, <i>J</i> = 1.7 Hz), 7.04 (1H, t, <i>J</i> = 7.5 Hz) & 6.96 (1H, t, <i>J</i> = 7.3 Hz)		
MeDap9	8.07 (1H, m)	4.52 (1H, m)	4.22 (1H, m)	1.05 (2H, d, <i>J</i> = 7.0 Hz), 6.88 (1H, m, NH)		
Ile10	7.91 (1H, d, <i>J</i> = 8.0 Hz)	4.35 (1H, m)	1.62 (1H, m) & 0.84 (1H, m)	1.43 (1H, m), 1.08 (1H, m) & 0.84 (3H, m)		
Asn11	9.25 (1H, d, <i>J</i> = 6.3 Hz)	4.14 (1H, m)	2.90 (1H, dd, <i>J</i> = 15.9 & 3.1 Hz) & 2.62 (1H, m)			
Gly12	8.35 (1H, br d, <i>J</i> = 7.6 Hz)	4.12 (1H, m) & 3.41 (1H, dd, <i>J</i> = 17.1 & 3.1 Hz)				
Gly13	7.73 (1H, m)	4.17 (1H, dd, <i>J</i> = 16.9 & 9.3 Hz) & 3.36 (1H, under H <sub>2</sub> O)				
Lipid	2.11 (2H, m, O=CCH <sub>2</sub> -), 1.46 (3H, -CH <sub>2</sub> CH(CH <sub>3</sub> ) <sub>2</sub> & O=CCH <sub>2</sub> CH <sub>2</sub> -), 1.20 (4H, -CH <sub>2</sub> CH <sub>2</sub> CH(CH <sub>3</sub> ) <sub>2</sub> ) & O=C(CH <sub>2</sub> ) <sub>2</sub> CH <sub>2</sub> -), 1.11 (2H, -CH <sub>2</sub> CH(CH <sub>3</sub> ) <sub>2</sub> ) & 0.83 (6H, -CH <sub>2</sub> CH(CH <sub>3</sub> ) <sub>2</sub> )					

NMR traces of all peptides can be found in the online supplementary material at DOI <https://doi.org/10.1039/D2SC00143H>

## Supplemental Schemes

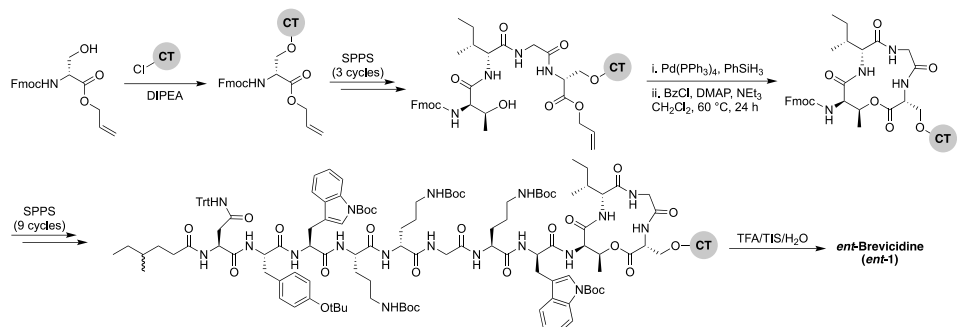


**Scheme S1.** Attempted synthesis of brevicidine failed due to deleterious O  $\rightarrow$  N acyl shift. CT = 2-chlorotrityl resin.

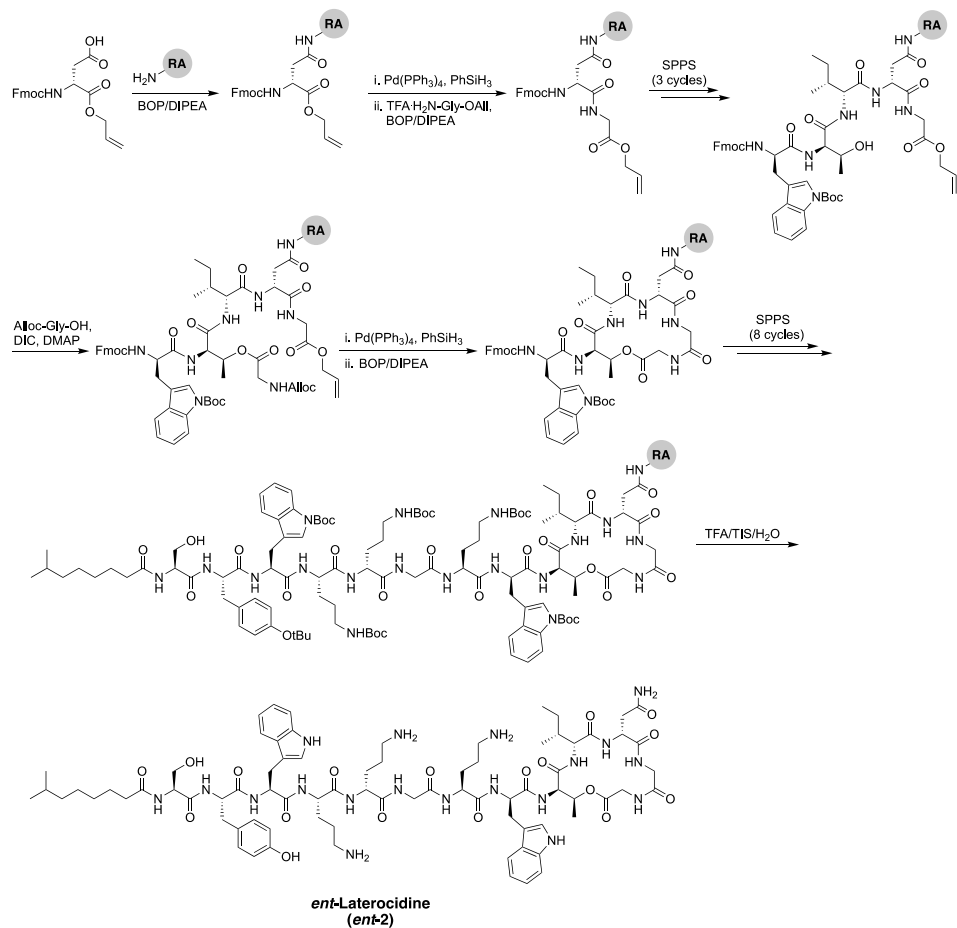


**Scheme S2.** Attempted synthesis of laterocidine failed at macrolactonization stage. RA = Rink amide resin.

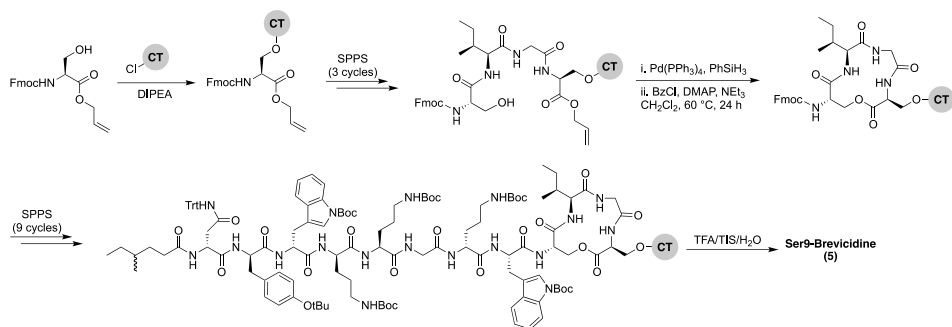
Synthetic Studies with the Brevicidine and Laterocidine Lipopeptide Antibiotics Including Analogues with Enhanced Properties and *In Vivo* Efficacy



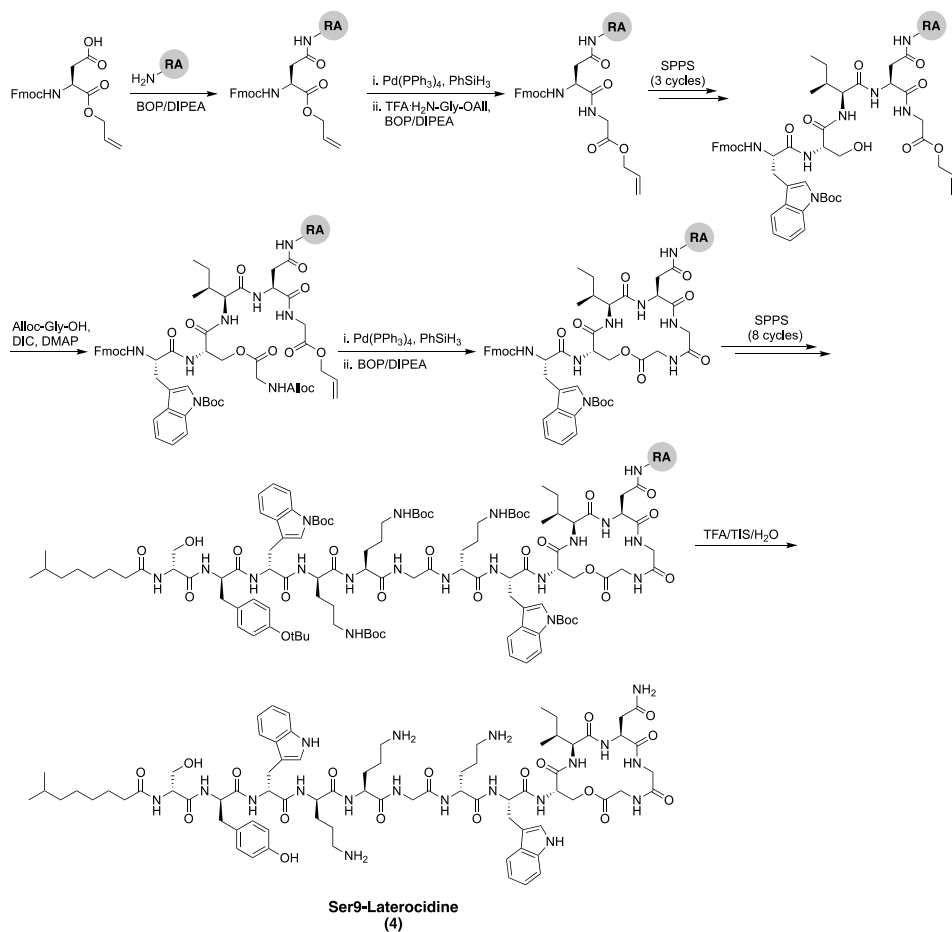
Scheme S3. Total SPPS of *ent*-brevicidine (*ent*-1). CT = 2-chlorotrityl resin.



Scheme S4. Total SPPS of *ent*-laterocidine (*ent*-2). RA = Rink amide resin.

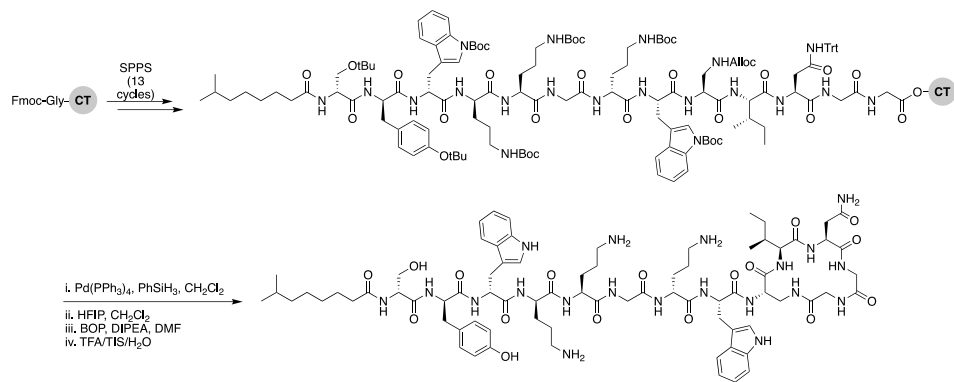


**Scheme S5.** Total SPPS of Ser9-brevicidine (3). CT = 2-chlorotrityl resin.



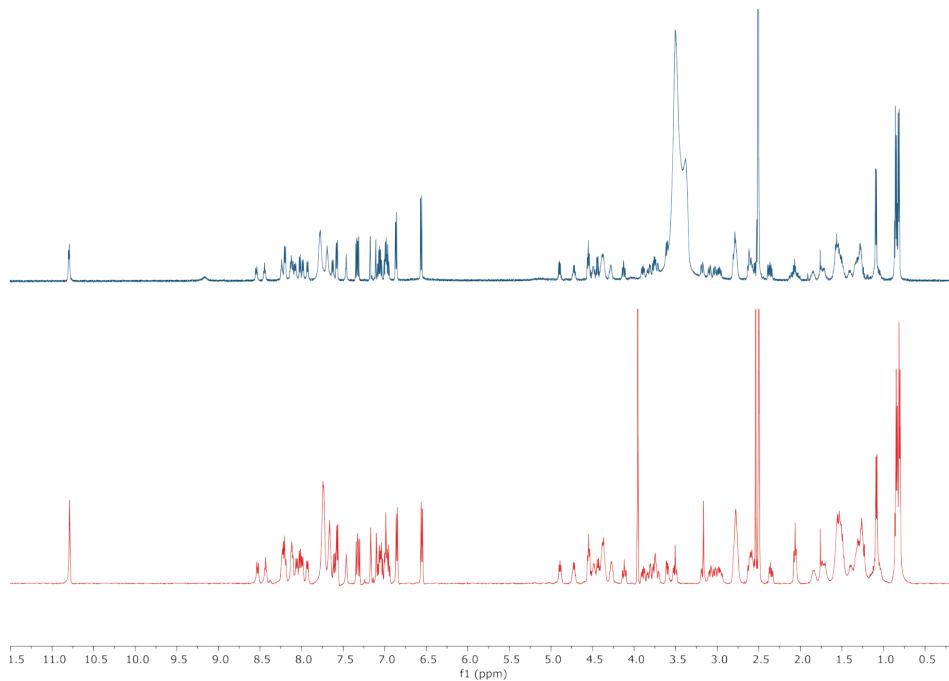
**Scheme S6.** Total SPPS of Ser9-laterocidine (4). RA = Rink amide resin.

Synthetic Studies with the Brevicidine and Laterocidine Lipopeptide Antibiotics  
Including Analogues with Enhanced Properties and *In Vivo* Efficacy



**Scheme S7.** Combination synthesis of Dap9-laterocidine (**6**) where the entire protected linear peptide is assembled by SPPS, and cyclized and deprotected in solution. CT = 2-chlorotrityl resin.



**Supplemental figures**

**Figure S1.** <sup>1</sup>H NMR (600 MHz, DMSO-d<sub>6</sub>) of synthetic brevicidine (top) overlaid with the previously published <sup>1</sup>H NMR (500 MHz, DMSO-d<sub>6</sub>) spectrum of natural brevicidine (bottom) isolated from fermentation of the producing organism. Spectra were recorded at room temperature. The spectrum for the synthetic material contains broad signals between 3.30-3.65 ppm due to H<sub>2</sub>O/HDO present in the NMR solvent. The peak at ca. 3.96 ppm in the published spectrum of brevicidine is attributed to an impurity not present in the synthetic material.

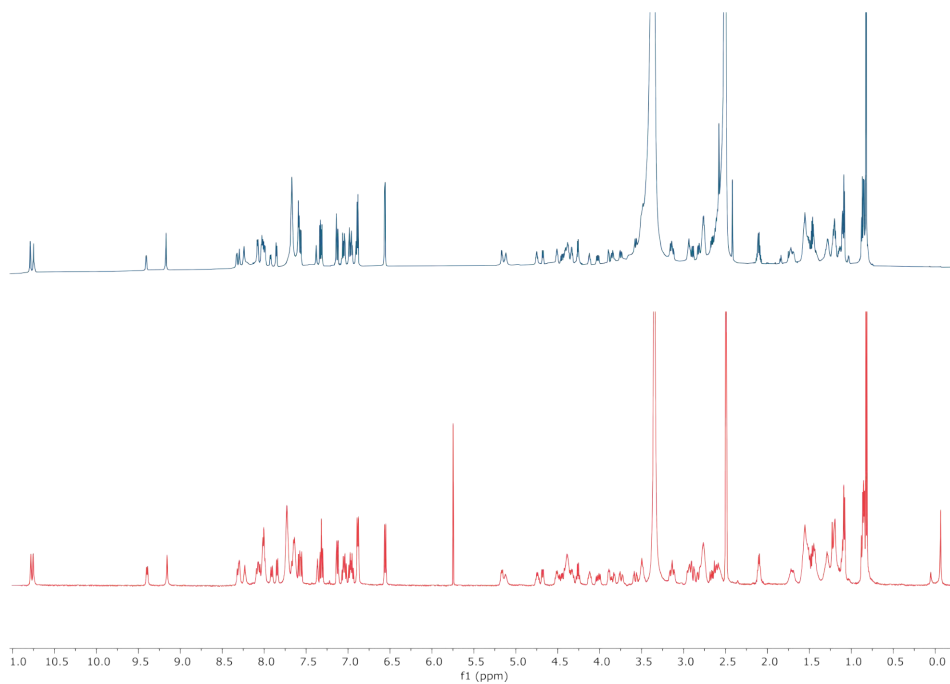
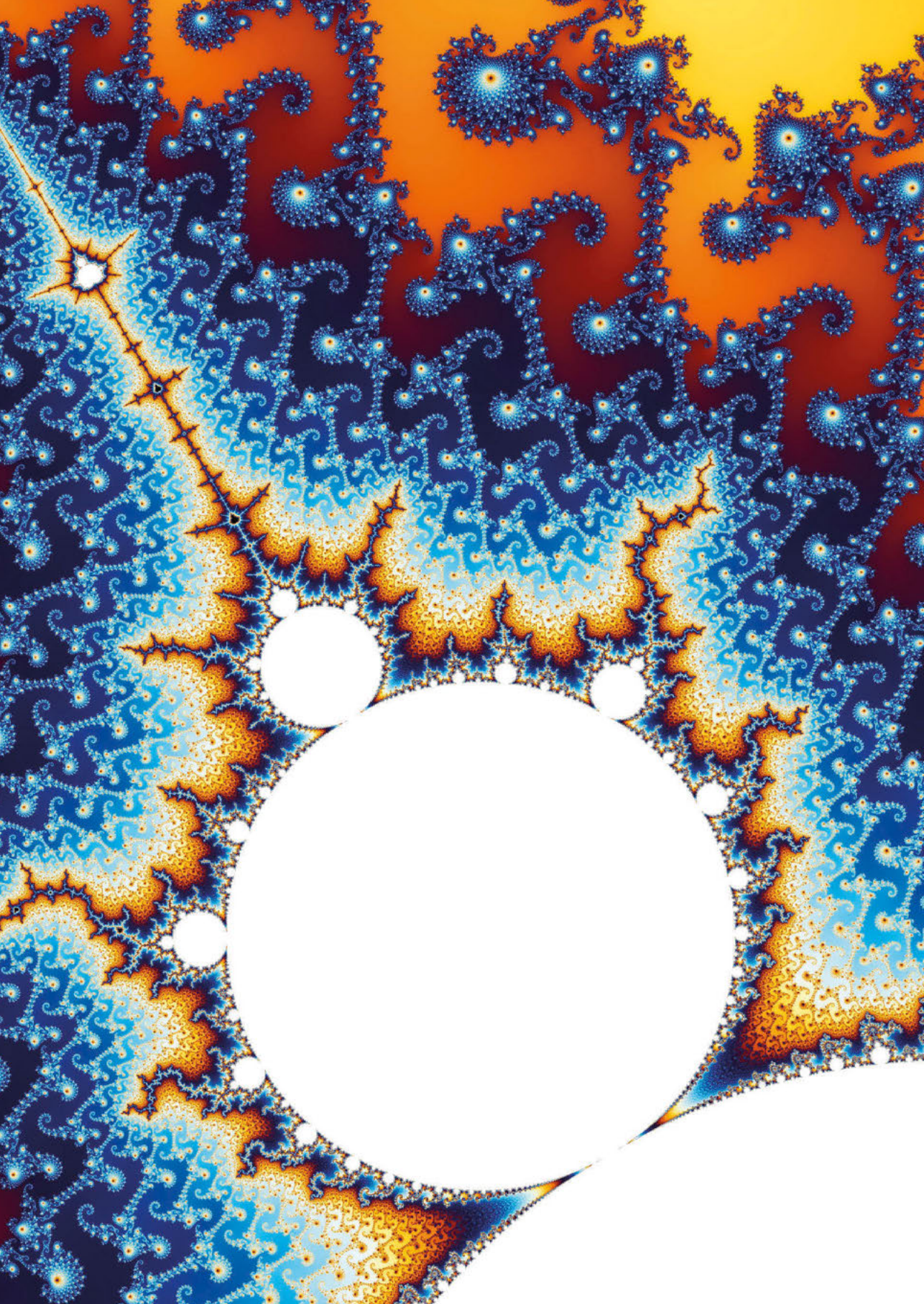


**Figure S2.** <sup>1</sup>H NMR (850 MHz, DMSO-d<sub>6</sub>) of synthetic laterocidine (top) overlaid with the previously published <sup>1</sup>H NMR (500 MHz, DMSO-d<sub>6</sub>) spectrum of natural laterocidine (bottom) isolated from fermentation of the producing organism. Spectra were recorded at room temperature.

## References

- (1) Bierbaum, G.; Sahl, H.-G. The Search for New Anti-Infective Drugs: Untapped Resources and Strategies. *International Journal of Medical Microbiology* **2014**, *304* (1), 1–2. <https://doi.org/10.1016/j.ijmm.2013.10.003>.
- (2) Brown, E. D.; Wright, G. D. Antibacterial Drug Discovery in the Resistance Era. *Nature* **2016**, *529* (7586), 336–343. <https://doi.org/10.1038/nature17042>.
- (3) Brown, E. D. Gram-Negative Resistance. *ACS Infect Dis* **2015**, *1* (11), 507–507. <https://doi.org/10.1021/acinfecdis.5b00123>.
- (4) O'Neill, J. *Antimicrobial Resistance: Tackling a Crisis for the Health and Wealth of Nations*; 2014. <https://amr-review.org/>.
- (5) WHO. <https://www.who.int/news-room/detail/27-02-2017-who-publishes-list-of-bacteria-for-which-new-antibiotics-are-urgently-needed>.
- (6) Li, Y. X.; Zhong, Z.; Zhang, W. P.; Qian, P. Y. Discovery of Cationic Nonribosomal Peptides as Gram-Negative Antibiotics through Global Genome Mining. *Nat Commun* **2018**, *9* (1). <https://doi.org/10.1038/s41467-018-05781-6>.
- (7) Morales, F. E.; Garay, H. E.; Muñoz, D. F.; Augusto, Y. E.; Otero-González, A. J.; Reyes Acosta, O.; Rivera, D. G. Aminocatalysis-Mediated on-Resin Ugi Reactions: Application in the Solid-Phase Synthesis of N-Substituted and Tetrazolo Lipopeptides and Peptidosteroids. *Org Lett* **2015**, *17* (11), 2728–2731. <https://doi.org/10.1021/acs.orglett.5b01147>.
- (8) Diamandas, M.; Moreira, R.; Taylor, S. D. Solid-Phase Total Synthesis of Dehydrotryptophan-Bearing Cyclic Peptides Tunicyclin B, Sclerotide A, CDA3a, and CDA4a Using a Protected  $\beta$ -Hydroxytryptophan Building Block. *Org Lett* **2021**, *23* (8), 3048–3052. <https://doi.org/10.1021/acs.orglett.1c00717>.
- (9) Al-Ayed, K.; Ballantine, R. D.; Zhong, Z.; Li, Y.; Cochrane, S.; Martin, N. Total Synthesis of the Brevicidine and Laterocidine Family of Lipopeptide Antibiotics. *ChemRxiv* **2021**, 1–8. <https://doi.org/10.26434/CHEMRXIV.13660949.V1>.
- (10) Pelay-Gimeno, M.; García-Ramos, Y.; Jesús Martín, M.; Spengler, J.; Molina-Guijarro, J. M.; Munt, S.; Francesch, A. M.; Cuevas, C.; Tulla-Puche, J.; Albericio, F. The First Total Synthesis of the Cyclodepsipeptide Pipecolidepsin A. *Nat Commun* **2013**, *4* (1), 2352. <https://doi.org/10.1038/ncomms3352>.
- (11) Hermant, Y.; Palpal-latoc, D.; Kovalenko, N.; Cameron, A. J.; Brimble, M. A.; Harris, P. W. R. The Total Chemical Synthesis and Biological Evaluation of the Cationic Antimicrobial Peptides, Laterocidine and Brevicidine. *J Nat Prod* **2021**, *84* (8), 2165–2174. <https://doi.org/10.1021/acs.jnatprod.1c00222>.
- (12) McDougal, P. G.; Griffin, J. H. Enantiotrascin. *Bioorg Med Chem Lett* **2003**, *13* (13), 2239–2240. [https://doi.org/10.1016/S0960-894X\(03\)00252-X](https://doi.org/10.1016/S0960-894X(03)00252-X).
- (13) Kleijn, L. H. J.; Vlieg, H. C.; Wood, T. M.; Sastre Toraño, J.; Janssen, B. J. C.; Martin, N. I. A High-Resolution Crystal Structure That Reveals Molecular Details of Target Recognition by the Calcium-Dependent Lipopeptide Antibiotic Laspartomycin C. *Angewandte Chemie International Edition* **2017**, *56* (52), 16546–16549. <https://doi.org/10.1002/anie.201709240>.
- (14) Cochrane, S. A.; Findlay, B.; Vederas, J. C.; Ratemi, E. S. Key Residues in Octyl-Tridecaptin A 1 Analogues Linked to Stable Secondary Structures in the Membrane. *ChemBioChem* **2014**, *15* (9), 1295–1299. <https://doi.org/10.1002/cbic.201402024>.
- (15) Vetterli, S. U.; Zerbe, K.; Müller, M.; Urfer, M.; Mondal, M.; Wang, S. Y.; Moehle, K.; Zerbe, O.; Vitale, A.; Pessi, G.; Eberl, L.; Wollscheid, B.; Robinson, J. A. Thanatin Targets the Intermembrane Protein Complex Required for Lipopolysaccharide Transport in Escherichia Coli. *Sci Adv* **2018**, *4* (11). [https://doi.org/10.1126/SCIADV.AAU2634/SUPPL\\_FILE/AAU2634\\_SM.PDF](https://doi.org/10.1126/SCIADV.AAU2634/SUPPL_FILE/AAU2634_SM.PDF).
- (16) Moreira, R.; Taylor, S. D. The Chiral Target of Daptomycin Is the 2R, 2'S Stereoisomer of Phosphatidylglycerol. *Angewandte Chemie International Edition* **2022**, *61* (4), e202114858. <https://doi.org/10.1002/anie.202114858>.
- (17) Nam, J.; Shin, D.; Rew, Y.; Boger, D. L. Alanine Scan of [L-Dap<sup>2</sup>]Ramoplanin A<sub>2</sub> Aglycon: Assessment of the Importance of Each Residue. *J Am Chem Soc* **2007**, *129* (28), 8747–8755. [https://doi.org/10.1021/JA068573K/SUPPL\\_FILE/JA068573KSI20070517\\_065843.PDF](https://doi.org/10.1021/JA068573K/SUPPL_FILE/JA068573KSI20070517_065843.PDF).
- (18) Bionda, N.; Stawikowski, M.; Stawikowska, R.; Cudic, M.; López-Vallejo, F.; Treitl, D.; Medina-Franco, J.; Cudic, P. Effects of Cyclic Lipodepsipeptide Structural Modulation on Stability, Antibacterial Activity, and

- Human Cell Toxicity. *ChemMedChem* **2012**, *7* (5), 871–882. <https://doi.org/10.1002/cmdc.201200016>.
- (19) Hart, P. T.; Kleijn, L. H. J.; de Bruin, G.; Oppedijk, S. F.; Kemmink, J.; Martin, N. I. A Combined Solid- and Solution-Phase Approach Provides Convenient Access to Analogues of the Calcium-Dependent Lipopeptide Antibiotics. *Org. Biomol. Chem.* **2014**, *12* (6), 913–918. <https://doi.org/10.1039/C3OB42238K>.
- (20) Gimenez, D.; Phelan, A.; Murphy, C. D.; Cobb, S. L. Fengycin A Analogues with Enhanced Chemical Stability and Antifungal Properties. *Org Lett* **2021**, *23* (12), 4672–4676. [https://doi.org/10.1021/ACS.ORGLETT.1C01387/ASSET/IMAGES/LARGE/OL1C01387\\_0004.JPEG](https://doi.org/10.1021/ACS.ORGLETT.1C01387/ASSET/IMAGES/LARGE/OL1C01387_0004.JPEG).
- (21) Li, Z.; Chakraborty, P.; de Vries, R. H.; Song, C.; Zhao, X.; Roelfes, G.; Scheffers, D. J.; Kuipers, O. P. Characterization of Two Relacidines Belonging to a Novel Class of Circular Lipopeptides That Act against Gram-Negative Bacterial Pathogens. *Environ Microbiol* **2020**, *22* (12), 5125–5136. <https://doi.org/10.1111/1462-2920.15145>.
- (22) Mukherjee, S.; van der Donk, W. A. Mechanistic Studies on the Substrate-Tolerant Lanthipeptide Synthetase ProcM. *J Am Chem Soc* **2014**, *136* (29), 10450–10459. <https://doi.org/10.1021/ja504692v>.
- (23) Ge, J.; Li, L.; Yao, S. Q. A Self-Immobilizing and Fluorogenic Unnatural Amino Acid That Mimics Phosphotyrosine. *Chemical Communications* **2011**, *47* (39), 10939. <https://doi.org/10.1039/c1cc14653j>.
- (24) Freire, F.; Fisk, J. D.; Peoples, A. J.; Ivancic, M.; Guzei, I. A.; Gellman, S. H. Diacid Linkers That Promote Parallel  $\beta$ -Sheet Secondary Structure in Water. *J Am Chem Soc* **2008**, *130* (25), 7839–7841. <https://doi.org/10.1021/ja802042c>.
- (25) Chun, C.; Lee, S. M.; Kim, S. Y.; Yang, H. K.; Song, S.-C. Thermosensitive Poly(Organophosphazene)–Paclitaxel Conjugate Gels for Antitumor Applications. *Biomaterials* **2009**, *30* (12), 2349–2360. <https://doi.org/10.1016/j.biomaterials.2008.12.083>.
- (26) Moreira, R.; Barnawi, G.; Beriashvili, D.; Palmer, M.; Taylor, S. D. The Effect of Replacing the Ester Bond with an Amide Bond and of Overall Stereochemistry on the Activity of Daptomycin. *Bioorg Med Chem* **2019**, *27* (1), 240–246. <https://doi.org/10.1016/J.BMC.2018.12.004>.
- (27) Gude, M.; Ryf, J.; White, P. D. An Accurate Method for the Quantitation of Fmoc-Derivatized Solid Phase Supports. *Letters in Peptide Science* **2002**, *9* (4), 203–206. <https://doi.org/10.1023/A:1024148619149>.



## Chapter 3

# Synthesis and Structure–Activity Relationship Studies of N-terminal Analogues of the Lipopeptide Antibiotics Brevicidine and Laterocidine

### *Abstract*

The brevicidine and laterocidine family of lipopeptide antibiotics exhibit strong activity against multidrug-resistant Gram-negative bacteria, while showing low propensity to induce resistance. Both peptides feature a branched lipid tail on the N-terminal residue, which for brevicidine is chiral. Here, we report the synthesis and biological evaluation of a library of brevicidine and laterocidine analogues wherein the N-terminal lipid is replaced with linear achiral fatty acids. Optimal lipid chain lengths were determined and new analogues with strong activity against colistin-resistant *E. coli* produced.

### **Parts of this chapter have been published in RSC Medicinal Chemistry:**

Ballantine, R. D.\*; Al Ayed, K.\*; Bann, S. J.; Hoekstra, M.; Martin, N. I.; Cochrane, S. A. Synthesis and Structure-Activity Relationship Studies of N-Terminal Analogues of the Lipopeptide Antibiotics Brevicidine and Laterocidine. RSC Med. Chem. **2022**, 00, 1–3. <https://doi.org/10.1039/D2MD00281G>

### **Parts of the data in this chapter are part of a patent:**

"Antibiotic natural product analogues"; Cochrane, S.A.; Ballantine, R. D.; Martin, N. I.; Al Ayed, K.; Hoekstra, M.; Zamarbide Losada, S.D.; Priority Date: 28 January 2021; Published: 4 August 2022; WO2022162332A1

\*Authors contributed equally

## Introduction

Antimicrobial resistance (AMR) is set to become a major crisis within our lifetime. In addition to the economic costs, it is estimated that the number of deaths caused by AMR will rise to 10 million annually by 2050.<sup>1</sup> In fact, the number of deaths attributable to bacterial AMR surpassed the yearly deaths caused by breast cancer in 2019.<sup>2</sup> Given the pressing need for new antibacterial agents, synthesis and structure-activity relationship (SAR) studies with novel lead compounds remain valuable strategies for addressing the rising tide of AMR.

Non-ribosomal lipopeptides represent a gold mine of potential antimicrobials with desirable therapeutic advantages, including strong activity against multidrug-resistant bacteria, multifaceted modes of action,<sup>3</sup> and superior proteolytic stability when compared to ribosomal antimicrobial peptides.<sup>4-7</sup> Their superior stability arises from the presence of D-amino acids and/or macrocyclic motifs, both of which improve proteolytic stability. Lipopeptides are secondary metabolites produced by non-ribosomal peptide synthetases (NRPSs), and are often N-acylated with a lipid tail.<sup>8</sup> The lipids are biosynthetically derived from the branched amino acids (valine, leucine and isoleucine), therefore it is common that bacterial lipopeptides feature a similarly branched acyl group.<sup>9</sup> Owing to the synthetic challenge and expense associated with incorporating these features into peptide synthesis, a common focus of SAR studies is to vary the N-terminal lipid tail. Lipid tail libraries have been created for many lipopeptides, including tridecaptins,<sup>10</sup> paenibacterin,<sup>7</sup> cerexin A<sub>1</sub><sup>11</sup> and polymyxins.<sup>12</sup>

Brevicidine (**1**) and laterocidine (**2**) (Fig. 1) are two novel peptides that were recently reported by Li *et al.* following a biosynthetic gene cluster mining strategy.<sup>13</sup> Given their strong antimicrobial activity against Gram-negative bacteria (including colistin-resistant *E. coli*), along with their low cytotoxicity and low propensity to induce resistance, we recently developed methods to access both brevicidine and laterocidine by solid-phase peptide synthesis (SPPS).<sup>14</sup> The ability to synthesize this family of lipopeptides has allowed for the possibility of SAR studies including the structurally related relacidines.<sup>15</sup> Brevicidine (**1**) and laterocidine (**2**) each feature an N-terminal acyl chain; 4-methylhexanoyl in the former and 6-methyloctanoyl in the latter. Herein, we report the development of novel N-terminal lipid analogues of brevicidine and laterocidine with strong and selective activity against Gram-negative bacteria.

## Results and Discussion

Lipid analogues were synthesized following our previously reported methods.<sup>14</sup> Briefly: for analogues of brevicidine, Fmoc-Ser-OAllyl was first loaded on to 2-chlorotrityl (CT) chloride resin via the side chain and standard Fmoc-SPPS was performed to synthesize the tetrapeptide (**4**). Allyl ester deprotection, followed by an on-resin modified Yamaguchi esterification afforded the macrocyclic lactone portion of the peptide, which was subsequently extended through the N-terminus via SPPS to obtain the desired analogues. Similarly, for analogues of laterocidine, Fmoc-Asp-OAllyl was first loaded onto Rink Amide (RA) resin via its side chain. The allyl group was next removed and H-Gly-OAllyl was coupled after which SPPS was used to obtain linear pentapeptide (**7**). An on-resin Steglich esterification between the free hydroxyl of threonine and Alloc-Gly-OH was then performed. Both allyl and Alloc groups

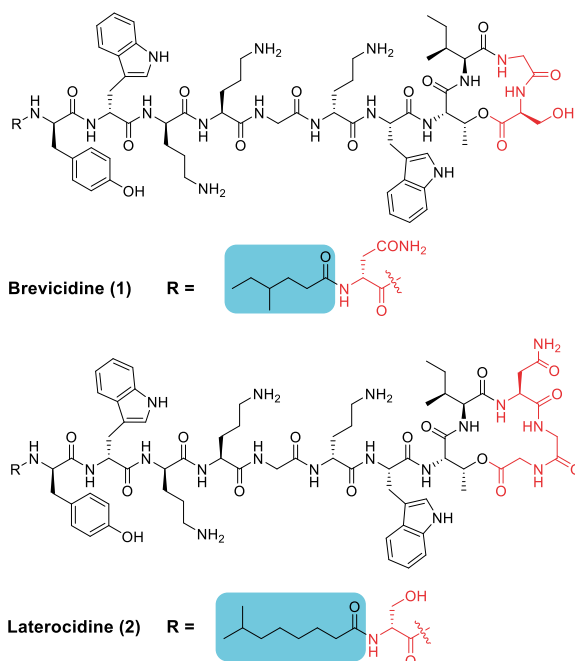


**Fig. 1.** Structures of brevicidine (1) and Laterocidine (2). N-terminal lipid tails are highlighted in blue and structural differences between the two lipopeptides in red.

were subsequently removed followed by an on-resin macrolactamization which yielded the laterocidine macrocycle. The cyclic intermediate was then further elaborated through to the N-terminus by SPPS. Natural brevicidine has a chiral 4-methylhexanoyl lipid tail, the configuration of which has not been previously reported. This likely has an (*S*)-configuration as such lipids are often derived from isoleucine.<sup>8</sup> As chiral lipids are expensive and/or must be chemically synthesized, we chose to synthesise lipid tail analogues containing cheaper, commercially available lipids. The brevicidine and laterocidine variants prepared included unacylated peptides (9 & 18) and C2 – C16 lipidated brevicidine (10 – 17) and laterocidine (19 – 26) analogues, with lipid length incrementally increasing by two carbons for each analogue. Peptides were synthesized in overall yields ranging between 5-27% (after HPLC purification).

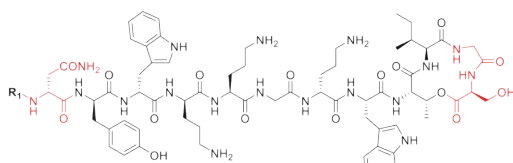
The minimum inhibitory concentrations (MICs) of brevicidine and laterocidine analogues were determined against a panel of clinically relevant ESKAPE pathogens; *Escherichia coli* (*E. coli*), *Klebsiella pneumoniae* (*K. pneumoniae*), *Acinetobacter baumannii* (*A. baumannii*), *Pseudomonas aeruginosa* (*P. aeruginosa*) and *Staphylococcus aureus* (*S. aureus*), which cause the majority of nosocomial infections in the United States.<sup>16</sup> Notably, while colistin (polymyxin E) is used as a last-resort antibiotic in the treatment of infections caused by many Gram-negative bacteria, the emergence of plasmid-borne genes conferring colistin resistance (*mcr*) threatens to render this drug ineffectual.<sup>17</sup> In this resistance mechanism, the polymyxin target (Lipid A) is modified, reducing binding affinity. For this reason, a strain of colistin-resistant *E. coli* carrying the *mcr-1* gene was also included in the panel.



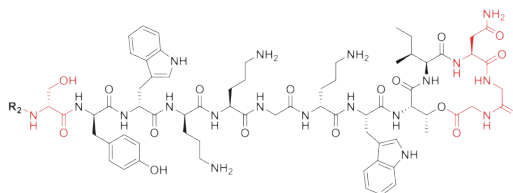
**Table 1.** Antimicrobial activity of brevicidine and laterocidine analogues 9 – 26.

Compound	Lipid Chain length	Antimicrobial Activity ( $\mu\text{g/mL}$ )						Hemolytic Activity (%)
		<i>E. coli</i> ATCC 25922	<i>E. coli</i> ATCC 2 5922 MCR-1	<i>K. pneumoniae</i> ATCC 1 3883	<i>A. baumannii</i> ATCC 17961	<i>P. aeruginosa</i> PAO1	<i>S. aureus</i> USA300	
1	C7	4	4	2	4	8	>32	0.8
9	H	>32	>32	>32	>32	16	>32	0.2
10	C2	>32	>32	>32	>32	8	>32	0.2
11	C4	32	32	8	32	16	>32	0.1
12	C6	8	8	4	16	>32	>32	0.3
13	C8	16	16	16	16	8	>32	0.4
14	C10	4	4	4	4	8	32	6.2
15	C12	8	8	8	4	16	32	13.3
16	C14	16	16	32	4	32	>32	18.0
17	C16	>32	>32	>32	32	>32	>32	13.3
2	C9	2	2	2-4	2	4	>32	0.4
18	H	>32	>32	>32	>32	>32	>32	0.2
19	C2	>32	>32	>32	>32	16	>32	0.2
20	C4	16	32	32	>32	8	>32	0.3
21	C6	4	8	8	16	4	>32	0.2
22	C8	2	2	2	4	2	>32	0.2
23	C10	2	2	2-4	2	2	>32	2.1
24	C12	4	4	8	2	8	32	21.5
25	C14	8	8	8	2	8	16	56.2
26	C16	32	32	>32	4	32	32	46.1
Colistin	C8/C9	0.5	8	0.5	$\leq 0.25$	4	>32	<0.1
0.1% TX100	ND	ND	ND	ND	ND	ND	ND	100

ND = not determined. All assays run in triplicate. [Peptide] in hemolytic assays = 64  $\mu\text{g/mL}$ . Additional strain information in supplementary information.

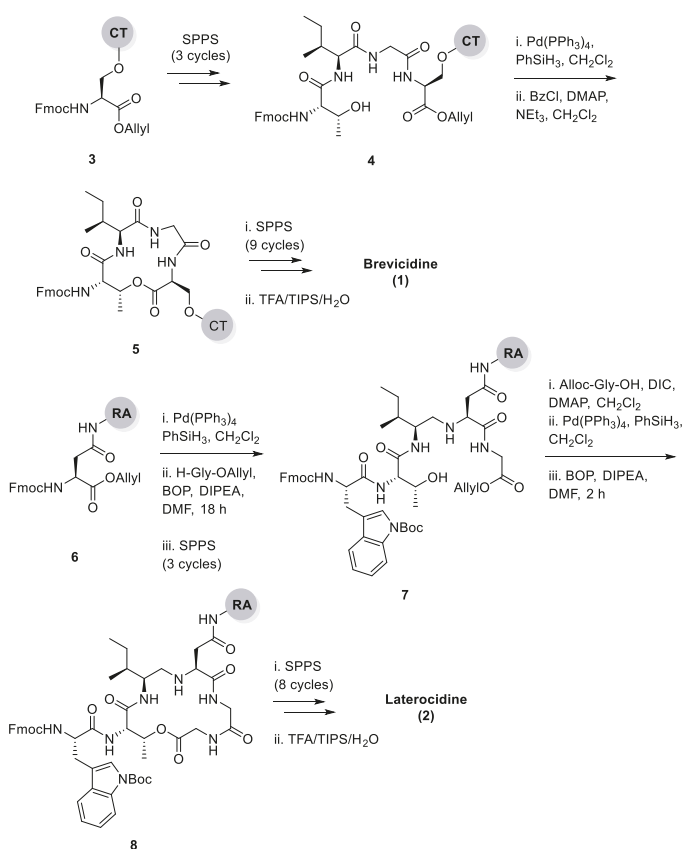


9: R<sub>1</sub> = H; 10: R<sub>1</sub> = C(O)CH<sub>3</sub>; 11: R<sub>1</sub> = C(O)C<sub>3</sub>H<sub>7</sub>; 12: R<sub>1</sub> = C(O)C<sub>6</sub>H<sub>11</sub>; 13: R<sub>1</sub> = C(O)C<sub>7</sub>H<sub>15</sub>;  
14: R<sub>1</sub> = C(O)C<sub>9</sub>H<sub>19</sub>; 15: R<sub>1</sub> = C(O)C<sub>11</sub>H<sub>23</sub>; 16: R<sub>1</sub> = C(O)C<sub>13</sub>H<sub>27</sub>; 17: R<sub>1</sub> = C(O)C<sub>15</sub>H<sub>31</sub>;



18: R<sub>2</sub> = H; 19: R<sub>2</sub> = C(O)CH<sub>3</sub>; 20: R<sub>2</sub> = C(O)C<sub>2</sub>H<sub>5</sub>; 21: R<sub>2</sub> = C(O)C<sub>6</sub>H<sub>11</sub>; 22: R<sub>2</sub> = C(O)C<sub>7</sub>H<sub>15</sub>;  
23: R<sub>2</sub> = C(O)C<sub>9</sub>H<sub>19</sub>; 24: R<sub>2</sub> = C(O)C<sub>11</sub>H<sub>23</sub>; 25: R<sub>2</sub> = C(O)C<sub>13</sub>H<sub>27</sub>; 26: R<sub>2</sub> = C(O)C<sub>15</sub>H<sub>31</sub>;

Synthesis and Structure–Activity Relationship Studies of N-terminal Analogues of the Lipopeptide Antibiotics Brevicidine and Laterocidine



**Scheme 1.** On-resin syntheses of brevicidine (1) (top) laterocidine (2) (bottom). CT: 2-Chlorotrityl chloride resin, RA: Rink amide resin.

For the brevicidine lipid analogues, H-Brev (9), C2-Brev (10) and C16-Brev (17) showed complete ablation of antimicrobial activity (>32 µg/mL). The latter could possibly be due to reduced solubility of the peptide in Mueller Hinton broth (MHB), despite using DMSO as an additive, or activity could be diminished by hydrophobic self-aggregation interfering with the peptide's ability to interact with the bacterial membrane. Inversely, peptides lacking a lipid tail or with a very short lipid are likely unable to insert into the bacterial membrane thus limiting their ability to disrupt the membrane or self-permeabilise through to the periplasm.<sup>18</sup> A similar observation has been made for unacylated analogues of polymyxin B and colistin which display no antimicrobial activity, despite retaining the ability to efficiently bind with high specificity to lipopolysaccharide (LPS).<sup>18</sup> Notably, our lipid scan with brevicidine and laterocidine revealed an apparent double “sweet-spot” in activity with C6-Brev (12), which generally showed a two-fold decrease in activity across strains, and C10-Brev (14) which maintained comparable activity to Brevicidine (1). C10-Brev (14) likely has similar hydrophobic properties to the natural branched C7 lipid in Brev, whereas C8-Brev (13) is less hydrophobic and less active. The higher activity of C6 vs C8 was unexpected but could

be due to improved solubility. In the case of the laterocidine analogues, a broader increase in antimicrobial activity was observed for analogues **20** – **25** with C8-Lat (**22**) and C10-Lat (**23**) exhibiting the same activity as Laterocidine (**2**).

H-Lat (**18**), C2-Lat (**19**) and C16-Lat (**26**) showed a marked decrease in activity – with the exception of C16-Lat (**26**) against *A. baumannii* (4 µg/mL). The more hydrophobic analogues are likely less active due to their poorer solubility in aqueous media. Gratifyingly, the activities of the brevicidine and laterocidine analogues against *E. coli* were unaffected by the presence of the *mcr-1* resistance gene, paralleling the early *in vitro* results by Li *et al.*<sup>13</sup> These findings further underscore the potential for this class of lipopeptide antibiotics to be developed as a therapeutic alternative against drug-resistant infections.

Having ascertained the antimicrobial activity of all synthetic peptides against a panel of ESKAPE pathogens, we next assessed their mammalian toxicity with hemolytic assays using sheep red blood cells. The % hemolysis for all peptides at 64 µg/mL was determined, with the hemolysis induced by the surfactant 0.1% Triton X-100 taken as 100%. The peptide concentration used is 32x the MIC of the most potent analogues. Hemolysis was <1% for all analogues with a C8 chain or shorter, including the strongest antibacterial peptide C8-Lat (**22**). Hemolytic activity increased up to C14 (>50% for C14-Lat) and then decreased at longer chain lengths, perhaps due to decreased solubility of peptides or aggregation.

## Conclusions

In summary, a library of *N*-terminal lipid analogues was generated for brevicidine (**9** – **17**) and laterocidine (**18** – **26**) using our previously established synthetic approaches. The peptides were assayed *in vitro* against a panel of ESKAPE pathogens to identify analogues with comparable activities to synthetic brevicidine (**1**) and laterocidine (**2**). The substitution with a decanoyl tail in both brevicidine (**14**) and laterocidine (**23**) had no effect on the antimicrobial activity, including colistin-resistant *E. coli*. This strong activity against drug-resistant Gram-negative bacteria coupled with the reduced synthetic cost highlights these analogues as potential therapeutic candidates for future development.

## Experimental methods

### Materials

**Brevicidine Analogues.** All proteinogenic Fmoc-amino acids used in this study were purchased from CEM. The remaining Fmoc-amino acids, including Fmoc-D-Trp(Boc)-OH, Fmoc-D-Tyr(tBu)-OH and Fmoc-D-Asn(Trt)-OH were purchased from Fluorochem. Fmoc-D-Orn(Boc)-OH was purchased from Merck. Fmoc-L-Orn(Boc)-OH was purchased from ChemImpex. Fmoc-Ser-OAllyl,<sup>19</sup> Fmoc-Asp-OAllyl,<sup>20</sup> TFA·H<sub>2</sub>N-Gly-OAllyl<sup>21</sup> were synthesized according to referenced literature procedures. Acetic anhydride, butyric acid, decanoic acid and dodecanoic acid were purchased from Alfa Aesar. Hexanoic acid and octanoic acid were purchased from Sigma-Aldrich. Myristic acid was sourced from the C6 to C14 Fatty Acid Kit by Matreya Inc. Palmitic acid was purchased from Fluorochem. [Bis(dimethylamino)methylene]-1*H*-1,2,3-triazolo[4,5-*b*]pyridinium-3-oxidhexafluorophosphate (HATU),

trifluoroacetic acid (TFA) and triisopropylsilane (TIPS) were also purchased from Fluorochem. 2-Chlorotrityl chloride resin and diisopropylethylamine (DIPEA) were purchased from Sigma-Aldrich. HPLC grade acetonitrile (MeCN), dichloromethane ( $\text{CH}_2\text{Cl}_2$ ) and dimethylformamide (DMF) were purchased from Merck. All chemicals were used without further purification.

**Laterocidine analogues.** Fmoc-L-Orn(Boc)-OH and Fmoc-D-Orn(Boc)-OH were purchased from Combi-Blocks. All other Fmoc-amino acids and the Rink amide MBHA resin were purchased from P3 BioSystems. Acetic anhydride, butyric acid, lauric acid, myristic acid, palmitic acid, sodium diethyldithiocarbamate trihydrate and pyridine were purchased from Acros Organics. Hexanoic acid, octanoic acid and decanoic acid were purchased from Alfa Aesar. ((1H-Benzo[d][1,2,3]triazol-1-yl)oxy)tris(dimethylamino)phosphonium hexafluorophosphate (BOP), N,N-Diisopropylcarbodiimide (DIC) and triisopropylsilane (TIPS) were purchased from Manchester Organics. 4-Dimethylaminopyridine (DMAP) was purchased from Sigma Aldrich. Diisopropylethylamine (DIPEA), piperidine, trifluoroacetic acid (TFA) and dimethyl sulfoxide (DMSO) were purchased from Carl Roth. Dichloromethane ( $\text{CH}_2\text{Cl}_2$ ) and petroleum ether were purchased from VWR Chemicals. Acetonitrile (MeCN), dimethylformamide (DMF) and methyl tertiary-butyl ether (MTBE) were purchased from Biosolve. Tetrakis(triphenylphosphine)palladium(0) and phenylsilane were purchased from Fluorochem.

### Antimicrobial testing

Colistin sulfate was purchased from Activate Scientific. Kanamycin monosulfate was purchased from MP Biomedicals. *E. coli* ATCC 25922, *S. aureus* USA300 (ATCC BAA1717), *K. pneumoniae* ATCC 13883 and *A. baumannii* ATCC 17961 belong to the American Type Culture Collection (ATCC). *P. aeruginosa* PAO1 was kindly provided by L.H.C. Quarles Van Ufford, Utrecht University, Utrecht, The Netherlands. *E. coli* ATCC 25922 MCR-1 was transfected in house using the pGDP2-MCR1 plasmid kindly provided by Yong-Xin Li, The University of Hong Kong, Hong Kong, China. Sheep blood agar plates (Ref. PB5039A) were purchased from Thermo Scientific. Tryptic soy broth (Ref. 02-200-500) was purchased from Scharlab. Mueller-Hinton broth (Ref. X927.1) was purchased from Carl Roth. Polypropylene 96-wells plates (Ref. 3879) were purchased from Corning.

### General procedure for manual peptide synthesis

**Brevicidine analogues.** Analogues of brevicidine were synthesized according to our previously reported synthesis.<sup>14</sup> To a flame dried 50 mL round bottom flask was added Fmoc-Ser-Oallyl (220 mg, 0.600 mmol) and dry dichloromethane ( $\text{CH}_2\text{Cl}_2$ ) (10.0 mL). 2-Chlorotrityl (CT) chloride resin (2.00 g, 0.81 mmol  $\text{g}^{-1}$ ) and DIPEA (420  $\mu\text{L}$ , 2.40 mmol) were added. The suspension was stirred under argon for 24 h at 45 °C, after which the resin was filtered through a manual SPPS vessel and washed with  $\text{CH}_2\text{Cl}_2$  (3 x 10 mL). The resin was then capped by adding a solution of MeOH, DIPEA and  $\text{CH}_2\text{Cl}_2$  (20 mL, 10 : 5 : 85) and bubbled with argon for 1 h. The resin was washed with DMF (3 x 10 mL) then  $\text{CH}_2\text{Cl}_2$  (3 x 10 mL) and dried under a positive pressure of argon. A small portion of resin was then used to ascertain the loading. Estimation of loading level of first residue onto resin (0.16 mmol  $\text{g}^{-1}$ ) was calculated via an Fmoc loading test, as described by Gude *et al.*<sup>22</sup>

Standard Fmoc SPPS protocol was used to extend the peptide to the linear Fmoc-Thr-Ile-Gly-Ser stage. Specifically, loaded resin (1.56 g, 0.25 mmol) was added to a manual SPPS vessel and bubbled in DMF (15 mL) for 15 min to swell. The solvent was discharged and the resin was bubbled in an Fmoc deprotection solution of 20% piperidine in DMF (3 x 15 mL, 2 x 1 min then 1 x 5 min) with argon. The resin was washed with DMF (3 x 15 mL) and a coupling solution of amino acid (5 equiv), HATU (5 equiv) and DIPEA (10 equiv) in DMF (15 mL) was added. The solution was then bubbled with argon for 1 h, before the solution was discharged and the resin washed with DMF (3 x 15 mL). The process was repeated to obtain on-resin linear Fmoc-tetrapeptide. An allyl deprotection solution of tetrakis(triphenylphosphine) palladium (578 mg, 0.500 mmol) and phenylsilane (308  $\mu$ L, 2.50 mmol) in  $\text{CH}_2\text{Cl}_2$  and DMF (1:1, 20 mL) was added. The solution was bubbled with argon for 2 h in darkness, after which the deprotection solution was discharged and the resin was washed with DMF (3 x 15 mL), 0.5% sodium diethyldithiocarbamate solution in DMF (4 x 15 mL), DMF (4 x 15 mL) and  $\text{CH}_2\text{Cl}_2$  (4 x 15 mL). The resin was dried under argon, then added to a 100 mL flame dried round bottom flask under argon. Dry dichloroethane (50 mL), benzoyl chloride (30  $\mu$ L, 0.258 mmol), triethylamine (139  $\mu$ L, 9.97 mmol) and catalytic DMAP (3.00 mg, 24.6  $\mu$ mol) were added. The mixture was stirred overnight at 60 °C. The reaction was cooled to room temperature before the resin was filtered through a manual SPPS vessel and washed with DMF (3 x 15 mL) and  $\text{CH}_2\text{Cl}_2$  (3 x 15 mL) and dried under argon. To ascertain a successful macrolactonisation, a small sample was cleaved using 2% TFA solution in  $\text{CH}_2\text{Cl}_2$  (1 mL). The cleavage cocktail was gently agitated for 1 h and filtered through a glass wool plug. The filtrate was concentrated with a gentle stream of argon before being analyzed by LC-MS. Desired cyclic product was identified ( $[\text{M}+\text{H}]^+$  calculated for  $\text{C}_{30}\text{H}_{36}\text{N}_4\text{O}_8$  581.2, found (LC-MS) 581.4. Following this modified Yamaguchi esterification, Fmoc SPPS was continued using the above protocol to complete the linear peptide portion. The resin was then divided and the lipid tails were attached to the *N*-terminus using the same procedure (0.05 mmol scale). Acetylated brevicidine (**11**) was synthesized by adding on-resin peptide (306 mg, 50.0  $\mu$ mol) to a manual SPPS vessel with DMF (5 mL) to swell for 10 min. The solvent was discharged and a solution of acetic anhydride (240  $\mu$ L, 2.54 mmol), DIPEA (440  $\mu$ L, 2.53 mmol) and DMAP (1 crystal) in DMF (5 mL) was added and bubbled for 2.5 h with argon. The resin was then washed with DMF (3 x 5 mL) and  $\text{CH}_2\text{Cl}_2$  (3 x 5 mL) then dried under argon. The dried resin was then added to a cleavage cocktail of TFA, TIPS and distilled water (3 mL, 95 : 2.5 : 2.5) and heated to 37 °C for 1 h. The suspension was filtered through a glass wool plug and the filtrate concentrated under vacuum. Diethyl ether was used to precipitate the crude peptide, which was then centrifuged and washed with additional diethyl ether. The suspension was centrifuged and the pellet dissolved in the minimal amount of 1:1 acetonitrile and water solution with 0.1% TFA. The crude mixture was subsequently purified by RP-HPLC Method A. Fractions were assessed by LC-MS and product containing fractions were pooled, frozen and lyophilized to yield the lipid analogues.

**Laterocidine analogues.** Rink amide MBHA (5.00 g, 0.67 mmol  $\text{g}^{-1}$ ) was loaded via the sidechain carboxyl group of Fmoc-Asp-Oallyl (2.65 g, 6.70 mmol) with BOP (2.96 g, 6.70 mmol) and DIPEA (2.33 mL, 13.4 mmol) in DMF (150 mL) overnight. The resin was capped with acetic anhydride and pyridine (3 : 2) for 30 min and the resin loading was determined as above (0.50 mmol  $\text{g}^{-1}$ ). Two batches of the loaded resin (1.00 g, 0.500 mmol) were bubbled in tetrakis(triphenylphosphine) palladium (150 mg, 0.130 mmol) and phenylsilane (1.50 mL,

12.2 mmol) in  $\text{CH}_2\text{Cl}_2$  (30 mL) with nitrogen for 1 h. The resin was subsequently washed with  $\text{CH}_2\text{Cl}_2$  (5 x 20 mL), sodium diethyldithiocarbamic acid trihydrate in DMF (5 mg  $\text{mL}^{-1}$ , 5 x 20 mL) and DMF (5 x 20 mL). TFA· $\text{H}_2\text{N}$ -Gly-OAllyl (230 mg, 1.00 mmol) was coupled using BOP (442 mg, 0.999 mmol) and DIPEA (350  $\mu\text{L}$ , 2.01 mmol) under nitrogen flow for 1 h. Fmoc SPPS was continued using a similar procedure as above: Fmoc was removed using a 20% piperidine solution (3 x 10 mL, 2 x 2 min then 1 x 10 min). The resin was washed and a coupling solution of amino acid (4 equiv), BOP (4 equiv) and DIPEA (8 equiv) in DMF (10 mL) was added and bubbled with nitrogen for 1 h. The process was repeated to extend the N-terminus to include Trp8. The resin was then treated with Alloc-Gly-OH (1.20 g, 7.54 mmol), DIC (1.20 mL, 7.66 mmol) and DMAP (30.0 mg, 0.246 mmol) in  $\text{CH}_2\text{Cl}_2$  and DMF (16 mL, 3 : 1) under nitrogen for 18 h. Alloc protecting groups were removed following the aforementioned protocol with tetrakis(triphenylphosphine) palladium. Cyclization was then achieved by adding a solution of BOP (442 mg, 0.999 mmol) and DIPEA (350  $\mu\text{L}$ , 2.01 mmol) in DMF (10 mL) and bubbling with nitrogen for 2 h. The remaining linear N-terminal section of the peptide was synthesized using the above SPPS protocol. The two batches of resin were divided and lipid tails were attached as above on a 0.1 mmol scale. Dried resin was subsequently added to cleavage cocktail containing TFA, TIPS and  $\text{H}_2\text{O}$  (5 mL, 95 : 2.5 : 2.5) for 1.5 h. The reaction mixture was then filtered through cotton and precipitated in MTBE and petroleum ether (1 : 1). The resulting precipitate was washed with fresh MTBE and petroleum ether (1 : 1) and lyophilized from *t*-butanol and water (1 : 1). The crude peptide was then purified by RP-HPLC Method B. Pure fractions were pooled and lyophilized.

### Purification and analysis of peptides

**Prep RP-HPLC purification of crude peptides.** Brevicidine analogues were purified by Reversed-Phase High Performance Column Chromatography (RP-HPLC). Purification was performed on a Perkin Elmer HPLC system composed of a 200 series binary pump, UV/Vis detector, vacuum degasser, Rheodyne 7725i injector. The system was operated using ThermoFisher Chromeleon 7.2 software. **Method A (Preparative):** Phenomenex Luna C18 column (5  $\mu\text{m}$ , 250 x 21.2 mm) equipped with a 2 mL sample loop. Runs were performed at a flow rate of 10 mL/min with UV detection at 220 nm. Solvent A = 0.1 % TFA in MilliQ water and solvent B = 0.1 % TFA in MeCN. A gradient method for  $\text{C}_0 - \text{C}_{12}$  brevicidine analogues was employed, starting from 5 % B and 95 % A for 5 min, ramping up to 8 % B over 20 min, then ramping up to 20 % B over 15 min, ramping up to 30 % B over 3 min, ramping again up to 95 % B over 4 min, remaining at 95 % B for 3 min, ramping down to 5 % B over 2 min before staying at 5 % B for 5 min. A gradient method for  $\text{C}_{14} - \text{C}_{16}$  brevicidine analogues was employed, starting from 5 % B and 95 % A for 5 min, ramping up to 27 % solvent B over 6 min, then ramping up to 44 % solvent B over 7 min, ramping up again to 78 % solvent B over 9 min, ramping to 95 % solvent B over 3 min, remaining at 95 % B for 2 min before ramping down to 5 % B over 3 min and remaining there for 5 min. **Method B (Preparative):** Purification was performed on a BESTA-Technik system with a Dr. Maisch ReproSil Gold 120 C18 column (10  $\mu\text{m}$ , 25 x 250 mm) and equipped with a ECOM Flash UV detector. Runs were performed at a flow rate of 12 mL/min with UV detection at 214 nm and 254 nm. Solvent A = 0.1% TFA in water/MeCN (95 : 5) and solvent B = 0.1% TFA in water/MeCN (5 : 95). A gradient method was employed, starting at 100 % solvent A for 5 min, ramping up to 70 % solvent B over 50 min, remaining at 70 % solvent B for 3 min before ramping down to 100 % solvent A over 1 min and remaining there for 5 min. Product containing fractions

were pooled, partially concentrated under vacuum, frozen and then lyophilized to yield pure peptides as white flocculent solids. A small amount of purified peptide was analyzed by analytical HPLC. **Method C (Analytical):** Analytical runs of brevicidine analogues were performed on a Perkin Elmer HPLC system composed of a 200 series quaternary pump, UV/Vis detector, vacuum degasser, Rheodyne 7725i injector equipped with a 200  $\mu$ L sample loop and Phenomenex Luna C18 column (5  $\mu$ m, 150 x 4.6 mm). The system was operated using ThermoFisher Chromeleon 7.2 software. Runs were performed at a flow rate of 2 mL/min with UV detection at 220 nm. Solvent A = 0.1 % TFA in MilliQ water and solvent B = 0.1 % TFA in MeCN. A gradient method was employed, starting from 20 % B and 80 % A for 2 min, ramping up to 95 % B over 18 min, ramping down to 20 % B over 0.1 min before staying at 20 % B for 3.9 min. **Method D (Analytical):** Analytical runs of laterocidine analogues were performed on a Shimadzu Prominence-i LC-2030 system with a Dr. Maisch ReproSil Gold 120 C18 (5  $\mu$ m, 4.6 x 250 mm) at 30 °C. Runs were performed at a flow rate of 1 mL/min with UV detection at 214 nm and 254 nm. Solvent A = 0.1% TFA in water/CAN (95 : 5) and solvent B = 0.1% TFA in water/CAN (5 : 95). A gradient method for C<sub>0</sub> - C<sub>12</sub> laterocidine was employed, starting at 100% solvent A for 2 min, ramping up to 50 % Solvent B over 45 min, ramping up to 100% solvent B over 1 min, remaining at 100% solvent B for 6 min before ramping down to 100% solvent A over 1 min and remaining there for 5 min. A gradient method for C<sub>14</sub> - C<sub>16</sub> laterocidine was employed, starting at 100% solvent A for 2 min, ramping up to 70 % solvent B over 45 min, ramping up to 100% solvent B over 1 min, remaining there for 6 min before ramping down to 100% solvent A and remaining there for 5 min. High resolution mass spectrometry (HRMS) spectra of brevicidine peptides were recorded by Analytical Services and Environmental Projects (ASEP) at Queen's University Belfast on a Waters LCT Premier ToF mass spectrometer using the electrospray ionisation (ESI) technique. HRMS spectra of laterocidine peptides were performed on a Thermo Scientific Dionex UltiMate 3000 HPLC system with a Phenomenex Kinetex C18 (2.6  $\mu$ m, 2.1 x 150 mm) column at 35 °C and equipped with a diode array detector. The following solvent system, at a flow rate of 0.3 mL/min, was used: solvent A = 0.1% formic acid in water, solvent B = 0.1% formic acid in acetonitrile. A gradient method was employed, starting at 95 % solvent A and 5 % solvent B for 1 min, ramping up to 95 % solvent B over 9 min, ramping up to 98 % solvent B over 1 min, remaining there for 1 min before ramping back down to 95 % solvent A over 2 min and remaining there for 1 min. The system was connected to a Bruker micrOTOF-Q II mass spectrometer (ESI ionization) calibrated internally with sodium formate. (HPLC traces of the peptides can be found in the online supplementary material at <https://doi.org/10.1039/D2MD00281G>)

### Antimicrobial testing

All minimum inhibitory concentrations (MICs) were determined according to Clinical and Standards Laboratory Institute (CLSI) guidelines. Blood agar plates were inoculated with glycerol stocks of *E. coli* ATCC 25922, *K. pneumoniae* ATCC 13883, *A. baumannii* ATCC 17961, *P. aeruginosa* PAO1 and *S. aureus* USA300. The inoculated agar plates were then incubated for 16 h at 37 °C. Individually grown colonies were subsequently used to inoculate 5 mL aliquots of TSB that were then incubated at 37 °C with shaking at 220 rpm. *E. coli* 25922 MCR-1 glycerol stock was used to inoculate 5 mL of TSB supplemented with kanamycin that was then incubated for 16 h at 37 °C with shaking at 220 rpm. The next day the culture was diluted 100 fold in TSB supplemented with kanamycin and incubated at 37 °C with shaking

at 220 rpm. In parallel, the lipopeptide antibiotics DMSO stocks to be assessed were serially diluted with MHB in polypropylene 96-well plates (50  $\mu\text{L}$  in each well). Colistin sulfate stocks were dissolved in water before being diluted with MHB. Aliquots of the inoculated TSB were incubated until an  $\text{OD}_{600}$  of around 0.5 was reached. The bacterial suspensions were then diluted with MHB ( $2 \times 10^5$  CFU  $\text{mL}^{-1}$ ) and added to the microplates containing the test compounds (50  $\mu\text{L}$  to each well). The well-plates were sealed with an adhesive membrane and after 18 h of incubation at 37 °C with shaking at 600 rpm, the wells were visually inspected for bacterial growth. MIC values reported are based on three technical replicates and defined as the lowest concentration of the compound that prevented visible growth of bacteria.

### Hemolytic assays

Experiments were performed in triplicate and Triton X-100 used as a positive control. Red blood cells from defibrinated sheep blood obtained from Thermo Fisher were centrifuged (400 g for 15 min at 4°C) and washed with Phosphate-Buffered Saline (PBS) containing 0.002% Tween20 (buffer) five times. Then, the red blood cells were normalized to obtain a positive control read-out between 2.5 and 3.0 at 415 nm to stay within the linear range with the maximum sensitivity. A serial dilution of the compounds (128 – 1  $\mu\text{g}/\text{mL}$ , 75  $\mu\text{L}$ ) was prepared in a 96-well polypropylene plate. The outer border of the plate was filled with 75  $\mu\text{L}$  buffer. Each plate contained a positive control (0.1% Triton-X final concentration, 75  $\mu\text{L}$ ) and a negative control (buffer, 75  $\mu\text{L}$ ) in triplicate. The normalized blood cells (75  $\mu\text{L}$ ) were added and the plates were incubated at 37 °C for 1 h while shaking at 500 rpm. A flat-bottom polystyrene plate with 100  $\mu\text{L}$  buffer in each well was prepared. After incubation, the plates were centrifuged (800 g for 5 min at room temperature) and 25  $\mu\text{L}$  of the supernatant was transferred to their respective wells in the flat-bottom plate. The values obtained from a read-out at 415 nm were corrected for background (negative control) and transformed to a percentage relative to the positive control.



### Yields and HRMS analysis of peptides

**Table 2.** Peptide number, name, chemical formula, exact mass, mass found and overall yield for peptides 1 – 26.

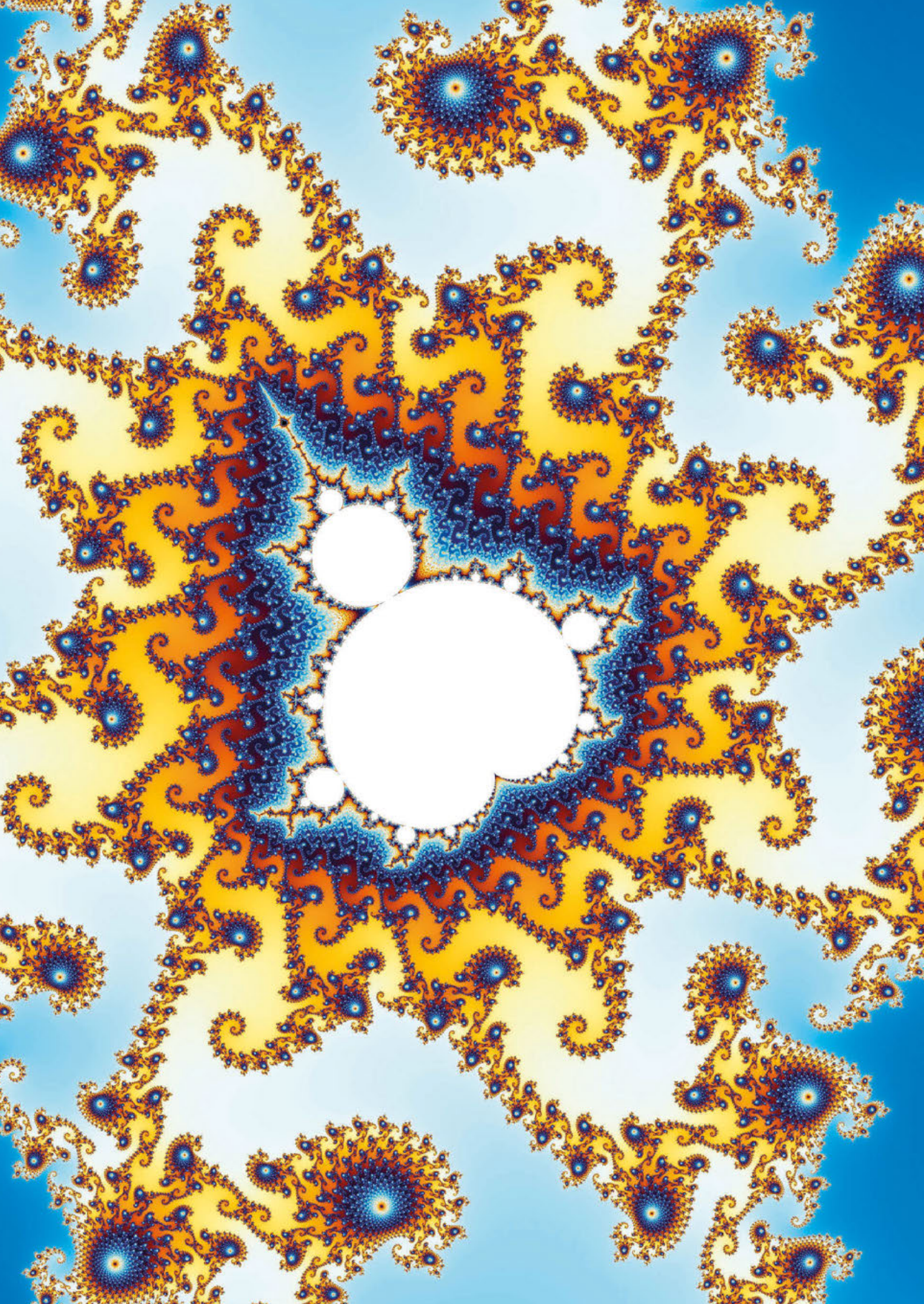
Peptide	Name	Chemical Formula	Calcd Exact Mass	Mass found	Calcd	Overall Yield [%]
1	Brevicidine	C <sub>74</sub> H <sub>106</sub> N <sub>18</sub> O <sub>17</sub>	1518.7983	507.2688 [M+3H] <sup>3+</sup>	507.2734	9
9	H-Brev	C <sub>67</sub> H <sub>94</sub> N <sub>18</sub> O <sub>16</sub>	1406.7095	704.3672 [M+2H] <sup>2+</sup>	704.3620	2
10	C2-Brev	C <sub>69</sub> H <sub>96</sub> N <sub>18</sub> O <sub>17</sub>	1448.7201	1449.7290 [M+H] <sup>+</sup>	1449.7274	3
11	C4-Brev	C <sub>74</sub> H <sub>100</sub> N <sub>18</sub> O <sub>17</sub>	1476.7514	1477.7579 [M+H] <sup>+</sup>	1477.7592	25
12	C6-Brev	C <sub>73</sub> H <sub>104</sub> N <sub>18</sub> O <sub>17</sub>	1504.7827	1505.8070 [M+H] <sup>+</sup>	1505.7905	19
13	C8-Brev	C <sub>75</sub> H <sub>108</sub> N <sub>18</sub> O <sub>17</sub>	1532.8140	1533.8483 [M+H] <sup>+</sup>	1533.8218	4
14	C10-Brev	C <sub>77</sub> H <sub>112</sub> N <sub>18</sub> O <sub>17</sub>	1560.8453	521.2809 [M+3H] <sup>3+</sup>	521.2809	4
15	C12-Brev	C <sub>79</sub> H <sub>116</sub> N <sub>18</sub> O <sub>17</sub>	1588.8766	795.4525 [M+2H] <sup>2+</sup>	795.4456	3
16	C14-Brev	C <sub>81</sub> H <sub>120</sub> N <sub>18</sub> O <sub>17</sub>	1616.9079	809.4640 [M+2H] <sup>2+</sup>	809.4612	2
17	C16-Brev	C <sub>83</sub> H <sub>124</sub> N <sub>18</sub> O <sub>17</sub>	1644.9392	823.4837 [M+2H] <sup>2+</sup>	823.4769	4
2	Laterocidine	C <sub>78</sub> H <sub>113</sub> N <sub>19</sub> O <sub>18</sub>	1603.8511	802.9326 [M+2H] <sup>2+</sup>	802.9329	2
18	H-Lat	C <sub>69</sub> H <sub>97</sub> N <sub>19</sub> O <sub>17</sub>	1463.7310	732.8731 [M+2H] <sup>2+</sup>	732.8728	2
19	C2-Lat	C <sub>71</sub> H <sub>99</sub> N <sub>19</sub> O <sub>18</sub>	1505.7415	753.8783 [M+2H] <sup>2+</sup>	753.8781	1
20	C4-Lat	C <sub>73</sub> H <sub>103</sub> N <sub>19</sub> O <sub>18</sub>	1533.7728	767.8944 [M+2H] <sup>2+</sup>	767.8937	3
21	C6-Lat	C <sub>75</sub> H <sub>107</sub> N <sub>19</sub> O <sub>18</sub>	1561.8041	781.9097 [M+2H] <sup>2+</sup>	781.9094	2
22	C8-Lat	C <sub>77</sub> H <sub>111</sub> N <sub>19</sub> O <sub>18</sub>	1589.8354	795.9254 [M+2H] <sup>2+</sup>	795.9250	2
23	C10-Lat	C <sub>79</sub> H <sub>115</sub> N <sub>19</sub> O <sub>18</sub>	1617.8667	809.9410 [M+2H] <sup>2+</sup>	809.9407	3
24	C12-Lat	C <sub>81</sub> H <sub>119</sub> N <sub>19</sub> O <sub>18</sub>	1645.8980	823.9567 [M+2H] <sup>2+</sup>	823.9563	0.4
25	C14-Lat	C <sub>83</sub> H <sub>123</sub> N <sub>19</sub> O <sub>18</sub>	1673.9293	851.9881 [M+2H] <sup>2+</sup>	851.9876	1
26	C16-Lat	C <sub>85</sub> H <sub>127</sub> N <sub>19</sub> O <sub>18</sub>	1701.9606	837.9722 [M+2H] <sup>2+</sup>	837.9720	1

## References

- (1) O'Neill, J. *Antimicrobial Resistance: Tackling a Crisis for the Health and Wealth of Nations.*; 2014.
- (2) Murray, C. J.; Ikuta, K. S.; Sharara, F.; Swetschinski, L.; Robles Aguilar, G.; Gray, A.; Han, C.; Bisignano, C.; Rao, P.; Wool, E.; Johnson, S. C.; Browne, A. J.; Chipeta, M. G.; Fell, F.; Hackett, S.; Haines-Woodhouse, G.; Kashef Hamadani, B. H.; Kumaran, E. A. P.; McManigal, B.; Agarwal, R.; Akech, S.; Albertson, S.; Amuasi, J.; Andrews, J.; Aravkin, A.; Ashley, E.; Bailey, F.; Baker, S.; Basnyat, B.; Bekker, A.; Bender, R.; Bethou, A.; Bielicki, J.; Boonkasidecha, S.; Bukosia, J.; Carvalheiro, C.; Castañeda-Orjuela, C.; Chansamouth, V.; Chaurasia, S.; Chiurchiù, S.; Chowdhury, F.; Cook, A. J.; Cooper, B.; Cressey, T. R.; Criollo-Mora, E.; Cunningham, M.; Darboe, S.; Day, N. P. J.; De Luca, M.; Dokova, K.; Dramowski, A.; Dunachie, S. J.; Eckmanns, T.; Eibach, D.; Emami, A.; Feasey, N.; Fisher-Pearson, N.; Forrest, K.; Garrett, D.; Gastmeier, P.; Giref, A. Z.; Greer, R. C.; Gupta, V.; Haller, S.; Haselbeck, A.; Hay, S. I.; Holm, M.; Hopkins, S.; Iregbu, K. C.; Jacobs, J.; Jarovsky, D.; Javanmardi, F.; Khorana, M.; Kissoon, N.; Kobeissi, E.; Kostyanev, T.; Krapp, F.; Krumkamp, R.; Kumar, A.; Kyu, H. H.; Lim, C.; Limmathurotsakul, D.; Loftus, M. J.; Lunn, M.; Ma, J.; Mturi, N.; Munera-Huertas, T.; Musicha, P.; Mussi-Pinhata, M. M.; Nakamura, T.; Nanavati, R.; Nangia, S.; Newton, P.; Ngoun, C.; Novotney, A.; Nwakanma, D.; Obiero, C. W.; Olivás-Martínez, A.; Olliaro, P.; Ooko, E.; Ortiz-Brizuela, E.; Peleg, A. Y.; Perrone, C.; Plakkal, N.; Ponce-de-Leon, A.; Raad, M.; Ramdin, T.; Riddell, A.; Roberts, T.; Robotham, J. V.; Roca, A.; Rudd, K. E.; Russell, N.; Schnall, J.; Scott, J. A. G.; Shivamallappa, M.; Sifuentes-Osornio, J.; Steenkeste, N.; Stewardson, A. J.; Stoeva, T.; Tasak, N.; Thaiprakong, A.; Thwaites, G.; Turner, C.; Turner, P.; van Doorn, H. R.; Velaphi, S.; Vongpradith, A.; Vu, H.; Walsh, T.; Waner, S.; Wangrangsimakul, T.; Wozniak, T.; Zheng, P.; Sartorius, B.; Lopez, A. D.; Stergachis, A.; Moore, C.; Dolecek, C.; Naghavi, M. Global Burden of Bacterial Antimicrobial Resistance in 2019: A Systematic Analysis. *Lancet* **2022**, 399 (10325), 629–655. [https://doi.org/10.1016/S0140-6736\(21\)02724-0](https://doi.org/10.1016/S0140-6736(21)02724-0).
- (3) Shukla, R.; Lavore, F.; Maity, S.; Derks, M. G. N.; Jones, C. R.; Vermeulen, B. J. A.; Melcrová, A.; Morris, M. A.; Becker, L. M.; Wang, X.; Kumar, R.; Medeiros-Silva, J.; van Beekveld, R. A. M.; Bonvin, A. M. J. J.; Lorent, J. H.; Lelli, M.; Nowick, J. S.; MacGillavry, H. D.; Peoples, A. J.; Spoering, A. L.; Ling, L. L.; Hughes, D. E.; Roos, W. H.; Breukink, E.; Lewis, K.; Weingarth, M. Teixobactin Kills Bacteria by a Two-Pronged Attack on the Cell Envelope. *Nature* **2022**, 608 (7922), 390–396. <https://doi.org/10.1038/s41586-022-05019-y>.
- (4) Wang, Z.; Koirala, B.; Hernandez, Y.; Zimmerman, M.; Brady, S. F. Bioinformatic Prospecting and Synthesis of a Bifunctional Lipopeptide Antibiotic That Evades Resistance. *Science* (80-. ). **2022**, 376 (6596), 991–996. <https://doi.org/10.1126/science.abn4213>.
- (5) Acedo, J. Z.; Chiorean, S.; Vederas, J. C.; van Belkum, M. J. The Expanding Structural Variety among Bacteriocins from Gram-Positive Bacteria. *FEMS Microbiology Reviews*. Oxford Academic November 1, 2018, pp 805–828. <https://doi.org/10.1093/femsre/fuy033>.
- (6) Kralt, B.; Moreira, R.; Palmer, M.; Taylor, S. D. Total Synthesis of A54145 Factor D. *J. Org. Chem.* **2019**, 84 (18), 12021–12030. [https://doi.org/10.1021/ACS.JOC.9B01938/SUPPL\\_FILE/JO9B01938\\_SI\\_002.CIF](https://doi.org/10.1021/ACS.JOC.9B01938/SUPPL_FILE/JO9B01938_SI_002.CIF).
- (7) Noden, M.; Moreira, R.; Huang, E.; Yousef, A.; Palmer, M.; Taylor, S. D. Total Synthesis of Paenibacterin and Its Analogues. *J. Org. Chem.* **2019**, 84 (9), 5339–5347. <https://doi.org/10.1021/acs.joc.9b00364>.
- (8) Cochrane, S. A.; Vederas, J. C. Lipopeptides from Bacillus and Paenibacillus Spp.: A Gold Mine of Antibiotic Candidates. *Med. Res. Rev.* **2016**, 36 (1), 4–31. <https://doi.org/10.1002/MED.21321>.
- (9) Kaneda, T. Iso- and Anteiso-Fatty Acids in Bacteria: Biosynthesis, Function, and Taxonomic Significance. *Microbiol. Rev.* **1991**, 55 (2), 288–302. <https://doi.org/10.1128/mr.55.2.288-302.1991>.
- (10) Cochrane, S. A.; Lohans, C. T.; Brandelli, J. R.; Mulvey, G.; Armstrong, G. D.; Vederas, J. C. Synthesis and Structure-Activity Relationship Studies of N-Terminal Analogues of the Antimicrobial Peptide Tridecaptin A1. *J. Med. Chem.* **2014**, 57 (3), 1127–1131. <https://doi.org/10.1021/jm401779d>.
- (11) Cochrane, S. A.; Surgenor, R. R.; Khey, K. M. W.; Vederas, J. C. Total Synthesis and Stereochemical Assignment of the Antimicrobial Lipopeptide Cerexin A 1. *Org. Lett.* **2015**, 17 (21), 5428–5431. <https://doi.org/10.1021/acs.orglett.5b02779>.
- (12) Sakura, N.; Itoh, T.; Uchida, Y.; Ohki, K.; Okimura, K.; Chiba, K.; Sato, Y.; Sawanishi, H. The Contribution of the N-Terminal Structure of Polymyxin B Peptides to Antimicrobial and Lipopolysaccharide Binding Activity. *Bull. Chem. Soc. Jpn.* **2004**, 77 (10), 1915–1924. <https://doi.org/10.1246/bcsj.77.1915>.
- (13) Li, Y. X.; Zhong, Z.; Zhang, W. P.; Qian, P. Y. Discovery of Cationic Nonribosomal Peptides as Gram-Negative

- Antibiotics through Global Genome Mining. *Nat. Commun.* **2018**, *9* (1). <https://doi.org/10.1038/s41467-018-05781-6>.
- (14) Al Ayed, K.; Ballantine, R. D.; Hoekstra, M.; Bann, S. J.; Wesseling, C. M. J.; Bakker, A. T.; Zhong, Z.; Li, Y. X.; Bröchle, N. C.; van der Stelt, M.; Cochrane, S. A.; Martin, N. I. Synthetic Studies with the Brevicidine and Laterocidine Lipopeptide Antibiotics Including Analogues with Enhanced Properties and in Vivo Efficacy. *Chem. Sci.* **2022**, *13* (12), 3563–3570. <https://doi.org/10.1039/d2sc00143h>.
- (15) Al Ayed, K.; Zamarbide Losada, D.; Machushynets, N. V.; Terlouw, B.; Elsayed, S. S.; Schill, J.; Trebosc, V.; Pieren, M.; Medema, M. H.; van Wezel, G. P.; Martin, N. I. Total Synthesis and Structure Assignment of the Relacidine Lipopeptide Antibiotics and Preparation of Analogues with Enhanced Stability. *ACS Infect. Dis.* **2023**, *9* (4), 739–748. <https://doi.org/10.1021/acscinfecdis.3c00043>.
- (16) Boucher, H. W.; Talbot, G. H.; Bradley, J. S.; Edwards, J. E.; Gilbert, D.; Rice, L. B.; Scheld, M.; Spellberg, B.; Bartlett, J. Bad Bugs, No Drugs: No ESKAPE! An Update from the Infectious Diseases Society of America. *Clin. Infect. Dis.* **2009**, *48* (1), 1–12. <https://doi.org/10.1086/595011>.
- (17) Gogry, F. A.; Siddiqui, M. T.; Sultan, I.; Haq, Q. M. R. Current Update on Intrinsic and Acquired Colistin Resistance Mechanisms in Bacteria. *Front. Med.* **2021**, *8*, 677720. <https://doi.org/10.3389/fmed.2021.677720>.
- (18) Velkov, T.; Thompson, P. E.; Nation, R. L.; Li, J. Structure–Activity Relationships of Polymyxin Antibiotics. *J. Med. Chem.* **2010**, *53* (5), 1898–1916. <https://doi.org/10.1021/jm900999h>.
- (19) Mukherjee, S.; Van Der Donk, W. A. Mechanistic Studies on the Substrate-Tolerant Lanthipeptide Synthetase ProcM. *J. Am. Chem. Soc.* **2014**, *136* (29), 10450–10459. <https://doi.org/10.1021/ja504692v>.
- (20) Ge, J.; Li, L.; Yao, S. Q. A Self-Immobilizing and Fluorogenic Unnatural Amino Acid That Mimics Phosphotyrosine. *Chem. Commun.* **2011**, *47* (39), 10939–10941. <https://doi.org/10.1039/c1cc14653j>.
- (21) Freire, F.; Fisk, J. D.; Peoples, A. J.; Ivancic, M.; Guzei, I. A.; Gellman, S. H. Diacid Linkers That Promote Parallel  $\beta$ -Sheet Secondary Structure in Water. *J. Am. Chem. Soc.* **2008**, *130* (25), 7839–7841. <https://doi.org/10.1021/ja802042c>.
- (22) Gude, M.; Ryf, J.; White, P. D. An Accurate Method for the Quantitation of Fmoc-Derivatized Solid Phase Supports. *Letts. Pept. Sci.* **2002**, *9* (4–5), 203–206. <https://doi.org/10.1007/BF02538384>.





## Chapter 4

# Linearization of the Brevicidine and Laterocidine Lipopeptides Yields Analogues that Retain Full Antibacterial Activity

### **Abstract**

Brevicidine and laterocidine are macrocyclic lipodepsipeptides with selective activity against Gram-negative bacteria, including colistin-resistant strains. Previously, the macrocyclic core of these peptides was thought essential for antibacterial activity. In this study, we show that C-terminal amidation of linear brevicidine and laterocidine scaffolds, and substitution of the native Thr9, yields linear analogues that retain the potent antibacterial activity and low hemolysis of the parent compounds. Furthermore, an alanine scan of both peptides revealed that the aromatic and basic amino acids within the common central scaffold are essential for antibacterial activity. This linearization strategy for modification of cyclic peptides is a highly effective way to reduce the time and cost of peptide synthesis and may be applicable to other non-ribosomal antibacterial peptides.

### **Parts of this chapter have been published in the Journal of Medicinal Chemistry:**

Ballantine, R. D.; Al Ayed, K.\*; Bann, S. J.; Hoekstra, M.; Martin, N. I.; Cochrane, S. A. Linearization of the Brevicidine and Laterocidine Lipopeptides Yields Analogues That Retain Full Antibacterial Activity. *J Med Chem* **2023**, 66 (8), 6002–6009. <https://doi.org/10.1021/acs.jmedchem.3c00308>.

### **Parts of the data in this chapter are part of a patent:**

"Antibiotic natural product analogues"; Cochrane, S.A.; Ballantine, R. D.; Martin, N. I.; Al Ayed, K.; Hoekstra, M.; Zamarbide Losada, S.D.; Priority Date: 28 January 2021; Published: 4 August 2022; WO2022162332A1

\*Authors contributed equally

## Introduction

Antimicrobial resistance (AMR) is a growing concern posing a threat to both global health and economics. Current estimations predict that by 2050, the number of deaths attributable to AMR will surpass the annual deaths caused by cancer.<sup>1,2</sup> In this context, it is imperative that renewed efforts be made to discover and develop new antibiotics, in particular for the ESKAPE pathogens (*E. coli*, *Klebsiella pneumoniae*, *Acinetobacter baumannii*, *Pseudomonas aeruginosa* and *Staphylococcus aureus*) which represent the most important nosocomial infections within the United States.<sup>3</sup> Non-ribosomal peptides (NRPs) represent a burgeoning class of antibacterial compounds with the potential to address resistance.<sup>4</sup> Several classes of NRPs, such as the polymyxins, daptomycin, and vancomycin, are already in clinical use,<sup>5</sup> and many more promising antibacterial NRPs have been discovered in recent years, including lysocin E,<sup>6</sup> teixobactin,<sup>7</sup> lugdunin,<sup>8</sup> malacidin<sup>9</sup> and cilagicin.<sup>10</sup> Although the structures of different classes of NRPs vary considerably, a significant majority contain one or more macrocyclic rings. These structural features complicate the chemical synthesis of NRPs, as additional orthogonal protecting groups and special cyclization conditions are required for their synthesis.<sup>10-14</sup> This increases the complexity and cost of their chemical synthesis, which can be a barrier to clinical uptake.

Structure-activity relationship (SAR) studies are frequently performed on NRPs to optimize activity, stability, and/or cost of synthesis. They can also provide an insight into the mode of action. Alanine scans have already been performed on a number of NRPs, including daptomycin, tridecaptin A<sub>1</sub> (TriA<sub>1</sub>), and the polymyxins to identify residues that are crucial for antibacterial activity.<sup>15-17</sup> Additionally, side chain substitution analogues have been generated for laspartomycin C,<sup>18</sup> and work on teixobactin has shown that *allo*-enduracididine 10 can be replaced with both Arg and Lys, with the resulting analogues retaining strong activity.<sup>19,20</sup> Although many SAR studies have been performed, the linearization of cyclic NRPs is rarely reported.<sup>21</sup> If this can be achieved without loss of activity, the cost of, and time required, for synthesis would be significantly reduced.

In 2018, the NRPs brevicidine (**1**) and laterocidine (**2**) were discovered and found to have potent antibacterial activity against Gram-negative bacteria, including colistin-resistant *Escherichia coli*.<sup>22</sup> Structurally related analogues, relacidine A and B, were subsequently discovered in 2020 (**Figure 1**).<sup>23</sup> All four peptides share a central scaffold between residues two and eight but vary at their lipidated N-terminal amino acid and C-terminal macrocycle. Although these peptides were only recently discovered, the naming convention has already become somewhat complicated. We therefore propose “*ornicidines*” as a family name for these peptides, given that all contain a conserved central scaffold bearing three ornithine residues.

We recently reported synthetic methods to access brevicidine and laterocidine, as well as novel cyclic analogues.<sup>24</sup> Subsequent SAR studies revealed that the natural branched and/or chiral N-terminal acyl chains can be substituted with more affordable linear alternatives containing between eight and twelve carbons.<sup>25</sup> The costliest part in the syntheses of these peptides arises from the need to cyclize the side chain of Thr9 with the C-terminus. This also presents a challenge for synthesis by automated Fmoc solid-phase peptide synthesis (SPPS), as on-resin cyclization requires low resin loading, the use of orthogonal protection strategies, and

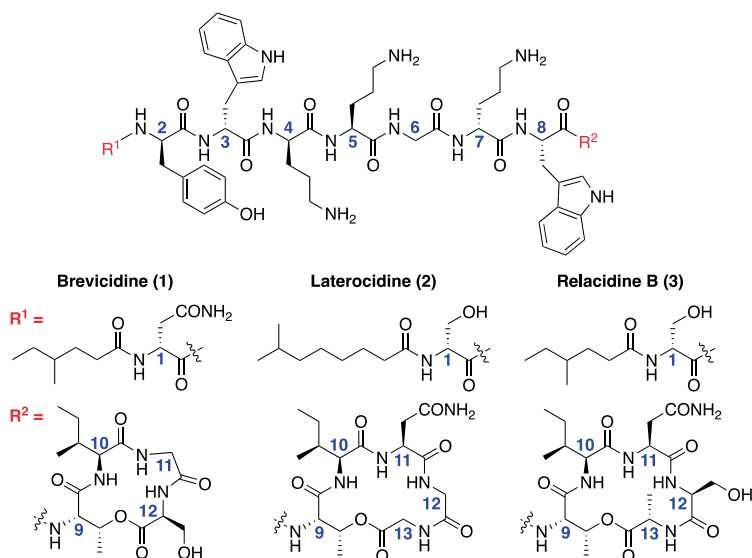


**Figure 1.** Structures of some known ornidicines: Brevicidine (1), laterocidine (2) and relacidine B (3).

extended reaction times for the cyclization step. Given that the macrocyclic rings found in the ornidicines differ both in size and amino acid composition, we were inspired to investigate the necessity of the macrocycle motif. In their seminal report on brevicidine and laterocidine, Li *et al.* found that a linear analogue of laterocidine was 8- to 32-fold less active than the natural cyclic peptide.<sup>22</sup> However, only one linear analogue was synthesized and tested in their study. To truly ascertain if the macrocyclic ring is essential for antibacterial activity, we embarked on the linearization of these peptides, the details of which are presented herein.

## Results and Discussion

Linear laterocidine (LL-OH, 4) and linear brevicidine (LB-OH, 5) were first synthesized by Fmoc SPPS, starting from 2-chlorotrityl (2-CT) chloride resin. The antibacterial activity of these peptides was then compared to brevicidine (1) and laterocidine (2) using minimum inhibitory concentration (MIC)/microbroth dilution assays (**Table 1**). The MICs of all peptides were determined against a panel of Gram-negative and Gram-positive ESKAPE pathogens. Additionally, a strain of *E. coli* carrying the *mcr-1* gene was included in the panel. The *mcr-1* gene is a transferable plasmid that confers resistance against colistin, a last-resort antibiotic for Gram-negative infections, by reducing the overall negative charge of lipopolysaccharide (LPS) through modification of lipid A with phosphoethanolamine. The propensity for cationic antibiotics to bind to the cell membrane is therefore reduced. This gene has been observed in more than 27 bacterial species over six continents.<sup>26</sup> The spread of the *mcr-1* gene could render colistin ineffectual, therefore novel antibacterials are urgently required to overcome this form of resistance.



In line with expectation, both LL-OH (**4**) and LB-OH (**5**) were found to be significantly less active than their cyclic counterparts. However, due to the presence of C-terminal carboxylic acids in both peptides, their net charge (2+) is lower than brevicidine/laterocidine (3+). The overall cationic charge of an antibacterial peptide is a critical property for preferential binding to the negatively charged phospholipids found throughout the bacterial membrane.<sup>27</sup> We therefore postulated that by masking the C-terminus with an amide, antibacterial activity could be improved. To this end, the linear C-terminal amide analogue of laterocidine (LL-NH<sub>2</sub>, **6**) and brevicidine (LB-NH<sub>2</sub>, **7**) were synthesized by Fmoc SPPS from rink amide resin and tested for antibacterial activity. Gratifyingly, both **6** and **7** showed a two-fold improvement in activity with respect to C-terminal acids **4** and **5**, overall a two/four-fold reduction compared to parent peptides.

Having demonstrated that the C-terminal macrocycle is not essential for antibacterial activity, we set out to determine whether the C-terminus of LB-NH<sub>2</sub> or LL-NH<sub>2</sub> could be truncated. Shorter peptides require less reagents and synthesis time and are therefore cheaper to synthesize. Amide analogues **8** – **16** were synthesized, whereby the C-terminal residues were removed sequentially up to and including Thr9. This revealed that for LB-NH<sub>2</sub> both Ser12 and Gly11 can be removed without diminishing antibacterial activity.

However, further removal of the third and fourth C-terminal residues as in analogues **13** and **15** respectively, resulted in substantial decreases in activity. Truncated LL-NH<sub>2</sub> analogues

**Table 1:** Activity of linear brevicidine and laterocidine C-terminal analogues. All assays run in triplicate. [Peptide] in hemolytic assays = 64 µg/mL. Additional strain information in supplementary information. LL, linear laterocidine; LB, linear brevicidine; Δ, deletion product.

Compound	Antibacterial Activity (µg/mL)						Hemolysis (%)
	<i>E. coli</i> ATCC 25922	<i>E. coli</i> (MCR-1)	<i>K. pneumoniae</i> ATCC 13883	<i>A. baumannii</i> ATCC 17961	<i>P. aeruginosa</i> PAO1	<i>S. aureus</i> USA300	Sheep red blood cells
Brev ( <b>1</b> )	4	4	2	4	8	>32	<0.1
Lat ( <b>2</b> )	2	2	2-4	2	4	>32	1.3
<sup>a</sup> LL-OH ( <b>4</b> )	8	16	8-16	16	8	>32	<0.1
<sup>b</sup> LB-OH ( <b>5</b> )	>32	>32	>32	>32	16	>32	<0.1
LL-NH <sub>2</sub> ( <b>6</b> )	4	8	4-8	8	4	>32	<0.1
LB-NH <sub>2</sub> ( <b>7</b> )	16	16	16	16	4	>32	<0.1
Δ13LL-NH <sub>2</sub> ( <b>8</b> )	8	8	4-8	4	4	>32	<0.1
Δ12LB-NH <sub>2</sub> ( <b>9</b> )	8	16	8	8	4	>32	3.8
Δ12-13LL-NH <sub>2</sub> ( <b>10</b> )	4	8	8-16	4	4	>32	3.0
Δ11-12LB-NH <sub>2</sub> ( <b>11</b> )	4	4-8	2	8	2	>32	<0.1
Δ11-13LL-NH <sub>2</sub> ( <b>12</b> )	4	4	2	4	4	32	2.3
Δ10-12LB-NH <sub>2</sub> ( <b>13</b> )	>32	>32	>32	>32	>32	>32	<0.1
Δ10-13LL-NH <sub>2</sub> ( <b>14</b> )	>32	32	>32	32	>32	>32	<0.1
Δ9-12LB-NH <sub>2</sub> ( <b>15</b> )	>32	>32	>32	>32	>32	>32	<0.1
Δ9-13LL-NH <sub>2</sub> ( <b>16</b> )	>32	>32	>32	32	>32	>32	<0.1

showed a similar trend, with removal of the three C-terminal residues (Asn11, Gly12 and Gly13) having no effect on the MIC values. Ile10 was equally implicated as a key residue. At this stage it must be emphasized that these linear analogues are substantially easier and cheaper to synthesize than brevicidine or laterocidine but retain full activity. Albeit, it is unclear whether these linear peptides operate via the same mechanism of action (MOA) as the parent peptides. Only minimal hemolysis (**Table 1**) was detected for these peptides at concentrations up to 32x higher than the MIC of the most potent peptides, showing that linearization does not increase hemolytic activity.

Given the ease with which these linear analogues could be prepared, we next proceeded to perform an alanine scan on both LB-NH<sub>2</sub> (analogues **17 – 28**) and LL-NH<sub>2</sub> (analogues **29 – 41**) (**Table 2**). Consistent with our truncation studies, substitution of Asn11, Gly12 or Gly13 in LL-NH<sub>2</sub>, or Ser12 in LB-NH<sub>2</sub>, had minimal effect on activity, giving analogues with MIC

**Table 2:** Alanine scan of linear brevicidamide and laterocidamide. All assays run in triplicate. Additional strain information in supplementary information.

Compound	Antibacterial Activity (µg/mL)					
	<i>E. coli</i> ATCC 25922	<i>E. coli</i> (MCR-1)	<i>K. pneumoniae</i> ATCC 13883	<i>A. baumannii</i> ATCC 17961	<i>P. aeruginosa</i> PAO1	<i>S. aureus</i> USA300
LB(D-Ala1)-NH <sub>2</sub> ( <b>17</b> )	16	16	16	8	8	>32
LB(D-Ala2)-NH <sub>2</sub> ( <b>18</b> )	>32	>32	>32	>32	16	>32
LB(D-Ala3)-NH <sub>2</sub> ( <b>19</b> )	>32	>32	>32	>32	32	>32
LB(D-Ala4)-NH <sub>2</sub> ( <b>20</b> )	>32	>32	>32	32	32	>32
LB(Ala5)-NH <sub>2</sub> ( <b>21</b> )	>32	>32	>32	>32	32	>32
LB(Ala6)-NH <sub>2</sub> ( <b>22</b> )	32	32	>32	32	32	>32
LB(D-Ala7)-NH <sub>2</sub> ( <b>23</b> )	>32	>32	>32	16	32	>32
LB(Ala8)-NH <sub>2</sub> ( <b>24</b> )	>32	>32	>32	>32	32	>32
LB(Ala9)-NH <sub>2</sub> ( <b>25</b> )	8	16	16	16	4	>32
LB(Ala10)-NH <sub>2</sub> ( <b>26</b> )	>32	>32	>32	>32	16	>32
LB(Ala11)-NH <sub>2</sub> ( <b>27</b> )	32	32	>32	32	16	>32
LB(Ala12)-NH <sub>2</sub> ( <b>28</b> )	8	8	8	4	8	>32
LL(D-Ala1)-NH <sub>2</sub> ( <b>29</b> )	8	8	>32	32	8	>32
LL(D-Ala2)-NH <sub>2</sub> ( <b>30</b> )	32	32	>32	>32	16	>32
LL(D-Ala3)-NH <sub>2</sub> ( <b>31</b> )	>32	>32	>32	>32	>32	>32
LL(D-Ala4)-NH <sub>2</sub> ( <b>32</b> )	>32	>32	>32	32	>32	>32
LL(Ala5)-NH <sub>2</sub> ( <b>33</b> )	32	>32	>32	>32	32	>32
LL(Ala6)-NH <sub>2</sub> ( <b>34</b> )	4-8	8	8	16	16	>32
LL(D-Ala7)-NH <sub>2</sub> ( <b>35</b> )	>32	>32	>32	32	32	>32
LL(Ala8)-NH <sub>2</sub> ( <b>36</b> )	>32	>32	>32	>32	32	>32
LL(Ala9)-NH <sub>2</sub> ( <b>37</b> )	4	4-8	4	8	4	>32
LL(Ala10)-NH <sub>2</sub> ( <b>38</b> )	>32	>32	>32	>32	16	>32
LL(Ala11)-NH <sub>2</sub> ( <b>39</b> )	8	8	8	8	4	>32
LL(Ala12)-NH <sub>2</sub> ( <b>40</b> )	8	8	8	8	8	>32
LL(Ala13)-NH <sub>2</sub> ( <b>41</b> )	4-8	8	8	8	4	>32

values of 4-8  $\mu\text{g mL}^{-1}$ . Interestingly, the replacement of Gly11 in LB-NH<sub>2</sub> was significantly detrimental to activity, showing that although both laterocidine and brevicidine have very similar peptide sequences, changes that work on one are not guaranteed to work on the other. Furthermore, for both the LB-NH<sub>2</sub> and LL-NH<sub>2</sub> peptides, the N-terminal residues (D-Tyr2, D-Trp3, D-Orn4, Orn5, D-Orn7 and Trp8) were found to be integral to antibacterial activity (**Figure 2**). These residues are either aromatic or cationic. The former may be important for maintaining an active conformation through  $\pi$ -stacking or increasing the hydrophobicity of the peptide to aid passage through the bacterial membrane,<sup>28</sup> while the latter may play a role in target binding through electrostatic interactions, in addition to binding phospholipids present in the membrane.<sup>29</sup>

The results of the alanine scans are notably like those observed with the tridecaptins, a class of linear antibacterial NRPs. In TriA<sub>1</sub>, three cationic residues (D- and L-Dab) and two aromatic amino acids are also essential for antibacterial activity (**Figure 2**).<sup>15</sup> TriA<sub>1</sub> kills Gram-negative bacteria by binding to LPS on the outer membrane, entering the periplasm, selectively binding to Gram-negative lipid II, and disrupting the proton motive force (PMF).<sup>30</sup> Brevicidine, laterocidine, and the relacidines also bind to LPS,<sup>21, 22</sup> although the relacidines were reported not to bind lipid II,<sup>22</sup> and brevicidine interacts with phosphatidylglycerol and cardiolipin on the inner membrane to disrupt the PMF.<sup>31</sup> Our studies suggest that the central scaffold of these peptides represents a key epitope responsible for LPS binding and/or membrane disruption.

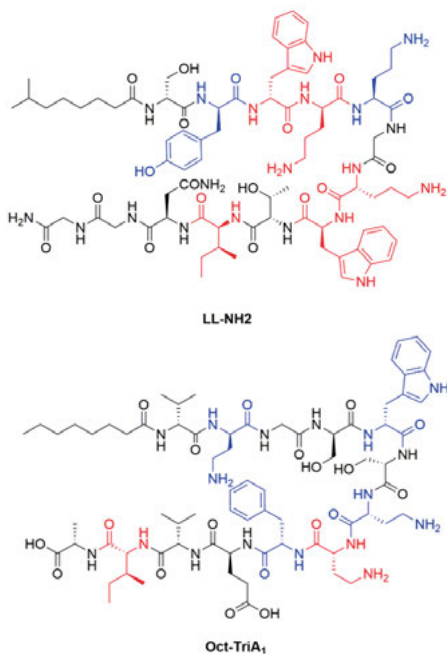


**Figure 2.** Comparison of essential residues in linear laterocidamide and Oct-TriA<sub>1</sub>.<sup>15</sup> Blue residues result in a 4- to 8-fold loss in activity against *E. coli* ATCC 25922 upon substitution with alanine, and red residues result in a 16-fold or greater loss.

Another particularly interesting observation is that Thr9, whose side-chain cyclizes with the C-terminus in natural ornicidines, is not essential for activity. This led us to consider amino acid substitutions at this position that may enhance the antibacterial activity of the linear peptides. To study this, a library of position 9-modified LL-NH<sub>2</sub> analogues (**42** – **52**), and ΔSer12-LB-NH<sub>2</sub> analogues (**53** – **63**) were synthesized and assessed for antibacterial activity (**Table 3**).

ΔSer12-LB-NH<sub>2</sub>, rather than LB-NH<sub>2</sub> was selected as the scaffold so that the effect of the well tolerated truncation and position 9 modification could be studied concurrently and compared to full length LL-NH<sub>2</sub>. In both peptides, position 9 modifications were surprisingly well tolerated, with hydrophobic residues (Leu, Phe, Met and Trp) and polar residues (Ser, Asn, Gln, MeAbu, Dap(Alloc) and Glu(OAll)) having little to no effect on antibacterial activity. Inclusion of an anionic acid at this position (Asp) abolished activity against most strains (excluding *P. aeruginosa*), showing the importance of having a net +3 charge on the peptide.

**Table 3:** Position 9 modification of peptides. All assays run in triplicate. [Peptide] in hemolytic assays = 64 µg/mL. Additional strain information in supplementary information.

Compound	Antibacterial Activity (µg/mL)						Hemolysis (%)
	<i>E. coli</i> ATCC 25922	<i>E. coli</i> (MCR-1)	<i>K. pneumoniae</i> ATCC 13883	<i>A. baumannii</i> ATCC 17961	<i>P. aeruginosa</i> PAO1	<i>S. aureus</i> USA300	Sheep red blood cells
LL(Leu9)-NH <sub>2</sub> ( <b>42</b> )	4	8	8	4	8	>32	<0.1
LL(Phe9)-NH <sub>2</sub> ( <b>43</b> )	4	4	8	4	8	>32	0.6
LL(Met9)-NH <sub>2</sub> ( <b>44</b> )	4	4	4	4	4	>32	0.6
LL(Trp9)-NH <sub>2</sub> ( <b>45</b> )	4	4	4	4	16	>32	2.1
LL(Ser9)-NH <sub>2</sub> ( <b>46</b> )	4	8	4	8	4	>32	<0.1
LL(Asn9)-NH <sub>2</sub> ( <b>47</b> )	8	8	8-16	16	8	>32	<0.1
LL(Gln9)-NH <sub>2</sub> ( <b>48</b> )	4	8	4	8	4	>32	0.6
LL(MeAbu9)-NH <sub>2</sub> ( <b>49</b> )	4	4	4	2	4	>32	<0.1
LL(Dap[Alloc]9)-NH <sub>2</sub> ( <b>50</b> )	2	4	4	4	8	>32	<0.1
LL(Glu[OAll]9)-NH <sub>2</sub> ( <b>51</b> )	16	16	>32	16	>32	>32	<0.1
LL(Dap9)-NH <sub>2</sub> ( <b>52</b> )	8	8	32	16	18	>32	<0.1
Δ12LB (Leu9)-NH <sub>2</sub> ( <b>53</b> )	4	4	4	4	8	>32	1.1
Δ12LB (Phe9)-NH <sub>2</sub> ( <b>54</b> )	2	2-4	2-4	4	4	>32	1.1
Δ12LB (Met9)-NH <sub>2</sub> ( <b>55</b> )	4	4	4	4	4	>32	0.7
Δ12LB (Trp9)-NH <sub>2</sub> ( <b>56</b> )	4	4	8	4	8	16	0.8
Δ12LB (Ser9)-NH <sub>2</sub> ( <b>57</b> )	4	8	4	8	2	>32	0.6
Δ12LB (Asn9)-NH <sub>2</sub> ( <b>58</b> )	8	8	16	16	2	>32	0.2
Δ12LB (Gln9)-NH <sub>2</sub> ( <b>59</b> )	8	8	16	16	2	>32	0.5
Δ12LB (MeAbu9)-NH <sub>2</sub> ( <b>60</b> )	4	4	2	2	4	>32	0.7
Δ12LB (Dap[Alloc]9)-NH <sub>2</sub> ( <b>61</b> )	4	4	2	2	4	>32	<0.1
Δ12LB (Glu[OAll]9)-NH <sub>2</sub> ( <b>62</b> )	4	8	4	8	2	>32	1.1
Δ12LB (Asp9)-NH <sub>2</sub> ( <b>63</b> )	>32	>32	>32	>32	4	>32	0.3
Δ12LB (Dap9)-NH <sub>2</sub> ( <b>64</b> )	8	8	>32	16	4	>32	0.3

However, addition of an additional cationic residue (Dap) did not increase antibacterial activity. At this stage, with 60 novel linear peptides assessed, our most active analogues were  $\Delta$ Ser12-LB(Phe9)-NH<sub>2</sub> (**54**), and LL(Dap(Alloc)9)-NH<sub>2</sub> (**61**), both showing MICs of 2-4  $\mu\text{g mL}^{-1}$  against most strains, including MCR-1 producing *E. coli*. As for the initial series of linear analogues (**Table 1**), we also investigated whether the structural alterations to brevicidine and laterocidine in analogues 42-64 would impart an antibacterial MOA based on a general detergent effect. Such a non-specific MOA is often identified by an increase in hemolytic activity compared to the natural peptides. To this end, all novel LB-NH<sub>2</sub> and LL-NH<sub>2</sub> analogues prepared were incubated with sheep erythrocytes for 1 hour at 37 °C and the hemolysis assessed. Gratifyingly, all peptides displayed low hemolytic activity (< 5%) when tested at 32x MIC with only slight hemolysis observed for  $\Delta$ 12LB-NH<sub>2</sub> (**9**) and  $\Delta$ 12-13LL-NH<sub>2</sub> (**10**) measured at 3.8% and 3.0% respectively (**Table 3**). The low levels of hemolysis observed suggest a specific MOA is at play. However, future studies will be required to elucidate the exact mechanism by which these peptides operate.

## Conclusion

Cyclic NRPs are a common class of antibacterial agents encountered in Nature. Through the work described above, we have shown that the C-terminal macrocycles in brevicidine (**1**) and laterocidine (**2**) are not required for antibacterial activity. Although linear peptides bearing C-terminal carboxylates were significantly less active than their cyclic counterparts, amidation of the C-terminus increased the activity of the linear species to levels comparable to the natural products without introducing hemolytic effects. Further modification at Thr9, whose side chain forms the macrocycle with the C-terminus, yielded novel linear analogues that exhibit potent anti-Gram-negative activity, including against MCR-1 producing *E. coli*. *P. aeruginosa* is a major contributor to nosocomial infection rates, in fact the World Health Organisation (WHO) has listed carbapenem resistant *P. aeruginosa* as one of the top three critical priority pathogens that require antibiotic research.<sup>32</sup> Gratifyingly, the peptides presented herein also demonstrate equipotent or improved activity against *P. aeruginosa*. These linear peptides are more economical to synthesize as they do not require additional orthogonal protecting groups or extra cyclization steps. The convenience offered by the linear C-terminal amide brevicidine and laterocidine analogues also enabled an alanine scan study. This revealed that for both peptides, the residues (D-Tyr2, D-Trp3, D-Orn4, Orn5, D-Orn7 and Trp8) are essential for bioactivity. These residues are either cationic or aromatic (hydrophobic), which are key for target binding and maintaining an active conformation to cross the bacterial cell membrane. Of course, further MOA studies will be required to confirm how these peptides elicit their activity. The results of such assays will likely complement the findings of our alanine scan. Additionally, linear peptides are often more prone to proteolytic degradation than their cyclic counterparts. The large number of D-amino acids present in these novel linear analogues likely impart excellent protection against proteolytic degradation but further studies will be required to confirm this.

In nature, cyclic NRPs are prepared by non-ribosomal peptide synthetases, with the cyclization step performed by the thioesterase domain. To the best of our knowledge, this is the only natural method by which microorganisms can mask the C-terminus of NRPs. To date, the linearization of NRPs has not been frequently reported, raising the intriguing

possibility that the “linearization + amidation strategy” here reported might also be used in preparing functional linear analogues of other cyclic NRPs. Due to their constrained structures, cyclic peptides are intrinsically more ordered and suffer a lower entropic penalty upon target binding than linear peptides. However, many NRAPs are amphiphilic in nature and adopt ordered secondary structures upon interacting with the bacterial membrane. This may help offset the entropic penalty for some linear NRAPs (e.g., TriA<sub>1</sub><sup>33</sup>) and account for the retention of activity observed with the linear ornididine analogues reported in this study. Efforts to further establish the general applicability of this approach with cyclic NRPs that possess promising biological activities, and to assess the mechanism of action of the reported linear ornididine analogues, are now underway and will be reported in due course.

## Experimental Section

**General:** All proteinogenic Fmoc-amino acids used in this study were purchased from CEM or P3 BioSystems. For brevicidine analogues, Fmoc-D-Asn(Trt)-OH, Fmoc-D-Tyr(tBu)-OH, Fmoc-D-Trp(Boc)-OH, Fmoc-L-Glu(OAll)-OH, diisopropylethylamine (DIPEA), 2-(7-Aza-1H-benzotriazole-1-yl)-1,1,3,3-tetramethyluronium hexafluorophosphate (HATU), triisopropylsilane (TIPS), 4-methylpiperidine, phenylsilane, trifluoroacetic acid (TFA) and tetrakis(triphenylphosphine)palladium were purchased from Fluorochem. Fmoc-L-Orn(Boc)-OH, Fmoc-D-Orn(Boc)-OH, Fmoc-L-Dap(Alloc)-OH and (2S,3R)-(Fmoc-amino)-3-azidobutyric acid were purchased from ChemImpex. 4-Methylhexanoic acid and 2-chlorotriyl chloride (2-CT) resin (200-400 mesh) were purchased from Sigma Aldrich. Rink amide MBHA resin (100-200 mesh), diethyl ether, HPLC grade acetonitrile (ACN), dichloromethane (DCM) and N,N-dimethylformamide (DMF) were purchased from Sigma Aldrich. For laterocidine analogues, Fmoc-L-Orn(Boc)-OH, Fmoc-D-Orn(Boc)-OH, Fmoc-L-Dap(Alloc)-OH and Fmoc-L-Glu(OAll)-OH were purchased from CombiBlocks. 2-CT resin and Rink Amide MBHA were purchased from P3 BioSystems and Iris Biotech respectively. Isopelargonic acid was purchased from Enamine. ((1H-Benzo[d][1,2,3]triazol-1-yl)oxy)tris(dimethylamino) phosphonium hexafluorophosphate (BOP), N,N-diisopropylcarbodiimide (DIC), ethyl cyanohydroxyiminoacetate (Oxyma) and TIPS were purchased from Manchester Organics. DIPEA, piperidine, TFA and dimethylsulfoxide (DMSO) were purchased from Carl Roth. DCM and petroleum ether were purchased from VWR Chemicals. ACN, DMF and methyl tertiary-butyl ether (MTBE) were purchased from Biosolve. All chemicals were used without further purification. All synthetic compounds are >95% pure by HPLC analysis.

**Peptide Synthesis:** Peptides **1** and **2** were synthesized and purified as previously described.<sup>22,23</sup> Brevicidine analogues with a C-terminal acid were synthesized manually on a 0.05 mmol scale on 2-CT resin pre-loaded with Fmoc-Gly-OH in a Merrifield vessel. The resin loading was determined to be 0.73 mmol g<sup>-1</sup>. The resin was initially swollen by bubbling in DMF (3 mL) for 10 min. The solvent was discharged and the Fmoc group removed by addition of a 20% solution of 4-methylpiperidine in DMF (3 x 3 mL, 2 x 1 min then 1 x 3 min). The resin was washed with DMF (3 x 3 mL) and a coupling solution of amino acid (6 eq.), HATU (6 eq.) and DIPEA (12 eq.) in DMF (3 mL) was added. The coupling was bubbled with argon for 1 hour before being discharged and the resin was washed with DMF (3 x 3 mL). The

cycle of deprotections and couplings was repeated to obtain the full lipopeptide. Brevicidine analogues with a C-terminal amide were synthesized using a Liberty Blue HT12 system. Automated SPPS was performed on a 0.05 mmol scale using Fmoc chemistry on Rink amide resin. Factory settings were used for all coupling and deprotection cycles. Asymmetrically protected amino acids were used as 0.2 M solutions in DMF, with amino acid subunits being coupled using HATU as the activator and DIPEA as the activator base and heated to 70 °C for 3 min. Upon completion of synthesis, the peptide resin was washed with DCM (3 x 5 mL) and dried under a positive pressure of argon for 15 min. Global deprotection and resin cleavage was performed using a cocktail of TFA/TIPS/H<sub>2</sub>O (5 mL, 95 : 2.5 : 2.5) at 37 °C for 1 hour with frequent agitation. The cleavage solution was filtered through a glass wool plug and concentrated *in vacuo*. Cold diethyl ether was added to crash out the peptide, the suspension was centrifuged (3500 rpm, 3 min) and the solvent was decanted. The pellet was re-suspended in fresh diethylether and centrifuged (3500 rpm, 3 min) again. The solvent was decanted and the crude pellet was dissolved in a minimal amount of 20% acetonitrile solution in water with 0.1% TFA. The peptides were subsequently purified by Reversed-Phase High Performance Liquid Chromatography (RP-HPLC) (**Method A**). Laterocidine analogues containing a C-terminal acid were synthesized manually on a 0.1 mmol scale on 2-CT resin pre-loaded with Fmoc-Gly-OH. The resin loading was determined to be 0.73 mmol g<sup>-1</sup>. All couplings with the exception of the lipid were performed using amino acid (4 eq.), BOP (4 eq.) and DIPEA (8 eq.) in DMF (5 mL) for 1 hour at room temperature under a positive pressure of nitrogen. The lipid was coupled by treating the resin with isopelargonic acid (2 eq.), BOP (2 eq.) and DIPEA (4 eq.) in DMF (5 mL) overnight at room temperature. Fmoc removal was performed by treating the resin with 20% piperidine solution in DMF (5 mL, 1 x 5 min then 1 x 15 min). Laterocidine analogues with a C-terminal amide were synthesized automatically using a CEM Liberty Blue automated peptide synthesizer with microwave irradiation. Couplings were performed at 0.125 M concentration using amino acid (5 eq.), DIC (5 eq.) and Oxyma (5 eq.). Fmoc removal was performed using piperidine : DMF (1 : 4, v/v). Final sidechain deprotection and cleavage from resin was carried out by treating the resin with a cocktail of TFA/TIPS/H<sub>2</sub>O (5 mL, 95 : 2.5 : 2.5, v/v) for 90 min. The reaction mixture was filtered through cotton, the filtrate precipitated with MTBE/petroleum ether (1 : 1, v/v) and centrifuged (4500 rpm, 5 min). The pellet was resuspended in MTBE/petroleum ether (1 : 1, v/v) and centrifuged again (4500 rpm, 5 min). The crude pellet was dissolved in tBuOH/H<sub>2</sub>O (1 : 1, v/v) and lyophilized overnight. The crude mixtures were subsequently purified by RP-HPLC (**Method B**).

**Purification and analysis of peptides:** Brevicidine analogues were purified by Reversed-Phase High Performance Liquid Chromatography (RP-HPLC). Purification was performed on a Perkin Elmer HPLC system composed of a 200 series binary pump, UV/Vis detector, vacuum degasser, Rheodyne 7725i injector. The system was operated using ThermoFisher Chromeleon 7.2 software. **Method A:** Phenomenex Luna C18 column (5 µg, 250 x 21.2 mm) equipped with a 2 mL sample loop. Runs were performed at a flow rate of 10 mL/min with UV detection at 220 nm. Solvent A = 0.1% TFA in MilliQ water and solvent B = 0.1 % TFA in ACN. A gradient method was employed, starting from 5 % B and 95 % A for 5 min, ramping up to 8 % B over 20 min, then ramping up to 20 % B over 15 min, ramping up to 30 % B over 3 min, ramping again up to 95 % B over 4 min, remaining at 95 % B for 3 min, ramping down to 5 % B over 2 min before staying at 5 % B for 5 min. **Method B:** Purification was performed

on a BESTATEchnik system with a Dr. Maisch ReproSil Gold 120 C18 column (10  $\mu\text{m}$ , 25 x 250 mm) and equipped with a ECOM Flash UV detector. Runs were performed at a flow rate of 12 mL/min with UV detection at 214 nm and 254 nm. Solvent A = 0.1% TFA in water/ACN (95 : 5) and solvent B = 0.1% TFA in water/ACN (5 : 95). A gradient method was employed, starting at 100 % solvent A for 5 min, ramping up to 70 % solvent B over 50 min, remaining at 70 % solvent B for 3 min before ramping down to 100 % solvent A over 1 min and remaining there for 5 min. Product containing fractions were pooled, partially concentrated under vacuum, frozen and then lyophilized to yield pure peptides as white flocculent solids. A small amount of purified peptide was analyzed by analytical HPLC. Peptide purity was quantified by analytical HPLC (Brevicidine analogues – Method C, laterocidine analogues – Method D). **Method C (Analytical):** A Phenomenex Luna C18 column (5  $\mu\text{m}$ , 150 x 4.6 mm) was used, with samples injection to a 200  $\mu\text{L}$  sample loop. The flow rate was set at 2 mL/min and UV/Vis absorbance measured at 220 nm. Gradient elution was again employed using the same solvents, A and B. It began at 20 % B and 80 % A for 2 min, before ramping to 95 % B over 18 min. B was then decreased to 20 % over 0.1 min and held for 3.9 min. **Method D (Analytical):** Analytical runs of laterocidine analogues were performed on a Shimadzu Prominence-i LC-2030 system with a Dr. Maisch ReproSil Gold 120 C18 (5  $\mu\text{m}$ , 4.6 x 250 mm) at 30 °C. Runs were performed at a flow rate of 1 mL/min with UV detection at 214 nm and 254 nm. Solvent A = 0.1% TFA in water/ACN (95 : 5) and solvent B = 0.1% TFA in water/ACN (5 : 95). A gradient method was employed, starting at 100% solvent A for 2 min, ramping up to 50 % Solvent B over 45 min, ramping up to 100% solvent B over 1 min, remaining at 100% solvent B for 6 min before ramping down to 100% solvent A over 1 min and remaining there for 5 min. Electrospray ionization high resolution mass spectrometry (ESI-HRMS) was carried out on all purified brevicidine analogues by the Analytical Services and Environmental Projects (ASEP) Department at Queen's University Belfast. A Waters LCT Premier ToF mass spectrometer was used to obtain the relevant spectra. HRMS spectra of laterocidine peptides were performed on a Thermo Scientific Dionex UltiMate 3000 HPLC system with a Phenomenex Kinetex C18 (2.6  $\mu\text{m}$ , 2.1 x 150 mm) column at 35 °C and equipped with a diode array detector. The following solvent system, at a flow rate of 0.3 mL/min, was used: solvent A = 0.1% formic acid in water, solvent B = 0.1% formic acid in acetonitrile. A gradient method was employed, starting at 95 % solvent A and 5 % solvent B for 1 min, ramping up to 95 % solvent B over 9 min, ramping up to 98 % solvent B over 1 min, remaining there for 1 min before ramping back down to 95 % solvent A over 2 min and remaining there for 1 min. The system was connected to a Bruker micrOTOF-Q II mass spectrometer (ESI ionization) calibrated internally with sodium formate.

**Antibacterial Testing:** All minimum inhibitory concentrations (MICs) were determined according to Clinical and Laboratory Standards Institute (CLSI) guidelines. Blood agar plates were inoculated with glycerol stocks of *E. coli* ATCC 25922, *K. pneumoniae* ATCC 13883, *A. baumannii* ATCC 17961, *P. aeruginosa* PAO1 and *S. aureus* USA300. The inoculated agar plates were then incubated for 16 h at 37 °C. Individually grown colonies were subsequently used to inoculate 5 mL aliquots of TSB that were then incubated at 37 °C with shaking at 220 rpm. *E. coli* 25922 MCR-1 glycerol stock was used to inoculate 5 mL of TSB supplemented with kanamycin that was then incubated for 16 h at 37 °C with shaking at 220 rpm. The next day the culture was diluted 100-fold in TSB supplemented with kanamycin and incubated at 37 °C with shaking at 220 rpm. In parallel, the lipopeptide antibiotics DMSO stocks to be



assessed were serially diluted with MHB in polypropylene 96-well plates (50  $\mu\text{L}$  in each well). Colistin sulfate stocks were dissolved in water before being diluted with MHB. Aliquots of the inoculated TSB were incubated until an  $\text{OD}_{600}$  of around 0.5 was reached. The bacterial suspensions were then diluted with MHB ( $2 \times 10^5 \text{ CFU mL}^{-1}$ ) and added to the microplates containing the test compounds (50  $\mu\text{L}$  to each well). The well-plates were sealed with an adhesive membrane and after 18 h of incubation at 37 °C with shaking at 600 rpm, the wells were visually inspected for bacterial growth. MIC values reported are based on three technical replicates and defined as the lowest concentration of the compound that prevented visible growth of bacteria.

**Hemolytic assays:** Experiments were performed in triplicate and Triton X-100 used as a positive control. Red blood cells from defibrinated sheep blood obtained from ThermoFisher were centrifuged (400 g for 15 min at 4°C) and washed with Phosphate-Buffered Saline (PBS) containing 0.002% Tween20 (buffer) five times. Then, the red blood cells were normalized to obtain a positive control read-out between 2.5 and 3.0 at 415 nm to stay within the linear range with the maximum sensitivity. A serial dilution of the compounds (128 – 1  $\mu\text{g/mL}$ , 75  $\mu\text{L}$ ) was prepared in a 96-well polypropylene plate. The outer border of the plate was filled with 75  $\mu\text{L}$  buffer. Each plate contained a positive control (0.1% Triton-X final concentration, 75  $\mu\text{L}$ ) and a negative control (buffer, 75  $\mu\text{L}$ ) in triplicate. The normalized blood cells (75  $\mu\text{L}$ ) were added, and the plates were incubated at 37 °C for 1 h while shaking at 500 rpm. A flat-bottom polystyrene plate with 100  $\mu\text{L}$  buffer in each well was prepared. After incubation, the plates were centrifuged (800 g for 5 min at room temperature) and 25  $\mu\text{L}$  of the supernatant was transferred to their respective wells in the flat-bottom plate. The values obtained from a read-out at 415 nm were corrected for background (negative control) and transformed to a percentage relative to the positive control.

### Linear Brevicidines and Laterocidines Hemolysis (%) at 64 $\mu\text{g/ml}$ , 1 h incubation

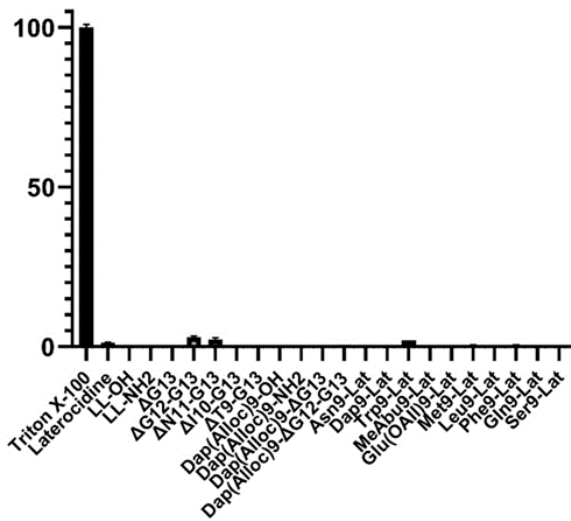
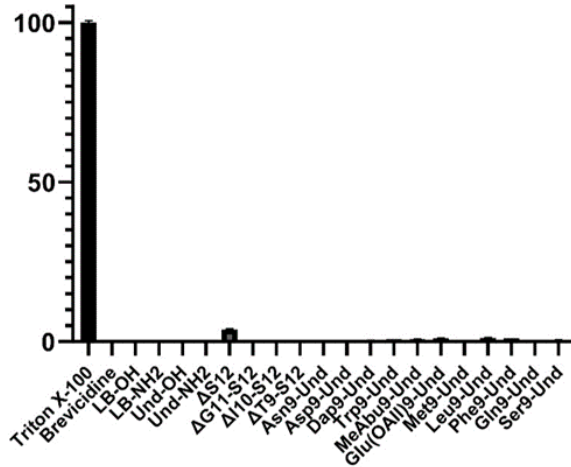


**Figure 3.** Hemolytic assays of ornucidine analogues at 64  $\mu\text{g mL}^{-1}$  following 1 hour incubation with sheep blood cells.

## HPLC and HRMS analysis of peptides

**Table S1.** Peptide number, name, chemical formula, exact mass, mass found and overall yield for peptides 4 – 64. HPLC traces of all peptides can be found at <https://doi.org/10.1021/acs.jmedchem.3c00308>

Peptide	Name	Chemical Formula	Calcd Exact Mass	Mass found	Calcd	Overall Yield [%]
4	LL-OH	C <sub>78</sub> H <sub>115</sub> N <sub>19</sub> O <sub>19</sub>	1621.8617	811.9386 [M+2H] <sup>2+</sup>	811.9381	19
5	LB-OH	C <sub>74</sub> H <sub>108</sub> N <sub>18</sub> O <sub>18</sub>	1536.8089	769.4144 [M+2H] <sup>2+</sup>	769.4117	8
6	LL-NH <sub>2</sub>	C <sub>78</sub> H <sub>116</sub> N <sub>20</sub> O <sub>18</sub>	1620.8776	811.4464 [M+2H] <sup>2+</sup>	811.4461	29
7	LB-NH <sub>2</sub>	C <sub>74</sub> H <sub>109</sub> N <sub>19</sub> O <sub>17</sub>	1535.8249	768.9221 [M+2H] <sup>2+</sup>	768.9200	8
8	Δ13LL-NH <sub>2</sub>	C <sub>76</sub> H <sub>113</sub> N <sub>19</sub> O <sub>17</sub>	1563.8562	782.9358 [M+2H] <sup>2+</sup>	782.9354	29
9	Δ12LB-NH <sub>2</sub>	C <sub>76</sub> H <sub>108</sub> N <sub>18</sub> O <sub>15</sub>	1448.7929	1471.7715 [M+H] <sup>+</sup>	1471.7821	38
10	Δ12-13LL-NH <sub>2</sub>	C <sub>74</sub> H <sub>110</sub> N <sub>18</sub> O <sub>16</sub>	1506.8347	754.4248 [M+2H] <sup>2+</sup>	754.4247	24
11	Δ11-12LB-NH <sub>2</sub>	C <sub>69</sub> H <sub>101</sub> N <sub>17</sub> O <sub>14</sub>	1391.7714	1392.7838 [M+H] <sup>+</sup>	1392.7787	13
12	Δ11-13LL-NH <sub>2</sub>	C <sub>70</sub> H <sub>104</sub> N <sub>16</sub> O <sub>14</sub>	1392.7918	697.4037 [M+2H] <sup>2+</sup>	697.4032	20
13	Δ10-12LB-NH <sub>2</sub>	C <sub>63</sub> H <sub>90</sub> N <sub>16</sub> O <sub>13</sub>	1278.6873	1279.7019 [M+H] <sup>+</sup>	1279.6946	14
14	Δ10-13LL-NH <sub>2</sub>	C <sub>64</sub> H <sub>93</sub> N <sub>15</sub> O <sub>13</sub>	1279.7077	640.8614 [M+2H] <sup>2+</sup>	640.8612	29
15	Δ9-12LB-NH <sub>2</sub>	C <sub>59</sub> H <sub>83</sub> N <sub>15</sub> O <sub>11</sub>	1177.6396	1178.6526 [M+H] <sup>+</sup>	1178.6469	13
16	Δ9-13LL-NH <sub>2</sub>	C <sub>60</sub> H <sub>86</sub> N <sub>14</sub> O <sub>11</sub>	1178.6600	1179.6670 [M+H] <sup>+</sup>	1179.6673	14
17	LB(D-Ala1)-NH <sub>2</sub>	C <sub>73</sub> H <sub>107</sub> N <sub>17</sub> O <sub>17</sub>	1493.8031	747.4174 [M+2H] <sup>2+</sup>	747.4175	11
18	LB(D-Ala2)-NH <sub>2</sub>	C <sub>68</sub> H <sub>104</sub> N <sub>16</sub> O <sub>17</sub>	1444.7827	1466.7829 [M+Na] <sup>+</sup>	1466.7885	6
19	LB(D-Ala3)-NH <sub>2</sub>	C <sub>65</sub> H <sub>103</sub> N <sub>17</sub> O <sub>18</sub>	1421.7667	1421.7842 [M+H] <sup>+</sup>	1421.7905	9
20	LB(D-Ala4)-NH <sub>2</sub>	C <sub>72</sub> H <sub>103</sub> N <sub>17</sub> O <sub>18</sub>	1493.7667	747.4002 [M+2H] <sup>2+</sup>	747.3992	3
21	LB(Ala5)-NH <sub>2</sub>	C <sub>72</sub> H <sub>103</sub> N <sub>17</sub> O <sub>18</sub>	1493.7667	747.3993 [M+2H] <sup>2+</sup>	747.3992	8
22	LB(Ala6)-NH <sub>2</sub>	C <sub>75</sub> H <sub>110</sub> N <sub>18</sub> O <sub>18</sub>	1550.8245	775.9287 [M+2H] <sup>2+</sup>	775.9281	7
23	LB(D-Ala7)-NH <sub>2</sub>	C <sub>72</sub> H <sub>102</sub> N <sub>17</sub> O <sub>18</sub>	1493.7667	747.3990 [M+2H] <sup>2+</sup>	747.3992	8
24	LB(Ala8)-NH <sub>2</sub>	C <sub>66</sub> H <sub>103</sub> N <sub>17</sub> O <sub>18</sub>	1421.7667	711.3997 [M+2H] <sup>2+</sup>	711.3992	19
25	LB(Ala9)-NH <sub>2</sub>	C <sub>73</sub> H <sub>106</sub> N <sub>18</sub> O <sub>17</sub>	1506.7983	1528.7998 [M+Na] <sup>+</sup>	1528.8041	17
26	LB(Ala10)-NH <sub>2</sub>	C <sub>71</sub> H <sub>102</sub> N <sub>18</sub> O <sub>18</sub>	1494.7619	1494.7811 [M+H] <sup>+</sup>	1494.7858	9
27	LB(Ala11)-NH <sub>2</sub>	C <sub>75</sub> H <sub>110</sub> N <sub>18</sub> O <sub>18</sub>	1550.8245	775.9284 [M+2H] <sup>2+</sup>	775.9281	7
28	LB(Ala12)-NH <sub>2</sub>	C <sub>74</sub> H <sub>108</sub> N <sub>18</sub> O <sub>17</sub>	1520.8140	760.9227 [M+2H] <sup>2+</sup>	760.9228	15
29	LL(D-Ala1)-NH <sub>2</sub>	C <sub>75</sub> H <sub>111</sub> N <sub>20</sub> O <sub>17</sub>	1604.8827	803.4487 [M+2H] <sup>2+</sup>	803.4487	34
30	LL(D-Ala2)-NH <sub>2</sub>	C <sub>72</sub> H <sub>112</sub> N <sub>20</sub> O <sub>17</sub>	1528.8514	765.4331 [M+2H] <sup>2+</sup>	765.4330	31
31	LL(D-Ala3)-NH <sub>2</sub>	C <sub>70</sub> H <sub>111</sub> N <sub>19</sub> O <sub>18</sub>	1505.8354	753.9254 [M+2H] <sup>2+</sup>	753.9250	37
32	LL(D-Ala4)-NH <sub>2</sub>	C <sub>76</sub> H <sub>111</sub> N <sub>19</sub> O <sub>18</sub>	1577.8354	789.9256 [M+2H] <sup>2+</sup>	789.9250	27
33	LL(Ala5)-NH <sub>2</sub>	C <sub>76</sub> H <sub>111</sub> N <sub>19</sub> O <sub>18</sub>	1577.8354	789.9255 [M+2H] <sup>2+</sup>	789.9250	30
34	LL(Ala6)-NH <sub>2</sub>	C <sub>79</sub> H <sub>118</sub> N <sub>20</sub> O <sub>18</sub>	1634.8933	818.4544 [M+2H] <sup>2+</sup>	818.4539	34
35	LL(D-Ala7)-NH <sub>2</sub>	C <sub>76</sub> H <sub>111</sub> N <sub>19</sub> O <sub>18</sub>	1577.8354	789.9256 [M+2H] <sup>2+</sup>	789.9250	28
36	LL(Ala8)-NH <sub>2</sub>	C <sub>70</sub> H <sub>111</sub> N <sub>19</sub> O <sub>18</sub>	1505.8354	753.9254 [M+2H] <sup>2+</sup>	753.9250	31
37	LL-(Ala9)-NH <sub>2</sub>	C <sub>77</sub> H <sub>114</sub> N <sub>20</sub> O <sub>17</sub>	1590.8671	796.4409 [M+2H] <sup>2+</sup>	796.4408	43
38	LL(Ala10)-NH <sub>2</sub>	C <sub>75</sub> H <sub>110</sub> N <sub>20</sub> O <sub>18</sub>	1578.8307	790.4229 [M+2H] <sup>2+</sup>	790.4226	34
39	LL(Ala11)-NH <sub>2</sub>	C <sub>75</sub> H <sub>115</sub> N <sub>20</sub> O <sub>17</sub>	1577.8718	789.9429 [M+2H] <sup>2+</sup>	789.9432	20
40	LL(Ala12)-NH <sub>2</sub>	C <sub>78</sub> H <sub>118</sub> N <sub>20</sub> O <sub>18</sub>	1634.8933	818.4546 [M+2H] <sup>2+</sup>	818.4539	29
41	LL(Ala13)-NH <sub>2</sub>	C <sub>79</sub> H <sub>118</sub> N <sub>20</sub> O <sub>18</sub>	1634.8933	818.4541 [M+2H] <sup>2+</sup>	818.4539	32
42	LL(Leu9)-NH <sub>2</sub>	C <sub>80</sub> H <sub>120</sub> N <sub>20</sub> O <sub>17</sub>	1632.9140	817.4644 [M+2H] <sup>2+</sup>	817.4643	10
43	LL(Phe9)-NH <sub>2</sub>	C <sub>83</sub> H <sub>118</sub> N <sub>20</sub> O <sub>17</sub>	1666.8984	834.4563 [M+2H] <sup>2+</sup>	834.4565	22
44	LL(Met9)-NH <sub>2</sub>	C <sub>79</sub> H <sub>118</sub> N <sub>20</sub> O <sub>17</sub> S	1650.8705	826.4424 [M+2H] <sup>2+</sup>	826.4425	17
45	LL(Trp9)-NH <sub>2</sub>	C <sub>85</sub> H <sub>119</sub> N <sub>21</sub> O <sub>17</sub>	1705.9093	853.9619 [M+2H] <sup>2+</sup>	853.9619	20
46	LL(Ser9)-NH <sub>2</sub>	C <sub>77</sub> H <sub>114</sub> N <sub>20</sub> O <sub>18</sub>	1606.8620	804.4386 [M+2H] <sup>2+</sup>	804.4383	22

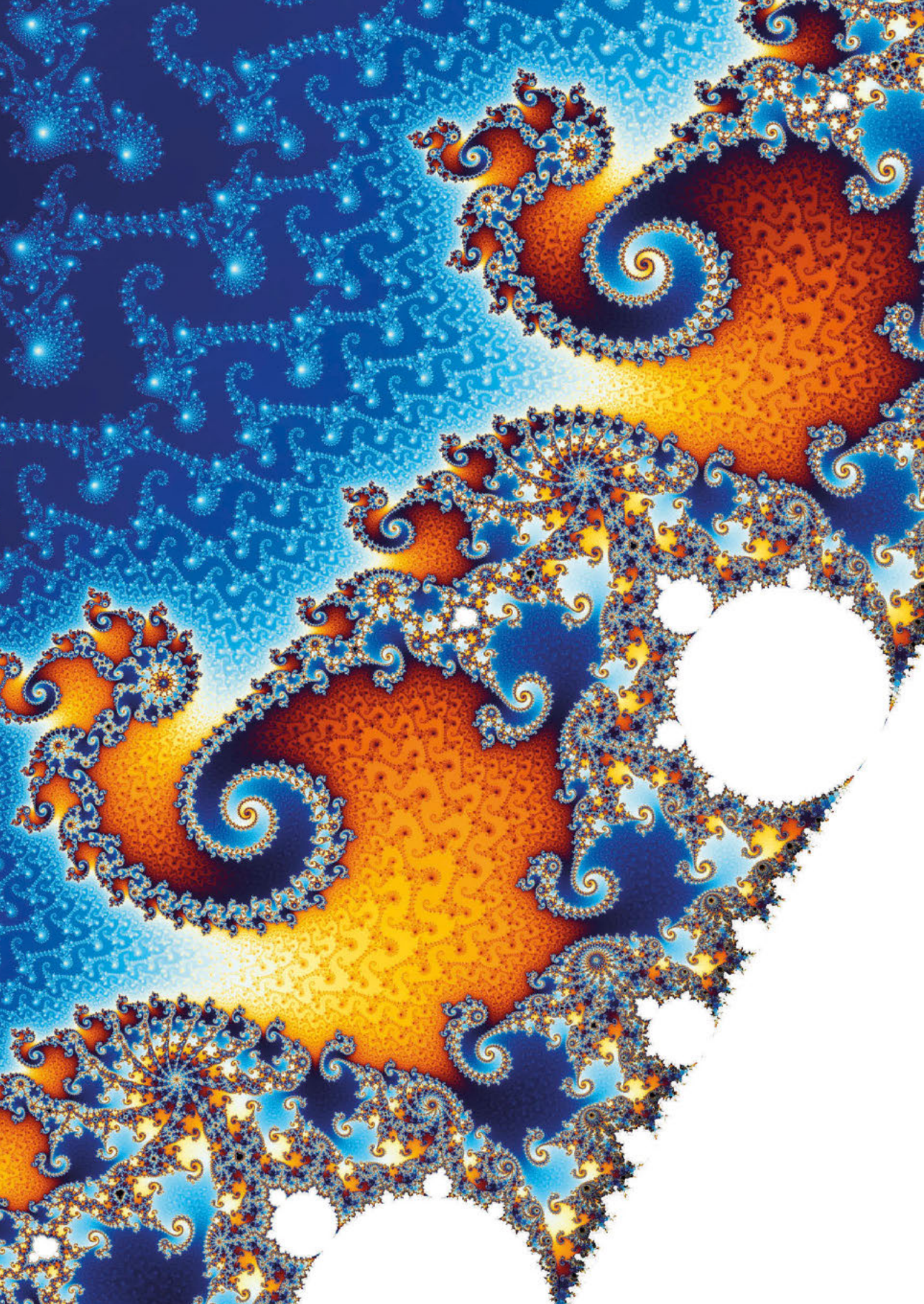
47	LL(Asn9)-NH <sub>2</sub>	C <sub>78</sub> H <sub>115</sub> N <sub>21</sub> O <sub>18</sub>	1633.8729	817.9438 [M+2H] <sup>2+</sup>	817.9437	20
48	LL(Gln9)-NH <sub>2</sub>	C <sub>79</sub> H <sub>117</sub> N <sub>21</sub> O <sub>18</sub>	1647.8885	824.9519 [M+2H] <sup>2+</sup>	824.9516	17
49	LL(MeAbu9)-NH <sub>2</sub>	C <sub>78</sub> H <sub>115</sub> N <sub>23</sub> O <sub>17</sub>	1645.8841	823.9495 [M+2H] <sup>2+</sup>	823.9494	13
50	LL(Dap[Alloc]9)-NH <sub>2</sub>	C <sub>81</sub> H <sub>119</sub> N <sub>21</sub> O <sub>19</sub>	1689.8991	845.9574 [M+2H] <sup>2+</sup>	845.9569	15
51	LL(Glu[OAlI]9)-NH <sub>2</sub>	C <sub>82</sub> H <sub>120</sub> N <sub>20</sub> O <sub>19</sub>	1688.9039	845.4595 [M+2H] <sup>2+</sup>	845.4592	14
52	LL(Dap9)-NH <sub>2</sub>	C <sub>77</sub> H <sub>115</sub> N <sub>23</sub> O <sub>17</sub>	1605.8780	803.9465 [M+2H] <sup>2+</sup>	803.9463	21
53	Δ12LB(Leu9)-NH <sub>2</sub>	C <sub>75</sub> H <sub>108</sub> N <sub>18</sub> O <sub>14</sub>	1460.8292	1461.8273 [M+H] <sup>+</sup>	1461.8365	38
54	Δ12LB(Phe9)-NH <sub>2</sub>	C <sub>76</sub> H <sub>108</sub> N <sub>18</sub> O <sub>14</sub>	1494.8136	748.4111 [M+2H] <sup>2+</sup>	748.4141	30
55	Δ12LB(Met9)-NH <sub>2</sub>	C <sub>77</sub> H <sub>108</sub> N <sub>18</sub> O <sub>14</sub> S	1478.7857	1479.7827 [M+H] <sup>+</sup>	1479.7930	13
56	Δ12LB(Trp9)-NH <sub>2</sub>	C <sub>78</sub> H <sub>107</sub> N <sub>19</sub> O <sub>14</sub>	1533.8245	512.2821 [M+2H] <sup>2+</sup>	512.2717	24
57	Δ12LB(Ser9)-NH <sub>2</sub>	C <sub>79</sub> H <sub>102</sub> N <sub>18</sub> O <sub>16</sub>	1434.7772	1435.7797 [M+H] <sup>+</sup>	1435.7845	42
58	Δ12LB(Asn9)-NH <sub>2</sub>	C <sub>71</sub> H <sub>103</sub> N <sub>19</sub> O <sub>15</sub>	1461.7881	1484.7651 [M+H] <sup>+</sup>	1484.7773	12
59	Δ12LB(Gln9)-NH <sub>2</sub>	C <sub>72</sub> H <sub>105</sub> N <sub>19</sub> O <sub>15</sub>	1475.8038	492.9408 [M+3H] <sup>3+</sup>	493.9358	24
60	Δ12LB(MeAbu9)-NH <sub>2</sub>	C <sub>71</sub> H <sub>103</sub> N <sub>21</sub> O <sub>14</sub>	1473.7993	737.9129 [M+H] <sup>+</sup>	737.9069	22
61	Δ12LB(Dap[Alloc]9)-NH <sub>2</sub>	C <sub>74</sub> H <sub>107</sub> N <sub>19</sub> O <sub>16</sub>	1517.8143	749.9157 [M+2H] <sup>2+</sup>	749.9144	33
62	Δ12LB(Glu[OAlI]9)-NH <sub>2</sub>	C <sub>75</sub> H <sub>108</sub> N <sub>18</sub> O <sub>16</sub>	1516.8191	506.6093 [M+3H] <sup>3+</sup>	506.6136	21
63	Δ12LB(Asp9)-NH <sub>2</sub>	C <sub>71</sub> H <sub>103</sub> N <sub>18</sub> O <sub>16</sub>	1462.7721	732.3873 [M+2H] <sup>2+</sup>	732.3933	27
64	Δ12LB(Dap9)-NH <sub>2</sub>	C <sub>70</sub> H <sub>103</sub> N <sub>19</sub> O <sub>14</sub>	1433.7932	717.9044 [M+2H] <sup>2+</sup>	717.9039	22

## References

- O'Neill, J. Review on Antibacterial Resistance, **2014**
- Antibacterial resistance collaborators, Global burden of bacterial antimicrobial resistance in 2019. *Lancet* **2022**, 399, 629 – 655. DOI: 10.1016/S0140-6736(21)02724-0
- Boucher, H. W.; Talbot, G. H.; Bradley, J. S.; Edwards, J. E.; Gilbert, D.; Rice, L. B.; Scheld, M.; Spellberg, B.; Bartlett, No Drugs: No ESCAPE! An Update from the Infectious Diseases Society of America. *Clin. Infect. Dis.* **2009**, 48 (1), 1 – 12. DOI: 10.1086/595011
- Liu, Y.; Ding, S.; Shen, J.; Zhu, K. Nonribosomal antibacterial peptides that target multidrug-resistant bacteria. *Nat. Prod. Rep.* **2019**, 36, 573 – 592. DOI: 10.1039/C8NP00031J
- Koo, H. B.; Seo, J. Antimicrobial peptides under clinical investigation. *Pept. Sci.* **2019**, 111 (5), e24122. DOI: 10.1002/pep2.24122
- Hamamoto, H.; Urai, M.; Ishii, K.; Yasukawa, J.; Paudel, A.; Murai, M.; Kaji, T.; Kuranaga, T.; Hamase, K.; Katsu, T.; Su, J.; Adachi, T.; Uchida, R.; Tomoda, H.; Yamada, M.; Souma, M.; Kurihira, H.; Inoue, M.; Sekimizu, K. Lysocin E is a new antibiotic that targets menaquinone in the bacterial membrane. *Nat. Chem. Biol.* **2015**, 11 (2), 123 – 133. DOI: 10.1038/nchembio.171
- Ling, L. L.; Schneider, T.; Peoples, A. J.; Sporing, A. L.; I. Engels, Conlon, B. P.; Mueller, A.; Schäberle, T. F.; Hughes, D. E.; Epstein, S.; Jones, M.; Lazarides, L.; Steadman, V. A.; Cohen, D. R.; Felix, C. R.; Fetterman, K. A.; Millett, W. P.; Nitti, A. G.; Zullo, A. M.; Chen, C.; Lewis, K. A new antibiotic kills pathogens without detectable resistance. *Nature* **2015**, 517, 455 – 459. DOI: 10.1038/nature14098
- Zipperer, A.; Konnerth, M. C.; Laux, C.; Berscheid, A.; Janek, D.; Weidenmaier, C.; Burian, M.; Schilling, N. A.; Slavetinsky, C.; Marschal, M.; Willmann, M.; Kalbacher, H.; Schitteck, B.; Brötz-Oesterheld, H.; Grond, S.; Peschel, A.; Krismer, B. Human commensals producing a novel antibiotic impair pathogen colonization. *Nature* **2016**, 535, 511 – 516. DOI: 10.1038/nature18634
- Hover, B. M.; Kim, S.-H.; Katz, M.; Charlop-Powers, Z.; Owen, J. G.; Ternei, M. A.; Maniko, J.; Estrela, A. B.; Molina, H.; Park, S.; Perlin, D. S.; Brady, S. F. Culture-independent discovery of the malacidins as calcium-dependent antibiotics with activity against multidrug-resistant Gram-positive pathogens. *Nat. Microbiol.* **2018**, 3, 415 – 422. DOI: 10.1038/s41564-018-0110-1
- Wang, Z.; Koirala, B.; Hernandez, Y.; Zimmerman, M.; Brady, S.F. Bioinformatic prospecting and synthesis of a bifunctional lipopeptide antibiotic that evades resistance. *Science* **2022**, 376 (6596), 991 – 996. DOI: 10.1126/science.abn4213

- (11) Murai, M.; Kaji, T.; Kuranaga, T.; Hamamoto, H.; Sekimizu, K.; Inoue, M. Total Synthesis and Biological Evaluation of the Antibiotic Lysocin E and Its Enantiomeric, Epimeric, and N-Demethylated Analogues. *Angew. Chem. Int. Ed.* **2015**, *54* (5), 1556 – 1560. DOI: 10.1002/anie.201410270
- (12) Jin, K.; Sam, I. H.; Po, K. H. L.; Lin, D.; Zadeh, E. H. G.; Chen, S.; Yuan, Y.; Li, X. Total synthesis of teixobactin. *Nat. Commun.* **2016**, *7* (12394), 1 – 6. DOI: 10.1038/ncomms12394
- (13) Schilling, N. A.; Berscheid, A.; Schumacher, J.; Saur, J. S.; Konnerth, M. C.; Wirtz, S. N.; Beltrán-Beleña, J. M.; Zipperer, A.; Krismer, B.; Peschel, A.; Kalbacher, H.; Brötz-Oesterhelt, H.; Steinem, C.; Grond, S. Synthetic Lugdunin Analogues Reveal Essential Structural Motifs for Antimicrobial Action and Proton Translocation Capability. *Angew. Chem. Int. Ed.* **2019**, *58* (27), 9234 – 9238. DOI: 10.1002/anie.201901589
- (14) Kovalenko, N.; Howard, G. K.; Swain, J. A.; Hermant, Y.; Cameron, A. J.; Cook, G. M.; Ferguson, S. A.; Stubbing, L. A.; Harris, P. W. R.; Brimble, M. A. A Concise Synthetic Strategy Towards the Novel Calcium-dependent Lipopeptide Antibiotic, Malacidin A and Analogues. *Front. Chem.* **2021**, *9* (687875), 1 – 11. DOI: 10.3389/fchem.2021.687875
- (15) Chow, H. Y.; Po, K. H. L.; Jin, K.; Qiao, G.; Sun, Z.; Ma, W.; Ye, X.; Zhou, N.; Chen, S.; Li, X. Establishing the Structure-Activity Relationship of Daptomycin. *ACS Med. Chem. Lett.* **2020**, *11*, 1442 – 1449. DOI: 10.1021/acsmchemlett.0c00175
- (16) Cochrane, S. A.; Findlay, B.; Vederas, J. C.; Rastemi, E. S. Key Residues in Octyl-Tridecaptin A<sub>1</sub> Analogues Linked to Stable Secondary Structures in the Membrane. *ChemBioChem* **2014**, *15*, 1295 – 1299. DOI: 10.1002/cbic.201402024
- (17) Kanazawa, K.; Sato, Y.; Ohki, K.; Okimura, K.; Uchida, Y.; Shindo, M.; Sakura, N. Contribution of each amino acid residue polymyxin B(3) to antimicrobial and lipopolysaccharide binding activity. *Chem. Pharm. Bull.* **2009**, *57* (3), 240 – 244. DOI: 10.1248/cpb.57.240
- (18) Wood, T.; Zeronian, M. R.; Buijs, N.; Bertheussen, K.; Abedian, H. K.; Johnson, A. V.; Pearce, N. M.; Lutz M.; Kemmink, J.; Seirnsma, T.; Hamoen, L. W.; Janssen, B. J. C.; Martin, N. I. Mechanistic insights into the C<sub>55</sub>-P targeting lipopeptide antibiotics revealed by the structure-activity studies and high-resolution crystal structures. *Chem. Sci.* **2022**, *13*, 2985 – 2991. DOI: 10.1039/D1SC07190D
- (19) Parmar, A.; Iyer, A.; Prior, S. H.; Lloyd, D. G.; Goh, E. T. L.; Vincent, C. S.; Palmal-Pallag, T.; Bachrati, C.; Breukink, E.; Maddar, A.; Lakshminarayanan, R.; Taylor, E. J.; Singh, I. Teixobactin analogues reveal enduracididine to be non-essential for highly potent antibacterial activity and lipid II binding. *Chem. Sci.* **2017**, *8*, 8183 – 8192. DOI: 10.1039/C7SC03241B
- (20) Parmar, A.; Lakshminarayanan, R.; Iyer, A.; Mayandi, V.; Goh, E. T. L.; Lloyd, D. G.; Chalasani, M. L. S.; Verma, N. K.; Prior, S. H.; Beuerman, R. W.; Maddar, A.; Taylor, E. J.; Singh, I. Design and Syntheses of Highly Potent Teixobactin Analogues against *Staphylococcus aureus*, Methicillin-Resistant *Staphylococcus aureus* (MRSA), and Vancomycin-Resistant Enterococci (VRE) *in Vitro* and *in Vivo*. *J. Med. Chem.* **2018**, *61*, 2009 – 2017. DOI: 10.1021/acs.jmedchem.7b01634
- (21) Malik, E.; Phoenix, D. A.; Snape, T. J.; Harris, F.; Singh, J.; Morton, L. H. G.; Dennison, S. R. Linearized esculentin-2EM shows pH dependent antibacterial activity with an alkaline optimum. *Mol. Cell Biochem.* **2021**, *476* (10), 3729 – 3744. DOI: 10.1007/s11010-021-04181-7
- (22) Li, X. Y.; Zhong, Z.; Zhang, W. P.; Qian, P. Y. Discovery of cationic nonribosomal peptides as Gram-negative antibiotics through global genome mining. *Nat. Commun.* **2018**, *9*, 3273 – 3281. DOI: 10.1038/s41467-018-05781-6
- (23) Li, Z.; Chakraborty, P.; de Vries, R. H.; Song, C.; Zhao, X.; Roelfes, G.; Scheffers, D.-J.; Kuipers, O. P. Characterization of two relacidines belonging to a novel class of circular lipopeptides that act against Gram-negative bacterial pathogens. *Environ. Microbiol.* **2020**, *22* (12), 5125 – 5136. DOI: 10.1111/1462-2920.15145
- (24) Al-Ayed, K.; Ballantine, R. D.; Hoekstra, M.; Bann, S. J.; Wesseling, C. M. J.; Bakker, A. T.; Zhong, Z.; Li, Y. X.; Brühle, N. C.; van der Stelt, M.; Cochrane, S. A.; Martin, N. I. Synthetic studies with the brevicidine and laterocidine lipopeptide antibiotics including analogues with enhanced properties and *in Vivo* efficacy. *Chem. Sci.* **2022**, *13*, 3563 – 3570. DOI: 10.1039/D2SC00143H
- (25) Ballantine, R. D.; Al Ayed, K.; Bann, S. J.; Hoekstra, M.; Martin, N. I.; Cochrane, S. A. Synthesis and structure-activity relationship studies of N-terminal analogues of the lipopeptide antibiotics brevicidine and laterocidine. *RSC Med. Chem.* **2022**, *13* (12), 1640 – 1643. DOI: 10.1039/D2MD00281G

- (26) Gogry, F. A.; Siddiqui, M. T.; Sultan, I.; Haq, Q. M. R. Current Update on Intrinsic and Acquired Colistin Resistance Mechanisms in Bacteria. *Front. Med.* **2021**, *8* (677720). DOI: 10.3389/frmed.2021.677720
- (27) Omardien, S.; Brul, S.; Zaat, S. A. J. Antimicrobial Activity of Cationic Antimicrobial Peptides against Gram-Positives: Current Progress Made in Understanding the Mode of Action and the Response of Bacteria. *Front. Cell Dev. Biol.* **2016**, *4* (111), 1 – 16. DOI: 10.3389/fcell.2016.00111
- (28) de Araujo, A. D.; Hoang, H. N.; Lim, J.; Mak, J. Y. W.; Fairlie, D. P. Tuning Electrostatic and Hydrophobic Surfaces of Aromatic Rings to Enhance Membrane Association and Cell Uptake of Peptides. *Angew. Chem. Intl. Ed.* **2022**, *61* (29), e202203995. DOI: 10.1002/anie.202203995
- (29) Chou, H-T.; Wen, H-W.; Kuo, T-Y.; Lin, C-C.; Chen, W-J. Interactions of cationic antimicrobial peptides with phospholipid vesicles and their antibacterial activity. *Peptides* **2010**, *31* (10), 1811 – 1820. DOI: 10.1016/j.peptides.2010.06.021
- (30) Cochrane, S. A.; Findlay, B.; Bakhtiary, A.; Acedo, J. Z.; Mercier, P.; Vederas, J. C. Antimicrobial lipopeptide tridecaptin A1 selectively binds to Gram-negative lipid II. *Proc. Natl. Acad. Sci. USA* **2016**, *113* (41), 11561 – 11566. DOI: 10.1073/pnas.1608623113
- (31) Zhao, X.; Zhong, Z.; Yang, S.; Deng, K.; Liu, L.; Song, X.; Zou, Y.; Li, L.; Zhou, Z.; Jia, R.; Lin, J.; Tang, H.; Ye, G.; Yang, J.; Zhao, S.; Lang, Y.; Wan, H.; Yin, Z.; Kuipers, O. P. Elucidating the Mechanism of Action of the Gram-Negative-Pathogen-Selective Cyclic Antimicrobial Lipopeptide Brevicidine. *Antimicrob. Agents Chemother.* **2023**, e00010-23. DOI: 10.1128/aac.00010-23
- (32) World Health Organization. Prioritization of pathogens to guide discovery, research, and development of new antibiotics for drug-resistant bacterial infections, including tuberculosis. Geneva. 2017. WHO/EMP/IAU/2017.12.
- (33) Bann, S. J.; Ballantine, R. D.; Cochrane, S. A. The tridecaptins: non-ribosomal peptides that selectively target Gram-negative bacteria. *RSC Med. Chem.* **2021**, *12*, 538.551. DOI: 10.1039/D0MD00413H.



## Chapter 5

# Total Synthesis and Structure Assignment of the Relacidine Lipopeptide Antibiotics and Preparation of Analogues with Enhanced Stability

### **Abstract**

The unabated rise of antibiotic resistance has raised the specter of a post-antibiotic era underscoring the importance of developing new classes of antibiotics. The relacidines are a recently discovered group of non-ribosomal lipopeptide antibiotics that show promising activity against Gram-negative pathogens and share structural similarities with brevicidine and laterocidine. While the first reports of the relacidines indicated that they possess a C-terminal five-amino acid macrolactone, an N-terminal lipid tail, and an overall positive charge, no stereochemical configuration was assigned precluding a full structure determination. To address this issue we here report a bioinformatics guided total synthesis of relacidine A and B and show that the authentic natural products match our predicted and synthesized structures. Following on this, we also synthesized an analogue of relacidine A wherein the ester linkage of the macrolactone was replaced by the corresponding amide. This analogue was found to possess enhanced hydrolytic stability while maintaining the antibacterial activity of the natural product in both *in vitro* and *in vivo* efficacy studies.

### **Parts of this chapter have been published in ACS Infectious Diseases:**

Al Ayed, K.; Zamarbide Losada, D.; Machushynets, N. V.; Terlouw, B.; Elsayed, S. S.; Schill, J.; Trebosc, V.; Pieren, M.; Medema, M. H.; van Wezel, G. P.; Martin, N. I. Total Synthesis and Structure Assignment of the Relacidine Lipopeptide Antibiotics and Preparation of Analogues with Enhanced Stability. *ACS Infect Dis* **2023**, *9* (4), 739–748. <https://doi.org/10.1021/acsinfecdis.3c00043>.

### **Parts of the data in this chapter are part of a patent:**

"Antibiotic natural product analogues"; Cochrane, S.A.; Ballantine, R. D.; Martin, N. I.; Al Ayed, K.; Hoekstra, M.; Zamarbide Losada, S.D.; Priority Date: 28 January 2021; Published: 4 August 2022; WO2022162332A1



## Introduction

Antimicrobial resistance (AMR) is recognized as a serious threat to public health today and has been projected to become a major global health crisis in the near future. A recently published study estimated that in 2019 there were 4.95 million deaths associated with bacterial AMR, including 1.27 million deaths directly attributable to AMR.<sup>1</sup> Beyond these current numbers, some have estimated that AMR could kill upwards of 10 million people per year globally by 2050.<sup>2,3</sup> Moreover, a recent report from the US Centers for Disease Control and Prevention found that the COVID-19 pandemic has further accelerated the spread of AMR, particularly in hospital settings.<sup>4</sup> In assessing the threat posed by AMR, the so-called ESKAPE pathogens have risen to prominence comprising: *Enterococcus faecium*, *Staphylococcus aureus*, *Klebsiella pneumoniae*, *Acinetobacter baumannii*, *Pseudomonas aeruginosa*, and *Enterobacter* species.<sup>5</sup> These pathogens are prone to developing antibiotic resistance and the infections they cause are often difficult to treat. Notable among the ESKAPE pathogens are the Gram-negative species which the World Health Organization has exclusively categorized as threat-level 'critical'. While there is a dire need for antibacterial agents that can effectively combat these particularly dangerous Gram-negative bacteria, the development of new antibiotics has stagnated since the 1980s.<sup>6</sup> Clearly, innovative approaches are needed to discover and develop new antibiotics that act against these pathogens.

In 2018, Qian and coworkers reported two new lipopeptide antibiotics discovered by mining bacterial genomes.<sup>7</sup> These natural products, termed brevicidine and laterocidine (Fig. 1), were found to exhibit potent anti-Gram-negative specific activity and low eukaryotic cell toxicity.

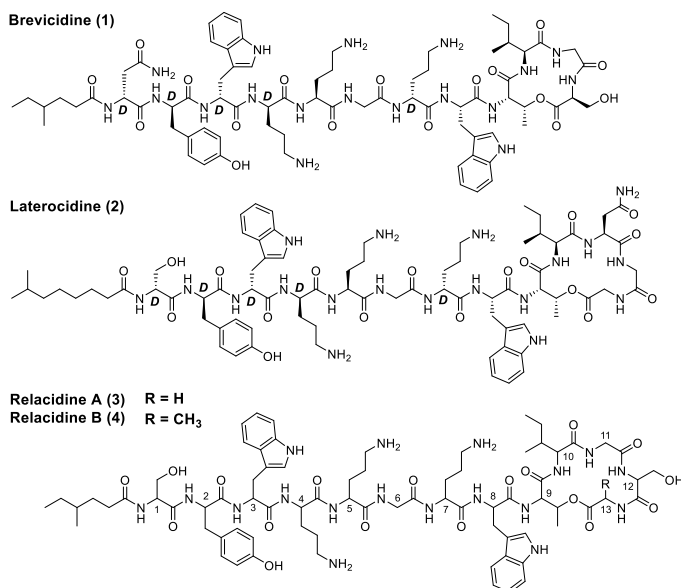


**Figure 1.** Structures of brevicidine (1), laterocidine (2), and previously proposed structures for relacidine A (3) and B (4). For the structures of brevicidine and laterocidine D-amino acids labeled D. Amino acid numbering indicated for relacidine A and B.

The low yields associated with the isolation of brevicidine and laterocidine via fermentative methods prompted us to pursue a total synthesis approach for their production which we also recently reported.<sup>8</sup> Shortly after brevicidine and laterocidine were discovered, the Kuipers group reported a series of structurally similar lipopeptides they named the relacidines.<sup>9</sup> As for brevicidine and laterocidine, the relacidines were found to specifically affect the growth of Gram-negative bacteria via a mechanism involving interactions with lipopolysaccharide (LPS).<sup>9</sup> Based on the relacidine biosynthetic gene clusters, and subsequent NMR and mass-spectrometric analysis of the natural products isolated, the Kuipers group proposed two main relacidine structures: relacidine A and relacidine B (Fig. 1).

While the stereochemical configurations of the amino acids comprising relacidine A and B were not assigned in the original report, the compounds are clearly similar in structure to brevicidine and laterocidine. In terms of their primary sequences, relacidine A and B differ only in the C-terminal residue that is esterified with the side chain of Thr9 to form the macrolactone. In relacidine A this C-terminal residue is Gly, while in relacidine B it is Ala (Fig. 1). In comparing the relacidines to brevicidine and laterocidine, it is apparent that they more closely resemble laterocidine. The sequence of the exocyclic linear peptide is the same for the relacidines and laterocidine and they also both have a five-amino acid macrocycle, while the brevicidine macrocycle consists of four residues. It is in the amino acids of the macrocycle that the relacidines differ from laterocidine. Specifically, the three C-terminal residues in the relacidines are Gly11, Ser12, and Gly13/Ala13 while in laterocidine they are Asn11, Gly12, and Gly13. These differences, and the lack of stereochemical assignments, prompted us to consider a total synthesis approach to the relacidines as a means of unambiguously establishing their structures. Furthermore, as for brevicidine and laterocidine, isolation of the relacidines from fermentation of the producing organism *Brevibacillus laterosporus*, requires laborious purification while yielding low quantities of pure material (sub-milligram per liter). In such cases total synthesis can provide an attractive alternative for obtaining quantities of material suitable for more comprehensive studies. To this end, we here report the total synthesis of a series of relacidine A and B diastereomers that, when compared with the natural product, allowed for unambiguous stereochemical assignments. In addition, we describe the synthesis of an analogue of relacidine A that exhibits increased stability in serum while retaining potent *in vitro* activity against a number of Gram-negative pathogens and *in vivo* activity in an established *Galleria mellonella* larvae infection model.

## Results and Discussion

Prior to embarking on the synthesis of relacidine A and B, we used a bioinformatics-based approach to predict the stereochemical configuration of the amino acids. To this end, we first analyzed the genome of *Brevibacillus laterosporus* MG64 (GenBank accession NZ\_QJJD01000001), the producing strain originally characterized by Kuipers and coworkers, using antiSMASH (v6.0.0; default settings).<sup>9,10,11</sup> This allowed us to readily identify the relacidine biosynthetic gene cluster (BGC, see Supplemental Information) based on biosynthetic logic. Subsequently, the architecture of the non-ribosomal peptide synthetase (NRPS) modules that assemble the relacidine peptide scaffold were studied. Particularly, we determined which modules contain epimerization domains, i.e. domains which catalyze the conversion from an L- to D-amino acid. Modules 1, 2, 3, 4, and 7 of *rlcC*, which incorporate serine, tyrosine,

tryptophan, ornithine, and ornithine, respectively, were all predicted to contain epimerization domains (Fig. 2A). Therefore, these residues were predicted to have a D-configuration in the final relacidine scaffold. To further confirm this, the relacidine BGC was compared to those of brevicidine and laterocidine, using the MIBiG database (MIBiG accessions BGC0001536 and BGC0002432 respectively), which showed that, barring a missing terminal module in the brevicidine BGC, the module architectures of all three BGCs are identical.<sup>12</sup> As the stereochemical configurations of brevicidine and laterocidine have been fully assigned, we could confirm that the epimerization domains in the brevicidine and laterocidine BGCs correspond exactly to the positions of the D-amino acids observed in their respective products.<sup>7</sup> Therefore, we predicted that the relacidines likely have the same stereochemical configurations at the same amino acid positions compared to brevicidine and laterocidine (Fig. 2B).

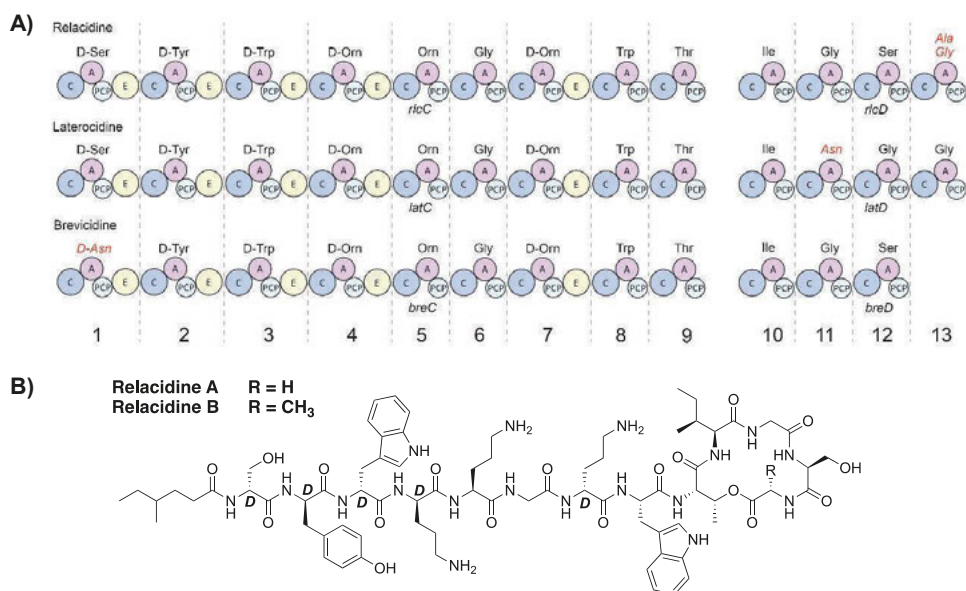


**Figure 2. Comparison of the relacidine, laterocidine, and brevicidine biosynthetic gene clusters. A)** Architecture of the NRPS modules of the relacidine, laterocidine, and brevicidine BGCs. **B)** Predicted chemical structures of relacidine A and B including stereochemical assignments. (C=Condensation domain; A=Adenylation domain; PCP=Peptidyl Carrier Protein domain; E=Epimerization domain). D-amino acids labeled D.

The peptide backbones of the relacidines, brevicidine, and laterocidine show differences at various positions (Fig. 2A). We analyzed the genetic basis for these differences by examining the active site sequences of the adenylation (A) domains, which are responsible for selecting the amino acid building blocks in non-ribosomal peptide biosynthesis. We uncovered a curious difference between the relacidine and laterocidine BGCs in the fourth module of *rlcD* (*latD*), which incorporates Gly in laterocidine biosynthesis and either Ala or Gly in relacidine biosynthesis.

Specifically, the relacidine BGC encodes Tyr at position 290, while the laterocidine BGC encodes Trp at the same position (labeled as position 291 in the laterocidine BGC). This difference is notable as this residue is centrally located in the active site of the A-domain that incorporates the 13<sup>th</sup> amino acid of relacidine and laterocidine (Fig. 3A). Given that the only difference between relacidine A and B is the incorporation of Gly or Ala respectively as the 13<sup>th</sup> amino acid, we asked whether this could be due to substrate promiscuity of the A-domain related to presence of Tyr rather than Trp at position 290 of the active site. This was further suggested by sequence analysis, which revealed that the active sites of all other Gly-only activating A-domains in relacidine, laterocidine, and brevicidine (Fig. 3A) also contain a Trp rather than a Tyr residue at position 290. To investigate this further, the 3D protein structures of all Gly-recognizing A-domains encoded by the relacidine, laterocidine, and brevicidine BGCs were first predicted with AlphaFold2. We next investigated how the Gly or Ala substrates, corresponding to relacidine A and B respectively, would fit into the A-domain active sites.<sup>13</sup> Based on this analysis, we hypothesize that in domains that exclusively incorporate Gly, Trp serves as a “gatekeeper” by effectively limiting the size of the active site pocket so that only the Gly substrate can fit. When modeling the corresponding Ala substrate into the active sites, the predicted distance between the Trp side chain of Gly-exclusive domains and the Ala methyl group is 1.9-2.4Å, which would likely cause steric repulsion (Fig. 3B; Supplemental Table S1). In contrast, if the A-domain active site contains the smaller Tyr residue at position 290 (as observed for the 13<sup>th</sup> A-domain encoded by the relacidine BGC) it appears to tolerate recognition of the Ala substrate, with a predicted distance of 3.4Å between the Tyr side chain and the Ala methyl group. These findings suggest that a single substitution in the active site of an A-domain can lead to substrate promiscuity, resulting in the production of NRPs with varying structural features encoded by the same BGC.

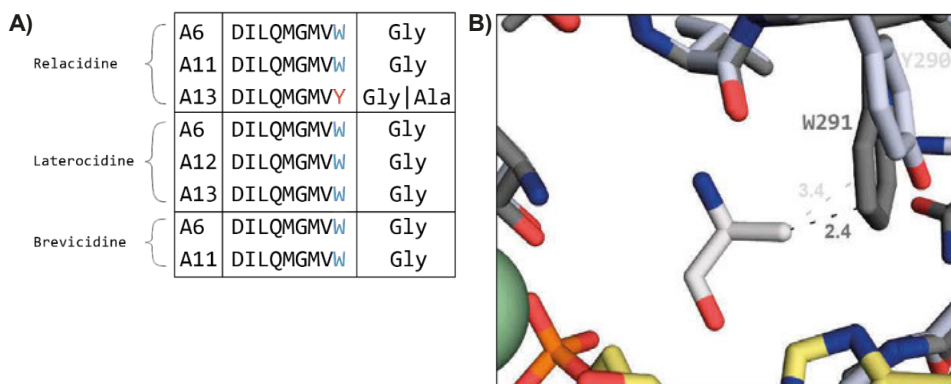


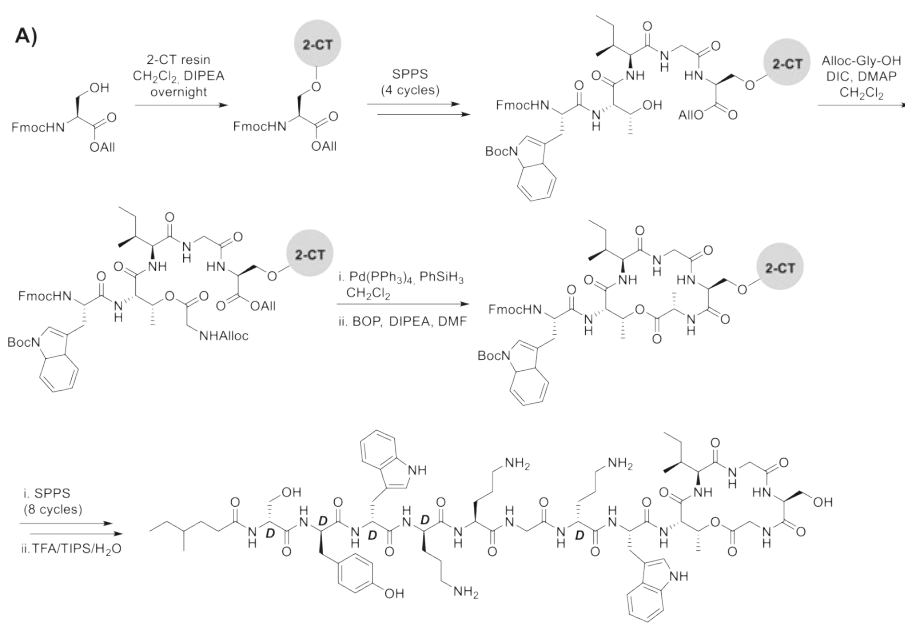
**Figure 3. Comparison of the Gly-recognizing A-domains in the relacidine, laterocidine, and brevicidine biosynthetic gene clusters.** A) Comparison of the active sites of the Gly-recognizing A-domains; B) Comparison of the 3-D structures predicted for the active sites of A-domain 13 containing Trp (laterocidine BGC; dark grey) or Tyr (relacidine BGC; grey), showing interactions of these residues with the Ala substrate.

Based on the stereochemical predictions generated from our analysis of the relacidine BGC, we next set out to synthesize relacidine A and B. The approach used was inspired by our earlier work on the total synthesis of brevicidine and laterocidine with some key differences.<sup>8,14</sup> Specifically, our previous solid phase peptide synthesis (SPPS) based preparation of laterocidine made use of the fact that the laterocidine macrocycle includes an Asn residue at position 11 which presented a viable option for resin attachment. However, because the relacidines lack an Asn residue at position 11, a different resin anchoring strategy was required. Instead, we identified the Ser at position 12 of the relacidine macrocycle as a viable option for resin attachment. To this end, the free sidechain hydroxyl of Fmoc-L-Ser-Oallyl was first attached to 2-chlorotrityl resin (2-CT) via an overnight coupling, which resulted in an acceptable loading of 0.37 mmol/g. The peptide was then extended to the pentapeptide using standard SPPS with the notable incorporation of Thr9 as the side-chain unprotected species (Scheme 1A). At this stage the required ester linkage between the Thr9 side chain hydroxyl and the C-terminal carboxylate of Gly13 was introduced by coupling Alloc-Gly using an on-resin Steglich esterification. After the subsequent simultaneous removal of the allyl and Alloc protecting groups, the macrocycle was formed using a BOP/DIPEA mediated amide bond formation between Ser12 and Gly13. The remaining exocyclic peptide was then elongated through eight additional rounds of SPPS, including an N-terminal lipidation using racemic 4-methylhexanoic acid. Cleavage of the peptide from resin with concomitant global deprotection was achieved using acidic conditions after which RP-HPLC purification afforded the desired relacidine A diastereomer **3a**. The same route was then applied to the synthesis of relacidine B diastereomer **4a** with the only difference being that Alloc-L-Ala was instead used to install the ester linkage with Thr9. Given that the relacidines differ from laterocidine only at positions 12 and 13, we also opted to prepare the full suite of possible relacidine A and B diastereomers based on L/D-Ser at position 12 and Gly or L/D-Ala at position 13 (Scheme 1B).

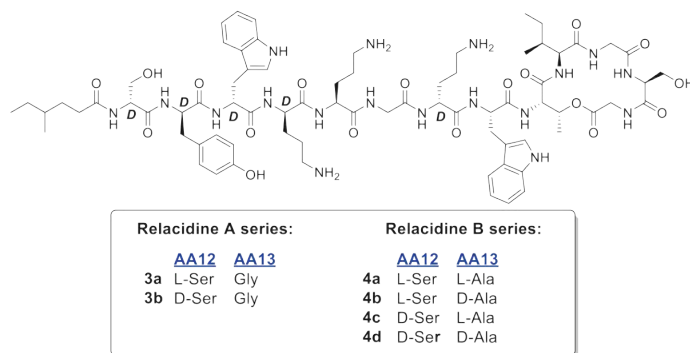
With access to relacidine A diastereomers **3a,b** and relacidine B diastereomers **4a-d** via chemical synthesis, we next set out to confirm the stereochemical configuration of the natural products by comparison with the relacidines obtained from fermentation of the producing strain. To do so, the relacidines were extracted from the cellular fraction of a *B. laterosporus* MG64 culture fermented in LB broth for 24 h. The crude extract thus obtained was analyzed using liquid chromatography-mass spectrometry (LC-MS) in order to compare the retention times of the natural and synthetic relacidines. Co-elution studies clearly demonstrated that the retention times of relacidine A and B from the bacterial extracts matched compounds **3a** and **4a**, respectively (Fig. 4). These findings support an L-configuration for Ser12 in relacidine A and B and an L-configuration for Ala13 in relacidine B, in accordance with the predictions based on our assessment of the BGC. Furthermore, analysis of the <sup>1</sup>H-NMR spectra of relacidine B diastereomers **4a-4d** (Supplemental Fig. S1) clearly show that the spectra obtained for diastereomer **4a** match the data previously published for relacidine B<sup>9</sup> (note: due to the extremely low isolated yield of relacidine A from fermentation, no NMR data were reported for the natural product which prevented comparison with our synthetic relacidine A diastereomers).

With the structures of relacidine A and B established, we next explored the synthesis of a relacidine A analogue wherein the ester linkage of the macrolactone ring was replaced by the corresponding amide. Our interest in this “relacidamide” analogue was two-fold: first, we

Total Synthesis and Structure Assignment of the Relacidine Lipopeptide Antibiotics and Preparation of Analogues with Enhanced Stability



**B) Diastereomers Prepared:**



**Scheme 1.** A) Representative total SPPS of relacidine A (**3a**) and B) structures of various diastereomers of relacidine A and B also prepared.

hypothesized that the amide analogue would be more readily synthesized and second, that the macrolactam ring would be more stable to hydrolysis than the corresponding macrolactone. The synthesis of relacidamide (**5**) is depicted in Scheme 2 and was inspired by our previous work with laterocidine and brevicidine analogues.<sup>8</sup> Using SPPS the linear precursor peptide was assembled on 2-CT resin with the notable introduction of 3-azido-L-alanine at position 9 instead of Thr. Notably, our initial approach involved the incorporation of Alloc-L-diaminopropionic acid at position 9, however, the required on-resin deprotection of the Alloc group following completion of the linear precursor peptide was found to proceed very sluggishly. By comparison, reduction of the azide in the 3-azido-L-alanine containing peptide

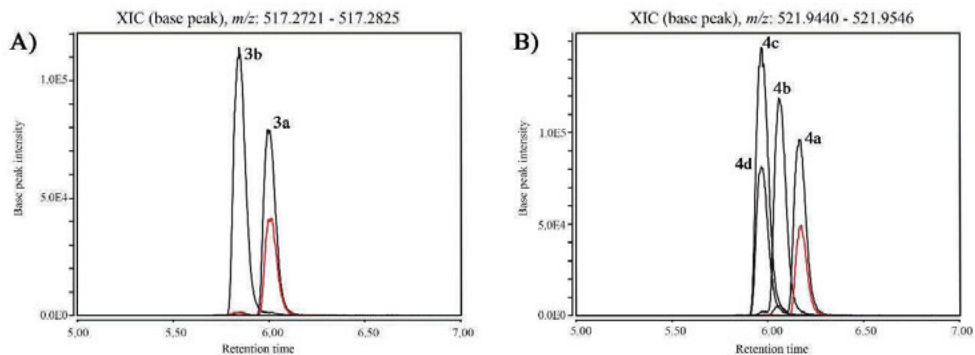
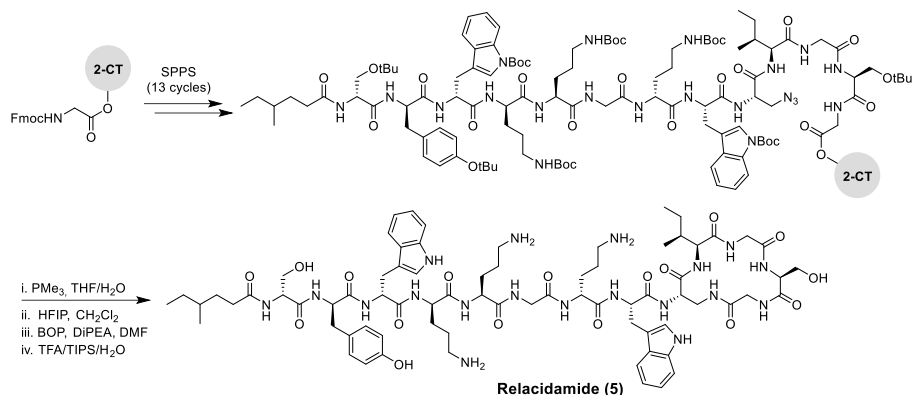


**Figure 4.** Extracted ion chromatograms (EICs) of: **A)** relacidine A with  $m/z$  517.2776 and **B)** relacidine B with  $m/z$  521.9492 from the crude extracts of *B. laterosporus* (red), overlaid with traces obtained for relacidine A diastereomers **3a,b** and relacidine B diastereomers **4a-d**. Synthetically prepared **3a** and **4a** co-elute with relacidine A and B from *B. laterosporus* MG64, respectively.

proceeded smoothly upon treatment of  $\text{PMe}_3$ , affording the amine cleanly after 3 hours. The protected linear peptide was then cleaved from the resin using mild acidic condition (HFIP/DCM) and then cyclized in solution using BOP/DIPEA. Finally, global deprotection and purification using RP-HPLC afforded pure relacidamide (**5**) in 18% yield over 30 steps.

The antibacterial activities of relacidine A (**3a**) and B (**4a**) along with diastereomers **3b** and **4b-d** as well as relacidamide (**5**) were assessed using a standard microbroth dilution assay to establish minimum inhibitory concentration (MIC) values against a panel of Gram-negative bacteria (Table 1). The MIC values measured for synthetic relacidine A (**3a**) and B (**4a**) agree well with those previously published.<sup>9</sup> Interestingly, the unnatural diastereomers of relacidine A and B as well as the relacidamide analogue (**5**) exhibited antibacterial activities similar to the natural products. As in the case of brevicidine and laterocidine, the biological activity of the relacidines was found to be unaffected by the clinically relevant *mcr-1* type colistin resistance. Relacidine A (**3a**) and B (**4a**) as well as relacidamide (**5**) were further tested against a panel of colistin-resistant *A. baumannii* clinical isolates which confirmed their ability to prevent the



**Scheme 2.** Synthesis of relacidamide (**5**).

growth of colistin-resistant isolates (Supplemental Table S2). The hemolytic activity of the compounds was also assessed showing them to cause little-to-no hemolysis when tested at 128 µg/ml (Supplemental Fig. S2). Notably, while relacidine A (**3a**) showed the highest level of hemolysis at 15 % under these conditions, relacidamide analogue (**5**) showed essentially no hemolysis (1%). Also of interest was the finding that while relacidine B (**4a**) induced <1% hemolysis, substitution of either the L-Ala or L-Ser to D-Ala or D-Ser increased hemolytic activity to 8-12%. Serum stability assays were also performed revealing relacidamide (**5**) to be significantly more stable than relacidine A (**3a**), in line with expectation (Supplemental Fig. S3). LC-MS analysis indicated that the most prominent degradation product of relacidine A corresponds to the hydrolyzed species (+18 amu), presumably due to cleavage of the ester linkage between Thr9 and Gly13. Somewhat surprisingly, relacidine B (**4a**) was also found to be highly resistant to degradation in human serum even after 24h incubation. The greater hydrolytic stability of relacidine B would appear to be attributable to the increased steric bulk of the Ala sidechain next to the ester linkage (compared to the methylene of Gly in relacidine A) which may hinder the nucleophilic attack of water at the ester carbonyl.

**Table 1.** *In vitro* minimum inhibitory concentrations (MICs) of relacidines

Peptide	Antibacterial Activity (µg/mL)				
	<i>E. coli</i> ATCC 25922	<i>E. coli</i> ATCC 25922 mcr-1	<i>K. pneumoniae</i> ATCC 13883	<i>P. aeruginosa</i> PAO1	<i>S. aureus</i> USA300
<b>3a</b>	2	2-4	4	4	>32
<b>3b</b>	2-4	4	4	2	>32
<b>4a</b>	1	2	4	4	>32
<b>4b</b>	2	2-4	4	4	>32
<b>4c</b>	1-2	1-2	2-4	4	>32
<b>4d</b>	2	2-4	2-4	8	>32
<b>5</b>	2-4	2-4	4	8	>32
<b>Colistin</b>	1	4	0.25-0.5	1	>32

Given the promising *in vitro* activity of relacidamide (**5**), along with its high serum stability, low hemolytic activity, and ease of synthesis, we further evaluated its efficacy in an established *in vivo* infection model using *G. mellonella* larvae. The *G. mellonella* infection model has gained popularity in recent years and provides a convenient method to assess the *in vivo* effectiveness and toxicity of novel antibiotics.<sup>15,16</sup> Relacidamide (**5**) was found to be well tolerated up to the highest tested dose after which its ability to treat infection with a colistin-resistant *A. baumannii* isolate (strain no. BV94) was assessed (Fig. 5). The larvae were first injected with either vehicle (PBS) or *A. baumannii* BV94 suspension in the right second proleg. The moth larvae were then injected in the left second proleg with either PBS (untreated), colistin at 100 mg/kg or 200 mg/kg, or relacidamide (**5**) at 100 mg/kg or 200 mg/kg. The *G. mellonella* larvae were then incubated for 72 h and their survival assessed twice per day. Relacidamide (**5**) induced 50% survival after 72 h at 100 mg/kg and 70 % survival at 200 mg/kg whereas none of the larvae treated with colistin survived and only 10 % of the untreated larvae survived after 72 h. These results also reflect the differences observed for the *in vitro* activity of relacidamide (**5**) which showed an MIC of 8 µg/ml against *A. baumannii* BV94 while colistin showed no activity at the highest concentration tested of 64 µg/ml (Supplemental Table S2).



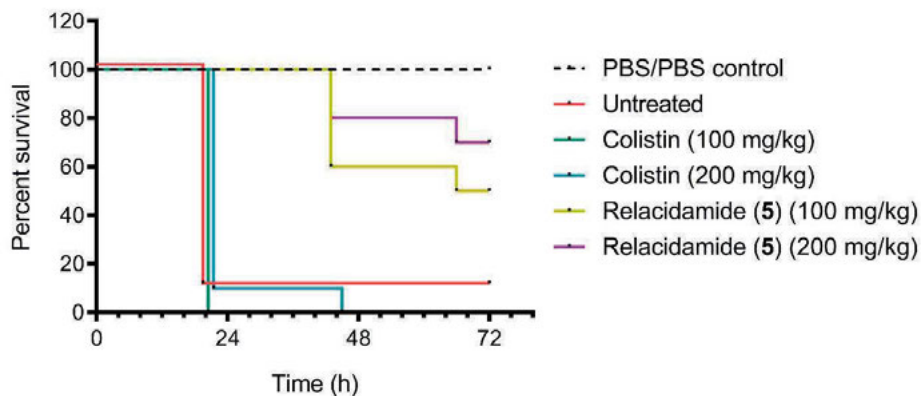


**Figure 5.** Percent survival of *G. mellonella* larvae after infection with colistin resistant *A. baumannii* isolate BV94 and subsequent treatment with test articles.

## Conclusion

In conclusion, we here report the total synthesis of the recently discovered lipopeptide antibiotics relacidine A and B, which was guided by bioinformatic analysis of the BGC. By examining the positions of the epimerization domains encoded by the relacidine BGC, we were able to predict the structure of these natural products including the stereochemical assignments of their component amino acids. Also of note, our analysis suggests that a single Trp to Tyr mutation in the active site of A-domain 13 of RlcD may allow incorporation of Ala at position 13 in relacidine B. Following on this, we developed a robust SPPS route that provided access to relacidine A and B including a number of diastereomers. Subsequent comparison of the synthetic lipopeptides with the natural products confirmed the structural predictions based on our analysis of the relacidine BGC. Furthermore, comparison of the NMR data published for relacidine B with the data obtained for the synthetic relacidine B diastereomers confirmed the predicted stereochemical configuration of relacidine B, validating our bioinformatics predictions. The antibacterial activities of the synthetic relacidines prepared, including the amide-for-ester relacidamide analogue, were evaluated against a panel of Gram-negative bacteria. All of the relacidines exhibited similar antibacterial potency while also exhibiting low hemolytic activity. In line with expectation, the relacidamide analogue (5) exhibited high serum stability, while retaining potent activity *in vitro*, and was therefore further evaluated *in vivo* in a *G. mellonella* larvae infection model. The compound was well tolerated at the highest dose tested and exhibited efficacy against a colistin-resistant *A. baumannii* isolate. These results showcase the relacidines as promising new lipopeptide antibiotics and indicate that further studies to more fully assess their therapeutic potential may be warranted.

## Experimental Methods

### Bioinformatics

We extracted the A-domains from the relacidine, laterocidine and brevicidine BGCs with HMMer (3.3.2) (<http://hmmmer.org>), using the AMP-binding domain profile hidden Markov model (HMM) also used by antiSMASH:

[https://github.com/antismash/antismash/blob/master/antismash/detection/hmm\\_detection/data/AMP-binding.hmm](https://github.com/antismash/antismash/blob/master/antismash/detection/hmm_detection/data/AMP-binding.hmm)

We extracted the active sites of these A-domains and predicted their substrates using PARAS (v0.0.1; unpublished; code available at <https://pypi.org/project/paras/>). We predicted the structures of the Gly-recognizing A-domains of the relacidine, laterocidine and brevicidine BGCs (Table S1) with AlphaFold2, building separate structure models for the N-terminal A-subdomain and the C-terminal A-subdomain. In pymol, we combined the predicted subdomains into complete structures by aligning them to the PDB structure 1AMU, a published X-ray crystallography structure of an A-domain bound to its substrate phenylalanine. We positioned the alanine in the active site of the predicted A-domain structures by mutating the phenylalanine substrate in 1AMU to alanine and measured the distance between the alanine residue and W291/Y290 (or equivalent) with pymol's measurement wizard (Table 2).

**Table 2.** Distances between the modelled alanine substrate and residue 290 based on AlphaFold structure models. The domains visualized in Fig. 3B are indicated in bold.

Domain	Module nr	Residue at position 290 or equivalent	Distance between Ala substrate and residue 290
RlcC A6	6	W290	1.9Å
RlcD A2	11	W294	2.4Å
<b>RlcD A4</b>	<b>13</b>	<b>Y290</b>	<b>3.4Å</b>
LatC A6	6	W290	2.5Å
LatD A3	12	W297	2.2Å
<b>LatD A4</b>	<b>13</b>	<b>W291</b>	<b>2.4Å</b>
BreC A6	6	W290	2.3Å
BreD A2	11	W297	2.4Å

### Materials

All reagents employed were of American Chemical Society (ACS) grade or higher and were used without further purification unless otherwise stated. Fmoc-L-Ser-OAllyl and Fmoc-D-Ser-OAllyl<sup>17</sup> as well as Alloc-Gly-OH, Alloc-L-Ala-OH and Alloc-D-Ala-OH<sup>18</sup> were synthesized according to referenced literature procedures. Fmoc-L-Orn(Boc)-OH, Fmoc-D-Orn(Boc)-OH and 4-methylhexanoic acid were purchased from Combi-Blocks. All other Fmoc-amino acids were purchased from P3 BioSystems. 2-Chloro trityl chloride (2-CT) resin was purchased from Iris Biotech. ((1H-Benzo[d][1,2,3]triazol-1-yl)oxy)tris(dimethylamino) phosphonium hexafluorophosphate (BOP), N,N-Diisopropylcarbodiimide (DIC) and triisopropylsilane (TIPS) were purchased from Manchester Organics. 1M PMe<sub>3</sub> in THF and 4-Dimethylaminopyridine (DMAP) were purchased from Sigma Aldrich. Phenylsilane

was purchased from Thermo Scientific ( $\text{PhSiH}_3$ ). Fmoc-L-azidoalanine was purchased from Chiralix. Diisopropylethylamine (DIPEA), piperidine, trifluoroacetic acid (TFA) and dimethyl sulfoxide (DMSO) were purchased from Carl Roth. Dichloromethane ( $\text{CH}_2\text{Cl}_2$ ) and petroleum ether were purchased from VWR Chemicals. Acetonitrile (MeCN), dimethylformamide (DMF) and methyl tertiary-butyl ether (MTBE) were purchased from Biosolve.

## General procedures for peptide synthesis

### Resin Loading

2-Chlorotrityl chloride resin (2-CT) (5 g, 1.55 mmol/g) was loaded by overnight coupling via the free sidechain hydroxyl of Fmoc-L-Ser-OAllyl (2.84 g, 7.75 mmol, 1 eq.) or Fmoc-D-Ser-OAllyl (1.5 g, 7.75 mmol, 1 eq.) with DIPEA (1.4 mL, 7.75 mmol, 1 eq.) in 23 mL of  $\text{CH}_2\text{Cl}_2$ . The suspension was stirred under argon at 45°C for 5 min. An additional volume of DIPEA (2.1 mL, 11.1 mmol, 1.5 eq.) was added, the suspension was stirred under argon at 45°C, overnight. After capping with MeOH (0.92 mL, 22.7 mmol, 3 eq.) and DIPEA (0.67 mL, 3.7 mmol, 0.5 eq.) for 15 min, the resin was filtered, washed and dried overnight under a stream of air. The resin loading was then determined to be 0.37 mmol/g and 0.33 mmol/g for 2-CT-Fmoc-L-Ser-OAllyl and 2-CT-Fmoc-D-Ser-OAllyl respectively.

### Synthesis of Relacidines (3a-4d)

Resin loaded with Fmoc-L-Ser-OAllyl (0.68 g, 0.25 mmol) or Fmoc-D-Ser-OAllyl (0.75 g, 0.25 mmol) was added to a manual SPPS cartridge and bubbled with nitrogen in DMF (5 mL, 30 min) to swell. Fmoc deprotections (1 min then 10 min) were carried out with 5 mL of dry piperidine in DMF (1 : 5, v/v). The next 4 amino acids (Gly11, Ile10, Thr9, Trp8) were coupled manually (1 h) under nitrogen flow via standard Fmoc solid-phase peptide synthesis (SPPS) (resin : Fmoc-AA : BOP : DIPEA, 1 : 4 : 4 : 8 molar eq.). The following Fmoc amino acids were used: Fmoc-Gly-OH, Fmoc-Ile-OH, Fmoc-Thr-OH (used without sidechain protection) and Fmoc-Trp(Boc)-OH. After coupling of Fmoc-Trp(Boc)-OH, esterification of the Thr sidechain was achieved by treating the resin-bound peptide with Alloc-Gly-OH (0.60 g, 3.75 mmol, 15 eq.), DIC (0.59 mL, 3.75 mmol, 15 eq.), and DMAP (15 mg, 0.13 mmol, 0.5 eq.) in 8 mL  $\text{CH}_2\text{Cl}_2$  : DMF (3 : 1, v/v) for 18 h under argon, for relacidine A; or Alloc-L-Ala-OH or Alloc-D-Ala-OH (0.65 g, 3.75 mmol, 15 eq.), DIC (0.59 mL, 3.75 mmol, 15 eq.), and DMAP (15 mg, 0.13 mmol, 0.5 eq.) in 8 mL  $\text{CH}_2\text{Cl}_2$  : DMF (3 : 1, v/v) for 18 h under argon, for relacidine B. The resin was treated with  $\text{Pd}(\text{PPh}_3)_4$  (75 mg, 0.075 mmol, 0.3 eq.), and  $\text{PhSiH}_3$  (0.75 mL, 7.5 mmol, 30 eq.) in  $\text{CH}_2\text{Cl}_2$  (16.5 mL) under argon for 2 h. The resin was subsequently washed with dry  $\text{CH}_2\text{Cl}_2$  (5 x 5 mL x 3 min), diethyldithiocarbamic acid trihydrate sodium salt in dry DMF (5 mg/mL, 5 x 5 mL x 3 min), and dry DMF (5 x 5 mL x 3 min). Subsequently, BOP (442 mg, 1.0 mmol, 4 eq.) and dry DIPEA (0.35 mL, 2.0 mmol, 8 eq.) were added to cyclize the peptide in 5 mL of DMF, the suspension was bubbled with nitrogen for 1 h. The remaining N-terminal section of the peptide was then synthesized using the standard SPPS protocol mentioned above. The following Fmoc amino acids were used: Fmoc-D-Orn(Boc)-OH, Fmoc-Gly-OH, Fmoc-L-Orn(Boc)-OH, Fmoc-D-Trp(Boc)-OH, Fmoc-D-Tyr(tBu)-OH, and Fmoc-D-Ser(tBu)-OH. Following the coupling of the last amino acid, the resin was split into two batches of 0.125 mmol. 4-Methylhexanoic acid (34 mg, 0.25 mmol, 2 eq.) was coupled using BOP (221 mg, 0.5 mmol, 4 eq.), and DIPEA (0.17 mL, 1.0 mmol, 8 eq.) in dry DMF (3 mL), under nitrogen flow for 2 h. Final deprotection was carried

out by treating the resins with TFA : H<sub>2</sub>O : TIPS (95 : 2.5 : 2.5, v/v, 5 mL) for 90 min while shaking. The reaction mixture was filtered through cotton, the filtrate was precipitated from MTBE : petroleum ether (1 : 1, v/v, 45 mL) and centrifuged (4500 rpm, 5 min). The pellet was then resuspended in MTBE : petroleum ether (1 : 1, v/v, 50 mL) and centrifuged again (4500 rpm, 5 min). Finally the pellet containing the crude lipopeptide was dissolved in tBuOH : H<sub>2</sub>O (1 : 1, v/v, 20 mL) and lyophilized overnight. The crude mixtures were subsequently purified by RP-HPLC (See Purification and analysis methods). Fractions were assessed by HPLC and LC-MS and product containing fractions were pooled, frozen and lyophilized to yield the pure lipopeptides as white powders in 3–10% yield over 28 steps. See section V, HPLC and HRMS analysis of peptides, for traces and individual yields.

### Synthesis of Relacidamide (5)

2-Chlorotrityl resin (2-CT) (5.0 g, 1.60 mmol/g) was loaded with 1 eq. Fmoc-Gly-OH following the same protocol as described above. Resin loading was determined to be 0.67 mmol/g. The linear peptide was assembled manually on a 0.25 mmol scale under nitrogen flow via standard Fmoc solid-phase peptide synthesis (SPPS) (1 h couplings, resin : Fmoc-AA : BOP : DIPEA, 1 : 4 : 4 : 8 molar eq.). DMF (5 mL) was used as solvent and Fmoc deprotections (5 min then 15 min) were carried out with 5 mL piperidine : DMF (1 : 4, v/v). The following Fmoc amino acids were used: Fmoc-D-Ser(tBu)-OH, Fmoc-D-Tyr(tBu)-OH, Fmoc-D-Trp(Boc)-OH, Fmoc-D-Orn(Boc)-OH, Fmoc-L-Orn(Boc)-OH, Fmoc-Gly-OH, Fmoc-Trp(Boc)-OH, Fmoc-L-azidoalanine, Fmoc-Ile-OH and Fmoc-Ser(tBu)-OH. Following the final Fmoc removal step, 4-methylhexanoic acid (65 mg, 0.5 mmol, 2 eq.) was coupled using BOP (221 mg, 0.5 mmol, 2 eq.) and DIPEA (0.17 mL, 1.0 mmol, 4 eq.) in 5 mL of DMF overnight, under nitrogen flow. The azide was reduced by treating the resin with 9 mL of 1M PMe<sub>3</sub> in THF and 1 mL of H<sub>2</sub>O for 3 hours. After washing the resin with DMF and CH<sub>2</sub>Cl<sub>2</sub>, the peptide was cleaved off the resin by treating it with HFIP : CH<sub>2</sub>Cl<sub>2</sub> (1 : 4, v/v, 20 mL) for 1 hour and rinsed with additional HFIP : CH<sub>2</sub>Cl<sub>2</sub> and CH<sub>2</sub>Cl<sub>2</sub>. The combined washings were then evaporated to yield the linear protected peptide with a free C-terminus and amino sidechain. The peptide was dissolved in 250 mL of CH<sub>2</sub>Cl<sub>2</sub> and 50 mL of DMF, treated with BOP (221 mg, 0.5 mmol, 2 eq.) and DIPEA (0.17 mL, 1.0 mmol, 4 eq.) and the solution was stirred overnight under nitrogen atmosphere. The reaction mixture was concentrated *in vacuo* and directly treated with TFA : H<sub>2</sub>O : TIPS (95 : 2.5 : 2.5, v/v, 10 mL) for 90 min while shaking. The reaction mixture was filtered through cotton, the filtrate was precipitated from MTBE : petroleum ether (1 : 1, v/v, 45 mL) and centrifuged (4500 rpm, 5 min). The pellet was then resuspended in MTBE : petroleum ether (1 : 1, v/v, 50 mL) and centrifuged again (4500 rpm, 5 min). Finally the pellet containing the crude lipopeptide was dissolved in tBuOH : H<sub>2</sub>O (1 : 1, v/v, 20 mL) and lyophilized overnight. The crude mixture were subsequently purified by RP-HPLC (See Purification and analysis methods). Fractions were assessed by HPLC and LC-MS and product containing fractions were pooled, frozen and lyophilized to yield the pure lipopeptide as white powder in 18% yield over 30 steps.

### Purification and analysis methods

**Preparative HPLC:** Purification was performed on a BESTA-Technik system with a Dr. Maisch Reprosil Gold 120 C18 column (10 μm, 25 x 250 mm) and equipped with a ECOM Flash UV detector. Runs were performed at a flow rate of 12 mL/min with UV detection at 214 nm and 254 nm. Solvent A = 0.1% TFA in water/MeCN (95 : 5) and solvent B = 0.1%

TFA in water/MeCN (5 : 95). A gradient method was employed, starting at 100 % solvent A for 2 min, ramping up to 100 % solvent B over 55 min, remaining at 100 % solvent B for 3 min before ramping down to 100 % solvent A over 1 min and remaining there for 1 min. Product containing fractions were pooled, partially concentrated under vacuum, frozen and then lyophilized to yield pure peptides as white flocculent solids. A small amount of purified peptide was analyzed by analytical HPLC.

**Analytical HPLC:** Analytical runs were performed on a Shimadzu Prominence-i LC-2030 system with a Dr. Maisch ReproSil Gold 120 C18 (5  $\mu\text{m}$ , 4.6 x 250 mm) at 30 °C. Runs were performed at a flow rate of 1 mL/min with UV detection at 214 nm and 254 nm. Solvent A = 0.1% TFA in water/MeCN (95 : 5) and solvent B = 0.1% TFA in water/MeCN (5 : 95). A gradient method was employed, starting at 100% solvent A for 2 min, ramping up to 50 % solvent B over 23 min, ramping up to 100% solvent B over 1 min, remaining there for 2 min before ramping down to 100% solvent A over 1 min and remaining there for 1 min.

**HRMS:** HRMS spectra were acquired on a Thermo Scientific Dionex UltiMate 3000 HPLC system with a Phenomenex Kinetex C18 (2.6  $\mu\text{m}$ , 2.1 x 150 mm) column at 35 °C and equipped with a diode array detector. The following solvent system, at a flow rate of 0.3 mL/min, was used: solvent A = 0.1% formic acid in water, solvent B = 0.1% formic acid in MeCN. A gradient method was employed, starting at 95 % solvent A and 5 % solvent B for 1 min, ramping up to 95 % solvent B over 9 min, ramping up to 98 % solvent B over 1 min, remaining there for 1 min before ramping back down to 95 % solvent A over 2 min and remaining there for 1 min. The system was connected to a Bruker micrOTOF-Q II mass spectrometer (ESI ionization) calibrated internally with sodium formate.

### **Culturing conditions and extraction of natural products**

*Brevibacillus laterosporus* MG64 was cultured on Luria-Bertani (LB) agar and colonies grown overnight in 5 ml LB broth at 37°C. This inoculum was transferred to 2 L Erlenmeyer flasks containing 500 ml of LB broth and incubated at 37°C with 220 rpm shaking for 24 h. Cells were collected by centrifugation (10,000  $\times$  g, 10 min, 4°C) and extracted with 100 mL of 70% isopropyl alcohol (IPA), pH 2 (acidified with 1 M HCl). Supernatant was separated by centrifugation (6000 $\times$ g, 10 min, 4 °C) and solvent was evaporated under vacuum using rotary evaporation. The crude extract was reconstituted in H<sub>2</sub>O and filtered with a 0.22  $\mu\text{m}$  syringe filter.

### **LC-MS/MS analysis**

LC-MS analysis was performed using a Shimadzu Nexera X2 UHPLC system coupled to a Shimadzu 9030 QTOF mass spectrometer as previously described.<sup>19</sup> Briefly, extracts and pure compounds were dissolved in H<sub>2</sub>O to a final concentration of 1 mg/mL and 0.01 mg/mL, and 2  $\mu\text{L}$  was injected into a Waters Acquity HSS C18 column (1.8  $\mu\text{m}$ , 100 Å, 2.1  $\times$  100 mm). The column was maintained at 30 °C, and run at a flow rate of 0.5 mL/min, using 0.1% formic acid in water as solvent A, and 0.1% formic acid in MeCN as solvent B. A gradient was employed for chromatographic separation starting at 5% B for 1 min, then 5 – 85% B for 9 min, 85 – 100% B for 1 min, and finally held at 100% B for 4 min. The column was re-equilibrated to 5% B for 3 min before the next run was started. The parameters used for the ESI source were:

interface voltage 4 kV, interface temperature 300 °C, nebulizing gas flow 3 L/min, and drying gas flow 10 L/min.

### Antimicrobial testing

**Table 3.** Minimum inhibitory concentrations (MICs) determined against panel of previously characterized colistin-resistant *A. baumannii* clinical isolates<sup>20</sup>

Strain	Antibacterial Activity ( $\mu\text{g/mL}$ )			
	Relacidine A (3a)	Relacidine B (4a)	Relacidamide (5)	Colistin
<i>A. baumannii</i> ATCC 17978	8	4	4	1
<i>A. baumannii</i> NCTC 13304	4	4	4	1
<i>A. baumannii</i> NCTC 13420	8	16	16	0.5
<i>A. baumannii</i> HUMC1	16	8	8	1
<i>A. baumannii</i> LAC-4	4	8	8	0.5
<i>A. baumannii</i> BV94	8	16	8	>64
<i>A. baumannii</i> BV95	8	8	8	32
<i>A. baumannii</i> BV172	16	16	16	>64
<i>A. baumannii</i> BV173	8	16	16	16

Colistin sulfate was purchased from Activate Scientific. Kanamycin monosulfate was purchased from MP Biomedicals. *E. coli* ATCC 25922, *S. aureus* USA300 (ATCC BAA1717) and *K. pneumoniae* ATCC 13883 belong to the American Type Culture Collection (ATCC). *P. aeruginosa* PAO1 was kindly provided by L.H.C. Quarles Van Ufford, Utrecht University, Utrecht, The Netherlands. *E. coli* ATCC 25922 MCR-1 was transfected in house using the pGDP2-MCR1 plasmid kindly provided by Yong-Xin Li, The University of Hong Kong, Hong Kong, China. Sheep blood agar plates (Ref. PB5039A) were purchased from Thermo Scientific. Tryptic soy broth (Ref. 02-200-500) was purchased from Scharlab. Mueller-Hinton broth (Ref. X927.1) was purchased from Carl Roth. Polypropylene 96-wells plates (Ref. 3879) were purchased from Corning.

All minimum inhibitory concentrations were determined according to Clinical and Standards Laboratory Institute (CLSI) guidelines. Blood agar plates were inoculated from glycerol stocks of the different *A. baumannii* strains used and then incubated for 16 h at 37 °C. Individually grown colonies were subsequently used to inoculate 5 mL aliquots of TSB that were then incubated at 37 °C. In parallel, the lipopeptide antibiotics DMSO stocks to be assessed were serially diluted with cation-adjusted MHB in polypropylene 96-well plates (50  $\mu\text{L}$  in each well). Colistin sulfate stocks were dissolved in water before being diluted with cation-adjusted MHB. The *A. baumannii* inoculated TSB aliquots were incubated until an  $\text{OD}_{600}$  of around 0.5 was reached. The bacterial suspensions were then diluted with cation-adjusted MHB ( $2 \times 10^5$  CFU  $\text{mL}^{-1}$ ) and added to the microplates containing the test compounds (50  $\mu\text{L}$  to each well). The well-plates were sealed with an adhesive membrane and after 18 h of incubation at 37 °C visually inspected for bacterial growth. MIC values reported are based on three technical replicates and defined as the lowest concentration of the compound that prevented visible growth of bacteria.

## Hemolytic assay

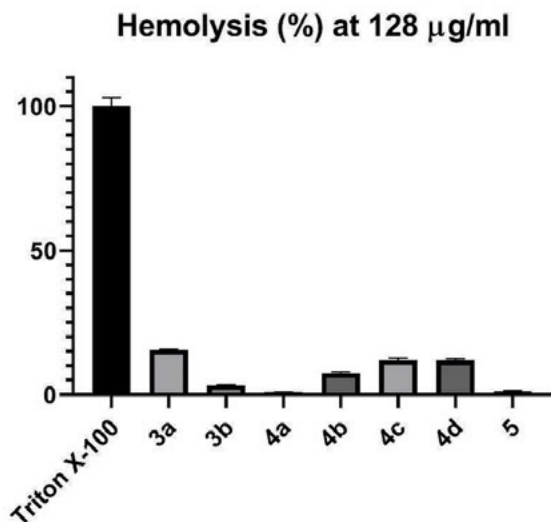


**Figure 6.** Hemolytic activity of compounds **3a-5** at 128  $\mu\text{g/mL}$  and 1 h incubation against sheep red blood cells. Colistin was also included as a reference and showed no detectable hemolysis (<0.1%) under the same conditions.

Experiments were performed in triplicate and Triton X-100 used as a positive control. Red blood cells from defibrinated sheep blood obtained from Thermo Fisher were centrifuged (400 g for 15 min at 4°C) and washed with Phosphate-Buffered Saline (PBS) containing 0.002% Tween20 (buffer) five times. Then, the red blood cells were normalized to obtain a positive control read-out between 2.5 and 3.0 at 415 nm to stay within the linear range with the maximum sensitivity. A serial dilution of the compounds (128 – 1  $\mu\text{g/mL}$ , 75  $\mu\text{L}$ ) was prepared in a 96-well polypropylene plate. The outer border of the plate was filled with 75  $\mu\text{L}$  buffer. Each plate contained a positive control (0.1% Triton-X final concentration, 75  $\mu\text{L}$ ) and a negative control (buffer, 75  $\mu\text{L}$ ) in triplicate. The normalized blood cells (75  $\mu\text{L}$ ) were added and the plates were incubated at 37 °C for 1 h while shaking at 500 rpm. A flat-bottom polystyrene plate with 100  $\mu\text{L}$  buffer in each well was prepared. After incubation, the plates were centrifuged (800 g for 5 min at room temperature) and 25  $\mu\text{L}$  of the supernatant was transferred to their respective wells in the flat-bottom plate. The values obtained from a read-out at 415 nm were corrected for background (negative control) and transformed to a percentage relative to the positive control.

## Serum Stability assay

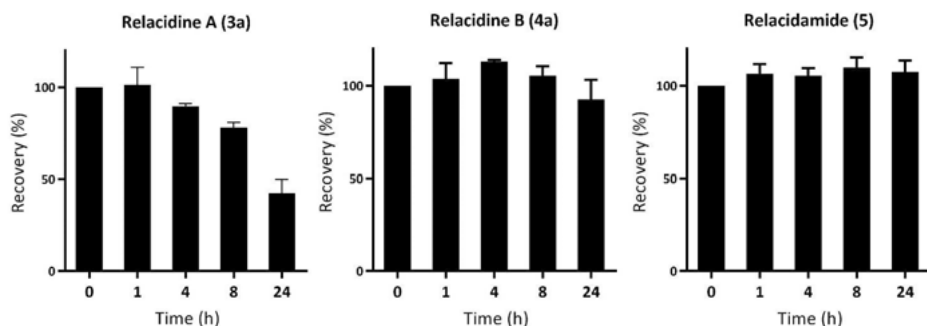


**Figure 7.** Serum stability assay comparing natural lipopeptides **3a** and **4a** to relacidamide analogue **5**.

10 mg/mL peptide solutions were prepared in Milli-Q water. Samples were prepared with 42  $\mu$ L peptide solution and 518  $\mu$ L human serum (obtained from Sigma Aldrich, product number: H4522) and incubated at 37  $^{\circ}$ C. Samples were taken at t = 0, 1, 4, 8 and 24 h. To 100  $\mu$ L of serum, 100  $\mu$ L of 6% trichloroacetic acid in acetonitrile (containing 0.2  $\mu$ g/mL D-Phenylalanine as internal standard) was added to precipitate the proteins. The samples were vortexed, left for 15 min at room temperature and stored at -20  $^{\circ}$ C. Before analysis the samples were centrifuged for 5 min at 13 000 rpm. The supernatant was analyzed by RP-HPLC using a Shimadzu Prominence-i LC-2030 system with a Dr. Maisch ReproSil Gold 120 C18 column (4.6  $\times$  250 mm, 5  $\mu$ m) at 30  $^{\circ}$ C and equipped with a UV detector monitoring at 220 nm and 254 nm. The following solvent system, at a flow rate of 1 mL/min, was used: solvent A, 0.1 % TFA in water/acetonitrile 95/5; solvent B, 0.1 % TFA in water/acetonitrile 5/95. Gradient elution was as follows: 100:0 (A/B) for 2 min, 100:0 to 50:50 (A/B) over 45 min, 50:50 (A/B) to 0:100 (A/B) over 1 min, 0:100 (A/B) for 6 min then reversion back to 100:0 (A/B) over 1 min, 100:0 (A/B) for 5 min. The peaks were integrated and normalized to the internal standard. The t=0 value was then set at 100% for each analogue and all time-points were calculated as a percentage of t=0. Biological duplicates of the experiment were performed.

## *In vivo* experiments

Ten *G. mellonella* larvae (Serum Therapeutics Inc., average weight 0.265 g) per group were infected using a 10- $\mu$ L injection in the right second proleg with mid-log phase ( $OD_{600} = 0.5$ ) growing bacteria resuspended and diluted in phosphate-buffered saline (PBS) to achieve the target inoculum of  $10^5$  colony forming unit (cfu) per larva. Inoculum density was verified by plating suitable dilutions on non-selective Luria-Bertani agar. Treatment was performed at 1 hour post-infection by injecting 10  $\mu$ L of the indicated compound dose in the left second proleg. The infected larvae were collected in a Petri dish and incubated at 37 $^{\circ}$ C. The viability of the larvae was assessed twice a day up to a total of 72 hours post-infection by checking for movement. Larvae were considered dead if no movement could be observed in response to stimulus with a pipette tip.



## HPLC and HRMS analysis of peptides

**Table 4.** Peptide number, name, chemical formula, exact mass, mass found and overall yield for peptides **3a-5**. HPLC traces of the peptides can be found in the online supplementary material at DOI <https://doi.org/10.1021/acsinfecdis.3c00043>

Compound	Name	Chemical Formula	Calcd Exact Mass	Mass found	Calcd	Overall Yield [%]
<b>3a</b>	Relacidine A	$C_{75}H_{108}N_{18}O_{18}$	1548.8089	775.4117	775.4118	5.4
<b>3b</b>	D-Ser12-Relacidine A	$C_{75}H_{108}N_{18}O_{18}$	1548.8089	775.4120	775.4118	6.8
<b>4a</b>	Relacidine B	$C_{76}H_{110}N_{18}O_{18}$	1562.8245	782.4199	782.4195	9.1
<b>4b</b>	D-Ala13, L-Ser12-Relacidine B	$C_{76}H_{110}N_{18}O_{18}$	1562.8245	782.4197	782.4195	9.5
<b>4c</b>	L-Ala13, D-Ser12-Relacidine B	$C_{76}H_{110}N_{18}O_{18}$	1562.8245	782.4199	782.4195	3.2
<b>4d</b>	D-Ala13, D-Ser12-Relacidine B	$C_{76}H_{110}N_{18}O_{18}$	1562.8245	782.4195	782.4195	5.7
<b>5</b>	Relacidamide	$C_{74}H_{107}N_{19}O_{17}$	1533.8092	767.9120	767.9119	18

## NMR characterization

**Table 5.**  $^1H$ -NMR ( $d_6$ -DMSO) characterization of relacidine A (**3a**)

Residue	-NH	H $\alpha$	H $\beta$	H $\gamma$	H $\delta$	H $\epsilon$
D-Ser1	7.88 (1H, d, $J = 7.4$ Hz)	4.27 (1H, m)	3.51 (2H, m)	5.11 (1H, t, $J = 5.4$ Hz)		
D-Tyr2	8.01 (1H, m)	4.36 (1H, m)	2.83 (1H, dd, $J = 14.2, 4.3$ Hz) & 2.62 (1H, m)	Phenol: 9.17 (1H, s), 6.89 (2H, d, $J = 8.5$ Hz), 6.57 (2H, d, $J = 8.5$ Hz)		
D-Trp3	8.00 (1H, m)	4.52 (1H, m)	3.17 (1H, m) & 2.95 (1H, m)	Indole: 10.79 (1H, s), 7.57 (1H, d, $J = 7.9$ Hz), 7.34 (1H, d, $J = 8.1$ Hz), 7.15 (1H, d, $J = 2.3$ Hz), 7.07 (1H, m), 6.99 (1H, t, $J = 7.2$ Hz)		
D-Orn4	8.04 (1H, d, $J = 8.1$ Hz)	4.38 (1H, m)	1.73 (1H, m) & 1.56 (1H, m)	1.56 (2H, m)	2.78 (2H, m)	7.69 (2H, br m)
Orn5	8.08 (1H, d, $J = 8.1$ Hz)	4.41 (1H, m)	1.71 (1H, m) & 1.53 (1H, m)	1.53 (2H, m)	2.77 (2H, m)	7.69 (2H, br m)
Gly6	8.26 (1H, m)	3.83 (1H, m) & 3.73 (1H, m)				
D-Orn7	8.11 (1H, m)	4.38 (1H, m)	1.40 (1H, m) & 1.28 (1H, m)	1.33 (2H, m)	2.59 (2H, m)	7.62 (2H, br m)
Trp8	8.18 (1H, d, $J = 8.2$ Hz)	4.76 (1H, m)	3.13 (1H, dd, $J = 14.5, 5.1$ Hz) & 2.95 (1H, m)	Indole: 10.77 (1H, s), 7.57 (1H, d, $J = 7.9$ Hz), 7.31 (1H, d, $J = 8.1$ Hz), 7.09 (1H, d, $J = 2.4$ Hz), 7.04 (1H, m), 6.95 (1H, t, $J = 7.2$ Hz)		
Thr9	8.08 (1H, d, $J = 8.1$ Hz)	4.58 (1H, dd, $J = 8.3, 4.1$ Hz)	4.96 (1H, m)	1.02 (3H, d, $J = 6.6$ Hz)		
Ile10	7.95 (1H, d, $J = 9.2$ Hz)	4.27 (1H, m)	1.67 (1H, m)	1.50 (1H, m) & 1.10 (1H, m), 0.84 (3H, d, $J = 6.8$ Hz)	0.86 (3H, t, $J = 7.4$ Hz)	
Gly11	9.19 (1H, t, $J = 5.1$ Hz)	3.94 (1H, m) & 3.33 (1H, under H <sub>2</sub> O)				
Ser12	8.56 (1H, d, $J = 8.1$ Hz)	4.12 (1H, m)	3.74 (1H, m) & 3.66 (1H, m)	4.88 (1H, t, $J = 5.7$ Hz)		
Gly13	8.12 (1H, m)	3.94 (1H, m) & 3.81 (1H, m)				
Lipid	2.12 (2H, m, O=CCH <sub>2</sub> ), 1.50 (2H, O=CCH <sub>2</sub> CH <sub>2</sub> ), 1.27 (5H, -CH <sub>2</sub> CH(CH <sub>3</sub> )CH <sub>2</sub> CH <sub>3</sub> ), 1.09 (2H, -CH <sub>2</sub> CH <sub>3</sub> ), 0.82 (6H, -CH(CH <sub>3</sub> )CH <sub>2</sub> CH <sub>3</sub> )					

**Table 6.**  $^1\text{H-NMR}$  ( $d_6$ -DMSO) characterization of D-Ser12-relacidine A (**3b**)

Residue	-NH	H $\alpha$	H $\beta$	H $\gamma$	H $\delta$	H $\epsilon$
D-Ser1	7.89 (1H, d, $J = 7.3$ Hz)	4.27 (1H, q, $J = 6.5$ Hz)	3.51 (2H, m)	5.14 (1H, br s)		
D-Tyr2	8.02 (1H, m)	4.34 (1H, m)	2.83 (1H, dd, $J = 14.2, 4.3$ Hz) & 2.62 (1H, m)	Phenol: 9.18 (1H, s), 6.89 (2H, d, $J = 8.6$ Hz), 6.57 (2H, d, $J = 8.4$ Hz)		
D-Trp3	8.01 (1H, m)	4.52 (1H, m)	3.16 (1H, m) & 2.95 (1H, m)	Indole: 10.80 (1H, s), 7.64 (1H, m), 7.34 (1H, d, $J = 8.1$ Hz), 7.15 (1H, d, $J = 2.4$ Hz), 7.07 (1H, t, $J = 7.5$ Hz), 6.99 (1H, t, $J = 7.4$ Hz)		
D-Orn4	8.02 (1H, m)	4.38 (1H, m)	1.73 (1H, m) & 1.56 (1H, m)	1.56 (2H, m)	2.78 (2H, m)	7.75 (2H, br m)
Orn5	8.09 (1H, d, $J = 8.4$ Hz)	4.41 (1H, m)	1.71 (1H, m) & 1.53 (1H, m)	1.53 (2H, m)	2.77 (2H, m)	7.75 (2H, br m)
Gly6	8.24 (1H, t, $J = 5.6$ Hz)	3.83 (1H, m) & 3.75 (1H, m)				
D-Orn7	8.04 (1H, d, $J = 8.5$ Hz)	4.38 (1H, m)	1.36 (1H, m) & 1.20 (1H, m)	1.28 (2H, m)	2.56 (2H, m)	7.65 (2H, br m)
Trp8	8.21 (1H, d, $J = 8.2$ Hz)	4.72 (1H, m)	3.16 (1H, m) & 2.91 (1H, m)	Indole: 10.76 (1H, s), 7.57 (1H, d, $J = 7.9$ Hz), 7.31 (1H, d, $J = 8.0$ Hz), 7.14 (1H, d, $J = 2.4$ Hz), 7.04 (1H, t, $J = 7.5$ Hz), 6.96 (1H, t, $J = 7.4$ Hz)		
Thr9	7.85 (1H, d, $J = 8.8$ Hz)	4.68 (1H, dd, $J = 8.9, 3.1$ Hz)	5.19 (1H, m)	1.14 (3H, d, $J = 6.2$ Hz)		
Ile10	8.40 (1H, d, $J = 3.7$ Hz)	3.90 (1H, dd, $J = 7.6, 3.7$ Hz)	1.64 (1H, m)	1.61 (1H, m) & 1.19 (1H, m), 0.88 (3H, d, $J = 6.8$ Hz)	0.90 (3H, t, $J = 7.3$ Hz)	
Gly11	9.22 (1H, t, $J = 5.5$ Hz)	3.73 (1H, m) & 3.65 (1H, m)				
D-Ser12	7.52 (1H, t, $J = 9.1$ Hz)	4.37 (1H, m)	3.98 (1H, m) & 3.83 (1H, m)	4.87 (1H, br s)		
Gly13	7.52 (1H, t, $J = 9.1$ Hz)	4.50 (1H, m) & 3.39 (1H, under H <sub>2</sub> O)				
Lipid	2.12 (2H, m, O=CCH <sub>2</sub> ), 1.50 (2H, O=CCH <sub>2</sub> CH <sub>2</sub> ), 1.27 (5H, -CH <sub>2</sub> CH(CH <sub>3</sub> )CH <sub>2</sub> CH <sub>3</sub> ), 1.09 (2H, -CH <sub>2</sub> CH <sub>3</sub> ), 0.82 (6H, -CH(CH <sub>3</sub> )CH <sub>2</sub> CH <sub>3</sub> )					

**Table 7.**  $^1\text{H-NMR}$  ( $d_6$ -DMSO) characterization of relacidine B (**4a**)

Residue	-NH	H $\alpha$	H $\beta$	H $\gamma$	H $\delta$	H $\epsilon$
D-Ser1	7.88 (1H, d, $J = 7.4$ Hz)	4.27 (1H, m)	3.51 (2H, m)	5.13 (1H, br s)		
D-Tyr2	8.02 (1H, m)	4.35 (1H, m)	2.83 (1H, m) & 2.62 (1H, m)	Phenol: 9.17 (1H, m), 6.90 (2H, d, $J = 8.5$ Hz), 6.57 (2H, d, $J = 8.4$ Hz)		
D-Trp3	8.01 (1H, m)	4.52 (1H, m)	3.16 (1H, dd, $J = 15.0, 4.5$ Hz) & 2.95 (1H, m)	Indole: 10.79 (1H, s), 7.57 (1H, d, $J = 8.0$ Hz), 7.34 (1H, d, $J = 8.1$ Hz), 7.15 (1H, d, $J = 2.4$ Hz), 7.07 (1H, m), 6.99 (1H, m)		
D-Orn4	8.03 (1H, m)	4.38 (1H, m)	1.73 (1H, m) & 1.56 (1H, m)	1.56 (2H, m)	2.78 (2H, m)	7.72 (2H, br m)
Orn5	8.09 (1H, d, $J = 8.3$ Hz)	4.41 (1H, m)	1.71 (1H, m) & 1.53 (1H, m)	1.53 (2H, m)	2.77 (2H, m)	7.72 (2H, br m)
Gly6	8.26 (1H, t, $J = 5.6$ Hz)	3.84 (1H, m) & 3.74 (1H, dd, $J = 16.9, 5.1$ Hz)				
D-Orn7	8.11 (1H, d, $J = 8.4$ Hz)	4.38 (1H, m)	1.41 (1H, m) & 1.29 (1H, m)	1.34 (2H, m)	2.59 (2H, m)	7.65 (2H, br m)
Trp8	8.22 (1H, d, $J = 8.1$ Hz)	4.75 (1H, m)	3.11 (1H, dd, $J = 14.7, 5.2$ Hz) & 2.96 (1H, m)	Indole: 10.78 (1H, s), 7.59 (1H, d, $J = 7.9$ Hz), 7.31 (1H, d, $J = 8.0$ Hz), 7.11 (1H, d, $J = 2.4$ Hz), 7.04 (1H, m), 6.96 (1H, m)		
Thr9	8.06 (1H, d, $J = 8.1$ Hz)	4.64 (1H, dd, $J = 8.1, 4.0$ Hz)	5.00 (1H, m)	0.99 (3H, d, $J = 6.5$ Hz)		
Ile10	7.72 (1H, m)	4.17 (1H, t, $J = 8.5$ Hz)	1.66 (1H, m)	1.54 (1H, m) & 1.11 (1H, m), 0.86 (3H, m)	0.87 (3H, m)	
Gly11	9.17 (1H, t, $J = 6.4$ Hz)	3.91 (1H, dd, $J = 14.3, 4.7$ Hz) & 3.36 (1H, under $\text{H}_2\text{O}$ )				
Ser12	8.46 (1H, d, $J = 7.8$ Hz)	4.10 (1H, m)	3.81 (1H, m) & 3.69 (1H, dd, $J = 11.0, 3.4$ Hz)	4.88 (1H, br s)		
Ala13	7.76 (1H, d, $J = 8.6$ Hz)	4.39 (1H, m)	1.43 (3H, d, $J = 7.2$ Hz)			
Lipid	2.12 (2H, m, O=CCH <sub>2</sub> ), 1.50 (2H, O=CCH <sub>2</sub> CH <sub>2</sub> ), 1.27 (5H, -CH <sub>2</sub> CH(CH <sub>3</sub> )CH <sub>2</sub> CH <sub>3</sub> ), 1.09 (2H, -CH <sub>2</sub> CH <sub>3</sub> ), 0.82 (6H, -CH(CH <sub>3</sub> )CH <sub>2</sub> CH <sub>3</sub> )					

**Table 8.**  $^1\text{H-NMR}$  ( $d_6$ -DMSO) characterization of D-Ala13, L-Ser12-relacidine B (**4b**)

Residue	-NH	H $\alpha$	H $\beta$	H $\gamma$	H $\delta$	H $\epsilon$
D-Ser1	7.88 (1H, d, $J = 7.4$ Hz)	4.27 (1H, m)	3.51 (2H, m)	5.14 (1H, br s)		
D-Tyr2	8.02 (1H, m)	4.35 (1H, m)	2.83 (1H, dd, $J = 14.2, 4.3$ Hz) & 2.62 (1H, m)	Phenol: 9.18 (1H, s), 6.90 (2H, d, $J = 8.5$ Hz), 6.57 (2H, d, $J = 8.4$ Hz)		
D-Trp3	8.01 (1H, m)	4.53 (1H, m)	3.16 (1H, dd, $J = 15.0, 4.5$ Hz) & 2.95 (1H, m)	Indole: 10.79 (1H, s), 7.58 (1H, d, $J = 2.9$ Hz), 7.34 (1H, d, $J = 8.1$ Hz), 7.15 (1H, d, $J = 2.4$ Hz), 7.07 (1H, t, $J = 7.5$ Hz), 6.99 (1H, t, $J = 7.4$ Hz)		
D-Orn4	8.03 (1H, m)	4.38 (1H, m)	1.73 (1H, m) & 1.56 (1H, m)	1.56 (2H, m)	2.78 (2H, m)	7.74 (2H, br m)
Orn5	8.09 (1H, d, $J = 8.2$ Hz)	4.41 (1H, m)	1.71 (1H, m) & 1.53 (1H, m)	1.53 (2H, m)	2.77 (2H, m)	7.74 (2H, br m)
Gly6	8.27 (1H, t, $J = 5.6$ Hz)	3.84 (1H, dd, $J = 16.9, 6.0$ Hz) & 3.72 (1H, dd, $J = 16.8, 5.1$ Hz)				
D-Orn7	8.11 (1H, d, $J = 8.5$ Hz)	4.38 (1H, m)	1.42 (1H, m) & 1.29 (1H, m)	1.35 (2H, m)	2.59 (2H, m)	7.66 (2H, br m)
Trp8	8.21 (1H, d, $J = 8.1$ Hz)	4.76 (1H, m)	3.13 (1H, dd, $J = 14.6, 5.0$ Hz) & 2.97 (1H, m)	Indole: 10.79 (1H, s), 7.57 (1H, d, $J = 3.0$ Hz), 7.31 (1H, d, $J = 8.0$ Hz), 7.10 (1H, d, $J = 2.4$ Hz), 7.04 (1H, t, $J = 7.5$ Hz), 6.95 (1H, t, $J = 7.4$ Hz)		
Thr9	7.95 (1H, d, $J = 8.4$ Hz)	4.58 (1H, dd, $J = 8.4, 3.9$ Hz)	5.07 (1H, m)	1.05 (3H, d, $J = 6.5$ Hz)		
Ile10	7.80 (1H, d, $J = 9.4$ Hz)	4.27 (1H, m)	1.74 (1H, m)	1.42 (1H, m) & 1.10 (1H, m), 0.84 (3H, m)	0.84 (3H, m)	
Gly11	8.96 (1H, t, $J = 5.8$ Hz)	3.95 (1H, dd, $J = 14.0, 5.1$ Hz) & 3.31 (1H, dd, $J = 14.0, 6.4$ Hz)				
Ser12	8.66 (1H, d, $J = 7.8$ Hz)	4.03 (1H, m)	3.65 (2H, m)	4.89 (1H, br s)		
D-Ala13	7.98 (1H, d, $J = 7.5$ Hz)	4.18 (1H, p, $J = 7.1$ Hz)	1.26 (3H, d, $J = 7.0$ Hz)			
Lipid	2.12 (2H, m, O=CCH <sub>2</sub> ), 1.50 (2H, O=CCH <sub>2</sub> CH <sub>2</sub> ), 1.27 (5H, -CH <sub>2</sub> CH(CH <sub>2</sub> ) <sub>2</sub> CH <sub>2</sub> CH <sub>3</sub> ), 1.09 (2H, -CH <sub>2</sub> CH <sub>3</sub> ), 0.82 (6H, -CH(CH <sub>3</sub> )CH <sub>2</sub> CH <sub>3</sub> )					

**Table 9.**  $^1\text{H-NMR}$  ( $d_6$ -DMSO) characterization of L-Ala13, D-Ser12-relacidine B (**4c**)

Residue	-NH	H $\alpha$	H $\beta$	H $\gamma$	H $\delta$	H $\epsilon$
D-Ser1	7.88 (1H, d, $J$ = 7.3 Hz)	4.26 (1H, q, $J$ = 6.5 Hz)	3.52 (2H, m)	5.12 (1H, t, $J$ = 5.5 Hz)		
D-Tyr2	8.02 (1H, m)	4.35 (1H, m)	2.83 (1H, dd, $J$ = 14.2, 4.3 Hz) & 2.62 (1H, dd, $J$ = 14.2, 9.5 Hz)	Phenol: 9.17 (1H, s), 6.89 (2H, m), 6.57 (2H, m)		
D-Trp3	8.00 (1H, m)	4.51 (1H, m)	3.16 (1H, m) & 2.95 (1H, dd, $J$ = 15.0, 9.4 Hz)	Indole: 10.79 (1H, s), 7.57 (1H, d, $J$ = 7.9 Hz), 7.34 (1H, d, $J$ = 8.0 Hz), 7.15 (1H, m), 7.07 (1H, m), 6.99 (1H, m)		
D-Orn4	8.02 (1H, d, $J$ = 8.4 Hz)	4.35 (1H, m)	1.73 (1H, m) & 1.56 (1H, m)	1.56 (2H, m)	2.77 (2H, m)	7.71 (2H, br m)
Orn5	8.08 (1H, d, $J$ = 8.2 Hz)	4.41 (1H, m)	1.71 (1H, m) & 1.53 (1H, m)	1.53 (2H, m)	2.77 (2H, m)	7.71 (2H, br m)
Gly6	8.24 (1H, t, $J$ = 5.6 Hz)	3.81 (1H, m) & 3.74 (1H, m)				
D-Orn7	8.04 (1H, d, $J$ = 8.4 Hz)	4.38 (1H, m)	1.35 (1H, m) & 1.20 (1H, m)	1.25 (2H, m)	2.54 (2H, m)	7.61 (2H, br m)
Trp8	8.20 (1H, d, $J$ = 8.2 Hz)	4.73 (1H, m)	3.16 (1H, m) & 2.90 (1H, dd, $J$ = 14.7, 9.7 Hz)	Indole: 10.74 (1H, s), 7.66 (1H, d, $J$ = 7.8 Hz), 7.31 (1H, d, $J$ = 8.1 Hz), 7.15 (1H, m), 7.04 (1H, m), 6.96 (1H, m)		
Thr9	7.84 (1H, d, $J$ = 8.9 Hz)	4.68 (1H, dd, $J$ = 9.0, 2.8 Hz)	5.26 (1H, m)	1.13 (3H, d, $J$ = 6.3 Hz)		
Ile10	8.39 (1H, d, $J$ = 3.1 Hz)	3.82 (1H, m)	1.66 (1H, m)	1.61 (1H, m) & 1.20 (1H, m), 0.88 (3H, d, $J$ = 6.7 Hz)	0.91 (3H, t, $J$ = 7.3 Hz)	
Gly11	9.17 (1H, m)	3.75 (1H, m) & 3.62 (1H, m)				
D-Ser12	7.47 (1H, d, $J$ = 9.0 Hz)	4.34 (1H, m)	3.99 (1H, m) & 3.84 (1H, m)	4.86 (1H, t, $J$ = 6.6 Hz)		
Ala13	7.45 (1H, d, $J$ = 9.2 Hz)	4.61 (1H, m)	1.18 (3H, d, $J$ = 6.9 Hz)			
Lipid	2.12 (2H, m, O=CCH <sub>2</sub> ), 1.50 (2H, O=CCH <sub>2</sub> CH <sub>2</sub> ), 1.27 (5H, -CH <sub>2</sub> CH(CH <sub>3</sub> )CH <sub>2</sub> CH <sub>3</sub> ), 1.09 (2H, -CH <sub>2</sub> CH <sub>3</sub> ), 0.82 (6H, -CH(CH <sub>3</sub> )CH <sub>2</sub> CH <sub>3</sub> )					

**Table 10.**  $^1\text{H-NMR}$  ( $d_6$ -DMSO) characterization of D-Ala13, D-Ser12-relacidine B (**4d**)

Residue	-NH	H $\alpha$	H $\beta$	H $\gamma$	H $\delta$	H $\epsilon$
D-Ser1	7.88 (1H, d, $J = 7.4$ Hz)	4.27 (1H, m)	3.51 (2H, m)	5.15 (1H, br s)		
D-Tyr2	8.02 (1H, m)	4.35 (1H, m)	2.83 (1H, dd, $J = 14.2, 4.3$ Hz) & 2.62 (1H, m)	Phenol: 9.18 (1H, s), 6.90 (2H, d, $J = 8.5$ Hz), 6.57 (2H, d, $J = 8.3$ Hz)		
D-Trp3	8.01 (1H, m)	4.52 (1H, m)	3.16 (1H, m) & 2.95 (1H, m)	Indole: 10.80 (1H, s), 7.58 (1H, t, $J = 7.3$ Hz), 7.34 (1H, d, $J = 8.1$ Hz), 7.15 (1H, d, $J = 2.4$ Hz), 7.07 (1H, t, $J = 7.5$ Hz), 6.99 (1H, t, $J = 7.4$ Hz)		
D-Orn4	8.03 (1H, m)	4.38 (1H, m)	1.73 (1H, m) & 1.56 (1H, m)	1.56 (2H, m)	2.78 (2H, m)	7.75 (2H, br m)
Orn5	8.09 (1H, m)	4.41 (1H, m)	1.71 (1H, m) & 1.53 (1H, m)	1.53 (2H, m)	2.77 (2H, m)	7.75 (2H, br m)
Gly6	8.25 (1H, t, $J = 5.6$ Hz)	3.83 (1H, dd, $J = 17.0, 6.0$ Hz) & 3.73 (1H, m)				
D-Orn7	8.11 (1H, m)	4.38 (1H, m)	1.41 (1H, m) & 1.29 (1H, m)	1.33 (2H, m)	2.59 (2H, m)	7.67 (2H, br m)
Trp8	8.20 (1H, d, $J = 8.1$ Hz)	4.78 (1H, m)	3.12 (1H, dd, $J = 14.6, 4.9$ Hz) & 2.96 (1H, m)	Indole: 10.78 (1H, s), 7.58 (1H, t, $J = 7.3$ Hz), 7.31 (1H, d, $J = 8.0$ Hz), 7.10 (1H, d, $J = 2.4$ Hz), 7.04 (1H, t, $J = 7.5$ Hz), 6.95 (1H, t, $J = 7.4$ Hz)		
Thr9	8.04 (1H, m)	4.65 (1H, dd, $J = 8.4, 4.0$ Hz)	5.05 (1H, m)	1.07 (3H, d, $J = 6.4$ Hz)		
Ile10	8.11 (1H, m)	4.24 (1H, t, $J = 7.8$ Hz)	1.68 (1H, m)	1.52 (1H, m) & 1.13 (1H, m), 0.86 (3H, m)	0.86 (3H, m)	
Gly11	8.97 (1H, t, $J = 5.4$ Hz)	3.73 (1H, m) & 3.58 (1H, m)				
D-Ser12	7.42 (1H, d, $J = 9.0$ Hz)	4.27 (1H, m)	3.71 (2H, m)	4.82 (1H, br s)		
D-Ala13	7.50 (1H, d, $J = 6.9$ Hz)	4.08 (1H, p, $J = 7.1$ Hz)	1.39 (3H, d, $J = 7.1$ Hz)			
Lipid	2.12 (2H, m, O=CCH <sub>2</sub> ), 1.50 (2H, O=CCH <sub>2</sub> CH <sub>2</sub> ), 1.27 (5H, -CH <sub>2</sub> CH(CH <sub>3</sub> )CH <sub>2</sub> CH <sub>3</sub> ), 1.09 (2H, -CH <sub>2</sub> CH <sub>3</sub> ), 0.82 (6H, -CH(CH <sub>3</sub> )CH <sub>2</sub> CH <sub>3</sub> )					

**Table 11.**  $^1\text{H-NMR}$  ( $d_6$ -DMSO) characterization of relacidamide (**5**)

Residue	-NH	H $\alpha$	H $\beta$	H $\gamma$	H $\delta$	H $\epsilon$
D-Ser1	7.89 (1H, d, $J = 7.4$ Hz)	4.27 (1H, m)	3.51 (2H, m)	5.14 (1H, br s)		
D-Tyr2	8.02 (1H, m)	4.35 (1H, m)	2.83 (1H, dd, $J = 14.3, 4.5$ Hz) & 2.62 (1H, m)	Phenol: 9.18 (1H, s), 6.90 (2H, d, $J = 8.5$ Hz), 6.57 (2H, d, $J = 8.4$ Hz)		
D-Trp3	8.01 (1H, m)	4.52 (1H, m)	3.16 (1H, dd, $J = 15.0, 4.5$ Hz) & 2.95 (1H, dd, $J = 14.9, 9.4$ Hz)	Indole: 10.80 (1H, s), 7.60 (1H, d, $J = 7.9$ Hz), 7.34 (1H, d, $J = 8.1$ Hz), 7.15 (1H, d, $J = 2.4$ Hz), 7.07 (1H, t, $J = 7.6$ Hz), 6.99 (1H, t, $J = 7.4$ Hz)		
D-Orn4	8.03 (1H, m)	4.38 (1H, m)	1.74 (1H, m) & 1.57 (1H, m)	1.57 (2H, m)	2.78 (2H, m)	7.75 (2H, br m)
Orn5	8.09 (1H, d, $J = 8.2$ Hz)	4.41 (1H, m)	1.71 (1H, m) & 1.54 (1H, m)	1.54 (2H, m)	2.78 (2H, m)	7.75 (2H, br m)
Gly6	8.27 (1H, m)	3.80 (1H, dd, $J = 16.8, 3.8$ Hz) & 3.76 (1H, m)				
D-Orn7	8.07 (1H, d, $J = 8.3$ Hz)	4.33 (1H, m)	1.39 (1H, m) & 1.28 (1H, m)	1.32 (2H, m)	2.59 (2H, m)	7.66 (2H, br m)
Trp8	8.17 (1H, d, $J = 8.3$ Hz)	4.63 (1H, m)	3.10 (1H, m) & 2.90 (1H, dd, $J = 14.7, 8.7$ Hz)	Indole: 10.78 (1H, s), 7.58 (1H, d, $J = 8.0$ Hz), 7.31 (1H, d, $J = 8.0$ Hz), 7.10 (1H, d, $J = 2.3$ Hz), 7.04 (1H, t, $J = 7.5$ Hz), 6.97 (1H, t, $J = 7.4$ Hz)		
Dap9	8.22 (1H, d, $J = 7.4$ Hz)	4.27 (1H, m)	3.56 (1H, m) & 2.80 (1H, m)	6.83 (1H, t, $J = 6.5$ Hz)		
Ile10	8.27 (1H, m)	4.10 (1H, t, $J = 9.7$ Hz)	1.76 (1H, m)	1.56 (1H, m) & 1.16 (1H, m), 0.83 (3H, m)	0.84 (3H, t, $J = 7.4$ Hz)	
Gly11	9.02 (1H, t, $J = 5.3$ Hz)	3.95 (1H, dd, $J = 14.8, 3.8$ Hz) & 3.45 (1H, m)				
Ser12	9.00 (1H, d, $J = 5.5$ Hz)	3.91 (1H, m)	3.74 (1H, m) & 3.68 (1H, m)	5.07 (1H, br s)		
Gly13	7.95 (1H, m)	3.92 (1H, m) & 3.51 (1H, m)				
Lipid	2.12 (2H, m, O=CCH <sub>2</sub> ), 1.50 (2H, O=CCH <sub>2</sub> CH <sub>2</sub> ), 1.27 (5H, -CH <sub>2</sub> CH(CH <sub>3</sub> )CH <sub>2</sub> CH <sub>3</sub> ), 1.09 (2H, -CH <sub>2</sub> CH <sub>3</sub> ), 0.82 (6H, -CH(CH <sub>3</sub> )CH <sub>2</sub> CH <sub>3</sub> )					

NMR traces of all peptides can be found in the online supplementary material at DOI <https://doi.org/10.1021/acsinfecdis.3c00043>

## Supplemental Figures

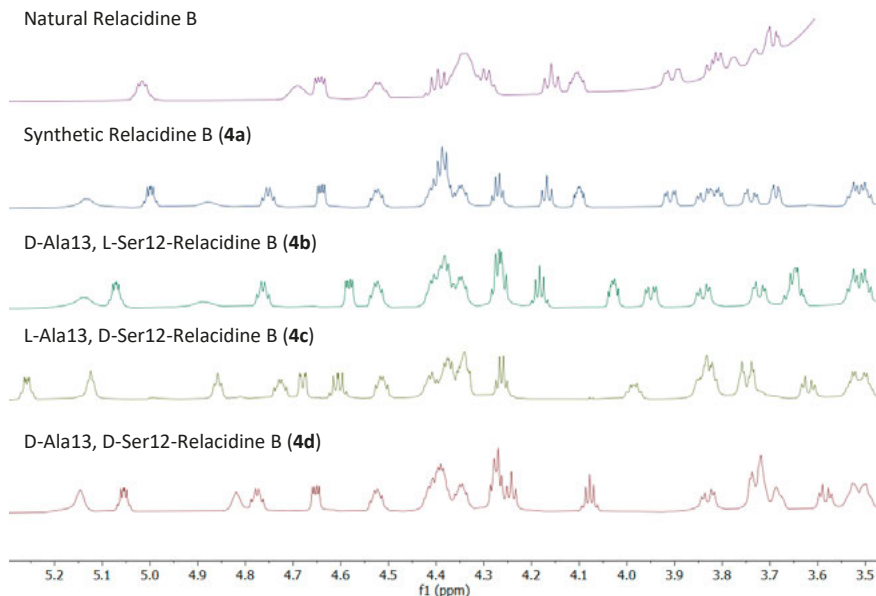


**Figure S1.** Previously published <sup>1</sup>H-NMR (600 MHz, *d*<sub>6</sub>-DMSO) spectrum of natural relacidine B isolated after fermentation of the producing organism overlaid with <sup>1</sup>H-NMR (850 MHz, *d*<sub>6</sub>-DMSO) spectra of synthetic relacidines **4a-4d**. Spectra were recorded at room temperature.

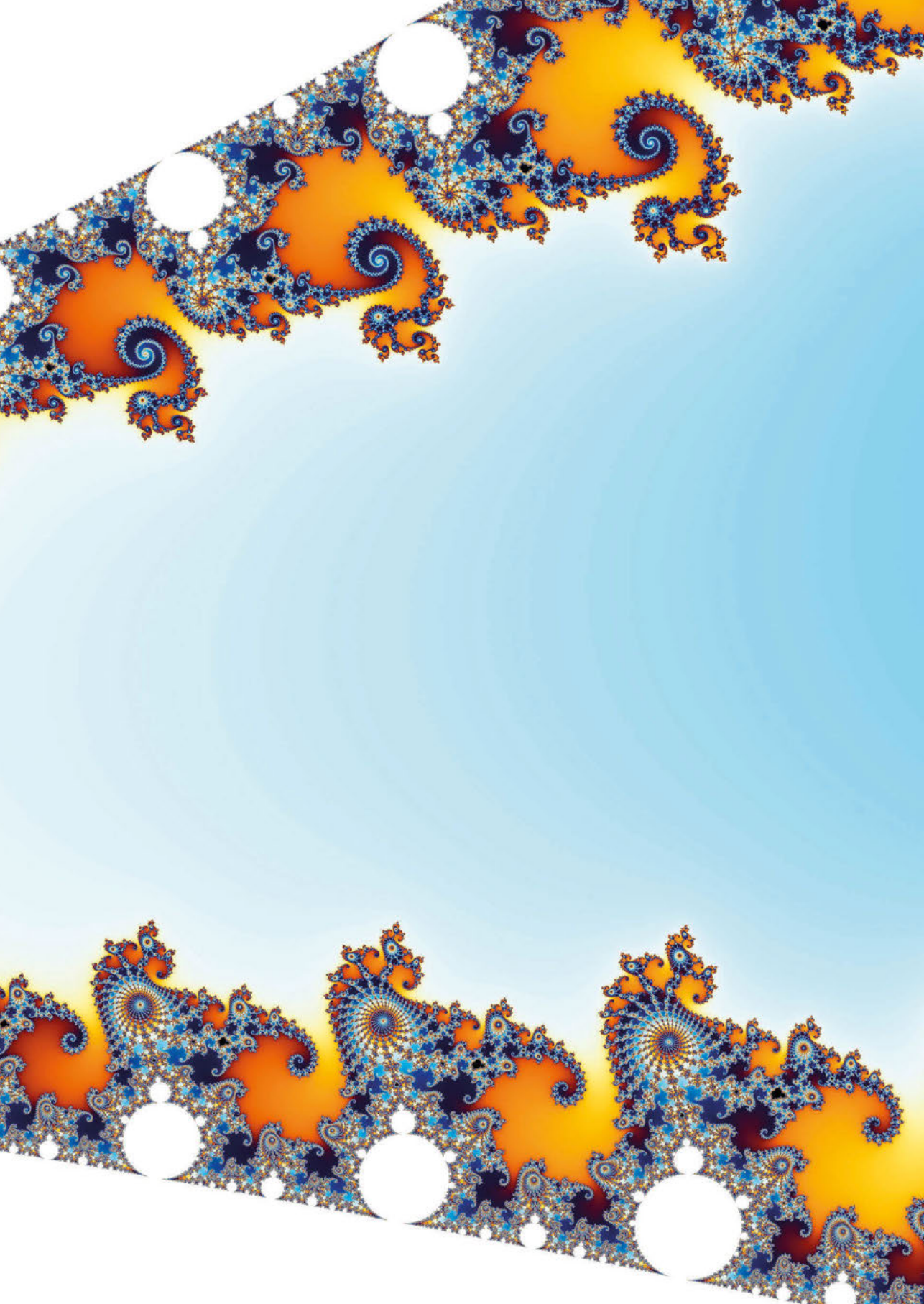
## References

- (1) Murray, C. J.; Ikuta, K. S.; Sharara, F.; Swetschinski, L.; Robles Aguilar, G.; Gray, A.; Han, C.; Bisignano, C.; Rao, P.; Wool, E.; Johnson, S. C.; Browne, A. J.; Chipeta, M. G.; Fell, F.; Hackett, S.; Haines-Woodhouse, G.; Kashef Hamadani, B. H.; Kumaran, E. A. P.; McManigal, B.; Agarwal, R.; Akech, S.; Albertson, S.; Amuasi, J.; Andrews, J.; Aravkin, A.; Ashley, E.; Bailey, F.; Baker, S.; Basnyat, B.; Bekker, A.; Bender, R.; Bethou, A.; Bielicki, J.; Boonkasidetcha, S.; Bukosia, J.; Carvalheiro, C.; Castañeda-Orjuela, C.; Chansamouth, V.; Chaurasia, S.; Chiurchiù, S.; Chowdhury, F.; Cook, A. J.; Cooper, B.; Cressey, T. R.; Criollo-Mora, E.; Cunningham, M.; Darboe, S.; Day, N. P. J.; De Luca, M.; Dokova, K.; Dramowski, A.; Dunachie, S. J.; Eckmanns, T.; Eibach, D.; Emami, A.; Feasey, N.; Fisher-Pearson, N.; Forrest, K.; Garrett, D.; Gastmeier, P.; Giref, A. Z.; Greer, R. C.; Gupta, V.; Haller, S.; Haselbeck, A.; Hay, S. I.; Holm, M.; Hopkins, S.; Iregbu, K. C.; Jacobs, J.; Jarovsky, D.; Javanmardi, F.; Khorana, M.; Kissoon, N.; Kobeissi, E.; Kostyanov, T.; Krapp, F.; Krumkamp, R.; Kumar, A.; Kyu, H. H.; Lim, C.; Limmathurotsakul, D.; Loftus, M. J.; Lunn, M.; Ma, J.; Mturi, N.; Munera-Huertas, T.; Musicha, P.; Mussi-Pinhata, M. M.; Nakamura, T.; Nanavati, R.; Nangia, S.; Newton, P.; Ngoun, C.; Novotney, A.; Nwakanma, D.; Obiero, C. W.; Olivas-Martinez, A.; Olliaro, P.; Ooko, E.; Ortiz-Brizuela, E.; Peleg, A. Y.; Perrone, C.; Plakkal, N.; Ponce-de-Leon, A.; Raad, M.; Ramdin, T.; Riddell, A.; Roberts, T.; Robotham, J. V.; Roca, A.; Rudd, K. E.; Russell, N.; Schnall, J.; Scott, J. A. G.; Shivamallappa, M.; Sifuentes-Osornio, J.; Steenkeste, N.; Stewardson, A. J.; Stoeva, T.; Tasak, N.; Thaiprakong, A.; Thwaites, G.; Turner, C.; Turner, P.; van Doorn, H. R.; Velaphi, S.; Vongpradith, A.; Vu, H.; Walsh, T.; Waner, S.; Wangrangsimakul, T.; Wozniak, T.; Zheng, P.; Sartorius, B.; Lopez, A. D.; Stergachis, A.; Moore, C.; Dolecek, C.; Naghavi, M. Global Burden of Bacterial Antimicrobial Resistance in 2019: A Systematic Analysis. *Lancet* **2022**, 399 (10325), 629–655. [https://doi.org/10.1016/S0140-6736\(21\)02724-0](https://doi.org/10.1016/S0140-6736(21)02724-0).



- (2) O'Neill, J. *Antimicrobial Resistance: Tackling a Crisis for the Health and Wealth of Nations.*; 2014.
- (3) O'Neill, J. *Tackling Drug-Resistant Infections Globally: Final Report and Recommendations.*; London, 2016.
- (4) CDC. *COVID-19: U.S. Impact on Antimicrobial Resistance, Special Report 2022*; Atlanta, Georgia, 2022. <https://doi.org/10.15620/cdc:117915>.
- (5) Rice, L. B. Federal Funding for the Study of Antimicrobial Resistance in Nosocomial Pathogens: No ESKAPE. *Journal of Infectious Diseases*. Oxford Academic April 15, 2008, pp 1079–1081. <https://doi.org/10.1086/533452>.
- (6) WHO. <https://www.who.int/news-room/detail/27-02-2017-who-publishes-list-of-bacteria-for-which-new-antibiotics-are-urgently-needed>.
- (7) Li, Y. X.; Zhong, Z.; Zhang, W. P.; Qian, P. Y. Discovery of Cationic Nonribosomal Peptides as Gram-Negative Antibiotics through Global Genome Mining. *Nat. Commun.* **2018**, *9* (1). <https://doi.org/10.1038/s41467-018-05781-6>.
- (8) Al Ayed, K.; Ballantine, R. D.; Hoekstra, M.; Bann, S. J.; Wesseling, C. M. J.; Bakker, A. T.; Zhong, Z.; Li, Y. X.; Brühle, N. C.; van der Stelt, M.; Cochrane, S. A.; Martin, N. I. Synthetic Studies with the Brevicidine and Laterocidine Lipopeptide Antibiotics Including Analogues with Enhanced Properties and in Vivo Efficacy. *Chem. Sci.* **2022**, *13* (12), 3563–3570. <https://doi.org/10.1039/d2sc00143h>.
- (9) Li, Z.; Chakraborty, P.; de Vries, R. H.; Song, C.; Zhao, X.; Roelfes, G.; Scheffers, D. J.; Kuipers, O. P. Characterization of Two Relacidines Belonging to a Novel Class of Circular Lipopeptides That Act against Gram-Negative Bacterial Pathogens. *Environ. Microbiol.* **2020**, *22* (12), 5125–5136. <https://doi.org/10.1111/1462-2920.15145>.
- (10) Li, Z.; Song, C.; Yi, Y.; Kuipers, O. P. Characterization of Plant Growth-Promoting Rhizobacteria from Perennial Ryegrass and Genome Mining of Novel Antimicrobial Gene Clusters. *BMC Genomics* **2020**, *21* (1), 1–11. <https://doi.org/10.1186/s12864-020-6563-7>.
- (11) Blin, K.; Shaw, S.; Kloosterman, A. M.; Charlop-Powers, Z.; van Wezel, G. P.; Medema, M. H.; Weber, T. AntiSMASH 6.0: Improving Cluster Detection and Comparison Capabilities. *Nucleic Acids Res.* **2021**, *49* (W1), W29–W35. <https://doi.org/10.1093/nar/gkab335>.
- (12) Medema, M. H.; Kottmann, R.; Yilmaz, P.; Cummings, M.; Biggins, J. B.; Blin, K.; de Bruijn, I.; Chooi, Y. H.; Claesen, J.; Coates, R. C.; Cruz-Morales, P.; Duddela, S.; Düsterhus, S.; Edwards, D. J.; Fewer, D. P.; Garg, N.; Geiger, C.; Gomez-Escribano, J. P.; Greule, A.; Hadjithomas, M.; Haines, A. S.; Helfrich, E. J. N.; Hillwig, M. L.; Ishida, A.; Jones, A. C.; Jones, C. S.; Jungmann, K.; Kegler, C.; Kim, H. U.; Kötter, P.; Krug, D.; Masschelein, J.; Melnik, A. V.; Mantovani, S. M.; Monroe, E. A.; Moore, M.; Moss, N.; Nützmann, H.-W.; Pan, G.; Pati, A.; Petras, D.; Reen, F. J.; Rosconi, F.; Rui, Z.; Tian, Z.; Tobias, N. J.; Tsunematsu, Y.; Wiemann, P.; Wyckoff, E.; Yan, X.; Yim, G.; Yu, F.; Xie, Y.; Aigle, B.; Apel, A. K.; Balibar, C. J.; Balskus, E. P.; Barona-Gómez, F.; Bechthold, A.; Bode, H. B.; Borriss, R.; Brady, S. F.; Brakhage, A. A.; Caffrey, P.; Cheng, Y.-Q.; Clardy, J.; Cox, R. J.; De Mot, R.; Donadio, S.; Donia, M. S.; van der Donk, W. A.; Dorrestein, P. C.; Doyle, S.; Driessen, A. J. M.; Ehling-Schulz, M.; Entian, K.-D.; Fischbach, M. A.; Gerwick, L.; Gerwick, W. H.; Gross, H.; Gust, B.; Hertweck, C.; Höfte, M.; Jensen, S. E.; Ju, J.; Katz, L.; Kaysser, L.; Klassen, J. L.; Keller, N. P.; Kormanec, J.; Kuipers, O. P.; Kuzuyama, T.; Kyrpides, N. C.; Kwon, H.-J.; Lautru, S.; Lavigne, R.; Lee, C. Y.; Linqun, B.; Liu, X.; Liu, W.; Luzhetskyy, A.; Mahmud, T.; Mast, Y.; Méndez, C.; Metsä-Ketelä, M.; Micklefield, J.; Mitchell, D. A.; Moore, B. S.; Moreira, L. M.; Müller, R.; Neilan, B. A.; Nett, M.; Nielsen, J.; O'Gara, F.; Oikawa, H.; Osbourn, A.; Osburne, M. S.; Ostash, B.; Payne, S. M.; Pernodet, J.-L.; Petricek, M.; Piel, J.; Ploux, O.; Raaijmakers, J. M.; Salas, J. A.; Schmitt, E. K.; Scott, B.; Seipke, R. F.; Shen, B.; Sherman, D. H.; Sivonen, K.; Smanski, M. J.; Sosio, M.; Stegmann, E.; Süßmuth, R. D.; Tahlan, K.; Thomas, C. M.; Tang, Y.; Truman, A. W.; Viaud, M.; Walton, J. D.; Walsh, C. T.; Weber, T.; van Wezel, G. P.; Wilkinson, B.; Willey, J. M.; Wohlleben, W.; Wright, G. D.; Ziemert, N.; Zhang, C.; Zotchev, S. B.; Breitling, R.; Takano, E.; Glöckner, F. O. Minimum Information about a Biosynthetic Gene Cluster. *Nat. Chem. Biol.* **2015**, *11* (9), 625–631. <https://doi.org/10.1038/nchembio.1890>.
- (13) Jumper, J.; Evans, R.; Pritzel, A.; Green, T.; Figurnov, M.; Ronneberger, O.; Tunyasuvunakool, K.; Bates, R.; Židek, A.; Potapenko, A.; Bridgland, A.; Meyer, C.; Kohl, S. A. A.; Ballard, A. J.; Cowie, A.; Romera-Paredes, B.; Nikolov, S.; Jain, R.; Adler, J.; Back, T.; Petersen, S.; Reiman, D.; Clancy, E.; Zielinski, M.; Steinegger, M.; Pacholska, M.; Berghammer, T.; Bodenstern, S.; Silver, D.; Vinyals, O.; Senior, A. W.; Kavukcuoglu, K.; Kohli, P.; Hassabis, D. Highly Accurate Protein Structure Prediction with AlphaFold. *Nature* **2021**, *596* (7873), 583–589. <https://doi.org/10.1038/s41586-021-03819-2>.
- (14) Ballantine, R. D.; Al Ayed, K.; Bann, S. J.; Hoekstra, M.; Martin, N. I.; Cochrane, S. A. Synthesis and Structure–

- Activity Relationship Studies of N-Terminal Analogues of the Lipopeptide Antibiotics Brevicidine and Laterocidine. *RSC Med. Chem.* **2022**, *00*, 1–3. <https://doi.org/10.1039/d2md00281g>.
- (15) Tsai, C. J.-Y.; Loh, J. M. S.; Proft, T. *Galleria Mellonella* Infection Models for the Study of Bacterial Diseases and for Antimicrobial Drug Testing. *Virulence* **2016**, *7* (3), 214–229. <https://doi.org/10.1080/21505594.2015.1135289>.
- (16) Pereira, M. F.; Rossi, C. C.; da Silva, G. C.; Rosa, J. N.; Bazzolli, D. M. S. *Galleria Mellonella* as an Infection Model: An in-Depth Look at Why It Works and Practical Considerations for Successful Application. *Pathog. Dis.* **2020**, *78* (8), 56. <https://doi.org/10.1093/femspd/ftaa056>.
- (17) Mukherjee, S.; Van Der Donk, W. A. Mechanistic Studies on the Substrate-Tolerant Lanthipeptide Synthetase ProcM. *J. Am. Chem. Soc.* **2014**, *136* (29), 10450–10459. <https://doi.org/10.1021/ja504692v>.
- (18) Dexter, H. L.; Williams, H. E. L.; Lewis, W.; Moody, C. J. Total Synthesis of the Post-Translationally Modified Polyazole Peptide Antibiotic Goadsporin. *Angew. Chemie Int. Ed.* **2017**, *56* (11), 3069–3073. <https://doi.org/10.1002/ANIE.201612103>.
- (19) Xiao, X.; Elsayed, S. S.; Wu, C.; Van Der Heul, H. U.; Metsä-Ketelä, M.; Du, C.; Prota, A. E.; Chen, C. C.; Liu, W.; Guo, R. T.; Abrahams, J. P.; Van Wezel, G. P. Functional and Structural Insights into a Novel Promiscuous Ketoreductase of the Lugdunomycin Biosynthetic Pathway. *ACS Chem. Biol.* **2020**, *15* (9), 2529–2538. <https://doi.org/10.1021/acscchembio.0c00564>.
- (20) Trebosc, V.; Gartenmann, S.; Tötzl, M.; Lucchini, V.; Schellhorn, B.; Pieren, M.; Lociuoro, S.; Gitzinger, M.; Tigges, M.; Bumann, D.; Kemmer, C. Dissecting Colistin Resistance Mechanisms in Extensively Drug-Resistant *Acinetobacter Baumannii* Clinical Isolates. *MBio* **2019**, *10* (4). <https://doi.org/10.1128/mBio.01083-19>.



# **Chapter 6**

## **Summary and Outlook**

**Chapter 1** briefly describes the history of infectious disease research giving examples of key discoveries recorded throughout written history. Building on the work of many generations of researchers, society today has a understanding of infectious diseases that only recently adopted the germ theory of disease over the miasma theory. The chapter also discusses the discovery of the first synthetic antibiotic Salvarsan and the first naturally derived antibiotic penicillin. Penicillin and antibiotics in general have helped transform the medical field but the threat of antibiotic resistance (AMR) looms over our society and the supply of efficacious antibiotics in the future is not a guarantee. The AMR threat was recently described eloquently by Cook and Wright as a kinetics problem.<sup>1</sup> The equilibrium can be shifted by either slowing the spread of resistance or increasing the rate of discovery. While antibiotic stewardship programs have been gaining traction, investment in antibiotic discovery is severely lacking with most research and development efforts currently led by academic institutions. The low cost per treatment, inevitable appearance of resistance, and the need to show superiority over existing treatments currently make antibiotic development too risky for most pharmaceutical companies.<sup>2</sup> In a perfect scenario a company could easily develop a drug that is potent and safe enough to treat an infection and that drug would then be saved for future use when other treatments have become ineffective. In such a scenario the rate of resistance spread is minimized and the rate of discovery optimized. In the real world, however, companies that develop a new antibiotic do not generate enough revenue to stay afloat, as currently there exist multiple cheap generic alternatives already in the clinic. Clearly a shift is needed in how the development of these lifesaving drugs is being funded in the current economic system. Luckily some things are changing as pilot initiatives are being explored involving new forms of financial incentives, such as those based on market entry awards which guarantee a return on investment for the developer, effectively decoupling revenue from the number of prescriptions written.<sup>3</sup> Recently people have also become more interested in alternative therapeutic strategies such as phage therapies,<sup>4</sup> endolysins,<sup>5</sup> vaccines,<sup>6</sup> antibody-antibiotic conjugates<sup>7</sup> and even bacterial proteolysis targeting chimeras.<sup>8</sup> While such strategies could hold immense therapeutic potential, until they are clinically validated classical approaches such as those described in this thesis will remain central to the fight against bacterial infections.

**Chapter 2** describes the first total synthesis of brevicidine and laterocidine (Fig. 1), which we, together with the group of Stephen Cochrane (Belfast) have proposed to constitute a new family of lipopeptide antibiotics we've termed the ornicidine class of antibiotics. Brevicidine and laterocidine were originally discovered by Li and coworkers using a genome mining strategy and shown to target Gram-negative bacterial via interaction with lipopolysaccharide (LPS). The subsequent isolation of both lipopeptides from fermentation of the producing organism led to limited amount of material and in the case of laterocidine only *in vitro* activity against Gram-negative pathogens could be shown due to sub-milligram per liter fermentation yields.<sup>9</sup> The approach described in this chapter made it possible to synthesize enough material for further biological evaluation and is currently being used to facilitate more elaborate mechanism of action (MOA) studies. This chapter also describes the synthesis of a number of analogues of both brevicidine and laterocidine, such as the enantiomers of the parent compounds, that were shown to be less active. Interestingly, the activities of the enantiomeric species were also shown to be antagonized by LPS. This finding raises the question if another biomolecular target might be involved in the MOA of these antibiotics. Given that the tridecaptins, which are structurally similar to the ornicidines were shown to bind Gram-negative Lipid II, it

might be fruitful to explore if the ornicidines display a similar MOA.<sup>10</sup> It can, however, be challenging to find a supply of Gram-negative Lipid II as it is typically made through labor intensive multi-step synthesis on a small scale. A small structure-activity relationship (SAR) study evaluating the importance of Thr9 is also described in **Chapter 2**. In doing so, Thr9 was substituted to Ser to study the effect of the side chain methyl group which resulted in analogues with comparable activity to the natural products. We also explored ester-to-amide modifications in the C-terminal macrocycles of brevicidine and laterocidine by replacing Thr9 with (S)-2,3-diaminopropanoic acid (Dap) or (2S,3R)-2,3-diaminobutanoic acid (MeDap). Interesting, while the amide analogues of brevicidine showed diminished activity, in the case of laterocidine the same substitutions were well tolerated and both the Dap9 and MeDap9 analogues retained activity against most of the tested bacterial strains. This discrepancy might arise from the difference in macrocycle size and/or conformation between the two scaffolds. An investigation into the folding of these peptides, with techniques such as X-ray diffraction or nuclear magnetic resonance (NMR) could shed light into these observed differences. Also of note is the recently finding reported by the group of Oscar Kuipers (Groningen) who discovered that a natural analogue of brevicidine named brevicidine B, possessing Phe instead of Tyr at position 2, shows broad spectrum activity against both Gram-negative and Gram-positive bacteria. Given these findings it would be interesting to ascertain if the effect could be replicated on the laterocidine scaffold.<sup>11</sup> Finally, efforts into increasing the potency and improving pharmacokinetic and pharmacodynamic properties of the ornicidines need to be taken before they can be considered proper drug candidates.

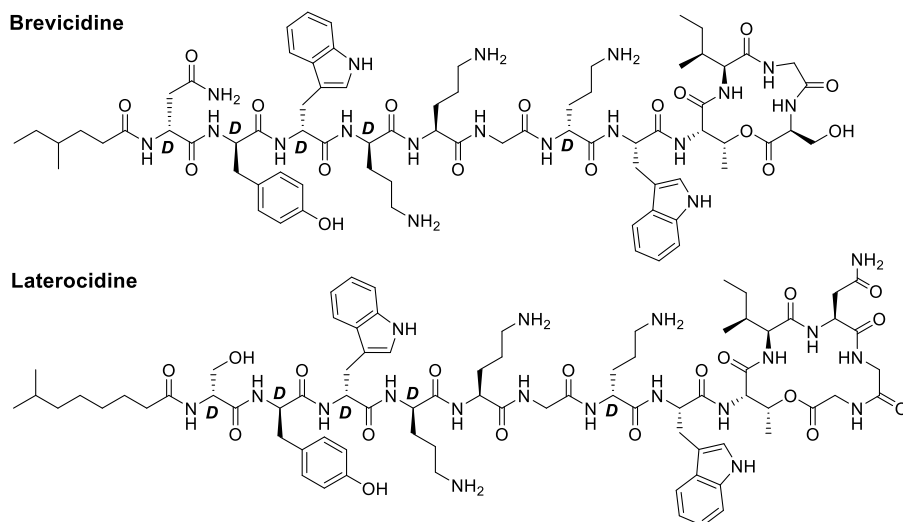


**Figure 1.** Structures of brevicidine and laterocidine. D-amino acids labeled D.

**Chapter 3** reports on the SAR study performed on the brevicidine and laterocidine scaffold in which the branched lipids found in the natural products were substituted for simpler linear saturated lipids of varying length. Although the exact function of the lipid has not been studied, removal of the lipid resulted in complete loss of antibacterial activity as observed

with other lipopeptides. For example, the polymyxins are thought to destabilize the outer membrane by binding LPS and eventually lead to the lysis of the cell.<sup>12</sup> The polymyxin B nonapeptide, the macrocyclic part of polymyxin B devoid of the lipid, however shows no considerable activity against most bacterial strains.<sup>13</sup> Although more data is needed to confirm this, the lipid tails of brevicidine and laterocidine are likely also necessary to insert into the bacterial membrane. Furthermore, the data presented in **Chapter 3** clearly shows that there exists a somewhat optimal lipid length of eight carbon atoms that closely approximates the lipid length of the natural products. Increasing the lipid length did not produce more active compounds. It did however result in more lysis of red blood cells, a parameter indicating non-selective membrane disruption.

**Chapter 4** outlines the discovery of linear brevicidine and laterocidine analogues that retain antibacterial activity. Previously, Li et al. found that linear analogue of brevicidine and laterocidine were less active than the natural products.<sup>14</sup> In this chapter, however, we were able to show that linear analogue of brevicidine and laterocidine can exhibit activity comparable to the parent compounds, provided they are prepared as the C-terminal amides. Because the linear analogues prepared by Li et al. bear a carboxylic acid at the C-terminus, at physiologic pH their overall charge is lower than their cyclic counterparts. The overall charge of antibacterial peptide is known to be of critical importance for activity due to binding interactions with charged phospholipids found throughout the bacterial membrane.<sup>15</sup> By masking the negative charge at the C-terminus through substitution of the carboxylic acid moiety to a neutrally charged amide we were able to produce analogues rivalling the natural products in potency. Furthermore, a full alanine scan of both linear peptide scaffolds was performed as well as truncation studies which gave further insight into residues that are key for activity. This revealed that for both peptides, the residues (D-Tyr2, D-Trp3, D-Orn4, Orn5, D-Orn7, and Trp8) are essential for bioactivity. These residues are either cationic or aromatic (hydrophobic) and are likely key for target binding and maintaining an active conformation to cross the bacterial cell membrane. Further MOA studies will be required to confirm how these peptides elicit their activity, as linearization might have impacted the MOA. Similarly, the proteolytic stability of these peptides needs to be assessed if they are to be taken further into development. The compounds, however, may be expected to be stable to proteolytic degradation due to the large number of D-amino acids in their sequences. Furthermore, the stability studies on brevicidine and laterocidine detailed in **Chapter 2** showed that the linear peptides were identified as the degradation products and these did not degrade further after 24 h incubation in human serum.

**Chapter 5** reports the total synthesis of the recently discovered lipodepsipeptide antibiotics relacidine A and B (Fig. 2), which was guided by bioinformatic analysis of the biosynthetic gene cluster (BGC). Like the brevicidines and laterocidines, relacidine A and B belong to the ornididine class of antibiotics and were recently discovered by the Kuipers group. Notably, the stereochemical configurations of the amino acids comprising relacidine A and B had not been determined in the initial report leading us to pursue a full structural assignment.<sup>16</sup> In doing so we were able to first predict these configurations by examining the position of the epimerization domains within the relacidine BGC. In addition the examination of the BGC led to the discovery of the potential cause of the promiscuity of the adenylation domain that incorporates the 13th amino acid in the relacidines, leading to production of two isoform.

It is likely that a tryptophan to a tyrosine mutation in this domain allows for the slightly larger alanine residue to be incorporated alongside the glycine incorporated at other positions in the ornididine family. Following this, we also synthesized relacidine A and B, as well as various analogues and in doing so validated our bioinformatic prediction by HPLC co-elution experiments and comparison with the NMR data reported by the Kuipers group. The serum stability of the synthesized lipopeptides was assessed, showing that an amide analogue containing a Thr9 to Dap9 substitution, exhibits increased stability while retaining potent activity. The amide analogue was therefore chosen for evaluation in a *Galleria mellonella* larvae infection model due to its high serum stability, low hemolytic activity, ease of synthesis and promising *in vitro* activity.

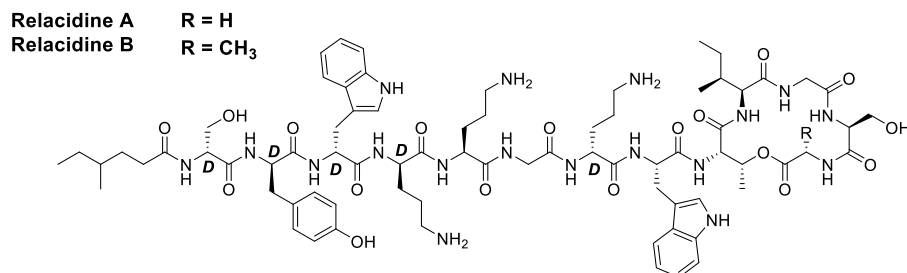


**Figure 2.** Structures of relacidine A and B. D-amino acids labeled D.

To conclude, the research described in this thesis has improved our understanding of the ornididine class of lipopeptide antibiotics. As genetic engineering of non-ribosomal peptide synthetases is still in its infancy, development of synthetic approaches to produce these natural products and their analogs has the power to increase access to these promising compounds and enable further study of their mechanisms of action. The data presented in this thesis has likewise shed light on some of the compelling characteristics of the ornididines and their analogues, such as their potency against drug-resistant strains of pathogenic bacteria *in vitro* as well as *in vivo*. Conversely, characteristics that pose a hurdle for further development have also been identified. Some of them, such as the proteolytic stability of the natural products has been already been addressed in this thesis but others, such as the toxicity and pharmacokinetics/pharmacodynamics profile need to be thoroughly optimized. Clearly, significant preclinical development will be required to advance these compounds further down the pipeline.

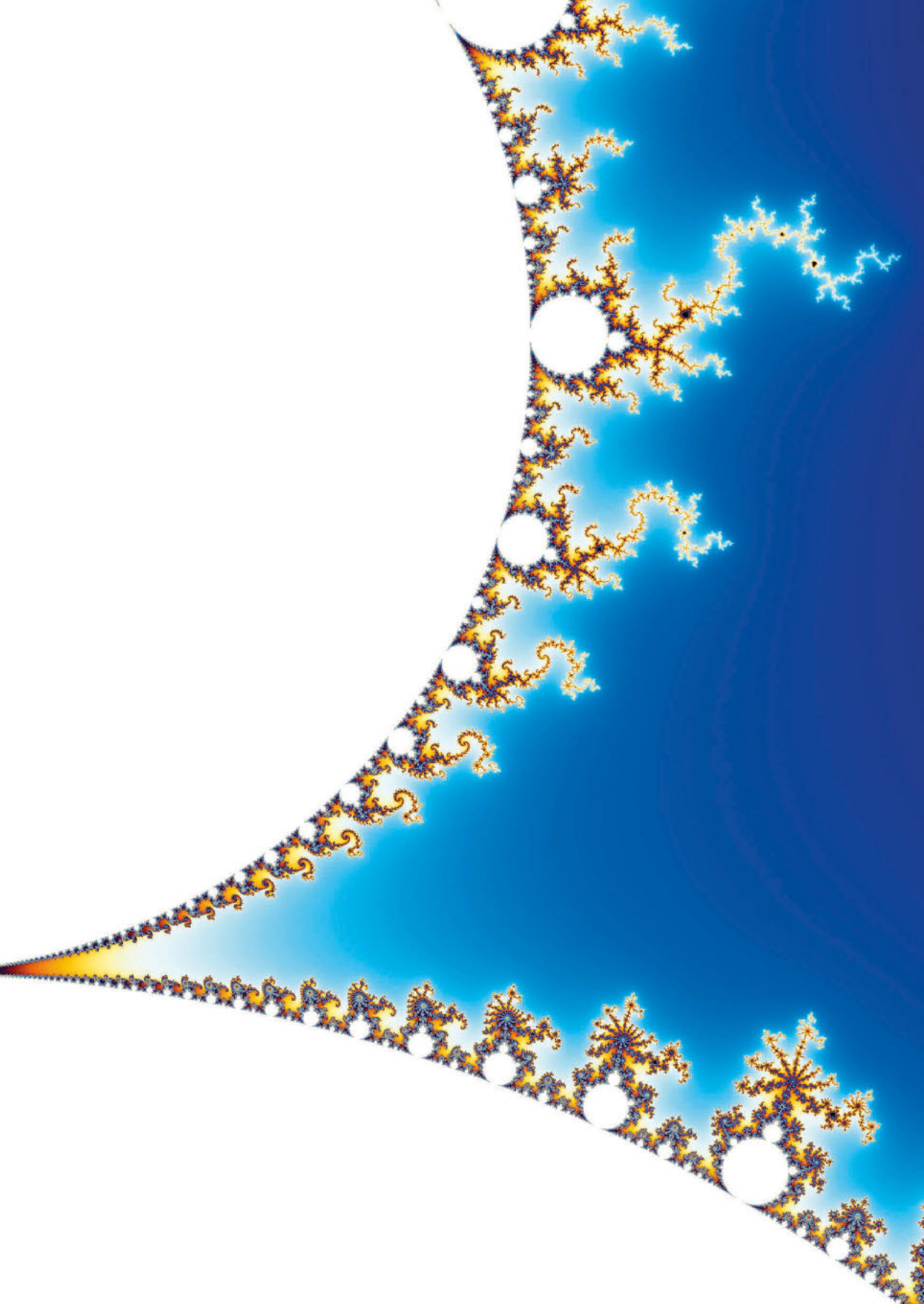
## References

- (1) Cook, M. A.; Wright, G. D. The Past, Present, and Future of Antibiotics. *Sci Transl Med* **2022**, *14* (657). <https://doi.org/10.1126/scitranslmed.abo7793>.
- (2) Jacobs, A. Crisis Looms in Antibiotics as Drug Makers Go Bankrupt. *The New York Times*. 2019, pp 1–3. <https://www.nytimes.com/2019/12/25/health/antibiotics-new-resistance.html> (accessed 2023-07-04).
- (3) Dutescu, I. A.; Hillier, S. A. Encouraging the Development of New Antibiotics: Are Financial Incentives the Right Way Forward? A Systematic Review and Case Study. *Infect Drug Resist* **2021**, *Volume 14*, 415–434. <https://doi.org/10.2147/IDR.S287792>.
- (4) Hatfull, G. F.; Dedrick, R. M.; Schooley, R. T. Phage Therapy for Antibiotic-Resistant Bacterial Infections.



- Annu. Rev. Med.* 2022 **2022**, 73, 173. <https://doi.org/10.1146/annurev-med-080219>.
- (5) Rahman, M. U.; Wang, W.; Sun, Q.; Shah, J. A.; Li, C.; Sun, Y.; Li, Y.; Zhang, B.; Chen, W.; Wang, S. Endolysin, a Promising Solution against Antimicrobial Resistance. *Antibiotics* **2021**, 10 (11), 1277. <https://doi.org/10.3390/antibiotics10111277>.
  - (6) Osterloh, A. Vaccination against Bacterial Infections: Challenges, Progress, and New Approaches with a Focus on Intracellular Bacteria. *Vaccines (Basel)* **2022**, 10 (5), 751. <https://doi.org/10.3390/vaccines10050751>.
  - (7) Lehar, S. M.; Pillow, T.; Xu, M.; Staben, L.; Kajihara, K. K.; Vandlen, R.; DePalatis, L.; Raab, H.; Hazenbos, W. L.; Hiroshi Morisaki, J.; Kim, J.; Park, S.; Darwish, M.; Lee, B.-C.; Hernandez, H.; Loyet, K. M.; Lupardus, P.; Fong, R.; Yan, D.; Chalouni, C.; Luis, E.; Khalifin, Y.; Plise, E.; Cheong, J.; Lyssikatos, J. P.; Strandh, M.; Koefoed, K.; Andersen, P. S.; Flygare, J. A.; Wah Tan, M.; Brown, E. J.; Mariathasan, S. Novel Antibody–Antibiotic Conjugate Eliminates Intracellular *S. Aureus*. *Nature* **2015**, 527 (7578), 323–328. <https://doi.org/10.1038/nature16057>.
  - (8) Morreale, F. E.; Kleine, S.; Leodolter, J.; Junker, S.; Hoi, D. M.; Ovchinnikov, S.; Okun, A.; Kley, J.; Kurzbauer, R.; Junk, L.; Guha, S.; Podlesainski, D.; Kazmaier, U.; Boehmelt, G.; Weinstabl, H.; Rumpel, K.; Schmiedel, V. M.; Hartl, M.; Haselbach, D.; Meinhart, A.; Kaiser, M.; Clausen, T. BacPROTACs Mediate Targeted Protein Degradation in Bacteria. *Cell* **2022**, 185 (13), 2338–2353.e18. <https://doi.org/10.1016/j.cell.2022.05.009>.
  - (9) Li, Y. X.; Zhong, Z.; Zhang, W. P.; Qian, P. Y. Discovery of Cationic Nonribosomal Peptides as Gram-Negative Antibiotics through Global Genome Mining. *Nat Commun* **2018**, 9 (1). <https://doi.org/10.1038/s41467-018-05781-6>.
  - (10) Cochrane, S. A.; Findlay, B.; Bakhtiary, A.; Acedo, J. Z.; Rodriguez-Lopez, E. M.; Mercier, P.; Vederas, J. C. Antimicrobial Lipopeptide Tridecaptin A1selectively Binds to Gram-Negative Lipid II. *Proc Natl Acad Sci U S A* **2016**, 113 (41), 11561–11566. <https://doi.org/10.1073/pnas.1608623113>.
  - (11) Zhao, X.; Kuipers, O. P. BrevicidineB, a New Member of the Brevicidine Family, Displays an Extended Target Specificity . *Frontiers in Microbiology* . 2021. <https://www.frontiersin.org/articles/10.3389/fmicb.2021.693117>.
  - (12) Ayoub Moubareck, C. Polymyxins and Bacterial Membranes: A Review of Antibacterial Activity and Mechanisms of Resistance. *Membranes (Basel)* **2020**, 10 (8), 181. <https://doi.org/10.3390/membranes10080181>.
  - (13) Tsubery, H.; Ofek, I.; Cohen, S.; Fridkin, M. Structure–Function Studies of Polymyxin B Nonapeptide: Implications to Sensitization of Gram-Negative Bacteria. *J Med Chem* **2000**, 43 (16), 3085–3092. <https://doi.org/10.1021/jm0000057>.
  - (14) Li, Y. X.; Zhong, Z.; Zhang, W. P.; Qian, P. Y. Discovery of Cationic Nonribosomal Peptides as Gram-Negative Antibiotics through Global Genome Mining. *Nat Commun* **2018**, 9 (1). <https://doi.org/10.1038/s41467-018-05781-6>.
  - (15) Omaidien, S.; Brul, S.; Zaat, S. A. J. Antimicrobial Activity of Cationic Antimicrobial Peptides against Gram-Positives: Current Progress Made in Understanding the Mode of Action and the Response of Bacteria. *Front Cell Dev Biol* **2016**, 4 (OCT), 208078. <https://doi.org/10.3389/fcell.2016.00111/BIBTEX>.
  - (16) Li, Z.; Chakraborty, P.; de Vries, R. H.; Song, C.; Zhao, X.; Roelfes, G.; Scheffers, D. J.; Kuipers, O. P. Characterization of Two Relacidines Belonging to a Novel Class of Circular Lipopeptides That Act against Gram-Negative Bacterial Pathogens. *Environ Microbiol* **2020**, 22 (12), 5125–5136. <https://doi.org/10.1111/1462-2920.15145>.





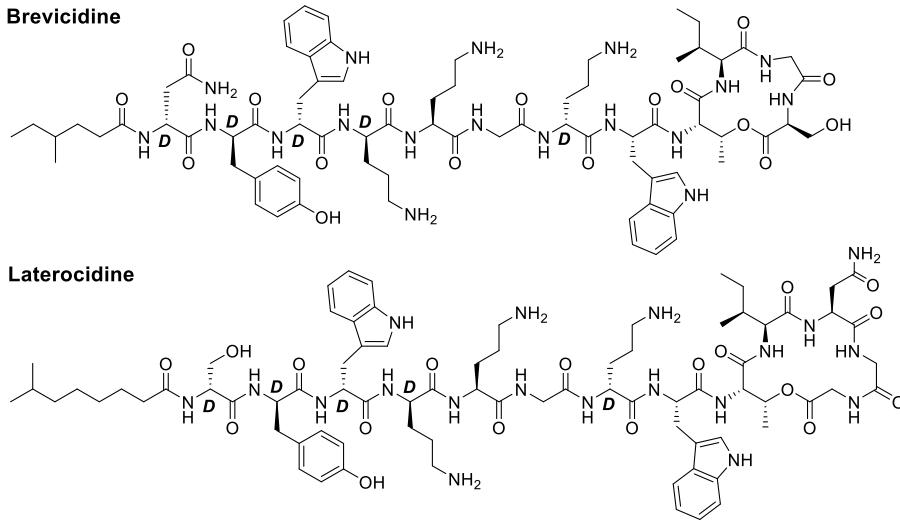
# Appendices

## **Samenvatting**

**Hoofdstuk 1** beschrijft kort de geschiedenis van het onderzoek naar infectieziekten en geeft voorbeelden van belangrijke ontdekkingen die in de loop van de geschiedenis zijn opgetekend. Voortbouwend op het werk van vele generaties onderzoekers heeft de hedendaagse samenleving een breed inzicht gekregen in infectieziekten en pas onlangs de ziektekiemtheorie overgenomen in plaats van de miasmatheorie. Het hoofdstuk bespreekt ook de ontdekking van het eerste synthetische antibioticum Salvarsan en het eerste natuurlijk verkregen antibioticum penicilline. Voornamelijk penicilline en antibiotica hebben geholpen de medische wereld te transformeren, maar de dreiging van antibioticaresistentie (AMR) hangt boven onze samenleving als het zwaard van Damocles en het aanbod van effectieve antibiotica in de toekomst is niet gegarandeerd. De AMR-dreiging is onlangs door Cook en Wright welsprekend beschreven als een kinetisch probleem.<sup>1</sup> Het evenwicht kan worden verschoven door de verspreiding van resistentie te vertragen of de snelheid van ontdekkingen te verhogen. Terwijl programma's voor antibioticabeheer steeds meer terrein winnen, ontbreekt het ernstig aan investeringen in de ontdekking van nieuwe antibiotica, waarbij de meeste onderzoeken en ontwikkelingsinspanningen momenteel worden geleid door academische instellingen. De lage kosten per behandeling, de onvermijdelijke schijn van resistentie en de noodzaak om superioriteit te tonen ten opzichte van bestaande behandelingen maken de ontwikkeling van antibiotica momenteel te riskant voor de meeste farmaceutische bedrijven.<sup>2</sup> In een perfect scenario zou een bedrijf gemakkelijk een medicijn kunnen ontwikkelen dat effectief en veilig genoeg is om een infectie te behandelen en zou dat medicijn bewaard worden voor toekomstig gebruik als andere behandelingen niet meer effectief zijn. In een dergelijk scenario wordt de verspreiding van resistentie geminimaliseerd en de snelheid van ontdekking geoptimaliseerd. In de echte wereld genereren bedrijven die een nieuw antibioticum ontwikkelen echter niet genoeg inkomsten om het hoofd boven water te houden, omdat er momenteel al meerdere goedkope generieke alternatieven in de kliniek bestaan. Er is duidelijk een verandering nodig in de manier waarop de ontwikkeling van deze levensreddende medicijnen in het huidige economische systeem wordt gefinancierd. Gelukkig zijn er een aantal dingen aan het veranderen nu proefinitiatieven worden onderzocht met nieuwe vormen van financiële prikkels, zoals in de vorm van beloningen voor markttoegang, die een rendement op de investering voor de ontwikkelaar garanderen, waardoor de inkomsten effectief worden losgekoppeld van het aantal uitgeschreven recepten.<sup>3</sup> Recentelijk is men ook steeds meer geïnteresseerd geraakt in alternatieve therapeutische strategieën zoals faagtherapieën,<sup>4</sup> endolysinen,<sup>5</sup> vaccins,<sup>6</sup> antilichaam-antibioticumconjugaten<sup>7</sup> en zelfs bacteriële proteolyse inducerende chimaera's.<sup>8</sup> Dergelijke strategieën zouden een enorm therapeutisch potentieel kunnen hebben, maar totdat ze klinisch gevalideerd worden, zullen klassieke benaderingen zoals die beschreven in dit proefschrift centraal blijven in de strijd tegen bacteriële infecties.

**Hoofdstuk 2** beschrijft de eerste totaalsynthese van brevicidine en laterocidine (Fig. 1), die wij samen met de groep van Stephen Cochrane (Belfast) hebben voorgesteld als een nieuwe familie van lipopeptide-antibiotica. Deze nieuwe familie hebben we de ornicidine-klasse van antibiotica genoemd. Brevicidine en laterocidine werden oorspronkelijk ontdekt door Li en collega's met behulp van een genominingstrategie. Daarmee werd aangetoond dat ze zich op Gram-negatieve bacteriën richten via interactie met lipopolysaccharide (LPS). De daaropvolgende isolatie van beide lipopeptiden uit de fermentatie van *Brevibacillus laterosporus* leidde tot een beperkte hoeveelheid materiaal. Daarnaast kon in het geval van laterocidine alleen *in vitro* activiteit tegen Gram-negatieve pathogenen worden aangetoond

vanwege fermentatieopbrengsten van minder dan een milligram per liter.<sup>9</sup> De beschreven aanpak in dit hoofdstuk maakte het mogelijk om voldoende materiaal te synthetiseren voor verdere biologische evaluatie en wordt momenteel gebruikt om meer uitgebreide studies van het werkingsmechanisme (MOA) mogelijk te maken. Dit hoofdstuk beschrijft ook de synthese van een aantal analogen van zowel brevicidine als laterocidine, zoals de enantiomeren van de moederverbindingen, waarvan is aangetoond dat ze minder actief zijn. Interessant is dat er ook werd aangetoond dat de activiteiten van de enantiomeren door LPS worden geantagoneerd. Deze bevinding roept de vraag op of er mogelijk een ander biomoleculair doelwit betrokken is bij de MOA van deze antibiotica. Aangezien tridecaptinen, die structureel vergelijkbaar zijn met de ornicidines, Gram-negatieve Lipid II binden, zou het interessant kunnen zijn om te onderzoeken of de ornicidines een vergelijkbare MOA vertonen.<sup>10</sup> Het kan echter een uitdaging zijn om een voorraad Gram-negatieve Lipid II te vinden, omdat het doorgaans wordt gemaakt via arbeidsintensieve meerstapssynthese op kleine schaal. Een klein onderzoek naar de structuur-activiteitsrelatie (SAR) waarin het belang van Thr9 werd geëvalueerd, wordt ook beschreven in **Hoofdstuk 2**. Daarbij werd Thr9 vervangen door Ser om het effect van de zijketenmethylgroep te bestuderen, wat resulteerde in analogen met vergelijkbare activiteit als de natuurlijke producten. We hebben ook ester-naar-amide-modificaties onderzocht in de C-terminale macrocycli van brevicidine en laterocidine door Thr9 te vervangen door (S)-2,3-diaminopropaanzuur (Dap) of (2S,3R)-2,3-diaminobutaanzuur (MeDap). Interessant is dat, hoewel de amide-analogen van brevicidine een verminderde activiteit vertoonden, in het geval van laterocidine dezelfde substituties goed werden verdragen en zowel de Dap9- als de MeDap9-analogen hun activiteit tegen de meeste van de geteste bacteriestammen behielden. Deze discrepantie zou kunnen voortkomen uit het verschil in macrocyclusgrootte en/of conformatie tussen de brevicidine- en laterocidine-scaffold. Een onderzoek naar de vouwing van deze peptiden, met technieken zoals röntgendiffractie of nucleaire magnetische resonantie (NMR), zou licht kunnen werpen op de waargenomen verschillen. Opmerkelijk is ook de recente bevinding gerapporteerd door de groep van Oscar Kuipers (Groningen). Zij ontdekten dat een natuurlijk analoog van brevicidine genaamd brevicidine B, dat Phe in plaats van Tyr op positie 2 bezit, een breed spectrum activiteit vertoont tegen zowel Gram-negatieve als Gram-positieve bacteriën. Gegeven deze bevindingen zou het interessant zijn om na te gaan of het effect kan worden gerepliceerd op het laterocidine-scaffold.<sup>11</sup> Ten slotte moeten er inspanningen worden geleverd om de potentie te vergroten en de farmacokinetische en farmacodynamische eigenschappen van de ornicidines te verbeteren voordat ze als geschikte kandidaat-geneesmiddelen kunnen worden beschouwd.



**Figuur 1.** Structuren van brevicidine and laterocidine. D-aminozuren aangegeven met D.

**Hoofdstuk 3** rapporteert over de SAR-studie uitgevoerd op het brevicidine- en laterocidine-scaffold waarin de vertakte lipiden, gevonden in de natuurlijke producten, werden vervangen door eenvoudigere lineaire verzadigde lipiden van variërende lengte. Hoewel de exacte functie van het lipide niet is onderzocht, resulteerde verwijdering van het lipide in een volledig verlies van antibacteriële activiteit, zoals waargenomen bij andere lipopeptiden. Er wordt bijvoorbeeld gedacht dat de polymyxines het buitenmembraan destabiliseren door LPS te binden en uiteindelijk tot de lyse van de cel leiden.<sup>12</sup> Het polymyxine B nonapeptide, het macrocyclische deel van polymyxine B zonder lipide, vertoont echter geen noemenswaardige activiteit tegen de meeste bacteriële stammen.<sup>13</sup> Hoewel er meer gegevens nodig zijn om dit te bevestigen, zijn de lipidestaarten van brevicidine en laterocidine waarschijnlijk ook nodig om in het bacteriële membraan te worden ingebracht. Bovendien laten de gegevens gepresenteerd in **Hoofdstuk 3** duidelijk zien dat er een enigszins optimale lipidelengte van acht koolstofatomen bestaat die de lipidelengte van de natuurlijke producten dicht benadert. Het vergroten van de lipidelengte produceerde geen actievere verbindingen. Het resulteerde echter wel in meer lyse van rode bloedcellen, een parameter die wijst op niet-selectieve membraanverstoring.

**Hoofdstuk 4** schetst de ontdekking van lineaire brevicidine- en laterocidine-analogen die antibacteriële activiteit behouden. Eerder vonden Li *et al.* dat de lineaire analogen van brevicidine en laterocidine minder actief waren dan de natuurlijke producten.<sup>14</sup> In dit hoofdstuk konden we echter aantonen dat de lineaire analogen van brevicidine en laterocidine een activiteit kunnen vertonen die vergelijkbaar is met de oorspronkelijke verbindingen, op voorwaarde dat ze worden bereid als de C-terminale amiden. Omdat de lineaire analogen bereid door Li *et al.* een carbonzuur aan het C-uiteinde bevatten, is bij fysiologische pH hun totale lading lager dan die van hun cyclische tegenhangers. Het is bekend dat de algehele lading van het antibacteriële peptide van cruciaal belang is voor de activiteit als gevolg van bindingsinteracties met geladen fosfolipiden die overal in het bacteriële membraan worden aangetroffen.<sup>15</sup> Door de negatieve lading aan de C-terminus te maskeren door vervanging



van de carbonzuurgroep naar een neutraal geladen amide, waren we in staat om analogen te produceren die qua potentie concurreren met de natuurlijke producten. Bovendien werd een volledige alaninescan van beide lineaire peptide scaffolds uitgevoerd, evenals verkortingsstudies die verder inzicht gaven in residuen die essentieel zijn voor activiteit. Hieruit bleek dat voor beide peptiden de residuen (D-Tyr2, D-Trp3, D-Orn4, Orn5, D-Orn7 en Trp8) essentieel zijn voor bioactiviteit. Deze residuen zijn kationisch of aromatisch (hydrofoob) en zijn waarschijnlijk de sleutel tot doelbinding en het behouden van een actieve conformatie om het bacteriële celmembraan te passeren. Verdere MOA-studies zullen nodig zijn om te bevestigen hoe deze peptiden hun activiteit opwekken, aangezien linearisatie de MOA mogelijk heeft beïnvloed. Op dezelfde manier moet de proteolytische stabiliteit van deze peptiden worden beoordeeld als ze verder in ontwikkeling willen worden gebracht. Er mag echter verwacht worden dat de verbindingen stabiel zijn tegen proteolytische afbraak vanwege het grote aantal D-aminozuren in hun sequenties. Bovendien lieten de stabiliteitsstudies met brevicidine en laterocidine, beschreven in **Hoofdstuk 2**, zien dat de lineaire peptiden werden geïdentificeerd als de afbraakproducten en dat deze niet verder werden afgebroken na 24 uur incubatie in menselijk serum.

**Hoofdstuk 5** rapporteert de totaalsynthese van de recent ontdekte lipodepsipeptide-antibiotica relacidine A en B (Fig. 2). Deze werd geleid door bioinformatische analyse van het biosynthetische gencluster (BGC). Net als de brevicidines en laterocidines behoren relacidine A en B tot de klasse van ornidicine-antibiotica en zijn onlangs ontdekt door de Kuipers-groep. Met name de stereochemische configuraties van de aminozuren die relacidine A en B omvatten, waren niet bepaald in het initiële rapport, wat ons ertoe bracht een volledige structurele karakterisatie na te streven.<sup>16</sup> Daarbij waren we in staat deze configuraties eerst te voorspellen door de positie van de epimerisatiedomeinen binnen de relacidine BGC te onderzoeken. Bovendien leidde het onderzoek van de BGC tot de ontdekking van de mogelijke oorzaak van de promiscuïteit van het adenylatiedomein dat het 13e aminozuur in de relacidines incorporeert, wat leidt tot de productie van twee isovormen. Het is waarschijnlijk dat een tryptofaan-naar-tyrosine mutatie in dit domein het mogelijk maakt dat het iets grotere alanineresidu ook wordt ingebouwd naast de glycine die op andere posities in de ornidicinefamilie wordt ingebouwd. Hierna hebben we ook relacidine A en B gesynthetiseerd, evenals verschillende analogen, en daarmee onze bioinformatische voorspelling gevalideerd door HPLC co-elutie-experimenten en vergelijking met de NMR-gegevens gerapporteerd door de Kuipers-groep. De serumstabiliteit van de gesynthetiseerde lipopeptiden werd beoordeeld, wat aantoont dat een amide-analoog die een Thr9-naar-Dap9-substitutie bevat, een verhoogde stabiliteit vertoont terwijl de krachtige activiteit behouden blijft. Het amide-analoog werd daarom gekozen voor evaluatie in een *Galleria mellonella*-larveninfectiemodel vanwege de hoge serumstabiliteit, lage hemolytische activiteit, het gemak van synthese en veelbelovende *in vitro* activiteit.



- Andersen, P. S.; Flygare, J. A.; Wah Tan, M.; Brown, E. J.; Mariathasan, S. Novel Antibody–Antibiotic Conjugate Eliminates Intracellular *S. Aureus*. *Nature* **2015**, *527* (7578), 323–328. <https://doi.org/10.1038/nature16057>.
- (8) Morreale, F. E.; Kleine, S.; Leodolter, J.; Junker, S.; Hoi, D. M.; Ovchinnikov, S.; Okun, A.; Kley, J.; Kurzbauer, R.; Junk, L.; Guha, S.; Podlesainski, D.; Kazmaier, U.; Boehmelt, G.; Weinstabl, H.; Rumpel, K.; Schmiedel, V. M.; Hartl, M.; Haselbach, D.; Meinhart, A.; Kaiser, M.; Clausen, T. BacPROTACs Mediate Targeted Protein Degradation in Bacteria. *Cell* **2022**, *185* (13), 2338–2353.e18. <https://doi.org/10.1016/j.cell.2022.05.009>.
- (9) Li, Y. X.; Zhong, Z.; Zhang, W. P.; Qian, P. Y. Discovery of Cationic Nonribosomal Peptides as Gram-Negative Antibiotics through Global Genome Mining. *Nat Commun* **2018**, *9* (1). <https://doi.org/10.1038/s41467-018-05781-6>.
- (10) Cochrane, S. A.; Findlay, B.; Bakhtiary, A.; Acedo, J. Z.; Rodriguez-Lopez, E. M.; Mercier, P.; Vederas, J. C. Antimicrobial Lipopeptide Tridecaptin A1selectively Binds to Gram-Negative Lipid II. *Proc Natl Acad Sci U S A* **2016**, *113* (41), 11561–11566. <https://doi.org/10.1073/pnas.1608623113>.
- (11) Zhao, X.; Kuipers, O. P. BrevicidineB, a New Member of the Brevicidine Family, Displays an Extended Target Specificity . *Frontiers in Microbiology* . 2021. <https://www.frontiersin.org/articles/10.3389/fmicb.2021.693117>.
- (12) Ayoub Moubareck, C. Polymyxins and Bacterial Membranes: A Review of Antibacterial Activity and Mechanisms of Resistance. *Membranes (Basel)* **2020**, *10* (8), 181. <https://doi.org/10.3390/membranes10080181>.
- (13) Tsubery, H.; Ofek, I.; Cohen, S.; Fridkin, M. Structure–Function Studies of Polymyxin B Nonapeptide: Implications to Sensitization of Gram-Negative Bacteria. *J Med Chem* **2000**, *43* (16), 3085–3092. <https://doi.org/10.1021/jm0000057>.
- (14) Li, Y. X.; Zhong, Z.; Zhang, W. P.; Qian, P. Y. Discovery of Cationic Nonribosomal Peptides as Gram-Negative Antibiotics through Global Genome Mining. *Nat Commun* **2018**, *9* (1). <https://doi.org/10.1038/s41467-018-05781-6>.
- (15) Omardien, S.; Brul, S.; Zaat, S. A. J. Antimicrobial Activity of Cationic Antimicrobial Peptides against Gram-Positives: Current Progress Made in Understanding the Mode of Action and the Response of Bacteria. *Front Cell Dev Biol* **2016**, *4* (OCT), 208078. <https://doi.org/10.3389/fcell.2016.00111/BIBTEX>.
- (16) Li, Z.; Chakraborty, P.; de Vries, R. H.; Song, C.; Zhao, X.; Roelfes, G.; Scheffers, D. J.; Kuipers, O. P. Characterization of Two Relacidines Belonging to a Novel Class of Circular Lipopeptides That Act against Gram-Negative Bacterial Pathogens. *Environ Microbiol* **2020**, *22* (12), 5125–5136. <https://doi.org/10.1111/1462-2920.15145>.

## List of publications

**Al Ayed, K.;** Zamarbide Losada, D.; Machushynets, N. V.; Terlouw, B.; Elsayed, S. S.; Schill, J.; Trebosc, V.; Pieren, M.; Medema, M. H.; van Wezel, G. P.; Martin, N. I. Total Synthesis and Structure Assignment of the Relacidine Lipopeptide Antibiotics and Preparation of Analogues with Enhanced Stability. *ACS Infect Dis* **2023**, 9 (4), 739–748. <https://doi.org/10.1021/acsinfectdis.3c00043>.

Ballantine, R. D.; **Al Ayed, K.\*;** Bann, S. J.; Hoekstra, M.; Martin, N. I.; Cochrane, S. A. Linearization of the Brevicidine and Laterocidine Lipopeptides Yields Analogues That Retain Full Antibacterial Activity. *J Med Chem* **2023**, 66 (8), 6002–6009. <https://doi.org/10.1021/acs.jmedchem.3c00308>.

Ballantine, R. D.\*; **Al Ayed, K.\*;** Bann, S. J.; Hoekstra, M.; Martin, N. I.; Cochrane, S. A. Synthesis and Structure-Activity Relationship Studies of N-Terminal Analogues of the Lipopeptide Antibiotics Brevicidine and Laterocidine. *RSC Med. Chem.* **2022**, 00, 1–3. <https://doi.org/10.1039/D2MD00281G>

**Al Ayed, K.\*;** Ballantine, R. D.\*; Hoekstra, M.; Bann, S. J.; Wesseling, C. M. J.; Bakker, A. T.; Zhong, Z.; Li, Y.-X.; Bröchle, N. C.; Van Der Stelt, M.; Cochrane, S. A.; Martin, N. I. Synthetic Studies with the Brevicidine and Laterocidine Lipopeptide Antibiotics Including Analogues with Enhanced Properties and in Vivo Efficacy. *Chem. Sci.* **2022**, 13 (12), 3563–3570. <https://doi.org/10.1039/D2SC00143H>

Zhou, J.\*; Mock, E. D.\*; **Al Ayed, K.;** Di, X.; Kantae, V.; Burggraaff, L.; Stevens, A. F.; Martella, A.; Mohr, F.; Jiang, M.; Van Der Wel, T.; Wendel, T. J.; Ofman, T. P.; Tran, Y.; De Koster, N.; Van Westen, G. J. P.; Hankemeier, T.; Van Der Stelt, M. Structure-Activity Relationship Studies of  $\alpha$ -Ketoamides as Inhibitors of the Phospholipase A and Acyltransferase Enzyme Family. *J. Med. Chem.* **2020**, 63 (17), 9340–9359. <https://doi.org/10.1021/acs.jmedchem.0c00522>

Zhou, J.; Mock, E. D.; Martella, A.; Kantae, V.; Di, X.; Burggraaff, L.; Baggelaar, M. P.; **Al-Ayed, K.;** Bakker, A.; Florea, B. I.; Grimm, S. H.; Den Dulk, H.; Li, C. T.; Mulder, L.; Overkleeft, H. S.; Hankemeier, T.; Van Westen, G. J. P.; Van Der Stelt, M. Activity-Based Protein Profiling Identifies  $\alpha$ -Ketoamides as Inhibitors for Phospholipase A2 Group XVI. *ACS Chem. Biol.* **2019**, 14 (2), 164–169. <https://doi.org/10.1021/acscchembio.8b00969>

de Bruin, G.; Huber, E. M.; Xin, B.-T.; van Rooden, E. J.; **Al-Ayed, K.;** Kim, K.-B.; Kisselev, A. F.; Driessen, C.; van der Stelt, M.; van der Marel, G. A.; Groll, M.; Overkleeft, H. S. Structure-Based Design of B1i or B5i Specific Inhibitors of Human Immunoproteasomes. *J. Med. Chem.* **2014**, 57 (14), 6197–6209. <https://doi.org/10.1021/jm500716s>

\*Authors contributed equally

A

## Curriculum Vitae

Karol Al Ayed was born on 5 July 1990 in Gdynia, Poland. In 2000 he moved to the Netherlands with his mother. After graduating high school at the Stanislas college in Delft, he started the bachelor life science & technology at Leiden University and TU Delft. During the bachelor program Karol became increasingly more interested in chemistry which led him to pursue an internship in the group of prof.dr. Hermen Overkleeft. There he worked on the synthesis and evaluation of selective immunoproteasome inhibitors. The work there sparked Karol's curiosity in chemistry even further and led him to pursue a master's degree in chemistry at Leiden University. During this time he worked on the discovery of novel phospholipase A/acyltransferase inhibitors in the group of prof.dr. Mario van der Stelt. After obtaining the degree of master in science in chemistry Karol pursued a PhD in the group of prof.dr. Nathaniel Martin, initially at Utrecht University and subsequently at Leiden University. There he mainly worked on the synthesis and assessment of lipopeptide antibiotics. As of February 2023, Karol is working as a Lead Scientist at the Nuclear Research and Consultancy Group (NRG) in Petten.



